

SERGEY N. MAKAROV • VISHWANATH IYER
SHASHANK KULKARNI • STEVEN R. BEST

ANTENNA AND EM MODELING WITH MATLAB® ANTENNA TOOLBOX™

SECOND EDITION

WILEY

ANTENNA AND EM MODELING WITH MATLAB® ANTENNA TOOLBOX

ANTENNA AND EM MODELING WITH MATLAB[®] ANTENNA TOOLBOX

SECOND EDITION

Dr. Sergey N. Makarov
Worcester Polytechnic Institute
Worcester, MA, USA

Dr. Vishwanath Iyer
MathWorks, Inc.
Sherborn, MA, USA

Dr. Shashank Kulkarni
MathWorks, Inc.
Khajaguda, Hyderabad, India

Dr. Steven R. Best
MegaWave, LLC
Worcester, MA, USA

WILEY

This second edition first published 2021
© 2021 John Wiley & Sons, Inc.

Edition History

First Edition: © John Wiley and Sons, Inc., New York, 2002

All rights reserved. No part of this publication may be reproduced, stored in a retrieval system, or transmitted, in any form or by any means, electronic, mechanical, photocopying, recording or otherwise, except as permitted by law. Advice on how to obtain permission to reuse material from this title is available at <http://www.wiley.com/go/permissions>.

The right of Dr. Sergey N. Makarov, Dr. Vishwanath Iyer, Dr. Shashank Kulkarni, and Dr. Steven R. Best to be identified as the authors of this work has been asserted in accordance with law.

Registered Office

John Wiley & Sons, Inc., 111 River Street, Hoboken, NJ 07030, USA

Editorial Office

111 River Street, Hoboken, NJ 07030, USA

For details of our global editorial offices, customer services, and more information about Wiley products visit us at www.wiley.com.

Wiley also publishes its books in a variety of electronic formats and by print-on-demand. Some content that appears in standard print versions of this book may not be available in other formats.

Limit of Liability/Disclaimer of Warranty

MATLAB® is a trademark of The MathWorks, Inc. and is used with permission. The MathWorks does not warrant the accuracy of the text or exercises in this book. This work's use or discussion of MATLAB® software or related products does not constitute endorsement or sponsorship by The MathWorks of a particular pedagogical approach or particular use of the MATLAB® software. While the publisher and authors have used their best efforts in preparing this work, they make no representations or warranties with respect to the accuracy or completeness of the contents of this work and specifically disclaim all warranties, including without limitation any implied warranties of merchantability or fitness for a particular purpose. No warranty may be created or extended by sales representatives, written sales materials or promotional statements for this work. The fact that an organization, website, or product is referred to in this work as a citation and/or potential source of further information does not mean that the publisher and authors endorse the information or services the organization, website, or product may provide or recommendations it may make. This work is sold with the understanding that the publisher is not engaged in rendering professional services. The advice and strategies contained herein may not be suitable for your situation. You should consult with a specialist where appropriate. Further, readers should be aware that websites listed in this work may have changed or disappeared between when this work was written and when it is read. Neither the publisher nor authors shall be liable for any loss of profit or any other commercial damages, including but not limited to special, incidental, consequential, or other damages.

Library of Congress Cataloging-in-Publication Data applied for:

ISBN: 9781119693697

Cover design by Wiley

Cover image: © Andrey Suslov/Shutterstock, sovika/iStock/Getty Images

Set in 10/12pt Times by SPi Global, Pondicherry, India

To our children



Contents

Preface and Text Organization	ix
List of Notations	xiii
About the Companion Website	xv
1 Antenna Circuit Model. Antenna Matching. Antenna Bandwidth	1
Section 1 Lumped Circuit Model of an Antenna. Antenna Input Impedance	1
Section 2 Antenna with Transmission Line. Antenna Reflection Coefficient. Antenna Matching. VSWR	18
2 Receiving Antenna: Received Voltage, Power, and Transmission Coefficient	31
Section 1 Analytical Model for the Receiving Antenna	31
Section 2 Model of a Two-Port Network for TX/RX Antennas	44
3 Antenna Radiation	55
Section 1 Maxwell Equations and Boundary Conditions	55
Section 2 Solution for Maxwell's Equations in Terms of Electric and Magnetic Potentials	63
Section 3 Antenna Radiation	71
Section 4 Antenna Directivity and Gain	84
4 Antenna Balun. Antenna Reflector. Method of Images	101
Section 1 Antenna Balun	101
Section 2 Antenna Reflector	116

5 Dipole Antenna Family: Broadband Antennas that Operate as Dipoles at Low Frequencies	135
Section 1 Broadband Dipoles and Monopoles	135
Section 2 Biconical, Wide Blade, and Vivaldi Antennas	141
6 Loop Antennas	155
Section 1 Loop Antenna vs. Dipole Antenna	155
7 Small Antennas	171
Section 1 Fundamental Limits on Antenna Bandwidth	171
Section 2 Practical Antenna Matching and Tuning for a Predefined (50Ω) Impedance	185
8 Patch and PIFA Antennas	197
Section 1 Patch Antennas	197
Section 2 Planar Inverted F (PIFA) Antenna. Bandwidth Estimations	219
9 Traveling Wave Antennas	233
Section 1 Long Wire Antenna and Yagi-Uda Antenna	233
Section 2 Helical and Spiral Antennas	241
10 Antenna Designer Including Circularly Polarized Antennas	251
Section 1 Fast Analysis and Design of Individual Antennas	251
Section 2 Meaning of Circular Polarization and Proper Antenna Orientation	259
11 Antenna Arrays	271
Section 1 Array Types. Array Factor. Concept of a Scanning Array	271
Section 2 Linear Arrays	287
Section 3 Planar Arrays	303
Index	317



Preface and Text Organization

The first edition of this book and the subsequent work of coauthors resulted in MATLAB® Antenna Toolbox™ – a dedicated learning and research software tool for major antenna and array types. Internally, the toolbox uses the Method of Moments (the method of integral equation) for modeling metal and metal-dielectric antennas. Rao–Wilton–Glisson basis functions on triangular facets are used for the metal parts and edge basis functions on tetrahedra are used for the dielectric parts. Accurate semi-analytical calculation of near-field interactions between neighbors facets and tetrahedra assures good solution accuracy.

The Antenna Toolbox has a relatively flexible 2.5D CAD geometry generator and it has an option to import an arbitrary surface antenna or an antenna platform mesh. In addition to multiple programmatic examples, it features over 60 different predesigned antenna configurations grouped by various families such as patch antennas, monopoles, dipoles, spirals, etc. and continues to grow.

In contrast to the first edition devoted to the development of numerical modeling, this second edition is structured differently. It is presented as a succinct yet self-contained introduction to basic antenna modeling and design with an emphasis on the antenna modeling with the already available MATLAB® Antenna Toolbox. Special attention is paid to small antennas where the Method of Moments remains the most accurate modeling tool. The present text has been used for a one-semester graduate or a senior-level undergraduate course for EE/ECE majors and other interested students. It can also be used for an independent study.

The text covers major antenna and array types, and concepts, along with the necessary theoretical background. The text also includes a number of practical antenna/array design examples performed by the authors. Wherever possible, we refer to more comprehensive and fundamental antenna books by C. A. Balanis, W. L. Stutzman, G. A. Thiele, R. C. Hansen, T. Milligan, and the others.

The text organization is shown in Table 1. It includes printed matter, MATLAB® Antenna Toolbox video laboratories, video tutorials, and video lectures, and is targeting either mixed or online material delivery. For running laboratories, MATLAB® 2018 or newer is required with Antenna Toolbox and RF Toolbox installed.

TABLE 1 Organization of printed matter, video laboratories, tutorials, and video lectures. The text content has been tentatively divided into 12 lectures; other arrangements are possible, indeed. Video laboratories (shadowed) teach how to use the Antenna Toolbox.

#	Topic	Antenna Toolbox laboratory recordings	Lecture recordings
1	Antenna circuit model, antenna impedance (Chapter 1 Section 1)	LabSession1.mp4 (10 minutes)	Lecture1_Recording.mp4 (20 minutes)
2	Antenna reflection coefficient, VSWR, antenna bandwidth (Chapter 1 Section 2)	LabSession2.mp4 (10 minutes)	Lecture2_Recording.mp4 (20 minutes)
3	Antenna-to-antenna link. Power transfer between TX/RX antennas (Chapter 2 Sections 1 and 2)	LabSession3.mp4 (13 minutes)	Lecture3_Recording.mp4 (20 minutes)
4	Maxwell's equations, boundary conditions, basic solutions (Chapter 3 Sections 1 and 2)		Lecture4_Recording.mp4 (20 minutes)
5	Antenna radiation: directivity, gain, realized gain, antenna aperture (Chapter 3 Sections 3 and 4)	LabSession4.mp4 (14 minutes)	Lecture5_Recording.mp4 (16 minutes)
6	Antenna balun, antenna reflector, method of images (Chapter 4 Sections 1 and 2)	LabSession5.mp4 (16 minutes)	Lecture6_Recording.mp4 (20 minutes)
7a	Dipole antenna family, broadband dipole like antennas (Chapter 5 Sections 1 and 2)	LabSession6Part1.mp4 (19 minutes) LabSession6Part2.mp4 (13 minutes)	Lecture7Part1_Recording.mp4 (12 minutes)
7b	Loop antennas (Chapter 6)	LabSession7.mp4 (16 minutes)	Lecture7Part2_Recording.mp4 (13 minutes)
8	Small antennas, bandwidth, antenna loss (Chapter 7, Video tutorials by Dr. S. Best)	VideoTutorial1.mp4 (15 minutes) VideoTutorial2.mp4 (15 minutes) LabSession8.mp4 (14 minutes)	Lecture8_Recording.mp4 (21 minutes)
9	Patch and PIFA antennas (Chapter 8 Sections 1 and 2)	LabSession9.mp4 (31 minutes)	Lecture9_Recording.mp4 (26 minutes)
10	Traveling wave antennas: Yagi-Uda, helix, spiral (Ch 9)	LabSession10.mp4 (30 minutes)	Lecture10_Recording.mp4 (22 minutes)

TABLE 1 (Continued)

#	Topic	Antenna Toolbox laboratory recordings	Lecture recordings
11	MATLAB® Antenna Designer (Chapter 10)	LabSession11 (21 minutes)	Lecture11_Recording. mp4 (23 minutes)
12	Antenna arrays (Chapter 11)	LabSession12Part1 (24 minutes) LabSession12Part2 (24 minutes)	Lecture12_Recording. mp4 (30 minutes)

One ongoing extension of the Antenna Toolbox is the utilization of the Fast Multipole Method (FMM) developed by the group of Dr. Leslie Greengard and the others. It is intended to enable modeling large antenna reflectors, antennas on large platforms (airplanes and cars), and large antennas arrays.

The online materials contain a suite of open-source MATLAB® scripts along with the supporting supplement, which demonstrate how to implement this approach and how to apply it to antenna reflectors and scatterers of large compared to the wavelength sizes.

We thank Dr. Angelo Puzella of Raytheon Technologies for numerous constructive comments and suggestions.

THE AUTHORS
Massachusetts 2021



List of Notations

Some notations used in the text

All complex-valued Roman quantities are denoted by **bold** letters. Examples include

1. Vector electric field, time domain $\vec{E}(\vec{r}, t)$
2. Vector electric field, complex phasor in frequency domain $\vec{E}(\vec{r})$
3. Electric field component, time domain $E_x(\vec{r}, t)$
4. Electric field component, complex phasor in frequency domain $E_x(\vec{r})$

All complex-valued Greek quantities are denoted by the *same* letters. Examples include

1. Electric potential, time domain $\varphi(\vec{r}, t)$
2. Electric potential, complex phasor in frequency domain $\varphi(\vec{r})$

Unit vectors in the directions of respective axes are denoted as \hat{x} , \hat{y} , etc.

In spherical co-ordinates $(\vec{r}, \theta, \varphi)$ or (\vec{r}, θ, ϕ) , θ is always computed from zenith. Azimuthal angle notations φ and ϕ are equivalent; they are used interchangeably. Time dependency $\exp(j\omega t)$ is used everywhere.



About the Companion Website

This book is accompanied by a companion website:



www.wiley.com/go/Makarov/AntennaandEMModelingwithMATLAB2e

The companion website is an important part of this text. It provides Antenna Toolbox laboratories in the sequential order. It also provides MATLAB® codes which employ the Fast Multipole Method (FMM) for large-size antenna/scattering problems.

CHAPTER 1



Antenna Circuit Model. Antenna Matching. Antenna Bandwidth

SECTION 1 LUMPED CIRCUIT MODEL OF AN ANTENNA. ANTENNA INPUT IMPEDANCE

1.1. Antenna Circuit Model. Antenna Loss	1
1.2. Maximum Power Transfer to (and from) Antenna	3
1.3. Antenna Efficiency	7
1.4. Antenna Input Impedance and Impedance Matching	8
1.5. Point of Interest: Input Impedance of a Dipole Antenna and Its Dependence on Dipole Length	10
1.6. Beyond the First Resonance	13
1.7. Numerical Modeling	13
References	15
Problems	16

1.1 ANTENNA CIRCUIT MODEL. ANTENNA LOSS

The generic transmitter (TX) circuit with an antenna is shown in Figure 1.1. The generator (g) is modeled as an ideal (sinusoidal or pulse) voltage source V_g in series

Antenna and EM Modeling with MATLAB® Antenna Toolbox, Second Edition. Sergey N. Makarov, Vishwanath Iyer, Shashank Kulkarni, and Steven R. Best.

© 2021 John Wiley & Sons, Inc. Published 2021 by John Wiley & Sons, Inc.

Companion website: www.wiley.com/go/Makarov/AntennaandEMModelingwithMATLAB2e

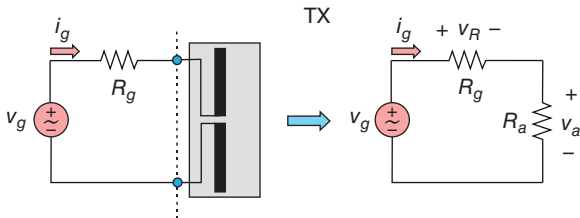


Figure 1.1 A generator (its Thévenin equivalent) connected to an antenna.

with the generator resistance R_g , connected to a TX antenna. The typical generator resistance is 50Ω . This model is known as Thévenin equivalent of the generator circuit. The Norton equivalent may also be used when necessary.

The portion depicted in the shaded box is an antenna. The antenna in Figure 1.1 is assumed to be *resonant*, which means that its equivalent impedance, Z_a , is purely real, i.e.

$$Z_a = R_a + jX_a = R_a, \quad X_a = 0. \quad (1.1)$$

In other words, the resonant antenna is simply modeled by a resistor R_a . The antenna resistance R_a includes two parts:

1. *Radiation resistance* of the antenna R_r that describes the circuit power loss due to *radiation* by the antenna into free space.
2. *Loss resistance* of the antenna R_L that describes the circuit power loss in the antenna itself. Case in point: a long thin wire with a significant ohmic resistance or a helical antenna with a ferrite lossy core.

One thus has

$$R_a = R_r + R_L > R_r. \quad (1.2)$$

Parasitic antenna resistance R_L has the following features:

- (a) it is zero for ideal antennas (a metal antenna made of perfect electric conductors);
- (b) it is usually relatively small for metal antennas covering the band 0.3–3 GHz (UHF, L-band, S-band) where it may be often ignored;
- (c) it may be very significant for printed antennas on lossy dielectric substrates and in the vicinity of lossy dielectric (such as FR4, ABS, human body, etc.);
- (d) it is vital for very small antennas whose size is much less than the wavelength.

Example 1.1

A small antenna operating at $f = 10$ MHz uses a thin copper wire with the diameter D of 0.25 mm and with the wire length l of 1 m. Calculate antenna loss resistance R_L .

Solution: The DC resistance of the wire is given by

$$R_{DC} = \frac{l}{A\sigma} \quad (1.3)$$

where σ is the material conductivity and A is the wire cross section. However, we cannot use this formula since most of the high-frequency current flows in a thin *skin layer* around the wire. The correct result has the form:

$$R_L = R_{HF} = \frac{l}{P} \sqrt{\frac{\omega\mu_0}{2\sigma}} = \frac{l}{\pi D} \sqrt{\frac{\omega\mu_0}{2\sigma}}, \quad \omega = 2\pi f, \quad (1.4)$$

where P is wire perimeter and μ_0 is vacuum permeability. A short MATLAB script given below accomplishes the task and gives R_L approximately equal to 1 Ω . This value may be comparable to the radiation resistance of a small antenna, and may even exceed it.

```
clear all;
mu      = 4*pi*1e-7; % Vacuum permeability, H/m
sigma   = 5.7e7; % Copper conductivity, S/m
D       = 0.25e-3; % Diameter, m
l       = 1; % Length, m
f       = 10e6; % Frequency, Hz
RHF = 1/(pi*D)*sqrt(mu*2*pi*f/(2*sigma)) % Loss resistance
```

1.2 MAXIMUM POWER TRANSFER TO (AND FROM) ANTENNA

One question you have to ask yourself is this: for a fixed resistance R_g , can the electric power delivered to the antenna be maximized, and at which value of R_a does the maximum occur? In other words, we would like to know what parameters the antenna should have in order to acquire and radiate *maximum* electric power from the *given* RF generator (an RF amplifier). In an electric circuit, the passive load – the antenna – may have only one such parameter – the antenna resistance.

All other antenna parameters (geometrical, material, etc.) are implicitly *included* into antenna's resistance.

The answer is given by the *maximum power transfer theorem* and found by solving the circuit in Figure 1.1. We assume that voltages and current are all functions of time and solve the circuit for *an arbitrary time moment*. First, the current is determined from the given voltage source $v_g(t)$ and the total resistance using the series equivalent,

$$i(t) = \frac{v_g(t)}{R_g + R_a}. \quad (1.5a)$$

This allows us to compute the (instantaneous) power delivered to the antenna based on

$$P_a(t) = R_a i(t)^2 = \frac{R_a v_g^2(t)}{(R_g + R_a)^2}. \quad (1.5b)$$

For a generator with fixed resistance R_g , the load resistance determines the power $P_a(t)$ at any time instant. Eq. (1.5b) is identical to the corresponding result at DC.

Example 1.2

Calculate and plot the average acquired antenna power when the generator with a periodic waveform $v_g(t) = v_g(t+T)$ is characterized by the *rms voltage* and generator resistance given by

$$V_{rms} = \sqrt{\frac{1}{T} \int_0^T v_g^2(t) dt} = 9 \text{ V} \text{ and } R_g = 50 \Omega \text{ in Figure 1.1.} \quad (1.5c)$$

Solution: We use Eq. (1.5b) and average it over period T to obtain *average power* $P_{avg} \equiv \overline{P_a(t)}$. The result has a form:

$$P_{avg} \equiv \overline{P_a(t)} \equiv \frac{1}{T} \int_0^T P_a(t) dt = \frac{R_a V_{rms}^2}{(R_g + R_a)^2}. \quad (1.5d)$$

Then, we plot the average antenna power as a function of the load resistance. The short MATLAB script given below accomplishes the task:

```
Rg = 50; % Generator resistance, Ohm
Vg = 9; % Generator rms voltage, V
RA = [0.01*Rg:0.01*Rg:10*Rg]; % Load resistance
PA = RA.*Vg.^2./(Rg + RA).^2; % Average antenna power
plot(RA, PA); grid on; title('Average antenna power, W')
xlabel('Load resistance, Ohm')
```

This important result is given in Figure 1.2. We see that the load power does have a maximum at a particular value of the load resistance. Our next step will be to find this maximum.

It is instructive to find the maximum of the average antenna power analytically since it gives us insight into the optimization process. We treat P_{avg} in Eq. (1.5d) as a function of R_a , i.e. $P_{avg} = P_{avg}(R_a)$. From basic calculus it is known that a function has a maximum where its first derivative is zero. Consequently, differentiating P_{avg} with respect to R_a gives

$$\frac{dP_{avg}}{dR_a} = V_{rms}^2 \left[\frac{1}{(R_g + R_a)^2} - 2 \frac{R_a}{(R_g + R_a)^3} \right] = V_{rms}^2 \left[\frac{R_g - R_a}{(R_g + R_a)^3} \right] = 0. \quad (1.6)$$

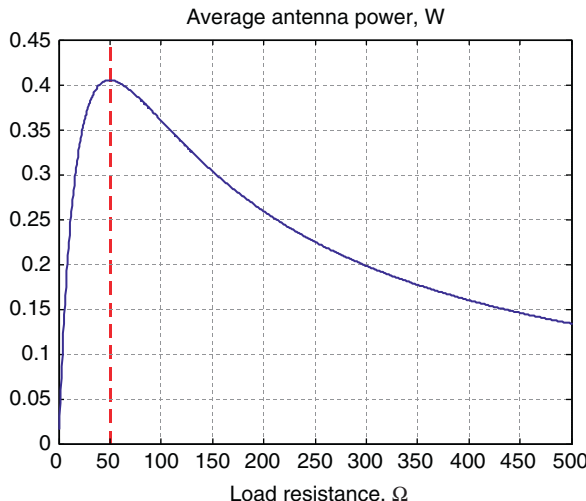


Figure 1.2 Average antenna power as a function of the antenna resistance for fixed $V_{rms} = 9$ V, $R_g = 50$ Ω .

The necessary and sufficient condition for Eq. (1.6) to hold, and thus maximizing the antenna power, is simply

$$R_a = R_g. \quad (1.7)$$

This result has a great practical value despite, or maybe thanks to, its simplicity. The maximum output radiated power is achieved when the antenna resistance is exactly equal to the internal resistance of the generator. In other words, the antenna is *matched* to the generator; it is called the *matched antenna*. The design of such an antenna over a frequency band of interest is called *antenna matching*. Such a design is a critical step, and it may be a great challenge for an RF engineer. It does not matter if the antenna radiates a sinusoidal or other periodic signal or a pulse; Eq. (1.7) holds in either case since it also maximizes power at *any* time instant.

However, it must be clearly stated that no more than 50% of the *total* generator power can be extracted even in this best case. This statement makes sense if we again examine the circuit in Figure 1.1 with two equal resistors. We see that the power delivered to each resistor is obviously the same. Since R_g is internal resistance, half of the total power is spent to heat up the generator.

Note: The power maximum in Figure 1.2 is relatively flat over the domain $R_a > R_g$; however, the power drops sharply when $R_a < R_g$. This last condition should be avoided if at all possible. The corresponding example is given below.

Example 1.3

A transmitting antenna in a radio handset features a monopole antenna. It is connected to a sine wave generator that has the same basic form as Figure 1.1 with an internal (generator) resistance of 50Ω . The antenna has the radiation resistance of 50Ω (which generates power loss in terms of electromagnetic radiation); its loss resistance is zero. The antenna, when properly matched to the power source, will radiate 50% of the total power. Now, a young RF engineer decides to “modify” the handset by cutting the monopole antenna and leaving only one-third of its length, so that the antenna’s radiation resistance is reduced to one-ninth of its original value. How does this affect the radiated signal?

Solution: For a periodic AC signal the average antenna power is given by Eq. (1.5d), that is

$$P_{avg} = \frac{R_a V_{rms}^2}{(R_g + R_a)^2} \quad (1.8)$$

The ratio of the two power levels for the two antenna configurations does not depend on generator voltage, i.e.

$$\frac{P_{a-\text{short}}}{P_{a-\text{original}}} = \frac{\frac{50/9}{(50+50/9)^2}}{\frac{50}{(50+50)^2}} = \frac{0.0018}{0.0050} = 0.36. \quad (1.9)$$

Thus, for the shorter antenna we will only achieve about 36% of radiated power compared to the original handset. In practice, this estimate becomes even much worse due to the appearance of a very significant antenna reactance as explained in the following text.

1.3 ANTENNA EFFICIENCY

After the antenna has been matched to the generator, the legitimate question to ask is how to find the antenna efficiency, E . Since $R_a = R_r + R_L > R_r$, only a part of the power delivered to the antenna is really radiated; another part is dissipated in the antenna itself and makes it a heater.

The corresponding equivalent circuit of the antenna with losses includes two resistors in series: the radiation resistance R_a and the loss resistance R_L . Since the same current $i(t)$ flows through both resistors at any time instant, we can find the *radiation efficiency* or simply the efficiency of the antenna in the form of the ratio of two powers: the *radiated power* and the *total power delivered to the antenna*. Those powers can either be given in terms of average values or by their instantaneous values. For example, at any time instant

$$E = \frac{P_{\text{radiated}}}{P_a} = \frac{R_r i(t)^2}{(R_r + R_L) i(t)^2} = \frac{R_r}{(R_r + R_L)} = \frac{1}{1 + R_L/R_r}. \quad (1.10)$$

In other words, the efficiency is a sole function of the ratio of two resistances. When the loss resistance is zero, the efficiency percentage is 100%; when the loss resistance is equal to the radiation resistance, the efficiency percentage is 50%. The efficiency definition Eq. (1.10) holds for any antenna, whether resonant or not.

Example 1.4

For a half-wave long patch antenna on a lossy dielectric substrate, the ratio of two resistances, R_L/R_r , is approximately given by [1]

$$R_L/R_r = \frac{3}{32} \sqrt{\epsilon_r} \frac{\lambda_0^2 \tan \delta}{hW}, \quad (1.11)$$

where h is the patch antenna thickness, W is the patch antenna width, $\lambda_0 = c_0/f$ is the *wavelength* in free space at frequency f in Hz, ϵ_r is the relative dielectric constant of the substrate, and $\tan \delta$ is the loss tangent of the substrate. Determine the antenna efficiency if $f = 930$ MHz, $W = 7$ cm, and the substrate is a low-cost 62 mil FR4 with $\epsilon_r=4.2$ and $\tan\delta=0.02$.

Solution: A simple MATLAB script given below programs Eq. (1.11) and outputs $R_L/R_r = 3.62$ and $E = 0.22$ or 22%. This result is remarkably discouraging; it says that 78% of power supplied to the matched antenna is lost in the antenna substrate itself whereas only 22% of the supplied power is really radiated! Better dielectric substrates with lower loss (and typically of higher cost) must be used at higher frequencies in order to reduce power loss to an acceptable level.

```
clear all;
epsilon = 8.85418782e-012;      % Diel. perm. vacuum, F/m
mu      = 1.25663706e-006;     % Magn. perm. vacuum, H/m
c       = 1/sqrt(epsilon*mu);   % Speed of light vacuum, m/s
h       = 62/1000*2.54e-2;      % Patch antenna thickness, m
W       = 0.07;                 % Patch antenna width, m
eps_r   = 4.2;                 % Rel. diel. constant, FR4
tand    = 0.02;                 % Loss tangent, FR4
f       = 930e6;                % Frequency, Hz
lambda0 = c/f;                % Wavelength in vacuum
Ratio   = 3/32*sqrt(eps_r)*lambda0^2*tand/(h*W)

E       = 1/(1 + Ratio)
```

1.4 ANTENNA INPUT IMPEDANCE AND IMPEDANCE MATCHING

Strictly speaking, practical antennae can be made resonant at only one single frequency, or at a discrete number of them. Unfortunately, no antennas of finite extent exist that are matched at all frequencies.

Consider now a harmonic generator with phasor voltage V_g . In frequency domain (in terms of phasors), the generic equivalent TX circuit looks like that shown in Figure 1.3 where Z_a is the complex *antenna impedance*, which depends on the antenna frequency. Z_a is also called the *input impedance* to the antenna. The complex impedance is the most important antenna circuit characteristic, the “business card” of the antenna. The generator circuit sees only the antenna impedance; the antenna radiation is not involved. The antenna impedance becomes real at certain frequencies when antenna resonates. Indeed, the equivalent circuit in Figure 1.3 is now restricted to harmonic (sinusoidal) RF excitation and is written in terms of phasor voltages and phasor current.

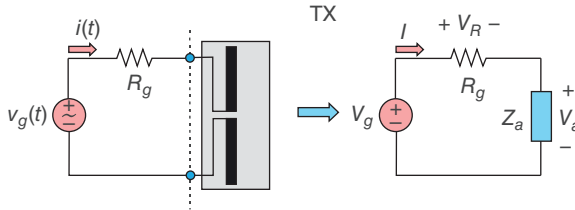


Figure 1.3 A generator (its Thévenin equivalent) connected to an antenna – the equivalent circuit in frequency domain (in the phasor form) for harmonic excitation.

We now write the input antenna impedance for an arbitrary antenna both in rectangular and in the polar form:

$$\mathbf{Z}_a = R_a + iX_a \text{ } [\Omega], \mathbf{Z}_a = |\mathbf{Z}_a| \angle \theta \text{ } [\Omega], R_a = |\mathbf{Z}_a| \cos \theta, X_a = |\mathbf{Z}_a| \sin \theta, \quad (1.12a)$$

$$|\mathbf{Z}_a| = \sqrt{R_a^2 + X_a^2} \text{ } [\Omega], \theta = \arctan \left(\frac{X_a}{R_a} \right), \quad (1.12b)$$

respectively. The real part of the impedance, R_a , is the *antenna resistance* introduced in the previous text; the imaginary part, X_a , is the *antenna reactance*. The antenna reactance may change its behavior from inductive ($X_a > 0$) to capacitive ($X_a < 0$) and vice versa when passing through the resonance.

The angle θ in Eq. (1.12a) and (1.12b) is equivalent to the *power angle* of a load in power electronics. The problem of antenna impedance matching is essentially equivalent to the problem of power factor correction in power electronics, with the same implications; although different means are used in both those cases. Of primary interest to us is the average power delivered to the antenna. In terms of phasors, this power may be written using several equivalent forms:

$$P_{avg} = \frac{\operatorname{Re}(\mathbf{V}_a \cdot \mathbf{I}^*)}{2} = \frac{\operatorname{Re}(\mathbf{Z}_a \cdot \mathbf{I} \cdot \mathbf{I}^*)}{2} = \frac{R_a |\mathbf{I}|^2}{2} = \frac{|\mathbf{Z}_a| |\mathbf{I}|^2}{2} \cos \theta = \frac{|\mathbf{V}_a| |\mathbf{I}|}{2} \cos \theta \text{ [W].} \quad (1.13a)$$

The circuit phasor current in Figure 1.3 is given by

$$\mathbf{I} = \frac{\mathbf{V}_g}{\mathbf{Z}_a + R_g} \text{ [A]} \quad (1.13b)$$

so that the average power delivered to the antenna becomes, according to Eq. (1.13a),

$$P_{avg} = \frac{R_a |\mathbf{I}|^2}{2} = \frac{R_a |\mathbf{V}_g|^2}{2 |\mathbf{Z}_a + R_g|^2} = \frac{1}{2} \frac{R_a |\mathbf{V}_g|^2}{(R_a + R_g)^2 + (X_a)^2} \text{ [W].} \quad (1.13c)$$

Similar to Eq. (1.6), it can be shown that its maximum value corresponds to the *ideal match*, i.e. to $X_a = 0$, $R_a = R_g$, that is

$$P_{avg} \Big|_{\text{max available}} = \frac{1}{8} \frac{|V_g|^2}{R_a} [\text{W}]. \quad (1.13d)$$

Thus, in order to design an efficient antenna, we must *match* the antenna impedance to the generator impedance, which has a typical value of 50Ω . For every antenna type, the matching is usually achieved by changing antenna dimensions and feed geometry.

1.5 POINT OF INTEREST: INPUT IMPEDANCE OF A DIPOLE ANTENNA AND ITS DEPENDENCE ON DIPOLE LENGTH

In order to become familiar with the problem of antenna matching, we now need a practical antenna example and a practical antenna impedance behavior. This example will also help us to define the *antenna impedance bandwidth* in future. To do so, we consider a cylindrical metal dipole antenna shown in Figure 1.4.

The antenna includes two dipole wings fed by a generator. In Figure 1.4, l_A is the total dipole length, a is the dipole radius.

During the last 70 or so years, a lot of efforts have been made to develop a good analytical terminal dipole model. As a result, one can use the following proven semi-analytical expression for the input dipole impedance [2]:

$$\begin{aligned} Z_a &= R_a(z) - j \left[120 \left(\ln \frac{l_A}{2a} - 1 \right) \cot z - X_a(z) \right] \\ R_a(z) &\approx -0.4787 + 7.3246z + 0.3963z^2 + 15.6131z^3 \\ X_a(z) &\approx -0.4456 + 17.0082z - 8.6793z^2 + 9.6031z^3. \end{aligned} \quad (1.14)$$

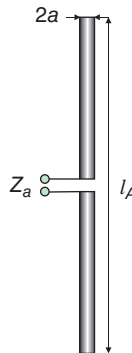


Figure 1.4 Dipole antenna for the evaluation of the reflection coefficient.

In Eq. (1.14), l_A is the total dipole length, a is the dipole radius, $z = kl_A/2$, and $k = \frac{2\pi}{\lambda}$, $\lambda = c_0/f$ is the *wavenumber* with c_0 being the speed of light in vacuum.

If a strip or blade dipole of width t is considered, then $a_{eq} = t/4$ [3] (providing the same equivalent capacitance of a dipole wing per unit length). We note here that a is the radius of a cylindrical dipole, while a_{eq} is the equivalent radius of a wire approximation to the strip dipole. Eq. (1.14) holds for relatively short nonresonant dipoles and for half-wave dipoles, i.e. in the frequency domain approximately given by

$$0.05 \leq f_C/f_{res} \leq 1.2, \quad (1.15)$$

where $f_{res} \equiv c_0/(2l_A)$ is the resonant frequency of an idealized dipole having exactly a *half-wave resonance* (c_0 is again the speed of light) and f_C is the center frequency of the band. This means that the ideal dipole resonates when its length is the half wavelength. When a monopole over an infinite ground plane is studied, the impedance in Eq. (1.14) halves.

Example 1.5

Plot to scale the input impedance for a dipole antenna with $l_A = 15$ cm, $a = 2$ mm and over the band 200–1200 MHz using Eq. (1.14) and MATLAB.

Solution: First, we find the resonant frequency of an idealized dipole, which is $f_{res} = c_0/(2l_A) = 3 \times 10^8/0.3 = 1$ GHz. A simple MATLAB script given below uses Eq. (1.14) and outputs the plot shown in Figure 1.5 for the dipole impedance. One can see that the true resonance occurs at a bit lower frequency of 928 MHz; the resonant radiation resistance appears to be 60Ω . According to Figure 1.2, this is still a very good match, which is close to the maximum radiated antenna power.

```

f = linspace(200e6, 1200e6, 1000); % Frequency, Hz
lA = 0.15; % Dipole total length, m
a = 0.002; % Dipole radius, m
Za = dipoleAnalytical(f, lA, a); % Find resonant frequency
Ra = real(Za); Xa = imag(Za); % Find resistance and reactance
[dummy, index] = min(abs(Xa)); % Find resonant frequency
fresMHz = f(index)/1e6
hold on; grid on;
plot(f/1e6, Ra, 'b', 'LineWidth', 2);
plot(f/1e6, Xa, 'r', 'LineWidth', 2);
xlabel('frequency, MHz'); ylabel('Impedance, \Omega');

```

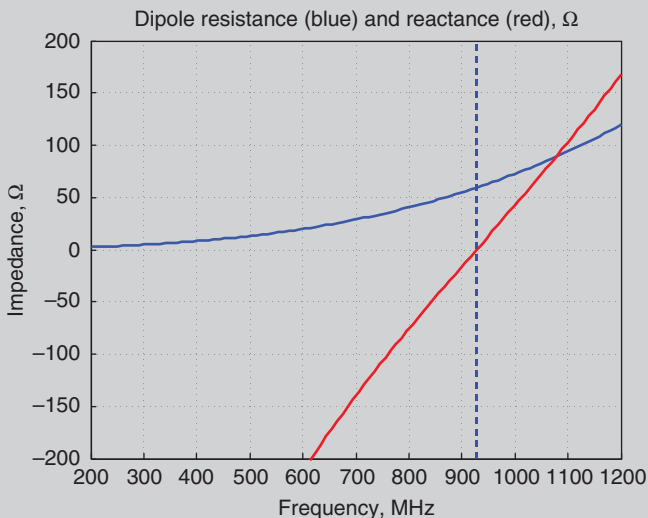


Figure 1.5 Dipole antenna impedance in the vicinity of its first (series) resonance. The dashed line shows the resonant frequency.

```

axis([min(f)/1e6 max(f)/1e6 -200 200]);
title('Dipole resistance(blue) and reactance(red), \Omega');
line([fresMHz fresMHz], [-200 200]);

```

The MATLAB script above uses function `dipoleAnalytical` that corresponds to Eq. (1.14):

```

function [Za] = dipoleAnalytical(f, lA, a); % EM data
    epsilon = 8.85418782e-012; % Vacuum, F/m
    mu = 1.25663706e-006; % Vacuum, H/m
    c = 1/sqrt(epsilon*mu); % Vacuum, m/s
    eta = sqrt(mu/epsilon); % Vacuum, Ohm
    l = lA/2; % Dipole half length
    k = 2*pi*f/c; % Wavenumber
    z = k*l; % Electrical length corresponding to l

    R = -0.4787 + 7.3246*z + 0.3963*z.^2 + 15.6131*z.^3;
    X = -0.4456 + 17.0082*z - 8.6793*z.^2 + 9.6031*z.^3;
    Za = R - j*( 120*(log(l/a)-1)*cot(z)-X );
    % Antenna impedance
end

```

Note: We will show later in the text that all metal antennas could be scaled in size so that a dipole with the size twice as small as the original one has the resonant frequency that is two times larger than the original resonant frequency. Similarly, a dipole with the size twice as large as the original one has the resonant frequency that is two times less. In other words, small antennas have high resonant frequencies and vice versa.

The scaling property of the antenna implies measuring its length l_A in terms of a dimensionless quantity called *electrical length*. The electrical length is simply the product of l_A and the *wavenumber* $k = 2\pi/\lambda$. The electrical length of the antenna does not depend on its operation frequency. A dipole antenna resonating at 100 MHz or at 5 GHz has the same electrical length.

1.6 BEYOND THE FIRST RESONANCE

The dipole antenna discussed thus far is a classic example of a narrow-band antenna that has its first resonance as a series resonance. In general, a resonance is characterized by a zero reactance, $X_a = 0$. However, the resistance value can vary dramatically depending on the type of resonance, i.e. series or parallel. Parallel resonances typically achieve large resistances. In the case of the dipole, the series resonances occur at odd multiples of f_{res} . In general, the dipole is not used at higher multiples of the fundamental resonance. The half-wavelength current distribution is no longer valid at these frequencies and therefore the radiation pattern of the antenna is also distorted.

1.7 NUMERICAL MODELING

Although impedances of many basic antenna types and geometries (dipoles, loops, patch antennas) are well documented (in particular, in *Antenna Engineering Handbook*, John L. Volakis, Ed., McGraw Hill, 2018, fifth edition), any particular antenna design heavily relies upon numerical electromagnetic modeling.

Let us compare the theoretical model for the dipole antenna impedance with a numerical model. The theoretical model is based on a cylindrical dipole (1.14). The modeling software used in this text is the Method of Moments software of the MATLAB® Antenna Toolbox™. This software has a library of antenna models that are parameterized to enable easy geometry setup and analysis. One such model is the dipole.

This model of the dipole in MATLAB will use the strip or blade approximation of the cylindrical dipole as discussed in [3]. We consider the same dipole as in Example 1.5, with the total length of 15 cm, and with the radius of 2 mm, and then

compare its theoretical impedance model given by Eq. (1.14) with numerical simulations, in the band from 200 to 1200 MHz. As discussed above, the equivalent radius of the strip dipole of width t is $a_{\text{eq}} = t/4$.

Example 1.6

Using MATLAB Antenna Toolbox, compare theory and numerical simulations for the strip dipole antenna with $l_A = 15$ cm, $t = 8$ mm over the band 200–1200 MHz. The theory model uses Eq. (1.14).

Solution: A simple MATLAB script given below initializes the dipole antenna, plots the antenna geometry, and computes the dipole input impedance over the frequency band of interest at the default computational mesh resolution. Figure 1.6 shows the resulting dipole geometry and the impedance comparison. The agreement between two solutions is good in the middle of the band, but it becomes worse at higher frequencies and at very low frequencies. There, the numerical solution generally becomes more accurate.

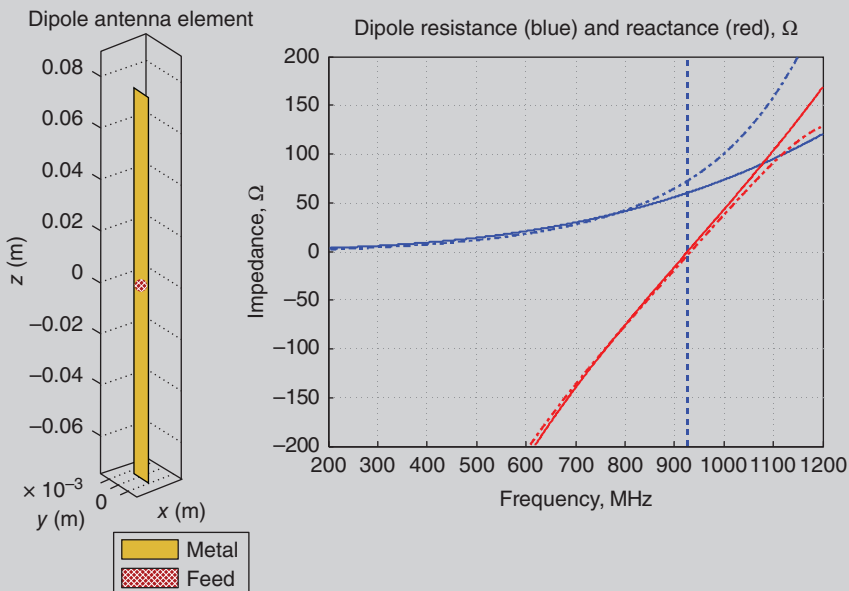


Figure 1.6 Dipole antenna impedance in the vicinity of its first (series) resonance. The dashed line shows the resonant frequency. The solid curves show the analytical antenna impedance. The dash-dot curves show the simulated antenna impedance.

```

%% Setup analysis parameters
f = linspace(200e6, 1200e6, 1000); % Frequency in Hz
lA = 0.15; % Dipole total length, m
a = 0.002; % Dipole radius, m
%% Antenna toolbox model and analysis
w = cylinder2strip(a); % Eq. strip width model
d = dipole('Length',lA,'Width',w); % Strip dipole model
figure; show(d) % Visualize geometry
Z = impedance(d, f); % Full-wave MoM solution
R = real(Z); % Resistance
X = imag(Z); % Reactance

```

Emphasize that the numerical solution uses an infinitesimally thin feed gap for the dipole antenna. An extension to a gap of finite thickness is possible.

We have already mentioned that, if a strip or blade dipole of width t is considered, then a twice as narrow cylindrical dipole provides the same equivalent capacitance of a dipole wing per unit length [3]. For example, the blade dipole of 8 mm in width and the cylindrical dipole of 4 mm in diameter should perform quite similarly.

The results from our numerical experiment suggest that the existing theory model is a good approximation for dipoles around the first resonance. Eq. (1.14) indeed quickly loses its validity above the first antenna resonance. The numerical model is also not perfect, but it is perhaps more reliable. We emphasize that the dipole theory model is still extremely useful in the estimation of the antenna path loss where its accuracy is quite sufficient; this question will be considered in the following text.

REFERENCES

1. D. R. Jackson, “Microstrip Antennas,” In *Antenna Engineering Handbook*, J. L. Volakis, Ed., McGraw Hill, New York, 2018, fifth edition.
2. C. -T. Tai and S. A. Long, “Dipoles and Monopoles,” In *Antenna Engineering Handbook*, J. L. Volakis, Ed., McGraw Hill, New York, 2007, fourth edition.
3. C. A. Balanis, *Antenna Theory: Analysis and Design*, Wiley, New York, 2016, fourth edition.

PROBLEMS

1. A small AM radio antenna operating at 1 MHz uses a thin copper wire with the diameter D of 0.2 mm and with the total wire length of 3 m.
 - (A) Calculate parasitic antenna's resistance (loss resistance) R_L .
 - (B) What is the antenna efficiency percentage if the radiation resistance is 1Ω ?
2. In Example 1.4, we replace the 62 mil FR4 substrate by a Rogers substrate material RO4003 with the same thickness and with $\epsilon_r=3.55$ and $\tan\delta=0.0027$. Is the efficiency of the patch antenna improved? What is the new efficiency value?
3. The generator's voltage source creates a sine wave with the amplitude of 10 V. The generator resistance is $R_g = 50 \Omega$. The antenna impedance at a frequency of interest measures
 - (A) $Z_a = 50 \Omega + j0 \Omega$;
 - (B) $Z_a = 75 \Omega + j0 \Omega$;
 - (C) $Z_a = 25 \Omega + j0 \Omega$;
 - (D) $Z_a = 50 \Omega + j50 \Omega$;
 - (E) $Z_a = 50 \Omega - j50 \Omega$;
 - (F) $Z_a = 50 \Omega + j100 \Omega$.

In every case, determine

- (I) Average power delivered to the antenna (show units).
- (II) Average power radiated by the antenna assuming loss resistance of 10Ω in every case.
4. The following antenna impedances are tested:
 - (A) $Z_a = 75 \Omega + j10 \Omega$;
 - (B) $Z_a = 25 \Omega + j0 \Omega$;
 - (C) $Z_a = 50 \Omega + j25 \Omega$.

Which antenna is best matched to the generator resistance of 50Ω (is characterized by the highest accepted power)?
- 5*. Approximately determine the resonant frequency of a strip dipole with the total length of 100 mm and the width of 2 mm. Prove your answer using MATLAB Antenna Toolbox and find the error. Present the text of the corresponding MATLAB script.
- 6*. Generate Figure 1.6 in MATLAB. Present the text of the corresponding MATLAB script.
- 7*. (A) Draw the equivalent circuit for a generic transmitting antenna in frequency domain including the generator and the antenna. Label all circuit parameters.

- (B) How do we define the “resonant” antenna condition?
 - (C) Create a strip dipole in MATLAB Antenna Toolbox with the length of 30 cm and the width of 2 mm. Use the *impedance* function over the frequency band 300–600 MHz and identify the frequency at which the antenna is resonant.
 - (D) What is the antenna radiation resistance at the resonance (assuming the lossless antenna)?
 - (E) Attach your MATLAB script to the homework report.
- 8*.** (A) Does the resonant frequency of a strip dipole increase or decrease with increasing its width? Prove your answer using MATLAB Antenna Toolbox.
- (B) Does the resonant frequency of a cylindrical dipole increase or decrease with increasing its radius? Justify your answer.
- 9*.** Use the dipole modeled in problem 7 C and analyze the impedance over the frequency band 300 MHz–1.5 GHz. Find all the series resonances in the impedance plot and annotate them. Report your results on the relationship between the resonant frequencies relative to the first resonance.
- 10*.** In MATLAB Antenna Toolbox, the amplitude of the port excitation voltage of the strip dipole antenna changes from 1 to 2 V. How will the antenna impedance change?

SECTION 2 ANTENNA WITH TRANSMISSION LINE. ANTENNA REFLECTION COEFFICIENT. ANTENNA MATCHING. VSWR

1.8.	Antenna Reflection Coefficient for a Lumped Circuit	18
1.9.	Antenna Reflection Coefficient with a Feeding Transmission Line	20
1.10.	Antenna Impedance Transformation. Antenna Match Via Transmission Line	22
1.11.	Reflection Coefficient Expressed in Decibels and Antenna Bandwidth	23
1.12.	VSWR of the Antenna	26
	References	28
	Problems	29

1.8 ANTENNA REFLECTION COEFFICIENT FOR A LUMPED CIRCUIT

If an antenna is connected to the generator via a short cable with the length being small compared to the wavelength, the lumped circuit in Figure 1.3 is entirely sufficient for antenna modeling. In practice, however, the antenna is usually connected via a longer cable. The cable connections are also common in *antenna arrays*; they are used to construct the *beamforming networks*.

Voltage and currents on long cables (transmission lines) are in fact electromagnetic waves, which may propagate back and forth between the antenna and the generator. A method of *scattering parameters* or *S-parameters* is useful in this case. S-parameters describe the complete behavior of a high-frequency *distributed linear circuit*. The term “scattering parameters” comes from the “Scattering Matrix” described in a 1965 IEEE article by K. Kurokawa entitled “Power Waves and the Scattering Matrix.” Today, S-parameter results are displayed on the *vector network analyzer* display screen with the simple push of the button.

We will consider the lumped circuit in Figure 1.3 first, with a real generator impedance, R_g , and an arbitrary antenna impedance, Z_a . The ratio of the available power delivered to the antenna (1.13c) to the maximum available power (1.13d) for the ideal match gives us an important parameter, the *normalized power delivered to the antenna*:

$$\frac{P_{avg}}{P_{avg}|_{\text{max available}}} = \frac{4R_aR_g}{|Z_a + R_g|^2} . \quad (1.16)$$

This result is nicely expressed in terms of the *complex reflection coefficient* (or *voltage reflection coefficient*), Γ , which is given by a combination of generator and antenna impedances [1]:

$$\frac{P_{avg}}{P_{avg}|_{\text{max available}}} = 1 - |\Gamma|^2, \quad \Gamma = \frac{Z_a - R_g}{Z_a + R_g}. \quad (1.17)$$

The corresponding proof task is cast as a homework problem at the end of this chapter. Emphasize that, if the antenna is connected to a microstrip transmission line or a cable, then R_g is replaced by the characteristic impedance of the transmission line, Z_0 , i.e. $R_g \rightarrow Z_0$.

In the general case of generator(s) and load(s) connected by cables/transmission lines, whose length is comparable to the wavelength, the reflection coefficient is formed by two *voltage or power waves* [1]. The *incident wave* V^+ propagates along a cable (the transmission line) from the generator depicted in Figure 1.3-left toward the antenna load. The *reflected wave* V^- propagates along the same cable but in the opposite direction, i.e. from the antenna to the generator. The complete voltage solution is the sum of both. The *complex reflection coefficient* of the antenna with a cable is defined as the ratio of two complex voltage values at the generator,

$$\Gamma \equiv \frac{V^-}{V^+}. \quad (1.18)$$

If there is no reflected wave, the reflection coefficient is exactly zero and there is an ideal match in Eq. (1.17). The transmitted wave is completely acquired by the antenna and is then radiated into the surrounding space.

The meaning of transmitted and reflected power waves is extremely useful in measurements (the vector network analyzer) and specifically for modeling networks with transmission lines (cables) of a significant length where the electromagnetic waves can propagate in a nontrivial way (change the phase or decay).

The size of the lumped circuit in Figure 1.3 was assumed to be *negligibly small* compared to the wavelength. In this case, both contributions $V^+ = V_0^+$ and $V^- = V_0^-$ may be deduced from the standard circuit analysis of lumped circuits (we use index 0 to distinguish this particular case). In that case, the meaning of the reflection coefficient is reduced to the standard circuit analysis; it simply reflects generator resistance and antenna impedance mismatch studied previously.

Example 1.7

Find V_0^+ and V_0^- for the lumped TX circuit shown in Figure 1.3-right.

Solution: The “incident voltage wave” is the antenna voltage for the ideal match,

$$V_0^+ = \frac{1}{2}V_g. \quad (1.19)$$

The “reflected voltage wave” is simply the actual antenna voltage minus the voltage for the ideal match, that is

$$V_0^- = \frac{Z_a}{Z_a + R_g} V_g - \frac{1}{2} V_g = \frac{1}{2} \frac{Z_a - R_g}{Z_a + R_g} V_g. \quad (1.20)$$

Their ratio is given by

$$\Gamma_0 = \frac{V_0^-}{V_0^+} = \frac{Z_a - R_g}{Z_a + R_g}, \quad (1.21)$$

which is exactly Eq. (1.17). The *reference plane* (at either generator or the antenna load) does not matter for the lumped circuit.

1.9 ANTENNA REFLECTION COEFFICIENT WITH A FEEDING TRANSMISSION LINE

Now, consider a generator connected to the antenna through a *lossless* transmission line (a coaxial cable, a printed microstrip, or a waveguide). The familiar lumped circuit in Figure 1.7a (and Figure 1.3) is transformed as shown in Figure 1.7b. In many practical situations, the transmission line is *precisely* matched to the generator; its *characteristic impedance* Z_0 is chosen to be *equal* to the generator resistance, that is

$$Z_0 = R_g. \quad (1.22)$$

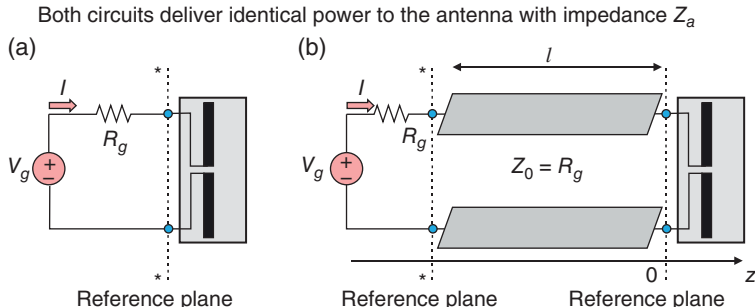


Figure 1.7 Equivalence of the TX circuits with and without the transmission line from the viewpoint of the *power* delivered to the antenna.

Our goal is to find the reflection coefficient of the combined system consisting of the antenna and the transmission line of length l in Figure 1.7b. The z -axis will be directed from the source to the antenna along the transmission line. To be consistent with the lumped-circuit approach from Example 1.7, we set the origin of the z -axis ($z = 0$) in the antenna reference plane in Figure 1.7b. Then, both the incident (traveling to the right) and the reflected (traveling to the left) waves in Figure 1.7b will have the following phasor form (time dependence is $\exp(j\omega t)$):

$$\mathbf{V}^+ = V_0^+ \exp(-jkz), \quad \mathbf{V}^- = V_0^- \exp(+jkz), \quad k = \frac{\omega}{c} \quad (1.23)$$

according to the familiar one-dimensional plane wave theory. Here, k is the real *wavenumber* of the lossless transmission line. It is equal to the angular frequency divided by the phase velocity (propagation speed), c , of the line. Voltage wave \mathbf{V}^+ propagates from left to right and corresponds to $\cos(\omega t - kz)$ in time domain while voltage wave \mathbf{V}^- propagates from right to left and corresponds to $\cos(\omega t + kz)$. Note that $k = \beta$ in Pozar's book [1].

According to Eq. (1.18) and (1.23), the reflection coefficient of the antenna with the transmission line in reference plane * in Figure 1.7b, i.e. at the generator where $z = -l$, has the form:

$$\Gamma^* \equiv \left. \frac{\mathbf{V}^-}{\mathbf{V}^+} \right|_{z=-l} = \frac{V_0^-}{V_0^+} \exp(-2jkl) = \Gamma_0 \exp(-2jkl), \quad (1.24)$$

where Γ_0 is given by Eq. (1.21) with $R_g = Z_0$. When transmission line length tends to zero, Eq. (1.24) is indeed reduced to Eq. (1.21). Eq. (1.24) is a simple yet powerful result; it will predict the average power delivered to the antenna with a cable or another transmission line.

Example 1.8 shows that the addition of the lossless transmission line perfectly matched at the generator does not change average power delivered to the antenna, irrespective of the value of its input impedance.

Example 1.8

Show that the addition of a lossless transmission line of any length, which is still perfectly matched at the generator, does not change average power delivered to the antenna of any input impedance. Only a phase of the reflection coefficient at the generator changes.

Solution: The solution is based on Eq. (1.24), which yields

$$|\Gamma^*| = |\Gamma_0 \exp(-2jkl)| = |\Gamma_0| |\exp(-2jkl)| = |\Gamma_0|. \quad (1.25)$$

Therefore, according to Eq. (1.17),

$$\frac{P_{avg}}{P_{avg}|_{\text{max available}}} = 1 - |\Gamma^*|^2 = 1 - |\Gamma_0|^2. \quad (1.26)$$

This example is perhaps overly optimistic. It needs two notes of caution.

First, if the transmission line is lossy, the factor $\exp(-2jkl)$ is becoming less than one (k is becoming complex) and the reflection coefficient decreases. An antenna connected by a very long lossy cable will be *perfectly matched* to the generator since $|\Gamma^*| \rightarrow 0$, but its radiated power will simply be zero. For example, a popular RG-58 50- Ω cable with the length of 10 m will accept 100 W from the generator but deliver only 33 W of power to the antenna. It is not a good practice to “match” the antennae by adding long lossy transmission lines.

Second, while one mismatch at the antenna still keeps the delivered power and $|\Gamma|$ unchanged, *two or more* arbitrary mismatches (the second mismatch is often at the generator) due to non-perfect cables, connectors, etc., may (or, sometimes, may not) lead to the “ripples” or visible oscillations of the measured $|\Gamma|$ as often seen on the network analyzer. This is because the factor $\exp(-2jkl)$ will appear not only multiplicatively, but also additively.

1.10 ANTENNA IMPEDANCE TRANSFORMATION. ANTENNA MATCH VIA TRANSMISSION LINE

Here, we use the well-known result for the antenna impedance transformation along a lossless transmission line of length l . In the plane labeled (*) in Figure 1.7b, the transformed antenna impedance (the equivalent impedance of the antenna with the transmission line) becomes [1]

$$\mathbf{Z}^* = \mathbf{Z}_0 \frac{\mathbf{Z}_a + j\mathbf{Z}_0 \tan(kl)}{\mathbf{Z}_0 + j\mathbf{Z}_a \tan(kl)}. \quad (1.27)$$

This result is obtained from impedance definition and by relating voltages and currents on the line via its characteristic impedance, \mathbf{Z}_0 .

We have shown in the previous section that adding the lossless transmission line perfectly matched at the generator does not change antenna power. Now, we are about to show that adding a transmission line mismatched *at both ends* does change antenna power. It may be quite beneficial for impedance matching.

Example 1.9

A quarter wave transmission line transformer is characterized by (from Eq. (1.27))

$$l = \frac{\lambda_{\text{line}}}{4} \Rightarrow kl = \frac{\pi}{2} \Rightarrow Z^* = \frac{Z_0^2}{Z_a} \quad (1.28)$$

An antenna with $Z_a = 200 \Omega$ is to be perfectly matched to the generator with $R_g = 50 \Omega$ by a proper choice of line characteristic impedance Z_0 .

Solution: The perfect match means that generator sees $Z^* = 50 \Omega$ in the reference plane. Then, from Eq. (1.28), one has

$$Z_0 = \sqrt{Z_a Z^*} = 100 \Omega. \quad (1.29)$$

It is not difficult to construct such a transmission line using, for example, a somewhat narrower microstrip as compared to the 50Ω microstrip line.

Emphasize that the quarter wave transformer is relatively narrowband; it cannot be used for antenna matching over a wide band. Also, some reflections and standing waves will occur along the quarter wave line.

1.11 REFLECTION COEFFICIENT EXPRESSED IN DECIBELS AND ANTENNA BANDWIDTH

It follows from the previous discussion that the major *dimensionless* parameter that characterizes antenna matching is the antenna reflection coefficient, Γ . To highlight the physical meaning of the reflection coefficient and its acceptable threshold, we rewrite Eq. (1.17) for the antenna power one more time:

$$\frac{P_{\text{avg}}}{P_{\text{avg}}|_{\text{max available}}} = 1 - |\Gamma|^2 \quad (1.30)$$

and let $|\Gamma|^2$ to have the value of 0.1. According to Eq. (1.30), this means that the power delivered to the antenna is exactly 90% of the maximum available antenna power. Simultaneously, the *reflection coefficient in dB* (or *power reflection coefficient*),

$$|\Gamma|_{\text{dB}} = 20 \log_{10} |\Gamma| = 10 \log_{10} |\Gamma|^2 \quad (1.31)$$

will attain the value of -10 dB . Since ideal antenna matching ($|\Gamma|=0$ or $|\Gamma|_{\text{dB}} = -\infty$) is never possible over the entire frequency band, it is a common agreement that, if

$$|\Gamma|_{\text{dB}} \leq -10 \text{dB} \quad (1.32)$$

uniformly over the band, then the antenna is said to be *matched over the band*. In other words, at least 90% of available power from the generator will be delivered to the antenna for any frequency within the band. When applied over a frequency band, Eq. (1.32) thus determines the *antenna impedance bandwidth* or simply the *antenna bandwidth*. Several such bands may be present for a *multiband antenna*.

The TX antenna may be treated as a one port (port 1) of *an electric linear network*, whereas the other ports (if present) are other antennas. An example is given by a transmit/receive antenna pair, which form a two-port linear network. In that and similar cases,

$$\Gamma = S_{11}, \quad (1.33)$$

where S_{11} is the *port 1 complex reflection coefficient* or the first diagonal term of a *multi-port scattering matrix* $\hat{S} = \{S_{ij}\}$ [1]. Similarly, Eq. (1.32) may be written in the form:

$$|S_{11}|_{\text{dB}} \leq -10 \text{dB}. \quad (1.34)$$

Note: Along with the reflection coefficient in dB, $|S_{11}|_{\text{dB}}$ is always nonpositive. The terminal condition $|S_{11}|_{\text{dB}} = 0$ dB corresponds to a complete reflection of the voltage generator signal from the antenna. Nothing is being radiated.

Note: Meanings of the complex reflection coefficient Γ itself and the dB measure of its magnitude, $20 \log_{10} |\Gamma|$, are often interchanged. For example, if an antenna datasheet reports “antenna reflection coefficient as a function of frequency,” it is $20 \log_{10} |\Gamma|$ that is being plotted (cf. Figure 1.8 as an example).

Example 1.10

Using MATLAB Antenna Toolbox, determine antenna impedance bandwidth for the blade dipole antenna with $l_A = 15$ cm, $w = 8$ mm.

Solution: The approximate resonant frequency of the half wave dipole with the length of 15 cm is about 1 GHz. We again choose the frequency band from 200 to 1200 MHz for testing. A simple MATLAB script given below initializes the dipole antenna, plots the antenna geometry, and computes the dipole reflection

coefficient $\Gamma = S_{11}$. Note that the computations are performed exactly following Eq. (1.17), i.e. without an extra cable. Figure 1.8 shows the resulting dipole geometry and the reflection coefficient comparison with the analytical result obtained from Eq. (1.14). The agreement between two solutions is good while the numerical solution is again expected to be somewhat more accurate for this particular geometry. Note that the exact reflection coefficient values below -10 dB *do not really matter*, they are very sensitive to small variations of the antenna impedance around 50Ω and are subject to noise.

```
%% Setup analysis parameters
f = linspace(200e6, 1200e6, 1000); % Frequency, Hz
lA = 0.15; % Dipole total length, m
a = 0.002; % Dipole radius, m
%% Antenna toolbox model and analysis
w = cylinder2strip(a); % Eq. strip width model
d = dipole('Length', lA, 'Width', w); % Strip dipole model
figure; show(d) % Visualize geometry
S11 = rfparam(sparameters(d, f, Rg), 1, 1); % Calculate s-parameters
S11dB = 20*log10(abs(S11));
```

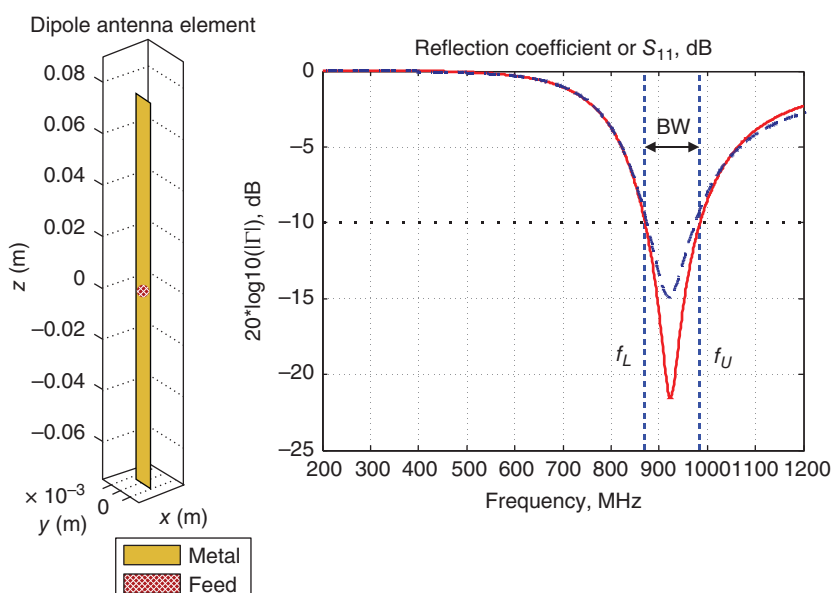


Figure 1.8 Magnitude of the reflection coefficient in dB for the dipole antenna and the antenna impedance bandwidth. Numerical solution is shown by a dashed curve.

In Figure 1.8, the antenna impedance bandwidth follows Eq. (1.32) or (1.34) with the minus 10 dB threshold. The threshold is shown by two dashed lines in Figure 1.8. The dipole antenna has the impedance bandwidth from the *lower frequency of the band*, $f_L = 870.7$ MHz, to the *upper frequency of the band*, $f_U = 985.8$ MHz (analytical solution is considered as an example). The *center frequency* of the band is given by

$$f_C = \frac{f_L + f_U}{2} = 928.25 \text{ MHz.} \quad (1.35)$$

The antenna *impedance bandwidth* BW (or fractional bandwidth) is determined in the form

$$BW = \frac{f_U - f_L}{f_C} \times 100\% \approx 12\%, \quad (1.36)$$

which is a very typical value for a wire dipole or a thin-blade dipole. Generally, we always want to increase the antenna bandwidth for a better throughput.

Note: Eq. (1.36) determines the bandwidth when it does not exceed 100%. For broadband antennas, the bandwidth is alternatively determined by the ratio of the upper-to-lower frequencies,

$$BW = f_U : f_L. \quad (1.37)$$

Both definitions may overlap. For example, if $f_U = 1\text{GHz}$, $f_L = 500\text{MHz}$, the antenna bandwidth according to Eq. (1.36) is 67% whereas the antenna bandwidth according to Eq. (1.37) is 2 : 1.

1.12 VSWR OF THE ANTENNA

Along with the reflection coefficient Γ or S_{11} , another measurable quantity of significant interest is the *voltage standing-wave ratio* or VSWR. On a transmission line connected to non-matched antenna, both waves – incident and reflected V^+ and V^- , respectively – form a prominent standing wave. At every point in space, this standing wave has a certain amplitude as a sinusoidal function of time. The VSWR is given by the ratio of maximum and minimum standing wave amplitudes on the line. It may be shown that [1–3]

$$VSWR = \frac{V_{max}}{V_{min}} = \frac{1 + |\Gamma|}{1 - |\Gamma|}. \quad (1.38a)$$

For the matched antenna, the VSWR is exactly one; for a non-matched antenna, it is always greater than one, and may even approach infinity for a short- or open-circuited antenna.

The VSWR may be used instead of the reflection coefficient to determine and plot the impedance bandwidth. In this case, the criterion of

$$|\Gamma|_{\text{dB}} \leq -10 \text{ dB} \quad (1.38\text{b})$$

corresponds to

$$\text{VSWR} \leq 2 \quad (1.38\text{c})$$

with a sufficient degree of accuracy.

Example 1.11

Plot the reflection coefficient in dB and VSWR for the dipole with $l_A = 15 \text{ cm}$, $a = 2 \text{ mm}$ over the band 200–1200 MHz using Eq. (1.14) and MATLAB, and determine the antenna impedance bandwidth.

Solution: We repeat the task of Example 1.5, but instead of the impedance plot, the reflection coefficient and the VSWR will be evaluated and plotted. Extra lines of the MATLAB code may be added such as

```
c = figure;
Rg = 50;
RC = (Za-Rg)./(Za+Rg);
temp = abs(RC);
VSWR = (1 + temp)./(1 - temp);
semilogy(f/1e6, VSWR, 'b', 'LineWidth', 2);
grid on; xlabel ('frequency, MHz'); ylabel ('VSWR, a.u.');
title('VSWR');
```

The result is shown in Figure 1.9. The same antenna impedance bandwidth is marked on every plot – for the reflection coefficient and for the VSWR, respectively. In fact, the $\text{VSWR} \leq 2$ bandwidth on the right plot is slightly greater than the $|\Gamma|_{\text{dB}} \leq -10 \text{ dB}$ bandwidth since, strictly speaking, the condition $\text{VSWR} = 2$ corresponds to $|\Gamma|_{\text{dB}} = -9.5 \text{ dB}$. This difference is usually ignored.

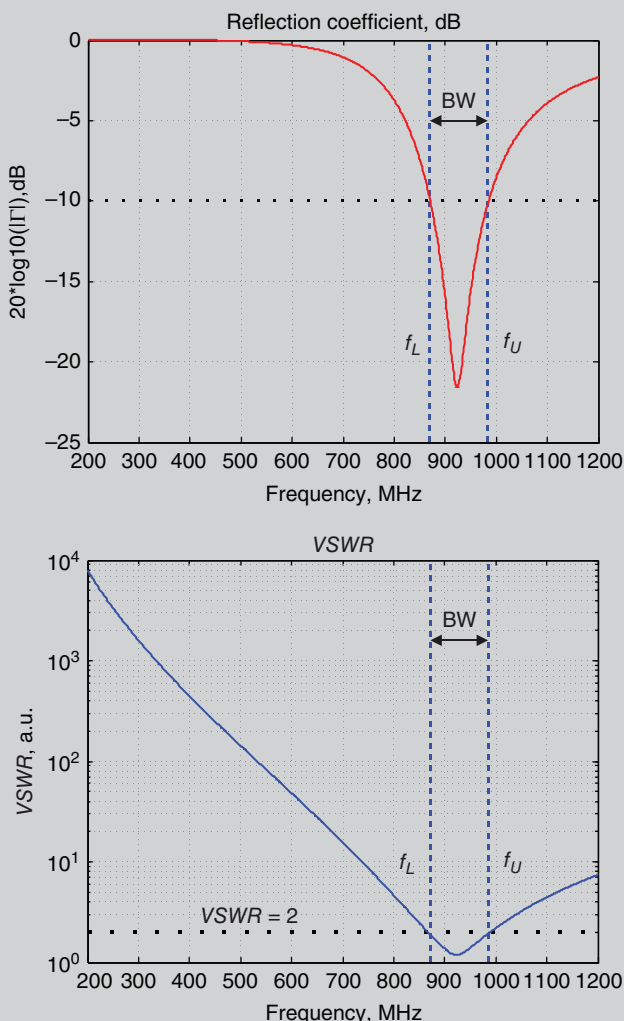


Figure 1.9 Reflection coefficient in dB (left) versus VSWR (right) for the same dipole antenna.

REFERENCES

1. D. M. Pozar, *Microwave Engineering*, Wiley, New York, 2011, fourth edition.
2. T. A. Milligan, *Modern Antenna Design*, Wiley, New York, 2005, second edition, pp. 17–18.
3. C. A. Balanis, *Antenna Theory: Analysis and Design*, Wiley, New York, 2016, fourth edition.

PROBLEMS

1. An antenna with
 - (A) $Z_a = 100 \Omega$
 - (B) $Z_a = 100 \Omega - j100 \Omega$
 - (C) $Z_a = 100 \Omega + j100 \Omega$

is directly connected to a generator with $R_g = 50 \Omega$. Determine the reflection coefficient Γ of the antenna, its magnitude, and normalized power delivered to the antenna in every case.
2. Repeat Problem 1 if
 - (A) a quarter wave transmission line with $Z_0 = 70.7 \Omega$ is added to the antenna;
 - (B) a full wave transmission line with $Z_0 = 70.7 \Omega$ is added to the antenna.
3. If an antenna is either an open or short circuit, what is its reflection coefficient, Γ ? Hint: The problem may be solved using the currents associated with the reflected and forward waves in Eq. (1.18), but introducing a minus sign to account for the opposite orientations of the two currents: $\Gamma = \frac{V^-}{V^+} = -\frac{I^-}{I^+}$.
4. Repeat Problem 3 if
 - (A) a quarter wave transmission line with $Z_0 = R_g$ is added to the antenna;
 - (B) a full wave transmission line with $Z_0 = R_g$ is added to the antenna.
5. The exact values of the antenna reflection coefficient Γ (computed vs. characteristic impedance of a 50Ω transmission line) are
 - (A) 0.1;
 - (B) 0.316;
 - (C) -0.5.
 1. Determine the reflection coefficient values in dB.
 2. Determine antenna impedance.
6. Calculate and plot to scale the phase of the reflection coefficient in Example 1.10.
7. In Example 1.10, a coaxial transmission cable RG-58 with $Z_0 = R_g = 50 \Omega$ and with the length of 1 m is added to the antenna. How does the plot in Figure 1.8 change?
8. The lower frequency of an antenna band is 2.5 GHz; the upper frequency of the band is 6 GHz. Determine the band center frequency and the antenna impedance bandwidth.
9. In Example 1.10, we use a generator with $R_g = 100 \Omega$. How does the antenna impedance bandwidth will change?

- 10***. A thick cylindrical tubular dipole has $l_A = 15$ cm, $a = 5$ mm. Using MATLAB Antenna Toolbox, determine the center frequency of the band and the impedance bandwidth percentage. How do those values relate to the values found in Example 1.10?
- 11***. Browsing the Antenna Toolbox Classes, provide at least one example of an antenna that has a significantly larger bandwidth than a thin dipole of the same length when matched to a $50\ \Omega$ generator/transmission line. Justify your answer by numerical simulations.
- 12***. A quantity that is also often used in analyzing the port characteristics of an antenna is *return loss*. What is it? How is it different from the reflection coefficient? Use the MATLAB Antenna Toolbox to plot the return loss and the reflection coefficient of a dipole antenna as described in Problem 10. Comment on the results.
- 13***. Your boss at the startup you have joined tells you about this new antenna that has been designed and called an ESD – an *electrically small dipole*. Your boss claims that the spatial radiation characteristics (far-field directivity/gain) do not change as the operating frequency is lowered. Investigate this claim by using the dipole in the MATLAB Antenna Toolbox library, modifying it as per the dimensions in Problem 10 and analyzing at the following frequencies: 200, 150, and 100 MHz. Do the following:
- (A) Calculate and plot the 3D radiation pattern of the antenna at the listed frequencies and make a table of the maximum directivity reported in the plot (look at top-left corner).
 - (B) Tabulate the impedance of this antenna at the listed frequencies.
- Comment on the results.
- 14.** Is the common household microwave oven an antenna? Justify your answer.

CHAPTER 2



Receiving Antenna: Received Voltage, Power, and Transmission Coefficient

In this chapter, we will establish and validate an equivalent circuit for the receiving antenna, establish open-circuit receive antenna voltage, and formulate an equivalent circuit for the antenna-to-antenna link between transmitter (with abbreviation TX) and receiver (with abbreviation RX) circuits. The antenna-to-antenna link is a *two-port linear network*; it is characterized by its *transfer function*. The transfer function expresses the received voltage and power in terms of the voltage and power at the transmitter. In other words, it establishes the *path loss*.

Why is the transfer function important? Because, ultimately we need to know the received voltage and power across the load at the receiver, but not exactly the antenna input impedance, antenna gain, or its radiation pattern, etc. The transfer functions may be found either numerically or, in simple cases, analytically. To perform this task, we must define the transfer function first, then express the transfer function using terminal antenna parameters, i.e. using the antenna circuit model.

SECTION 1 ANALYTICAL MODEL FOR THE RECEIVING ANTENNA

2.1. Model of the Receiving Antenna and Its Discussion	32
2.2. Finding Current of a Receive Dipole	33
2.3. Finding V_{OC} of a Receive Dipole. Induced EMF Method. Small Antennas Receive Much Less Power	34
2.4. Expressing V_{OC} of a Receive Dipole in Terms of Transmitter Parameters	37
2.5. Voltage and Power Transfer Functions	38
References	41
Problems	42

2.1 MODEL OF THE RECEIVING ANTENNA AND ITS DISCUSSION

One straightforward model of the receiving circuit with an antenna (in the form of its Thévenin equivalent) is shown in Figure 2.1 (the phasor form). The antenna has an input impedance Z_a , which is the physical property of the antenna itself and does not depend on its use – either in the transmit or receive mode. Indeed, antenna loading with a nearby metal or dielectric body may change input impedance. The rest of the receiving circuit is modeled by a load resistance R_{load} .

The circuit in Figure 2.1 has the following features:

1. The voltage source V_{OC} (phasor voltage) in series with the antenna input impedance is due to an incident electromagnetic signal; it is determined by its strength and polarization. However, it is also affected by a specific antenna construction and thus by its input impedance. An example is given by an *emf* induced in a small coil antenna due to an incident time-varying magnetic field following Faraday's law of induction.
2. The term V_{OC} simply means that the voltage source in Figure 2.1 is the voltage at the antenna terminals when the antenna is open-circuited.
3. At first sight, the circuit in Figure 2.1 is similar to the transmitter circuit in Figure 1.3 of Chapter 1 as long as V_{OC} is replaced by V_g .
4. The load resistance R_{load} is the input resistance/impedance of the receiving circuit (for example, an input impedance of a low-noise amplifier/filter). It is usually given to us and is usually equal or close to 50Ω .

However, the analysis of the circuit in Figure 2.1 is *not* equivalent to the circuit analysis for the transmitting antenna. It includes several paradoxes; some of them are listed below.

First, for a fixed voltage source V_{OC} , the maximum power transfer to the load resistance in Figure 2.1 is formally achieved not when $Z_a = R_{\text{load}}$ (the matching condition), but rather when $Z_a = 0$. However, an antenna with $Z_a = 0$ is a very small

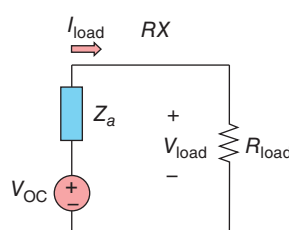


Figure 2.1 Model of the receiving antenna with a voltage source.

loop of wire which has $V_{OC} \approx 0$. Therefore, it is much more beneficial to increase the input impedance and simultaneously increase V_{OC} .

Second, for the matched receiving antenna with $Z_a = R_{load}$, exactly a half of circuit power is dissipated in the antenna itself. Where does this power go for an ideal antenna with zero loss resistance? The answer is given in particular in Ref. [1]: this power is “scattered” (or “reradiated”) into surrounding space. This very interesting fact is directly used for *passive RFID tag antenna design*; these antennas reradiate a part of the receiver power along with a proper modulation containing tag information.

Well, what happens then if we short out the load resistance? For example, we assume that $Z_a = R_{load}$ in Figure 2.1 and that R_{load} on the right of Figure 2.1 is shorted out. According to the same logic, more power should be reradiated back since the current through $Z_a = R_{load}$ doubles, which gives us a fourfold increase in the reradiated power.

Although the last observation is probably physically correct (a shorted-out dipole is a longer metal wire, which is a better scatterer), the test of the open-circuit condition meets some difficulties. When the circuit in Figure 2.1 is open ($R_{load} = \infty$), there is no current and thus no power dissipation on the antenna impedance. So, there should not be any scattering from the antenna, right? But we do know that the open-circuited dipole does scatter the incident field, and often quite significantly.

Those and other arguments rose questions about the validity of the circuit representation in Figure 2.1 [2]. It has been in particular stated that the Thévenin equivalent circuit of Figure 2.1 cannot be used for the receiving antenna [3–4] while many other textbooks still use that model (see, for example, [1]). Who is right and who is not?

A large part, if not the whole problem, is likely due to the fact that the voltage source V_{OC} in Figure 2.1 depends on both the transmitting signal and the receiving antenna itself. Therefore, in order to examine the circuit in Figure 2.1 and prove (or disprove) its validity, we must find V_{OC} first.

2.2 FINDING CURRENT OF A RECEIVE DIPOLE

We will consider a dipole antenna shown in Figure 2.2, with its radius approaching zero, i.e. $a \rightarrow 0$, for simplicity. The current distribution along the dipole antenna (in transmit or receive mode) is well approximated by a sinusoidal dependence [1] (the current is maximum at the antenna feed and is zero at the dipole tips since electric current cannot flow in the air). Analytically, one has with reference to Figure 2.2

$$\vec{I}(z) = \vec{a}_z I_0 \sin\left(k\left[\frac{l_A}{2} - |z|\right]\right), |z| \leq l_A/2, \quad (2.1)$$

where $k = 2\pi/\lambda$ is the wavenumber, λ is the wavelength, and \vec{a}_z is the unit vector in the z -direction. The constant I_0 in Eq. (2.1) is not yet the feed current I_a ; one

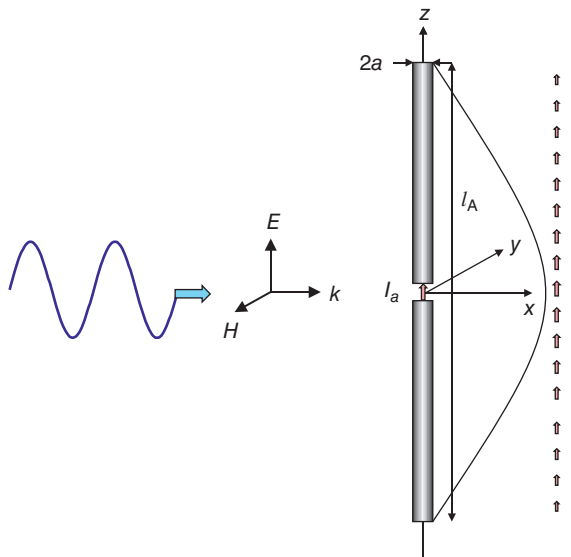


Figure 2.2 Receiving antenna configuration for finding V_{OC} . Both the incident signal and the receiving dipole have the same vertical polarization.

needs to normalize Eq. (2.1) in order to write it in terms of the feed current, I_a , in the form:

$$\vec{I}(z) = \vec{a}_z I_a \frac{\sin(k[\frac{l_A}{2} - |z|])}{\sin(k \frac{l_A}{2})}, |z| \leq l_A/2. \quad (2.2)$$

Eq. (2.2) is a good approximation for small dipoles and for dipoles close to the first resonance. Although the dipole radius a (for cylindrical dipoles) or dipole width t (for blade dipoles) is not explicitly present in Eq. (2.2), this result holds well for all relatively thin dipoles. However, it cannot be applied to dipole arrays [5].

2.3 FINDING V_{OC} OF A RECEIVE DIPOLE. INDUCED EMF METHOD. SMALL ANTENNAS RECEIVE MUCH LESS POWER

In the analytical form, the open-circuit voltage is most straightforwardly obtained through a complex power \mathbf{P} (Poynting vector) delivered by an *incident field*, \vec{E}^{inc} , to the open-circuited receiving antenna using the so-called *induced emf* method [1, 6–9]. For volumetric antennas, the complex received power \mathbf{P} is accumulated over the entire antenna surface and is thus an integral over the surface of the

receiving antenna, S_R . For linear antennas, this result is reduced to a line integral along the antenna in the form

$$V_{OC} I_a^* = - \int_{-\frac{l_A}{2}}^{+\frac{l_A}{2}} \vec{E}^{\text{inc}} \cdot \vec{I}^*(z) dz \Rightarrow V_{OC} = - \frac{1}{I_a^*} \int_{-\frac{l_A}{2}}^{+\frac{l_A}{2}} \frac{l_A}{2} \vec{E}^{\text{inc}} \cdot \vec{I}^*(z) dz \quad [\text{V}], \quad (2.3)$$

where \vec{E}^{inc} is an incident electric field; the star denotes complex conjugate.

Note: Eq. (2.3) simultaneously shows that, if the incident wave polarization (direction of \vec{E}^{inc}) is perpendicular to the antenna direction, then $\vec{a}_z \cdot \vec{E}^{\text{inc}} = 0$ and the antenna receives no power whatsoever. This effect is called *polarization mismatch*.

Note: Eq. (2.3) has a simple interpretation [6]. The factor $-dz \vec{E}^{\text{inc}} \cdot \vec{I}^*(z)/2$ or $+dV^{\text{inc}} I_a^*(z)/2$ where $dV^{\text{inc}} \equiv -dz \vec{a}_z \cdot \vec{E}^{\text{inc}}$ is the complex power of incident field per unit antenna length. Its integration/summation over the entire antenna length gives us the total antenna power in the feed, $V_{OC} I_a^*/2$. The factor $l_A/2$ is then canceled out.

For simplicity, we will assume here a plane wave incidence with exactly the same polarization (direction of the electric field) as the dipole axis shown in Figure 2.2. In that case, the dot product in Eq. (2.3) yields according to Eq. (2.2):

$$\vec{E}^{\text{inc}} \cdot \vec{I}^*(z) = + E_z^{\text{inc}} I_a^* \frac{\sin(k \frac{|z|}{2})}{\sin(k \frac{l_A}{2})}, |z| \leq l_A/2. \quad (2.4)$$

Note: The sign plus in Eq. (2.4) implies that the direction of the incident electric field and the direction of electric current induced along the receiving antenna coincide. In other words, they are in phase. This fact is additionally justified via numerical modeling via MATLAB Antenna Toolbox (function `planeWaveExcitation`).

The integral in Eq. (2.3) can now be computed analytically since E_z^{inc} is assumed to be constant. This yields the open-circuit voltage of the antenna in the simple closed form:

$$V_{OC} = - \frac{2}{k} E_z^{\text{inc}} \frac{\left[1 - \cos\left(\frac{k l_A}{2}\right) \right]}{\sin\left(\frac{k l_A}{2}\right)}. \quad (2.5)$$

This voltage clearly depends on

- (i) the strength of the incident signal (or field);
- (ii) the antenna length;
- (iii) the operation frequency.

In particular, it follows from Eq. (2.5) that the open-circuit voltage decreases when the dipole length l decreases (when the antenna becomes really small). The sign minus in Eq. (2.5) can be interchanged by switching the voltage polarity.

Example 2.1

Often, engineers are interested in the received voltage at *plane wave* incidence. The plane wave is so called because it has a plane phase front; it is not spherical or cylindrical wave.

Any radiated field at large distances from the source is locally represented by plane waves as explained later in the text. Such plane waves could be generated using different means, for example, by a GPS satellite, or by a base station antenna, or by your cellphone far away from it.

We assume here that a plane wave with the strength $E_z^{\text{inc}} = 1 \text{ V/m}$ at 1 GHz shown in Figure 2.2 is incident upon a dipole with the total length given by $l_A = 15, 10, 5, \text{ and } 2.5 \text{ cm}$. It is necessary to find the received open-circuit voltage amplitude for every dipole length.

Solution: We program Eq. (2.5) in MATLAB and create the script which evaluates the open-circuit voltage amplitude at different antenna lengths. Its text follows:

```
clear all
% EM data
epsilon = 8.85418782e-012; % Vacuum, F/m
mu = 1.25663706e-006; % Vacuum, H/m
c = 1/sqrt(epsilon*mu); % Vacuum, m/s
eta = sqrt(mu/epsilon); % Vacuum, Ohm
% Dipole parameters (receiver)
lA = [150 100 50 25]*1e-3; % Dipole length (m)
Einc = 1; % Incident field, V/m
f = 1e9; % Frequency of inc. field, Hz
lambda = c/f; % Wavelength
k = 2*pi/lambda; % Wavenumber
arg = k*lA/2; % Argument
VOC = abs(-(2/k)*Einc*(1-cos(arg))./sin(arg))
```

TABLE 2.1 Received open-circuit voltages for different dipole lengths.

l_A	15 cm	10 cm	5 cm	2.5 cm
V_{OC}	96 mV	55 mV	26 mV	13 mV

The above MATLAB script generates the data that are summarized in Table 2.1.

Thus, smaller antennas possess smaller received voltages and lower received powers. Two extreme voltage values in Table 2.1 differ by the factor of 7.4, which would give us a factor of 54.5 difference for the receiver power. The antenna of zero length receives nothing.

2.4 EXPRESSING V_{OC} OF A RECEIVE DIPOLE IN TERMS OF TRANSMITTER PARAMETERS

The next step of the analysis is to relate the incident field \vec{E}^{inc} to a signal radiated by the transmitter antenna. We assume a similar dipole transmitting antenna, located in the same plane as the receive dipole in Figure 2.2, with the same orientation, and with the similar feed position in the xy -plane – see Figure 2.3. In Figure 2.3, two dipole antennas are located *side by side*, which is the most favorable configuration. The antenna lengths could be different though. The antenna separation distance is r .

It will be shown in the next chapter that the incident field due to the transmitting antenna at significant separation distances (in the *far-field* or in the *Fraunhofer zone* where $r \geq 2l_A^2/\lambda$ in general for half-wave dipoles) is given by (cf. also [1])

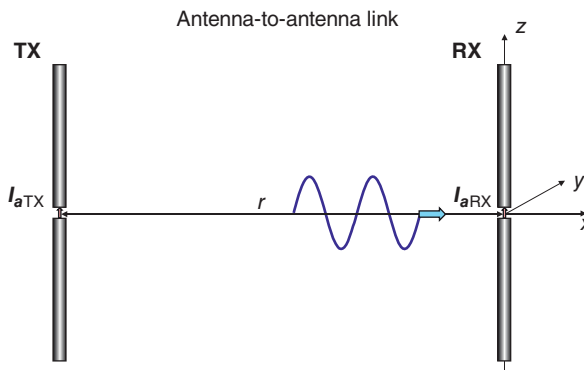


Figure 2.3 Geometry of the antenna-to-antenna link. Both antennas may have different lengths.

$$\vec{E}^{\text{inc}} = (0, 0, \mathbf{E}_z^{\text{inc}}), \quad \mathbf{E}_z^{\text{inc}} = -j\eta \frac{\mathbf{I}_a}{2\pi} \frac{1 - \cos(\frac{kl_a}{2})}{\sin(\frac{kl_a}{2})} \frac{\exp(-jkr)}{r}, \quad (2.6)$$

where all parameters in Eq. (2.6) are those for the transmitting antenna and $\eta = 377 \Omega$ is the *impedance of free space*. This result is also identical to that given in Kraus and Marhefka book [8] (Eq. [5.2.1.2.1]) if we take into account the definition of the feed current \mathbf{I}_a from Eq. (2.2) and the change of sign due to conversion from $\mathbf{E}_z^{\text{inc}}$ in Cartesian coordinates (directed up) to $\mathbf{E}_\theta^{\text{inc}}$ in spherical coordinates (directed down). Note that the factor $\frac{1 - \cos(\frac{kl_a}{2})}{\sin(\frac{kl_a}{2})}$ appears here again, similar to Eq. (2.5)! Combining Eq. (2.5) and (2.6) and taking into account the expression for the current of the transmitting antenna (see Chapter 1, Figure 1.3)

$$\mathbf{I}_a = \frac{\mathbf{V}_g}{R_g + \mathbf{Z}_{a\text{TX}}}, \quad (2.7)$$

we arrive at the expression for the received open-circuit voltage in terms of the transmitter generator voltage (phasor voltage) in the form:

$$\mathbf{V}_{\text{OC}} = \frac{j\eta}{\pi k} \frac{\left[1 - \cos\left(\frac{kl_{\text{ATX}}}{2}\right)\right]}{\sin\left(k \frac{l_{\text{ATX}}}{2}\right)} \frac{\left[1 - \cos\left(\frac{kl_{\text{ARX}}}{2}\right)\right]}{\sin\left(k \frac{l_{\text{ARX}}}{2}\right)} \frac{\exp(-jkr)}{r} \frac{1}{R_g + \mathbf{Z}_{a\text{TX}}} \mathbf{V}_g. \quad (2.8)$$

The antenna-to-antenna link is thus established. Eq. (2.8) simplifies to

$$\mathbf{V}_{\text{OC}} = \frac{j\eta}{\pi} \tan\left[\frac{kl_{\text{ATX}}}{4}\right] \tan\left[\frac{kl_{\text{ARX}}}{4}\right] \frac{\exp(-jkr)}{kr} \frac{1}{R_g + \mathbf{Z}_{a\text{TX}}} \mathbf{V}_g, \quad (2.9)$$

which is our final result. You could check that the open-circuit voltage indeed has the units of volts. Eq. (2.9) clearly demonstrates that voltage transmission problem is *linear*. Unfortunately, Eq. (2.9) is only valid for dipole and dipole-like antennas close to or below the first resonance. The polarization mismatch can be included into consideration by multiplying its right-hand side by a cosine of the angle between the two antenna directions.

2.5 VOLTAGE AND POWER TRANSFER FUNCTIONS

The last step is to establish the voltage and power *transfer functions* from the transmitter to the receiver. The *voltage transfer function*, \mathbf{T}_V , may be defined in a number of ways, for example, as the ratio of the voltage across the load resistor in

Figure 2.1 to the transmitter generator voltage, both in phasor form. One has from Eq. (2.9) and from the voltage divider circuit in Figure 2.1:

$$\mathbf{V}_{\text{load}} = \mathbf{T}_V \mathbf{V}_g, \quad \mathbf{T}_V = \frac{j\eta}{\pi} \tan \left[\frac{k l_{\text{ATX}}}{4} \right] \tan \left[\frac{k l_{\text{ARX}}}{4} \right] \frac{\exp(-jkr)}{kr} \frac{1}{R_g + Z_{a\text{TX}}} \frac{R_{\text{load}}}{R_{\text{load}} + Z_{a\text{RX}}}. \quad (2.10)$$

A *power transfer function*, T_P , can also be defined in a number of convenient ways. In every case, it is always proportional to $|\mathbf{T}_V|^2$. Assume, for example, that we are interested in the ratio of the average power across the load resistance of the receiver circuit (which is exactly the useful receiver power), P_{load} , to the total power delivered by the voltage source of the transmitter, P_{TX} (which is the total consumed RF power). The transmitter or generator circuit is assumed to be matched at any frequency, i.e. $Z_{a\text{TX}} = R_g$. This consumed power is the rated power of the transmitter; it is found from the TX circuit model in Figure 1.3 of Chapter 1 and does not depend on frequency. One thus has for the two corresponding powers and for the power transfer function

$$P_{\text{TX}} = \frac{|\mathbf{V}_g|^2}{4R_g}, \quad (2.11a)$$

$$P_{\text{load}} = \frac{|\mathbf{V}_{\text{load}}|^2}{2R_{\text{load}}}, \quad (2.11b)$$

$$T_P = \frac{P_{\text{load}}}{P_{\text{TX}}} = \frac{2R_g}{R_{\text{load}}} |\mathbf{T}_V|^2. \quad (2.11c)$$

Other definitions of the transfer function are indeed possible and will be considered later in this chapter.

Example 2.2

Both TX and RX circuits operating at 1 GHz make use of two identical 15 cm long side-by-side cylindrical dipole antennas separated by 1 m – see Figure 2.3. The dipole radius is 2 mm. Dipoles are facing each other. The TX circuit at matched conditions ($Z_{a\text{TX}} = R_g$) generates the total rated power P_{TX} of 1 W. The TX circuit also has $R_g = 50 \Omega$, the RX circuit has $R_{\text{load}} = 50 \Omega$ too. Find the useful received power P_{load} as a function of frequency (the *power spectrum*) over the band from 600 to 1200 MHz.

Solution: We program the voltage transfer function given by Eq. (2.10) and the power transfer given by Eq. (2.11c) in MATLAB and create a MATLAB script, the text of which is given below. The dipole's input impedance as a function of frequency is calculated from the analytical model described in Chapter 1, Example 1.5 (function `dipoleAnalytical`).



Figure 2.4 Power transfer function for two 15 cm long dipoles separated by 1 m in dB. To find the absolute value of the receiver power, we can simply multiply 1 W by T_P found from Eq. (2.11c).

The result for the power transfer function, T_P , in dB is plotted in Figure 2.4. It is rather unexpected: even at the most favorable frequency of 915 MHz the transfer function peaks just below -30 dB. This means that only 0.1% (!) of the total transmitter power reaches the receiver in the present configuration, even in the best possible case.

Where does the rest of the TX power go? The accurate answer will be given in the next chapter, based on the antenna radiation properties. It is based on the fact that the TX antenna radiates power in all possible directions, and that only a very small fraction of it is collected by even a closely spaced receiver antenna. This is a common feature of *omni-directional* antennae such as dipoles and loops.

```
% Analytical solution for the transfer function
clear all
% EM data
epsilon      = 8.85418782e-012;           % Vacuum, F/m
mu          = 1.25663706e-006;           % Vacuum, H/m
c           = 1/sqrt(epsilon*mu);         % Vacuum, m/s
eta          = sqrt(mu/epsilon);          % Vacuum, Ohm

% Dipole parameters (transmitter TX and receiver RX)
a            = 2.0e-3;       % Dipole radius (m) TX and RX
lA           = 150e-3;      % Dipole length (m) TX and RX
```

```

Rg           = 50;          % Generator resistance, Ohm
Rload        = 50;          % Receiver load, Ohm
antenna_spacing = 1000e-3; % Distance between antennas, m

% Frequency data
f      = linspace(600e6, 1200e6, 100);    % Frequency in Hz
% Dipole input impedance - TX
[ZTX] = dipoleAnalytical(f, lA, a);
% Dipole input impedance - RX
[ZRX] = dipoleAnalytical(f, lA, a);

% Transfer function
k      = 2*pi*f/c;
k1TX   = k*lA;
k1RX   = k*lA;
temp   = j*eta./(pi*k).*tan(k1TX/4).*tan(k1RX/4)...
.*exp(-j*k*antenna_spacing)./(antenna_spacing);
TV = temp.*Rload./((ZRX+Rload).* (ZTX+Rg)); % Voltage TF
TP = 10*log10(2*Rg/Rload*abs(TV).^2);         % Power TF in dB

% Plot transfer function
hold on; grid on; plot(f/1e6, TP, 'b', 'LineWidth', 2);
title('Power transfer function, dB');
xlabel('frequency, MHz'); ylabel('dB')
axis([600 1200 -60 -30])

```

REFERENCES

1. C. A. Balanis, *Antenna Theory: Analysis and Design*, Wiley, New York, 2016, fourth edition.
2. J. Van Bladel, “On the equivalent circuit of a receiving antenna,” *Antennas Prop. Magazine*, vol. 44, no. 1, pp. 164–165, 2002.
3. A. W. Love, “Comment: On the equivalent circuit of a receiving antenna,” *Antennas Prop. Magazine*, vol. 44, no. 5, pp. 124–125, 2002.
4. R. E. Collin, “Limitations of the Thévenin and Norton equivalent circuits for a receiving antenna,” *Antennas Prop. Magazine*, vol. 45, no. 2, pp. 119–124, 2003.
5. S. Makarov, A. Puzella, and V. Iyer, “Scan impedance for an infinite dipole array: Accurate theory model compared to numerical software,” *IEEE Antennas Prop. Magazine*, vol. 50, no. 6, pp. 132–149, 2008.

6. S. A. Schelkunoff, "Theory of antennas of arbitrary size and shape," *Proc. IEEE*, vol. 72, no. 9, pp. 1165–1190, 1984, doi: 10.1109/PROC.1984.12996.
7. R. F. Harrington, *Time-Harmonic Electromagnetic Fields*, McGraw Hill, New York, 1961 (Reprinted IEEE-Wiley, New York, 2001), p. 349.
8. J. D. Kraus and R. J. Marhefka, *Antennas for All Applications*, McGraw-Hill Science/Engineering/Math, New York, 2001, third edition.
9. W. L. Weeks, *Electromagnetic Theory for Engineering Applications*, Wiley, New York, 1964.

PROBLEMS

1. The open-circuit voltage of a receiver antenna depends on (make a list):
 - (A) ---
 - (B) ---
 - (C) ---
 - (D) ---
2. The power transfer function of the TX/RX link depends on (make a list):
 - (A) ---
 - (B) ---
 - (C) ---
 - (D) ---
3. Plot to scale (use MATLAB) electric current distribution along a dipole antenna with the total length of 15 cm and with the feed current of $10 \mu\text{A}$ for
 - (A) $f = 10 \text{ MHz}$;
 - (B) $f = 100 \text{ MHz}$;
 - (C) $f = 1000 \text{ MHz}$.
4. A co-polarized plane wave with the electric field strength of 1 V/m is normally incident upon a 15 cm long dipole at
 - (A) $f = 10 \text{ MHz}$;
 - (B) $f = 100 \text{ MHz}$;
 - (C) $f = 1000 \text{ MHz}$.

Determine the received open-circuit voltage for every frequency.
5. Repeat the previous when the direction of the E-field in the normally incident plane wave is
 - (i) perpendicular to the dipole axis;
 - (ii) forms the angle of 45° with the dipole axis.

Note: The corresponding power loss that you may encounter is known as the *polarization loss*.

- 6.** Using Eq. (2.9), establish limiting values of V_{OC} when
- (i) frequency tends to zero, but the distance between two antennas is fixed;
 - (ii) distance between two antennas tends to infinity, but the frequency is fixed;
 - (iii) antenna length tends to zero (for either TX or RX), but the frequency and distance are both fixed.

- 7.** You are given:

- (A) Both TX and RX antenna circuits with $R_g = R_{load} = 50 \Omega$.
- (B) A separation distance between the TX/RX antennas of 100 m.

Design two identical TX/RX dipole antennas (determine the length and the radius), which assure maximum output load power versus the rated input power when located side by side at

- (i) 433 MHz;
- (ii) 915 MHz;
- (iii) 2.45 GHz.

Present the value of the maximum output load power in every case.

- 8.** Could better results be obtained in the previous problem at

- (i) 433 MHz;
- (ii) 915 MHz;
- (iii) 2.45 GHz

when non-equal dipoles are used?

- 9.** For two half-wave dipole antennas separated by 1 km, what is approximately the power loss of the wireless link at 2.4 GHz? If the same dipoles are located 2 km apart, what do you think the new power loss would be? *Note:* Feel free to define a most appropriate expression for the power loss (power transfer function) at the beginning of your solution.

SECTION 2 MODEL OF A TWO-PORT NETWORK FOR TX/RX ANTENNAS

- 2.6. Impedance Matrix (Mutual Impedance) Approach to the Antenna-to-Antenna Link 44**
- 2.7. Transfer Function in Terms of Voltage Across the TX Antenna 46**
- 2.8. Scattering Matrix Approach (Transmission Coefficient) 47**
- 2.9. Power Transfer Function 48**
- 2.10. Mutual Impedance of Two Dipoles 49**
- 2.11. Two-port Network Antenna Model in MATLAB Antenna Toolbox 50**
- References 53**
- Problems 53**

2.6 IMPEDANCE MATRIX (MUTUAL IMPEDANCE) APPROACH TO THE ANTENNA-TO-ANTENNA LINK

Although the analytical approach introduced previously straightforwardly quantifies the antenna-to-antenna link, it is still based on the solution for the particular dipole-to-dipole antenna configuration and is not really generic. As another, more universal tool, we will consider a networking approach to the same problem [1, 2] instead of the approach of the Thévenin equivalent circuit from Section 1.

This approach does not explicitly introduce the questionable voltage source in Figure 2.1. Instead, it established a direct “conduction” path between the transmitting and receiving antennas using a *two-port linear network* concept. This path indeed implies antenna radiation and reception. In that way, a wireless link is represented in the circuit form. Such a model works in both frequency domain and in time domain as shown in Figure 2.5. The dependent voltage source shown in

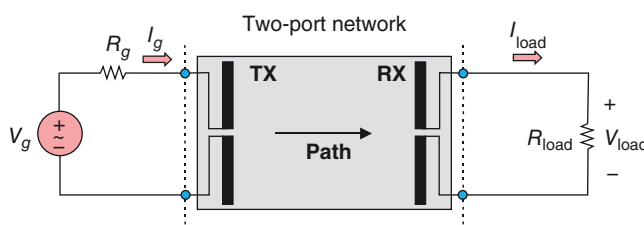


Figure 2.5 A path between the transmitting and receiving antennas in the form of a two-port network. The time-domain version is shown.

Figure 2.1 thus becomes unnecessary, at least formally. The only real source in the circuit in Figure 2.1 is now the generator voltage.

The model of Figure 2.5 becomes especially inviting in frequency domain (the phasor form) – see Figure 2.6 that follows. Of primary interest to us is the received load phasor voltage V_{load} as a function of the generator voltage V_g . This approach shall again provide us with the voltage transfer function T_V . In the phasor form,

$$T_V = \frac{V_{\text{load}}}{V_g}. \quad (2.12)$$

For a system with two lumped ports (TX and RX antennae terminals), one can use an *impedance matrix* \hat{Z} on the size 2×2 [3]. For example, such an impedance matrix is readily available in the MATLAB Antenna Toolbox at a given frequency. The impedance matrix is invariant to port impedances specified [3]. The TX–RX antenna network shown in Figure 2.6a is replaced by an equivalent two-port microwave network described by an impedance matrix, \hat{Z} , in Figure 2.6b:

$$\hat{Z} = \begin{bmatrix} Z_{11} & Z_{12} \\ Z_{21} & Z_{22} \end{bmatrix}, \quad (2.13)$$

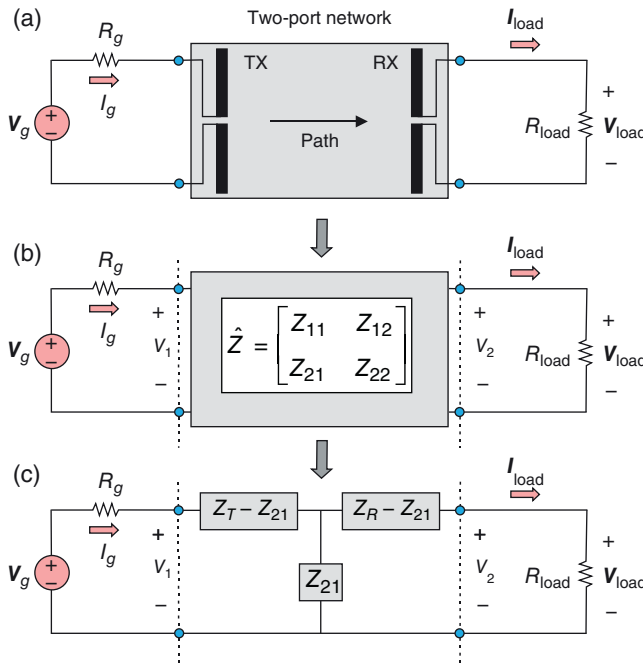


Figure 2.6 Transformations of the two-port antenna network in frequency domain.

where $\mathbf{Z}_{11} = \frac{V_1}{I_1} \Big|_{I_2=0}$, $\mathbf{Z}_{12} = \frac{V_1}{I_2} \Big|_{I_1=0}$, $\mathbf{Z}_{21} = \frac{V_2}{I_1} \Big|_{I_2=0}$, $\mathbf{Z}_{22} = \frac{V_2}{I_2} \Big|_{I_1=0}$.

Note that the formal definition of the impedance matrix implies that I_{load} in Figure 2.6 should flow as shown, i.e. *into* the RX port.

The impedance approach explicitly relates the antenna link to the circuit parameters and to the antenna input impedances, and allows us to directly employ the well-known analytical results for dipole and loop antennas when necessary. For reciprocal (non-ferrite) antennas, the *mutual impedances* are identical, i.e. $\mathbf{Z}_{12} = \mathbf{Z}_{21}$. We will assume that this condition is always valid.

In the far-field, self-impedances \mathbf{Z}_{11} , \mathbf{Z}_{22} coincide with the input impedances \mathbf{Z}_{aTX} , \mathbf{Z}_{aRX} of the transmitting and receiving antennas in free space, respectively.

Next, the two-port network in Figure 2.6b with the impedance matrix given by Eq. (2.13) is replaced by an equivalent T-network (the Π -equivalent is also possible, but it is not considered here). The resulting circuit is given in Figure 2.6c. The solution for the receiver voltage in Figure 2.6c then becomes an exercise in the basic circuit analysis. One has

$$V_{\text{load}} = \frac{R_{\text{load}} \mathbf{Z}_{21}}{(R_g + \mathbf{Z}_{11})(R_{\text{load}} + \mathbf{Z}_{22}) - \mathbf{Z}_{21}^2} V_g = \mathbf{T}_V V_g \quad (2.14)$$

for the voltage transfer function (which is also called the *forward voltage gain*). The result for the power transfer function(s) may be obtained in the same way. The component \mathbf{Z}_{21} – the *mutual impedance* – contains all the integral information about the path between the TX and RX antennas. It must be either calculated numerically or estimated experimentally.

For two antennas separated by a large distance, \mathbf{Z}_{21} is small. When the separation distance tends to infinity, $\mathbf{Z}_{21} \rightarrow 0$. In that case, the transmitter in Figure 2.6c is shorted out (\mathbf{Z}_{21} becomes a short circuit) and the receiver at infinity acquires no signal.

Thus, at large separation distances, $|\mathbf{Z}_{21}| < < \min(|\mathbf{Z}_{\text{aTX}}| = |\mathbf{Z}_{11}|, |\mathbf{Z}_{\text{aRX}}| = |\mathbf{Z}_{22}|)$. Therefore, one approximately has from Eq. (2.14):

$$V_{\text{load}} = \frac{R_{\text{load}} \mathbf{Z}_{21}}{(R_g + \mathbf{Z}_{\text{aTX}})(R_{\text{load}} + \mathbf{Z}_{\text{aRX}})} V_g = \mathbf{T}_V V_g. \quad (2.15)$$

2.7 TRANSFER FUNCTION IN TERMS OF VOLTAGE ACROSS THE TX ANTENNA

Quite often, we normalize the received voltage not by the generator voltage, V_g , but by the voltage across the TX antenna – see Figure 2.6b. The voltage transfer function so defined is denoted by \mathbf{T} . With reference to Figure 2.6b, one has

$$\mathbf{T} = \frac{\mathbf{V}_{\text{load}}}{\mathbf{V}_1}. \quad (2.16)$$

Solving the circuit in Figure 2.6c once again, one has

$$\mathbf{V}_{\text{load}} = \frac{R_{\text{load}} \mathbf{Z}_{21}}{\mathbf{Z}_{11}(R_{\text{load}} + \mathbf{Z}_{22}) - \mathbf{Z}_{21}^2} \mathbf{V}_1 = \mathbf{T} \mathbf{V}_1. \quad (2.17)$$

Eq. (2.17) is clearly a truncated version of Eq. (2.14) when $R_g = 0$.

2.8 SCATTERING MATRIX APPROACH (TRANSMISSION COEFFICIENT)

Although Eq. (2.14) through (2.17) for the transfer function may be (and have been) directly programmed in MATLAB or in another CEM package such as Ansys Electronics Desktop or CST Studio Suite of Dassault Systèmes, it is very useful to define the transfer function in terms of *S-parameters* (or *scattering parameters*) [3] of the two-port network in Figure 2.5 or in Figure 2.6a. This is the most common approach supported by the measurements with the network analyzer.

In Figure 2.7 that follows, the $\hat{\mathbf{Z}}$ -matrix network is replaced by an $\hat{\mathbf{S}}$ -matrix network. We assume that the characteristic transmission line impedance, \mathbf{Z}_0 , is equal to generator and load resistances for both the transmitter and receiver, i.e.

$$\mathbf{Z}_0 = R_g = R_{\text{load}}. \quad (2.18)$$

The straightforward way to reuse Eq. (2.14) and (2.17) in terms of scattering parameters is to employ two identities for the two-port network [3]:

$$S_{21} = \frac{2\mathbf{Z}_{21}\mathbf{Z}_0}{(\mathbf{Z}_{11} + \mathbf{Z}_0)(\mathbf{Z}_{22} + \mathbf{Z}_0) - \mathbf{Z}_{21}^2}, \quad (2.19a)$$

$$1 + S_{11} = 2 \frac{\mathbf{Z}_{11}(\mathbf{Z}_{22} + \mathbf{Z}_0) - \mathbf{Z}_{21}^2}{(\mathbf{Z}_{11} + \mathbf{Z}_0)(\mathbf{Z}_{22} + \mathbf{Z}_0) - \mathbf{Z}_{21}^2}. \quad (2.19b)$$

In view of this and taking into account Eq. (2.18), one precisely obtains a very simple and powerful result:

$$\mathbf{T}_V = \frac{1}{2} S_{21}, \quad (2.20a)$$

$$\mathbf{T} = \frac{S_{21}}{1 + S_{11}}, \quad (2.20b)$$

where S_{21} is the *transmission coefficient* between the two antennas. Emphasize that Eq. (2.20a) and (2.20b) are the exact result: no approximations of any kind have been involved into their derivation.

2.9 POWER TRANSFER FUNCTION

It has already been mentioned that the power transfer function, T_P , may be defined in a number of ways. The *most common way* is not to use Eq. (2.11c) but simply assign

$$T_P \equiv |S_{21}|^2. \quad (2.21)$$

Note that index P is now non-italic to underscore the difference of this result from Eq. (2.11c).

We again assume that $R_g = R_{\text{load}}$. In this case, the transfer function T_P from Eq. (2.21) will give us exactly the received load power – the power delivered to the load resistance in Figure 2.6 or 2.7,

$$P_{\text{load}} = \frac{1}{2} \frac{|V_{\text{load}}|^2}{R_{\text{load}}} \quad (2.22)$$

versus the power delivered to a transmitting antenna, which is *perfectly matched* to the generator resistance, that is

$$P_a = \frac{1}{8} \frac{|V_g|^2}{R_g}. \quad (2.23)$$

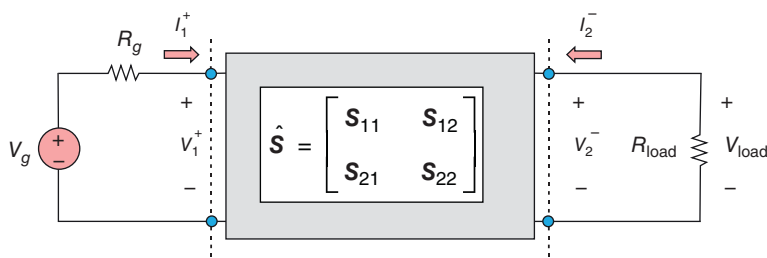


Figure 2.7 Network transformation of the antenna-to-antenna link – the S-matrix approach.

Note: Eq. (2.20a), (2.20b), and (2.21) for the transfer functions are valid in both near- and far-field of the antenna-to-antenna link. So is Eq. (2.14).

2.10 MUTUAL IMPEDANCE OF TWO DIPOLES

The major difficulty in solving Eq. (2.14) or Eq. (2.17) is in the evaluation of the antenna mutual impedance, Z_{21} [4]. Fortunately, once we know the open-circuit voltage, V_{OC} , of the receiving antenna – see Eq. (2.3) – then the mutual impedance, by definition, is given by

$$Z_{21} = \frac{V_{OC}}{I_{aTX}}. \quad (2.24)$$

Now, we substitute Eq. (2.9) for V_{OC} into Eq. (2.24) and obtain the mutual impedance in the form:

$$\begin{aligned} \frac{V_{OC}}{I_{aTX}} &= \frac{j\eta}{\pi} \tan \left[\frac{kl_{ATX}}{4} \right] \tan \left[\frac{kl_{ARX}}{4} \right] \underbrace{\frac{\exp(-jkr)}{kr}}_{V_g} \underbrace{\frac{1}{(R_g + Z_{aTX})I_{aTX}}} V_g \Rightarrow \\ Z_{21} &= \frac{j\eta}{\pi} \tan \left[\frac{kl_{ATX}}{4} \right] \tan \left[\frac{kl_{ARX}}{4} \right] \frac{\exp(-jkr)}{kr}. \end{aligned} \quad (2.25)$$

Finally, Z_{21} from Eq. (2.25) is plugged into Eq. (2.15) and the transfer function given by Eq. (2.12) is obtained. The result has the form,

$$T_V \equiv \frac{V_{load}}{V_g} = \frac{j\eta}{\pi} \tan \left[\frac{kl_{ATX}}{4} \right] \tan \left[\frac{kl_{ARX}}{4} \right] \frac{\exp(-jkr)}{kr} \frac{1}{R_g + Z_{aTX}} \frac{R_{load}}{R_{load} + Z_{aRX}}, \quad (2.26)$$

which is *identical* with the transfer function in Eq. (2.10) established with the Thévenin equivalent circuit from Figure 2.1. Thus, both approaches:

- (a) the Thévenin equivalent circuit for the receiving antenna; and
- (b) the impedance matrix approach

give us the same antenna-to-antenna transfer function *in the far-field*. In this and only this sense, the receiver circuit in Figure 2.1 is justified. This result may be straightforwardly generalized for arbitrary dipole antennas having different orientations.

2.11 TWO-PORT NETWORK ANTENNA MODEL IN MATLAB ANTENNA TOOLBOX

In a general case, both terminal matrices \hat{Z} and \hat{S} can either be measured or computed via full-wave numerical modeling. The MATLAB Antenna Toolbox makes it possible to compute all terminal matrices for an arbitrary number of diverse antennas forming an *N-port network*, and over any frequency band of interest.

A comparison will now be made of the theory model for the transfer function given by Eq. (2.10) with the transfer function found numerically in the MATLAB Antenna Toolbox. For the theoretical solution, we use the dipole input impedance model introduced in Chapter 1, Example 1.5. For the numerical solution, we are using Eq. (2.20a), which expresses the transfer function through the transmission coefficient.

A band from 600 to 1200 MHz is considered. The TX and RX antennae are the same strip dipoles as in Example 2.2, i.e. with the total length of 15 cm, and with the strip width of 8 mm (equivalent radius is 2 mm). The feed is modeled as a delta-gap. The antenna separation distance is 1 m. The TX and RX circuits have both $R_g = R_{\text{load}} = 50 \Omega$.

Example 2.3

Using an Antenna Toolbox project, compare theory and numerical simulations for the transfer function between two side-by-side dipole antennas with $l_A = 15$ cm, $a = 2$ mm separated by 1 m over the band 600–1200 MHz. The TX and RX circuits have both $R_g = R_{\text{load}} = 50 \Omega$. The theory model uses Eq. (2.10) and the analytical dipole input impedance model introduced in Chapter 1.

Solution: To obtain the analytical solution, we run the script from Example 2.2. The numerical solution aims to find the same power transfer function given by

$$T_P = 2|\mathbf{T}_V|^2 = \frac{1}{2}|\mathbf{S}_{21}|^2 \quad (2.27)$$

and its expression in dB, $10\log_{10}(T_P)$. To do so, we will append the following MATLAB script to the script of Example 2.2:

```
%> Create linear array of two dipoles
w      = cylinder2strip(a); % Strip width
d      = dipole('Length',lA,'Width',w); % Strip dipole model
l      = linearArray('Element',d,'ElementSpacing',antenna_spacing);
S      = sparameters(l,f);
S21   = rfparam(S,2,1);
TPn   = 10*log10(0.5*abs(S21).^2);
```

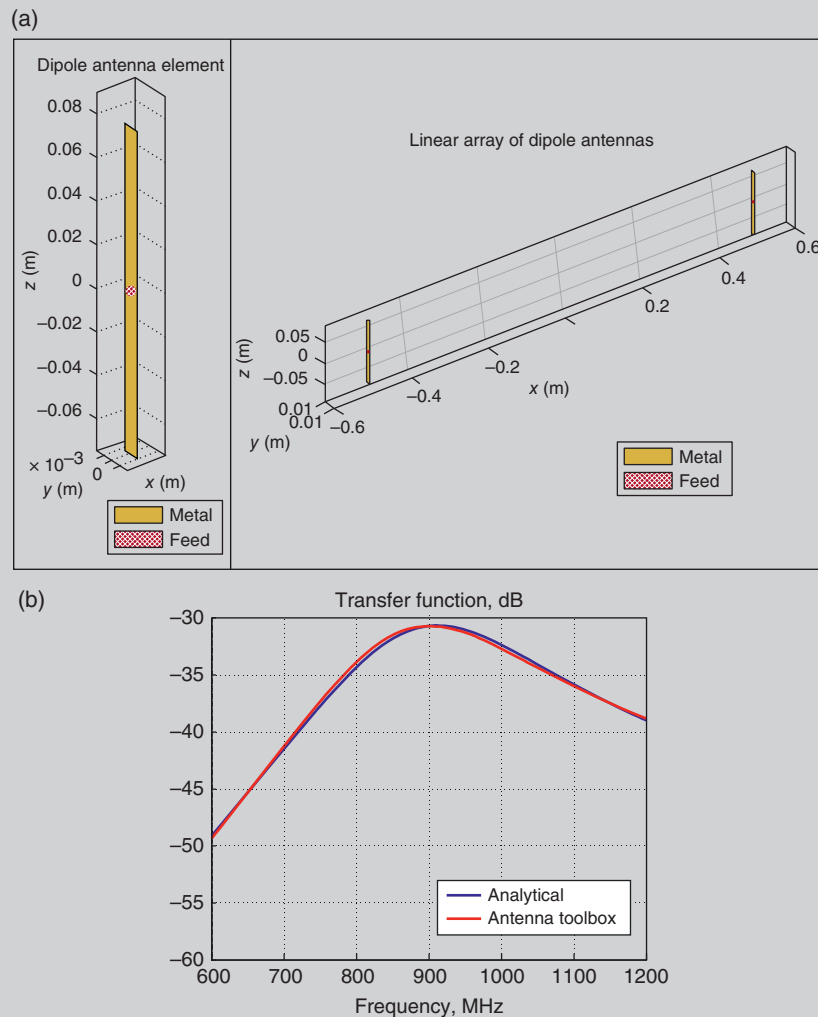


Figure 2.8 (a) Creation of a TX/RX geometry in the MATLAB Antenna Toolbox using `linearArray` function, (b) Transfer function in dB, $10\log_{10}T_P$ for two 15 cm long side-by-side dipole antennas with the radius 2 mm each, separated by 1 m as compared with the numerical solution.

```
%> Plot transfer function and compare
hold on;
grid on;
plot(f/1e6, TPn, 'r', 'LineWidth', 2);
title('Transfer function, dB')
```

```
legend('Analytical','Antenna Toolbox','Location','best');
xlabel('Frequency, MHz')
ylabel('Magnitude, dB')
```

This script uses function `linearArray` to create an array of two dipole antennas. You can visualize the individual array element using `show(d)` function and the entire array using `show(l)` function. An example is given in Figure 2.8a.

The transfer function comparison is shown in Figure 2.8b. The accuracy of the underlying theoretical dipole model [5] is truly amazing. Both solutions nearly coincide over the entire dynamic range of approximately 20 dB. We especially emphasize the agreement at higher frequencies where this theoretical model likely starts to fail. Furthermore, the results of Figure 2.8 also confirm the accuracy of the Thévenin equivalent circuit for the RX antenna introduced at the beginning of this chapter in Figure 2.1.

Note: In the Antenna Toolbox, you could also extract the impedance matrix of a TX/RX configuration (or an arbitrary antenna array) at any frequency of interest using the following commands:

```
S = sparameters(l,f);
Z = s2z(S.Parameters, 50);
```

The value of the characteristic transmission line impedance used here is 50Ω .

Note: Function `linearArray` is quite flexible and permits construction of arrays of arbitrary antennas arbitrarily oriented in space. As an example, the script given below creates an array of two dipoles (the TX/TX equivalent) with the second dipole titled by 45° :

```
d1      = dipole('Length',lA,'Width',w); % Strip dipole model
d2      = dipole('Length',lA,'Width',w); % Strip dipole model
d2.Tilt = 45;
l      = linearArray;
l.Element(1) = d1;
l.Element(2) = d2;
l.ElementSpacing = antenna_spacing;
```

REFERENCES

1. R. E. Collin, "Limitations of the Thévenin and Norton equivalent circuits for a receiving antenna," *Antennas Prop. Magazine*, vol. 45, no. 2, pp. 119–124, 2003.
2. S. Silver, *Microwave Antenna Theory and Design*, MIT Rad. Lab. Series vol. 12, McGraw Hill, New York, 1949.
3. D. M. Pozar, *Microwave Engineering*, Wiley, New York, 2011, fourth edition.
4. T. A. Milligan, *Modern Antenna Design*, Wiley, New York, 2005, second edition, pp. 17–18.
5. C. -T. Tai and S. A. Long, "Dipoles and monopoles," In *Antenna Engineering Handbook*, J. L. Volakis, Ed., McGraw Hill, New York, 2007, fourth edition, pp. 4-3 to 4-32.

PROBLEMS

1. (A) What units do the elements of the impedance matrix have?
 (B) What units do the elements of the scattering matrix have?
2. Mathematically establish the limiting value of Z_{21} when
 - (A) Frequency tends to zero, but the distance between two antennas is fixed.
 - (B) The distance between two antennas tends to infinity, but the frequency is fixed.
 - (C) Antenna length tends to zero (for either TX or RX), but the frequency and distance are both fixed.
- 3*. For two side-by-side cylindrical dipole antennas with $l_A = 15$ cm, $a = 2$ mm separated by 1 m plot to scale
 - (A) Real part of the mutual impedance Z_{21} ;
 - (B) Imaginary part of the mutual impedance Z_{21} ;
 - (C) Magnitude of the mutual impedance Z_{21} normalized by the magnitude of self-impedance Z_{11}
 over the band 600–1200 MHz using the MATLAB Antenna Toolbox. What meaning does the real part of the mutual impedance have?
- 4*. For two side-by-side cylindrical dipole antennas with $l_A = 15$ cm, $a = 2$ mm separated by 1 m plot to scale
 - (A) Magnitude of the transmission coefficient S_{21} ;
 - (B) Phase of the transmission coefficient S_{21}
 over the band 600 MHz–1200 MHz using the MATLAB Antenna Toolbox. What meaning does the magnitude of the transmission coefficient have?
- 5*. Two side-by-side TX/RX dipoles are separated by 100 m. Both of them have the total length of 6.25 cm and the radius of 1 mm. Plot the power

transfer function, $T_P \equiv |S_{21}|^2$, of this antenna link using the Antenna Toolbox over the frequency band from 2 to 3 GHz.

- (A) At what frequency value does the link transmission peak?
 - (B) Could you slightly modify the dipole length to achieve the peak at exactly 2.45 GHz? Report the resulting dipole length.
- 6*. In the previous problem, investigate the effect of dipole orientation on the transfer function. To do this, keep the TX dipole fixed in orientation, while changing the Tilt parameter on the RX dipole in steps of 10° from 0 to 90° . Choose the frequency at which the transfer function peaks (2.45 GHz) to run this study. Plot the transfer function in dB against the RX dipole orientation angle. Answer the following:
- (A) At what angle does the transfer function exhibit the peak value?
 - (B) At what angle does the transfer function exhibit the lowest value?
 - (C) What is the relative power loss (polarization loss) at 45° tilt as compared to the most favorable case?

CHAPTER 3



Antenna Radiation

SECTION 1 MAXWELL EQUATIONS AND BOUNDARY CONDITIONS

3.1. Maxwell's Equations	56
3.2. Boundary Conditions	57
3.3. About Electrostatic, Magnetostatic, and Direct Current Approximations	58
3.4. Analytical Solution to Maxwell's Equations in Time Domain.	
Plane Waves	59
References	61
Problems	62

In Chapter 2, we have used the fact that the radiated electric field of a dipole is given by Eq. (2.6). This was actually the major step in establishing the analytical transfer function for the antenna-to-antenna link. How is this equation obtained? How does the dipole radiate in other directions? How do other antennas radiate?

In order to answer these and similar questions and in order to establish the antenna radiation pattern, one needs to study Maxwell's equations for electromagnetic fields. This section provides a very basic introduction to Maxwell's equations and describes one simple yet exact solution. A comprehensive theory of engineering electromagnetics may be found elsewhere [1, 2].

3.1 MAXWELL'S EQUATIONS

Consider a medium with *electric permittivity* ϵ having the units of F/m and with *magnetic permeability* μ having the units of H/m. The *driving sources* for the electromagnetic fields are given by (generally volumetric) time-varying *free charge density* ρ with the units of C/m³ and by (generally volumetric) time-varying *electric current density* \vec{J} of free charges with the units of A/m². The free charges are free electrons in a metal or free electrons and/or holes in a semiconductor.

Instead of volumetric currents, one may consider surface currents (for metal antennas) or line current (for infinitesimally thin wire antennas). Similarly, instead of volumetric charges, one may consider surface charges (residing on surfaces of metal antennas) or line charges (for infinitesimally thin wire antennas).

Maxwell's equations for an electric field (or the *electric field intensity*) $\vec{E}(\vec{r}, t)$ [V/m] and for a magnetic field (or the *magnetic field intensity*) $\vec{H}(\vec{r}, t)$ [A/m] in time domain have the form:

$$\text{Ampere's law modified by displacement currents } \epsilon \frac{\partial \vec{E}}{\partial t} = \nabla \times \vec{H} - \vec{J}, \quad (3.1a)$$

$$\text{Faraday's law of induction } \mu \frac{\partial \vec{H}}{\partial t} = -\nabla \times \vec{E}, \quad (3.1b)$$

$$\text{Gauss' law for electric field } \nabla \cdot \epsilon \vec{E} = \rho, \quad (3.1c)$$

$$\text{Gauss' law for magnetic field (no magnetic charges)} \nabla \cdot \mu \vec{H} = 0, \quad (3.1d)$$

$$\text{Continuity equation for the electric current (from (3.1a), (3.1c)) } \frac{\partial \rho}{\partial t} + \nabla \cdot \vec{J} = 0. \quad (3.1e)$$

The continuity equation (3.1e) for the electric current is not independent; it is directly obtained from Eq. (3.1a) and (3.1c) keeping in mind that the divergence of the curl of any vector field is always zero and that the medium is locally homogeneous. Volumetric electric current is related to the electric field by a local form of Ohm's law,

$$\vec{J} = \sigma \vec{E}, \quad (3.1f)$$

where σ is (generally varying) *medium conductivity* with the units of S/m.

Note: If \vec{J} and ρ are equal to zero everywhere, the solution to Eq. (3.1a)–(3.1e) in unbounded space is given by $\vec{E} = \vec{H} = 0$. In other words, there are no fields in free space without the *sources*: the electric charges and the electric currents. On the other hand, if $\vec{E} = \vec{H} = 0$ everywhere in space, then \vec{J} and ρ must be equal to zero too.

Eq. (3.1d) has a general solution in the form,

$$\nabla \cdot \mu \vec{H} = 0 \Rightarrow \mu \vec{H} = \nabla \times \vec{A}, \quad (3.1g)$$

where \vec{A} is a new function – the *magnetic vector potential* – with the units of $V \cdot s/m$. Eq. (3.1g) follows from the vector calculus identity $\nabla \cdot (\nabla \times \vec{A}) = 0$, which is valid for any function $A(\vec{r}, t)$. Note that the substitution $A \rightarrow A + \nabla \psi$ does not change the form of this equation.

Question: What else except for Maxwell's equations do we need to know to establish antenna radiation characteristics and be able to model antennas and other RF circuits?

Answer: Boundary conditions for Maxwell's equations are critical for both analytical and numerical methods. They are briefly reviewed in Section 3.2.

3.2 BOUNDARY CONDITIONS

3.2.1 General Material Interface

Along with the electric and magnetic fields, \vec{E} and \vec{H} , we introduce the *electric flux density*, $\vec{D} = \epsilon \vec{E}$, and the *magnetic flux density*, $\vec{B} = \mu \vec{H}$. On the interface between two materials (dielectric, magnetic, or metal), the following boundary conditions are employed, either in time or frequency domain (medium I and medium II are those from Figure 3.1):

$$\vec{n} \cdot (\mu_2 \vec{H}_2 - \mu_1 \vec{H}_1) = 0 \text{ normal component of the } B\text{-field is continuous,} \quad (3.2a)$$

$$\vec{n} \cdot (\epsilon_2 \vec{E}_2 - \epsilon_1 \vec{E}_1) = 0 \text{ normal component of the } D\text{-field is continuous,} \quad (3.2b)$$

$$\vec{n} \times (\vec{H}_2 - \vec{H}_1) = 0 \text{ tangential component of the } H\text{-field is continuous,} \quad (3.2c)$$

$$\vec{n} \times (\vec{E}_2 - \vec{E}_1) = 0 \text{ tangential component of the } E\text{-field is continuous.} \quad (3.2d)$$

3.2.2 Metal-Dielectric (Metal-Air) Interface

On a metal surface S of a *perfect electric conductor* or PEC (represented by “inner” medium II in Figure 3.1), the tangential component of the total electric field vanishes, that is

$$\vec{E}_{tan1} = \vec{n} \times \vec{E}_1 = 0, \quad (3.2e)$$

where tan denotes the tangential component of the E -field that is parallel to the surface. The proof is based on Eq. (3.2d) which uses the fact that $\vec{E}_2 = 0$ within

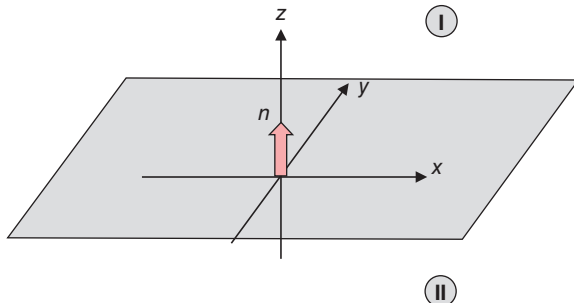


Figure 3.1 Problem geometry for boundary conditions at a media interface.

a perfect conductor. Otherwise, an infinite current would flow there, due to infinite conductivity.

Note: The PEC boundary condition (3.2e) is a good approximation to reality for antennas operating at approximately 10 GHz or lower. The PEC boundary condition implies *no loss*. At higher frequencies, the concept of a *surface impedance* should be used.

The normal component of the electric field at the PEC interface could have *any nonzero values* associated with the distributed surface charges. There is no electric or varying magnetic field within the perfect electric conductor. Therefore, the boundary condition for the magnetic field is trivially obtained from the Ampere's law Eq. (3.1a) using Eq. (3.2a):

$$\left(\nabla \times \vec{H} - \vec{J} \right)_{tan} = 0. \quad (3.2f)$$

This boundary condition is used less often than the boundary condition given by Eq. (3.2e).

Note: Boundary conditions for a non-perfect (finite-conductivity) metal surface or for an interface between two finite-conductivity (lossy) dielectrics are usually established in frequency domain. The original time domain form is less appropriate, even though it is also applicable.

3.3 ABOUT ELECTROSTATIC, MAGNETOSTATIC, AND DIRECT CURRENT APPROXIMATIONS

Certain approximations can be made when analyzing objects subject to electro-magnetic excitation. Consider an object under study on a certain size, D , with a given electromagnetic excitation at a frequency of $f = \omega/(2\pi)$ and the corresponding wavelength, λ , as shown in Figure 3.2; we assume that λ is the *shortest wavelength*

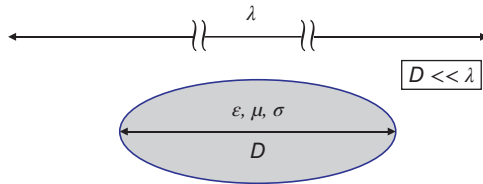


Figure 3.2 Illustration of electrostatic and magnetostatic approximations.

in the object material. The *necessary condition* for both electrostatic and magnetostatic approximations, and for the direct-current approximation to hold, is the condition [1]

$$D \ll \lambda, \lambda \equiv \frac{c}{f}, c = \frac{1}{\sqrt{\mu\epsilon}}. \quad (3.3)$$

In frequency domain, the time derivatives in Eq. (3.1a) and (3.1b) may be approximated as $\partial/\partial t \propto f$. On the other hand, the spatial derivatives may be approximated as $\partial/\partial x \propto \partial/\partial y \propto \partial/\partial z \propto 1/D$. Therefore, Eq. (3.3) rewritten in the form $f \ll c/D$ suggests that the two terms with time derivatives in both Eq. (3.1a) and (3.1b), respectively, are much smaller than the terms with spatial derivatives and can therefore be *neglected* entirely. The local speed of light, c , plays the role of the proportionality constant when such a comparison is made. The operation of neglecting all terms with time derivatives in Maxwell's equation is the *electrostatic and/or magnetostatic approximation* used in the majority of the general ECE circuit classes.

The word “static” used here may be somewhat confusing. It often means not only the true steady-state problems, but also a large number of problems where the time-dependence is present *parametrically*, through the time-dependent excitation conditions or otherwise. An example is given by currents and voltages in an AC circuit subject to a time-varying voltage. The current remains the same along the wire (follows a static pattern), which is then simply multiplied by a time-varying factor. At the same time, the absolute operating frequency may be still *quite high* – on the order of tens or hundreds of kHz or so. Therefore, the “static” approximation often also implies a low-frequency parametric approximation [1].

For antennas, Eq. (3.3) is not satisfied, except for the very small antennas. Indeed, any oscillating electromagnetic system eventually emits radio waves. However, the antennas comparable in size to the wavelength do it most efficiently.

3.4 ANALYTICAL SOLUTION TO MAXWELL'S EQUATIONS IN TIME DOMAIN. PLANE WAVES

Perhaps the most important solution to full Maxwell's equations is a *plane wave* shown in Figure 3.3. In Figure 3.3, the plane wave propagates with the speed of light in the y direction and has the vertical component of the electric field, E_z ,

and the (perpendicular) horizontal component of the magnetic field, H_x . It very much resembles an ocean wave coming toward you when you are on a beach where E_z plays the role of a vertical water movement. The only one (and principal) difference is that the plane wave has an extra field component (the H -field).

The plane wave is a one-dimensional solution for Maxwell's equations (3.1a)–(3.1e). With reference to Figure 3.3, Maxwell's equations in one dimension become

$$\text{Ampere's law } \epsilon \frac{\partial E_z}{\partial t} + \frac{\partial H_x}{\partial y} + J_z = 0, \quad (3.4a)$$

$$\text{Faraday's law } \mu \frac{\partial H_x}{\partial t} + \frac{\partial E_z}{\partial y} = 0. \quad (3.4b)$$

So far, no other equations become necessary. For simplicity, we assume that μ and ϵ are constants. Then, one can prove by direct substitution that one possible solution to Eq. (3.3), in a spatial domain where the excitation current J_z is zero, has the form,

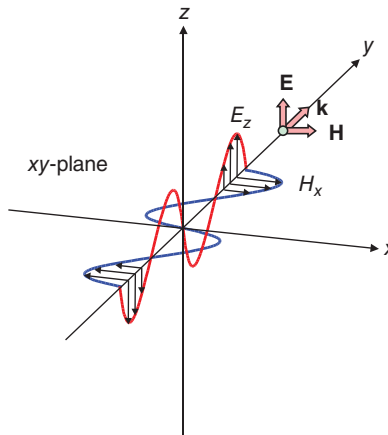


Figure 3.3 Plane electromagnetic wave that propagates along the x -axis.

$$E_z(y, t) = E_{z0} \cos \frac{\omega}{c}(y - ct), \quad (3.5a)$$

$$H_x(y, t) = \frac{1}{\eta} E_z(y, t), \quad (3.5b)$$

where

$$c = \frac{1}{\sqrt{\epsilon\mu}} \quad (3.5c)$$

is *speed of light* in a medium with dielectric permittivity ϵ and magnetic permeability μ (3.3×10^8 m/s in vacuum or air) and

$$\eta = \sqrt{\frac{\mu}{\epsilon}} \quad (3.5d)$$

is the *characteristic impedance* of the same medium with the units of ohms ($\sim 377 \Omega$ in vacuum or air). Such a solution in the form of a sinusoidal plane wave is shown in Figure 3.3.

The nature of the solution is better revealed if we differentiate Ampere's law with respect to time, plug in time derivative of H_x from Faraday's law, and finally arrive at (assuming there are no current sources in the domain of interest):

$$\frac{\partial^2 E_z}{\partial t^2} - c^2 \frac{\partial^2 E_z}{\partial y^2} = 0. \quad (3.6a)$$

Eq. (3.5a) is the famous *wave equation* appearing in many different disciplines. Its *general solution* is given by two arbitrary plane waves traveling with the speed of light in the two opposite directions:

$$E_z = f(y - ct) + g(y + ct). \quad (3.6b)$$

The first such wave is given by Eq. (3.5a) and (3.5b).

Note: The plane wave is so called because it has a plane *phase front* (the front of a constant phase); in contrast to spherical or cylindrical waves. In Figure 3.3, the phase front is given by any plane that is *parallel* to the xz -plane.

Any radiated field at large distances from any source is *locally* represented by plane waves. Such plane waves could be generated using different means, for example, by a GPS satellite, or by a base station antenna, or by your cell-phone far away from it, etc.

Note: It should be emphasized that Eq. (3.4a) and (3.4b) are *identical* to the equations for a radio-frequency (RF) transmission line if we replace the electric field by line voltage, the magnetic field – by line current, the dielectric constant – by line capacitance per unit length, and the magnetic permeability – by line inductance per unit length, i.e.

$$E \rightarrow V, H \rightarrow I, \epsilon \rightarrow C, \mu \rightarrow L.$$

This fact underscores a deep interconnection between the circuit quantities and the field quantities and allows us to better “visualize” the E - and H -fields as a “distributed” voltage and “distributed” current, respectively.

REFERENCES

1. C. A. Balanis, *Advanced Engineering Electromagnetics*, Wiley, New York, 2012, second edition.
2. R. F. Harrington, *Time-Harmonic Electromagnetic Fields*, McGraw Hill, New York, 1961 (Reprinted IEEE-Wiley, New York, 2001).

3. S. N. Makarov, G. M. Noetscher, and A. Nazarian, *Low-Frequency Electromagnetic Modeling for Electrical and Biological Systems Using MATLAB*. Wiley, New York, 2015.

PROBLEMS

1. (A) Express the speed of light in terms of medium's permittivity and permeability.
 (B) Express medium's characteristic impedance in terms of its permittivity and permeability.
 (C) State analogies between wave parameters and circuit parameters using comparison between the plane wave and the transmission line.
2. (A) Prove the vector identity $\nabla \cdot (\nabla \times \vec{A}) = 0$ for an arbitrary vector function $\vec{A}(\vec{r})$.
 (B) Prove the vector identity $\nabla \times (\nabla \phi) = 0$ for an arbitrary scalar function $\phi(\vec{r})$.
 (C) Prove the vector identity $\nabla \times \nabla \times \vec{A} = \nabla(\nabla \cdot \vec{A}) - \nabla^2 \vec{A}$ for an arbitrary vector function $\vec{A}(\vec{r})$.
 (D) Prove the vector identity $\vec{A} \times (\vec{B} \times \vec{C}) = (\vec{A} \cdot \vec{C})\vec{B} - (\vec{A} \cdot \vec{B})\vec{C}$ for three arbitrary vectors $\vec{A}, \vec{B}, \vec{C}$, either real or complex (bold).
3. 1. How many independent Maxwell's equations do we know?
 2. Why is Eq. (3.1a) called "Ampere's law"?
 3. What is a simple solution to Maxwell's equations with zero sources?
 4. What is the boundary condition on a surface of an ideal conductor (perfect metal)?
 5. How is Eq. (3.2d) transformed for the interface between a perfect conductor and air?
4. Prove by direct substitution that Eq. (3.5a)–(3.5c) for the plane wave are the solution to 1D Maxwell's equations (3.4a) and (3.4b). Provide all steps of your derivation.
5. Derive the wave equation, Eq. (3.6a). Provide all steps of your derivation.
6. Prove by direct substitution that Eq. (3.6b) is the solution of wave equation. Provide all steps of your derivation.

SECTION 2 SOLUTION FOR MAXWELL'S EQUATIONS IN TERMS OF ELECTRIC AND MAGNETIC POTENTIALS

3.5. Magnetic Vector Potential and Electric Scalar Potential	63
3.6. Comparison with the Static Case. Coulomb Gauge	64
3.7. Equations for Potentials. Lorentz Gauge	65
3.8. Wave Equations in Frequency Domain	66
3.9. Solution for Maxwell's Equations in Frequency Domain	67
References	69
Problems	69

3.5 MAGNETIC VECTOR POTENTIAL AND ELECTRIC SCALAR POTENTIAL

We will now obtain a general solution for Maxwell equations (3.1a)–(3.1e) in a homogeneous ($\mu = \mu_0 = \text{const}$, $\epsilon = \epsilon_0 = \text{const}$) unbounded medium (air) due to an arbitrary current and charge distribution. This solution describes the behavior of any high-frequency antenna or system, no matter what it is its particular shape or construction. We start with Eq. (3.1b) (Faraday's law) in the homogeneous medium

$$\mu_0 \frac{\partial \vec{H}}{\partial t} = -\nabla \times \vec{E} \quad (3.7a)$$

and use Eq. (3.1g) for the magnetic vector potential

$$\mu_0 \vec{H} = \nabla \times \vec{A}. \quad (3.7b)$$

This gives

$$\nabla \times \left[\vec{E} + \frac{\partial \vec{A}}{\partial t} \right] = 0. \quad (3.7c)$$

A general solution for Eq. (3.7c) has the form:

$$\vec{E} = -\nabla \varphi - \frac{\partial \vec{A}}{\partial t}. \quad (3.7d)$$

Here, φ can be an arbitrary function since $\nabla \times (\nabla \varphi) = 0$. Note that Eq. (3.7b) and (3.7d) define two vector fields (six unknowns total) in terms of two potentials: the (very familiar from static studies) *electric scalar potential* φ and the *magnetic*

vector potential \vec{A} , with *four* unknown total. This is a significant simplification of Maxwell equations.

3.6 COMPARISON WITH THE STATIC CASE. COULOMB GAUGE

Eq. (3.7d) is reduced to the well-known static result when time dependence is absent. In the *static case*, we obtain

$$\vec{E} = -\nabla\varphi \quad (3.8a)$$

where φ is the electric scalar potential with the units of volts. Substitution of this result into Gauss law, Eq. (3.1c), gives us *Poisson's equation* for the electric potential

$$\nabla \cdot \nabla\varphi = \nabla^2\varphi = -\frac{\rho}{\epsilon_0}, \quad (3.8b)$$

which is the basic equation of electrostatics. For a *given* charge distribution (electric charge is the source of the electric field), this equation determines the electric field potential and the electric field itself anywhere in space.

On the other hand, in the static case, Ampere's law Eq. (3.1a) yields

$$\nabla \times \vec{H} = \vec{J}. \quad (3.9a)$$

Substitution of Eq. (3.7b) into this expression gives

$$\nabla \times \nabla \times \vec{A} = \nabla(\nabla \cdot \vec{A}) - \nabla^2 \vec{A} = \mu_0 \vec{J}. \quad (3.9b)$$

The *Coulomb gauge* [1] is then used, which imposes the condition $\nabla \cdot \vec{A} = 0$. This yields

$$\nabla^2 \vec{A} = -\mu_0 \vec{J} \quad (3.9c)$$

or the basic equation of magnetostatics. Eq. (3.9c) is again *Poisson's equation* but now written for every component of the magnetic vector potential separately. For a given current distribution (electric current is the source of the magnetic field), this equation determines the magnetic vector potential and the magnetic field itself.

Question: What is the Coulomb gauge?

Answer: The magnetic vector potential in Eq. (3.7b) is defined to within a gradient of a certain function. The substitution $\vec{A} \rightarrow \vec{A} + \nabla\psi$ will still yield the same result, for an arbitrary function ψ . This function may be so chosen that $\nabla \cdot \vec{A} = 0$.

3.7 EQUATIONS FOR POTENTIALS. LORENTZ GAUGE

We will now use the full Ampere's law, i.e. Eq. (3.1a) and the so-called *Lorentz gauge* to derive the equations for both potentials. Applying the curl operation to both sides of Eq. (3.7b) yields

$$\mu_0 \nabla \times \vec{H} = \nabla \times \nabla \times \vec{A} = \nabla (\nabla \cdot \vec{A}) - \nabla^2 \vec{A}. \quad (3.10a)$$

Here, we have again used the vector identity $\nabla \times \nabla \times \vec{A} = \nabla (\nabla \cdot \vec{A}) - \nabla^2 \vec{A}$. We plug Eq. (3.10a) into Ampere's law (3.1a) and obtain

$$\epsilon_0 \mu_0 \frac{\partial \vec{E}}{\partial t} = \nabla (\nabla \cdot \vec{A}) - \nabla^2 \vec{A} - \mu_0 \vec{J}. \quad (3.10b)$$

As a final step, we substitute Eq. (3.7d) for the electric field, $\vec{E} = -\nabla \varphi - \frac{\partial \vec{A}}{\partial t}$. This gives

$$\nabla^2 \vec{A} - \epsilon_0 \mu_0 \frac{\partial^2 \vec{A}}{\partial t^2} = -\mu_0 \vec{J} + \left[\nabla (\nabla \cdot \vec{A}) + \epsilon_0 \mu_0 \nabla \frac{\partial \varphi}{\partial t} \right]. \quad (3.10c)$$

The term in square brackets is undesired, exactly as the term $\nabla(\nabla \cdot \vec{A})$ in magnetostatics, which was zeroed using the Coulomb gauge. To zero this entire term, we will use the *Lorentz gauge* Ref. [1], that is

$$\nabla \cdot \vec{A} + \epsilon_0 \mu_0 \frac{\partial \varphi}{\partial t} = 0 \Rightarrow \frac{\partial \varphi}{\partial t} = -\frac{1}{\epsilon_0 \mu_0} \nabla \cdot \vec{A}. \quad (3.10d)$$

Question: What is the Lorentz gauge?

Answer: The magnetic vector potential in Eq. (3.7b) is defined to within a gradient of a certain function. The substitution $\vec{A} \rightarrow \vec{A} + \nabla \psi$ will still yield the same result, for an arbitrary function ψ . This function may be so chosen that Eq. (3.10d) is satisfied.

Eq. (3.10c) and (3.10d) then become the required equations for both potentials:

$$\frac{\partial^2 \vec{A}}{\partial t^2} - \frac{1}{\epsilon_0 \mu_0} \nabla^2 \vec{A} = \mu_0 \vec{J}, \quad (3.11a)$$

$$\frac{\partial \varphi}{\partial t} = -\frac{1}{\epsilon_0 \mu_0} \nabla \cdot \vec{A}. \quad (3.11b)$$

Only the magnetic vector potential needs to be found from Eq. (3.11a) – the *inhomogeneous wave equation*. The electric scalar potential is then trivially

obtained from Eq. (3.11b). After the potentials are found, the fields are given by Eq. (3.7b) and (3.7d).

Note: Similar to the one-dimensional wave equation for plane waves from the previous section, we again arrive at wave equation (3.11a). However, now this is wave equation in *three dimensions*. Therefore, *multiple waves* may exist that propagate in all possible directions in the three-dimensional space.

Note: Eq. (3.11a) and (3.11b) in principle suffice to solve for the fields in any situation when the current source is known as a function of time; the current source may be either harmonic excitation or pulse excitation. This fact highlights the main practical purpose of the potentials: express the radiated fields in terms of the sources.

Well, one step is still remaining: we need to solve wave equation (3.11a). In order to do so, we will consider only time-harmonic fields and formulate this equation in frequency domain, i.e. in the phasor form.

3.8 WAVE EQUATIONS IN FREQUENCY DOMAIN

In phasor form or, which is the same, in the frequency domain, one introduces the time dependence in the form of a factor $\exp(j\omega t)$ for all the field quantities including

- the fields;
- the potentials;
- the sources.

The basic prerequisite for such a substitution is the linearity of Maxwell's equations. The factor $\exp(j\omega t)$ will then cancel out in every equation. The phasor method used here is equivalent to the phasor method for steady-state AC circuits studied in the ECE classes.

However, there is one significant difference. The phasors will no longer be complex constants, but they will become *complex functions* of the spatial coordinate, \vec{r} . The phasors will be denoted by the same letters as the original fields (and using bold letters for complex-valued vector quantities) and sources in time domain. Then, all spatial derivatives will remain the same while time derivatives will be transformed according to

$$\frac{\partial \varphi}{\partial t} \rightarrow j\omega \varphi, \quad \frac{\partial^2 \vec{A}}{\partial t^2} \rightarrow (j\omega)^2 \vec{A} = -\omega^2 \vec{A}. \quad (3.12)$$

The complex phasor vectors will again be denoted by bold letters, the phasors of scalar quantities with the Greek lowercase notations, e.g. the potential φ and charge density ρ , will be denoted by the same letters.

Example 3.1

Obtain wave equations for magnetic and electric potentials in frequency domain (such wave equations are called *Helmholtz equations* [1, 2]) and express the fields in terms of the potentials.

Solution: Wave equation (3.11a) for the magnetic vector potential is transformed to

$$\nabla^2 \vec{A} + k^2 \vec{A} = -\mu_0 \vec{J}, \quad k = \sqrt{\epsilon_0 \mu_0} \omega = \frac{\omega}{c_0}. \quad (3.13a)$$

Real scalar k is the familiar wave number. Applying the gradient operation to both sides of (3.13a) and using Eq. (3.11b) in frequency domain, $\nabla \cdot \vec{A} = -j\omega \epsilon_0 \mu_0 \varphi$, we obtain a similar equation for the electric scalar potential,

$$\nabla^2 \varphi + k^2 \varphi = -\frac{\rho}{\epsilon_0}. \quad (3.13b)$$

Eq. (3.13a) and (3.13b) form the so-called *mixed-potential formulation* of the Maxwell's equations. This formulation is very intuitive. It is also convenient from the numerical point of view and is widely used in the *Method of Moments* or *MoM* implemented in MATLAB Antenna Toolbox. Eq. (3.13a) and (3.13b) should be augmented with the current continuity equation in the phasor form,

$$j\omega \rho + \nabla \cdot \vec{J} = 0 \quad (3.13c)$$

expression for the electric field,

$$\vec{E} = -\nabla \varphi - j\omega \vec{A} \quad (3.13d)$$

and expression for the magnetic field,

$$\vec{H} = \frac{1}{\mu_0} \nabla \times \vec{A}. \quad (3.13e)$$

With all those steps done, the frequency-domain formulation becomes complete.

3.9 SOLUTION FOR MAXWELL'S EQUATIONS IN FREQUENCY DOMAIN

The inhomogeneous vector and scalar wave equations (3.13a) and (3.13b) have been studied by mathematicians and engineers for many years. About 120 years ago or so, it has been found that a general solution to those equations in an

unbounded medium, with the field decay at infinity, has the form of two similar volume (or surface, line) integrals

$$\vec{A}(\vec{r}) = \mu_0 \int \frac{\exp(-jk|\vec{r} - \vec{r}'|)}{4\pi|\vec{r} - \vec{r}'|} \vec{J}(\vec{r}') d\vec{r}', \quad (3.14a)$$

$$\varphi(\vec{r}) = \frac{1}{\epsilon_0} \int \frac{\exp(-jk|\vec{r} - \vec{r}'|)}{4\pi|\vec{r} - \vec{r}'|} \rho(\vec{r}') d\vec{r}' \quad (3.14b)$$

expressed in terms of the sources – the antenna currents and the charges. This fact again highlights the main practical purpose of the potentials: express the radiated fields in terms of the sources.

The structure of those integrals is of note. We integrate over \vec{r}' (the *integration variable*), but the result depends on \vec{r} (the *observation variable*). The integrand includes two parts: the source current $\vec{J}(\vec{r}')$ or the source charge $\rho(\vec{r}')$ and a function

$$G(\vec{r}, \vec{r}') = \frac{\exp(-jk|\vec{r} - \vec{r}'|)}{4\pi|\vec{r} - \vec{r}'|}, \quad (3.14c)$$

which is called the *Green's function* or the *fundamental solution* for hyperbolic Eq. (3.13a) and (3.13b).

Physically, the fundamental solution describes radiation of an infinitesimally small current element or, which is the same, radiation of an infinitesimally small oscillating charge. The radiated field is a spherical diverging wave. The fundamental solutions of the wave equation in spherical coordinates, Eq. (3.14a)–(3.14c), are valid at any frequency, all the way from DC to $f \rightarrow \infty$, and for any antenna or array geometry.

Note: The singularity is present in the denominator of the Green's function. Therefore, the integrals must be evaluated carefully.

Eq. (3.14a)–(3.14c) complete the formal solution of Maxwell's equations in the phasor form. If the current and charge distributions for an antenna are known and/or given, we find integrals (3.14a) and (3.14b) first. Then, we calculate the radiated fields from Eq. (3.13d) and (3.13e). Using these fields, we finally calculate the radiated power and the radiation pattern of an antenna.

Question: Is it so simple? Did we solve Maxwell's equations just in one lecture? Why are then so many engineers and software companies on the market spending a significant amount of time trying to solve Maxwell's equations?

Answer: There is a trick here that is often hidden in some electromagnetics texts until the very last moment. In fact, currents and charges in Eq. (3.14a) and (3.14b), are *not known* a priori. The only fact that we really know is the voltage in the antenna feed. But the current (and charge) distributions along an antenna body need to be computed separately.

This procedure is the main difficulty for all numerical methods. Before using Eq. (3.14a) and (3.14b) directly, these equations may be applied to antenna boundaries, with the corresponding boundary conditions. From those boundary conditions and from the known feeding source, currents and charges on the antenna may be established, by solving a (large) system of linear equations. This is the MoM formulation. Other modeling methods such as the finite element method (FEM) and the finite difference time domain method (FDTD) exist.

The sine current distribution along the dipole antenna introduced in Chapter 2 is also not the exact result, but is rather a (good) approximation to reality. In fact, according to the exact numerical analysis, the sine distribution should be augmented with a certain phase shift along the dipole axis and angular nonuniformity, which may become more significant for thick dipoles as well as dipole arrays [3].

REFERENCES

1. C. A. Balanis, *Advanced Engineering Electromagnetics*, Wiley, New York, 2012, second edition.
2. C. A. Balanis, *Antenna Theory: Analysis and Design*, Wiley, New York, 2016, fourth edition.
3. R. C. Hansen, “Carter dipoles and resonant dipoles,” *34th Antenna Applications Sym.*, Allerton Park, Monticello, IL, Sept. 2010.

PROBLEMS

1. (A) Which units does the electric scalar potential have?
 (B) Which units does the magnetic vector potential have?
 (C) Express the wavenumber in terms of (i) angular frequency;
 (ii) wavelength.
2. (A) Explain the meaning of the Coulomb gauge in your own words. What is it used for? How is it justified?
 (B) Explain the meaning of the Lorentz gauge in your own words. What is it used for? How is it justified?
 (C) How is the static result $\vec{E} = -\nabla\varphi$ known for college physics modified in a time-varying electromagnetic field?
 (D) Explain in your own words why are the electric and magnetic potentials important? What do they allow us to do?

3. Present a general solution for static Poisson equation (3.8b) if the charge distribution in space is known. Repeat for the magnetostatic equation (3.9c) if the current distribution in space is known.
4. Derive Eq. (3.13b) for the electric scalar potential. Provide all steps of your derivation.
5. For a given current distribution $\vec{J}(\vec{r})$, write a general solution to Maxwell's equations for E- and H-fields in an unbounded space at any frequency when *there are no free charges*: $\rho(\vec{r}) = 0$. A loop of a uniform time-varying electric current gives us an example of such a solution with $\rho(\vec{r}) = 0$.
6. (A) An infinitesimally small *static* electric charge generates an electric field. How fast does the electric field decrease with increasing the distance, r , from the source?
(B) A hypothetical infinitesimally small oscillating charge radiates into free space. How fast does the electric field decrease with increasing the distance, r , from the source?
(C) An infinitesimally small yet realistic current element radiates into free space. How fast does the electric field decrease with increasing the distance, r , from the source?

Based on your answers, do you see *one major advantage* of electromagnetic radiation over the static or quasistatic fields?

SECTION 3 ANTENNA RADIATION

3.10. Radiation of a Small Uniform Current Element ($I_A \ll \lambda$)	71
3.11. Near- and Far-field Regions for a Small Antenna	75
3.12. Radiation of a Dipole with the Sinusoidal Current Distribution	77
References	80
Problems	81

3.10 RADIATION OF A SMALL UNIFORM CURRENT ELEMENT ($I_A \ll \lambda$) [1]

Now, the first problem of practical importance – radiation of a small current element (*current dipole*) into free space – will be solved. The corresponding geometry is shown in Figure 3.4. A current element in the form of an infinitesimally thin cylinder of length l_A carries a uniform in space but sinusoidally varying in time electric current with a constant phasor amplitude I_0 . We will assume that I_0 is some real number although this is not a significant assumption. The length of the current element is small compared to the wavelength at any frequency of interest, that is $l_A \ll \lambda$.

Strictly speaking, the uniform current element cannot be used as a small dipole antenna: the current must be zero at the dipole tips, irrespective of the dipole size. However, we could further subdivide any nonuniform current into small uniform pieces and then add up the fields of every such piece. This approach explains why the idealized current element is important.

Thus, the electric current along the hypothetical current element in Figure 3.4 is a constant in space *line current*. For the line current, we may still define the volumetric *current density*, $\vec{J}(\vec{r})$, in the form,

$$\vec{J}(\vec{r}) = \delta(x)\delta(y)I_0 \vec{a}_z, \quad -l_A/2 < z < l_A/2, \quad (3.15)$$

where $\delta(x)$, $\delta(y)$ are two delta functions, \vec{a}_z is the unit vector in the direction of the z -axis. We substitute this result in Eq. (3.14a), which originally includes the volumetric integral,

$$\vec{A}(\vec{r}) = \mu_0 \int \frac{\exp(-jk|\vec{r} - \vec{r}'|)}{4\pi|\vec{r} - \vec{r}'|} \vec{J}(\vec{r}') d\vec{r}' \quad (3.16a)$$

and then evaluate this integral analytically when $l_A \rightarrow 0$ and $|\vec{r}| \rightarrow \infty$. Two delta functions reduce the volume integral to a line integral, i.e.

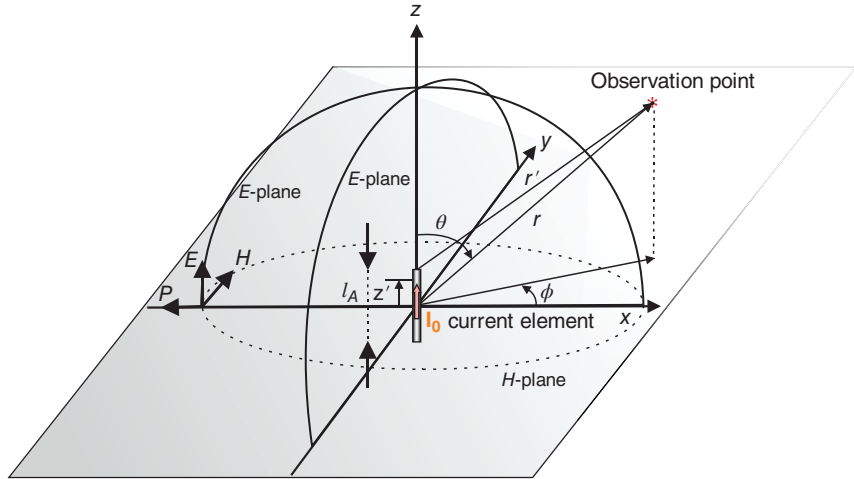


Figure 3.4 Coordinate system and radiating configuration for a small current element (the current dipole).

$$\vec{A}(\vec{r}) = \mu_0 I_0 \vec{a}_z \int_{-\frac{l_A}{2}}^{\frac{l_A}{2}} \frac{\exp(-jk|\vec{r} - (0, 0, z')|)}{4\pi|\vec{r} - (0, 0, z')|} dz' \rightarrow$$

$$\vec{A}(\vec{r}) = \vec{a}_z \frac{\mu_0 I_0 l_A}{4\pi|\vec{r}|} \exp(-jk|\vec{r}|) \text{ when } l_A \rightarrow 0 \text{ and } |\vec{r}| \rightarrow \infty.$$
(3.16b)

This result becomes exact for any observation point in space in the limit $l_A \rightarrow 0$. Note that the magnetic vector potential always behaves *similar* to the exciting current. For example, in the present case it has also only one vertical component, strictly parallel to the current dipole.

The magnetic field is found by finding the curl of the magnetic vector potential,

$$\vec{H} = \frac{1}{\mu_0} \nabla \times \vec{A},$$
(3.16c)

which is a nontrivial operation. Before doing this, we will switch to the spherical coordinate system from the rectangular coordinate system as shown in Figure 3.4. The standard conversion approach for vector \vec{A} utilizes the matrix–vector product and is given by

$$\begin{bmatrix} A_r \\ A_\theta \\ A_\phi \end{bmatrix} = \begin{bmatrix} \sin \theta \cos \varphi & \sin \theta \sin \varphi & \cos \theta \\ \cos \theta \cos \varphi & \cos \theta \sin \varphi & -\sin \theta \\ -\sin \varphi & \cos \varphi & 0 \end{bmatrix} \begin{bmatrix} A_x \\ A_y \\ A_z \end{bmatrix}.$$
(3.17)

Since Eq. (3.16b) predicts only the z -component of the magnetic vector potential, we obtain from (3.17) three components of the magnetic vector potential in the spherical coordinate system in the form:

$$\mathbf{A}_r = \mathbf{A}_z \cos \theta = \frac{\mu_0 I_0 l_A}{4\pi |\vec{r}|} \exp(-jk|\vec{r}|) \cos \theta,$$

$$\mathbf{A}_\theta = -\mathbf{A}_z \sin \theta = -\frac{\mu_0 I_0 l_A}{4\pi |\vec{r}|} \exp(-jk|\vec{r}|) \sin \theta, \mathbf{A}_\varphi = 0. \quad (3.18)$$

Next, one uses Eq. (3.18) to calculate the magnetic field, \vec{H} . The curl expansion in spherical coordinates is as follows:

$$\begin{aligned} \nabla \times \vec{A} &= \vec{a}_r \frac{1}{|\vec{r}| \sin \theta} \left[\frac{\partial}{\partial \theta} (\mathbf{A}_\varphi \sin \theta) - \frac{\partial \mathbf{A}_\theta}{\partial \varphi} \right] \\ &\quad + \vec{a}_\theta \frac{1}{|\vec{r}|} \left[\frac{1}{\sin \theta} \frac{\partial \mathbf{A}_r}{\partial \varphi} - \frac{\partial}{\partial r} (|\vec{r}| \mathbf{A}_\varphi) \right] + \vec{a}_\varphi \frac{1}{|\vec{r}|} \left[\frac{\partial}{\partial r} (|\vec{r}| \mathbf{A}_\theta) - \frac{\partial \mathbf{A}_r}{\partial \theta} \right], \end{aligned} \quad (3.19)$$

where \vec{a}_r , \vec{a}_θ , \vec{a}_φ are directional unit vectors in spherical coordinates. Note that according to Eq. (3.18) the azimuthal component of the vector potential is zero while the radial and elevation components do not possess any azimuthal variation due to the axial symmetry. Therefore, only the last azimuthal term on the right-hand side of Eq. (3.19) is different from zero and the H-field has only one azimuthal component in the form:

$$\begin{aligned} \vec{H} &= \frac{1}{\mu_0} \nabla \times \vec{A} = \vec{a}_\varphi \frac{1}{\mu_0 |\vec{r}|} \left[\frac{\partial}{\partial r} (|\vec{r}| \mathbf{A}_\theta) - \frac{\partial \mathbf{A}_r}{\partial \theta} \right] \\ &\rightarrow \vec{H} = \vec{a}_\varphi \frac{jk I_0 l_A \sin \theta}{4\pi |\vec{r}|} \left[1 + \frac{1}{jk |\vec{r}|} \right] \exp(-jk|\vec{r}|). \end{aligned} \quad (3.20)$$

The electric field is found next. We use Ampere's law in the phasor form and obtain

$$\vec{E} = \frac{1}{j\omega \epsilon_0} \nabla \times \vec{H} \quad (3.21)$$

everywhere in space except the current element itself. To evaluate (3.21), we apply the similar procedure and use the fact that that radial and elevation components of the magnetic field are zero. Therefore, the curl of the magnetic field becomes

$$\nabla \times \vec{H} = \vec{a}_r \frac{1}{|\vec{r}| \sin \theta} \left[\frac{\partial}{\partial \theta} (\mathbf{H}_\varphi \sin \theta) \right] + \vec{a}_\theta \frac{1}{|\vec{r}|} \left[-\frac{\partial}{\partial r} (|\vec{r}| \mathbf{H}_\varphi) \right]. \quad (3.22)$$

Calculating the various partial derivatives in Eq. (3.22) and substituting $k/\omega\epsilon_0 = \eta$, we finally arrive at

$$\begin{aligned}\vec{E} &= \vec{a}_r \frac{\eta I_0 l_A \cos \theta}{2\pi |\vec{r}|^2} \left(1 + \frac{1}{jk|\vec{r}|} \right) \exp(-jk|\vec{r}|) \\ &+ \vec{a}_\theta \frac{j\eta k I_0 l_A \sin \theta}{4\pi |\vec{r}|} \left(1 + \frac{1}{jk|\vec{r}|} - \frac{1}{k^2 |\vec{r}|^2} \right) \exp(-jk|\vec{r}|).\end{aligned}\quad (3.23)$$

Example 3.2

Summarize the exact analytical solution for the radiation of an infinitesimally short current dipole ($l_A \rightarrow 0$).

Solution: With reference to Figure 3.4, Eq. (3.23) and (3.20) yield

E-field:

$$\begin{aligned}\mathbf{E}_r &= \frac{\eta I_0 l_A \cos \theta}{2\pi |\vec{r}|^2} \left(1 + \frac{1}{jk|\vec{r}|} \right) \exp(-jk|\vec{r}|), \\ \mathbf{E}_\theta &= \frac{j\eta k I_0 l_A \sin \theta}{4\pi |\vec{r}|} \left(1 + \frac{1}{jk|\vec{r}|} - \frac{1}{k^2 |\vec{r}|^2} \right) \exp(-jk|\vec{r}|), \\ \mathbf{E}_\varphi &= 0\end{aligned}\quad (3.24a)$$

H-field:

$$\begin{aligned}\mathbf{H}_r &= 0, \\ \mathbf{H}_\theta &= 0, \\ \mathbf{H}_\varphi &= \frac{j k I_0 l_A \sin \theta}{4\pi |\vec{r}|} \left[1 + \frac{1}{jk|\vec{r}|} \right] \exp(-jk|\vec{r}|).\end{aligned}\quad (3.24b)$$

Note that in the far field, only the components \mathbf{E}_θ and \mathbf{H}_φ remain important.

3.11 NEAR- AND FAR-FIELD REGIONS FOR A SMALL ANTENNA

For small antennas (shorter than half of the wavelength):

1. The *near-field (or reactive near field) region* is defined as that region where $|\vec{r}| \leq \frac{\lambda}{2\pi} \approx 0.16\lambda$ [1].
2. The *far-field (or the radiating field) region* is commonly defined as that region where $|\vec{r}| \geq 2\lambda$ [1].
3. The *transition region (or radiating near field region)* can then be defined by $\frac{\lambda}{2\pi} \leq |\vec{r}| \leq 2\lambda$ [1].

Emphasize, that the factor $k|\vec{r}|$ in Eq. (3.24a) and (3.24b) is equal to $2\pi|\vec{r}|/\lambda$. Therefore,

1. In the near-field region, the factor $\frac{1}{k|\vec{r}|}$ is greater than one and dominates the solution. In this region, the fields are very strong, i.e. $\mathbf{E}_r \propto \frac{1}{|\vec{r}|^3}$, $\mathbf{E}_\theta \propto \frac{1}{|\vec{r}|^3}$, $\mathbf{H}_\phi \propto \frac{1}{|\vec{r}|^2}$. As a result, any object placed in the near field of an antenna may significantly alter antenna operation.
2. In the far-field region, the factor $\frac{1}{k|\vec{r}|}$ is much less than one. In this region, only two nontrivial field components are: $\mathbf{E}_\theta \propto \frac{1}{|\vec{r}|}$, $\mathbf{H}_\phi \propto \frac{1}{|\vec{r}|}$.
3. All other components such as $\mathbf{E}_r \propto \frac{1}{|\vec{r}|^2} \rightarrow 0$ can be neglected in the far field.

Eq. (3.24a) and (3.24b) are valid both in the far and near fields. In the far field, the E- and H-fields are those in a locally plane wave; they are related through the medium impedance η as shown in Section 1 of this chapter.

In the near field, the situation is quite different. Therefore, a legitimate question to ask is the following: which field (electric or magnetic) is the largest in the near field of the small dipole antenna? To answer this question, we may want to define a *local wave impedance*. The classical wave impedance (medium impedance) for a plane wave in free space is known to be $\eta = 377 \Omega$. This impedance can be expressed in the form,

$$\frac{|\vec{\mathbf{E}}|}{|\vec{\mathbf{H}}|} = \eta = 377 \Omega \quad (3.25a)$$

everywhere in space. When the plane wave assumption is discarded (the near field) one still could use Eq. (3.25a) and define a *local wave impedance magnitude*, which in the present case is expressed by

$$\frac{|\vec{E}|}{|\vec{H}|} = \eta_{wave} = \frac{\sqrt{|E_r|^2 + |E_\theta|^2 + |E_\phi|^2}}{\sqrt{|H_r|^2 + |H_\theta|^2 + |H_\phi|^2}} = \frac{\sqrt{|E_r|^2 + |E_\theta|^2}}{\sqrt{|H_\phi|^2}}. \quad (3.25b)$$

Example 3.3

Evaluate the “local wave impedance magnitude” (ratio of the magnitudes of electric and magnetic fields), Eq. (3.25b), for the small radiating current dipole and discuss the importance of the near field.

Solution: After substituting the solution Eq. (3.24a) and (3.24b) into Eq. (3.25b) and programming the corresponding result in MATLAB, one obtains a plot of the local wave impedance shown in Figure 3.5. Certainly, the electric field strongly dominates very close to the radiating current element, at the distances of about 0.1 wavelength whereas the magnetic field slightly dominates at the distances from 0.1 to 0.5 wavelength. Further, the local impedance approaches the wave impedance – the radiated field becomes a plane wave propagating from the dipole. The dominance of the electric field close to the radiator is one reason why the dipole antenna is sometimes called the *electric antenna*. For an infinitesimally small loop, the opposite situation occurs – the loop is therefore called the *magnetic antenna*.

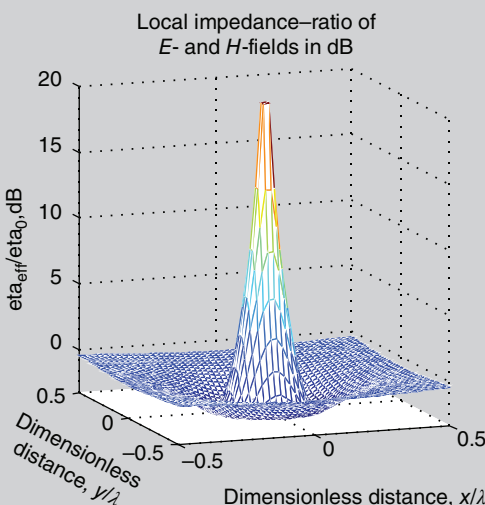


Figure 3.5 Plot of the ratio of the magnitudes of electric and magnetic fields in dB in the near field of the radiating current dipole. The plot corresponds to the *xy*-plane in Figure 3.4 or to the *H*-plane.

The electric field is more sensitive to dielectric-material loading whereas the magnetic field is more sensitive to magnetic-material loading. Therefore, a loop antenna in close proximity to a human body (a lossy dielectric but a nonmagnetic material) may still perform reasonably well whereas the dipole antenna may lose its performance.

The corresponding MATLAB script follows:

```
% EM data
epsilon = 8.85418782e-012; % Vacuum, F/m
mu = 1.25663706e-006; % Vacuum, H/m
c = 1/sqrt(epsilon*mu); % Vacuum, m/s
eta = sqrt(mu/epsilon); % Vacuum, Ohm

% Field data
f = 1e9; % Frequency, Hz
lambda = c/f; % Wavelength, m
k = 2*pi/lambda; % Wavenumber, 1/m
D = lambda/2; % Half size of the observation plane, m
x = linspace(-D, D, 50);
y = linspace(-D, D, 50);
[X,Y] = meshgrid(x, y);
r = sqrt(X.^2 + Y.^2);

% Local wave impedance
kr = k*r;
ETA = sqrt((1 - 1./kr.^2 + 1./kr.^4)./(1 + 1./kr.^2));
ETA(find(ETA>10)) = 10;
% ETA(find(ETA<1)) = 1;
mesh(X/lambda, Y/lambda, 10*log10(ETA.^2));
view(-20, 10); axis tight;
title('Local impedance - ratio of E- and H-fields in dB');
xlabel('dimensionless distance, x/lambda');
ylabel('dimentionless distance, y/lambda');
zlabel('eta, dimensionless in dB'); colormap jet;
```

3.12 RADIATION OF A DIPOLE WITH THE SINUSOIDAL CURRENT DISTRIBUTION

3.12.1 Problem Statement

The next and more complicated problem is the radiation of a dipole with a sinusoidal current distribution – see Figure 3.6 that follows. Based on the solution for the infinitesimal radiating current element, one can derive the solution for a dipole with the sinusoidal current distribution.

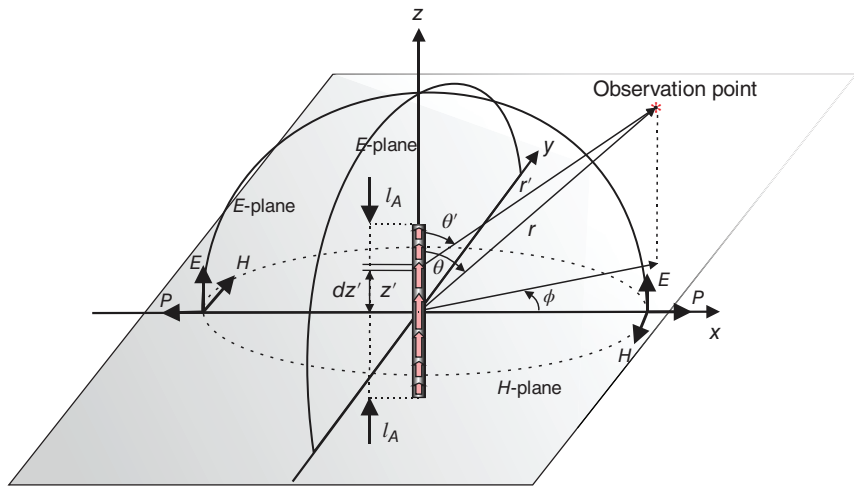


Figure 3.6 Coordinate system and radiating configuration for a finite dipole element.

According to Eq. (2.2), the sinusoidal current distribution along the dipole in Figure 3.6 is assumed to have the form,

$$\vec{I}(z') = \vec{a}_z I_a \frac{\sin\left(k\left[\frac{l_A}{2} - |z'|\right]\right)}{\sin\left(k\frac{l_A}{2}\right)}, \quad |z'| \leq l_A/2, \quad (3.26)$$

where $k = 2\pi/\lambda$ is again the wavenumber and \vec{a}_z is the unit vector in the z -direction (dipole direction), I_a is the antenna feed current, either real or complex. Although the dipole radius a (for cylindrical dipoles) or dipole width t (for blade dipoles) is not explicitly present in Eq. (3.26), this result still holds for relatively thin dipoles.

The idea is now to subdivide the entire current along the dipole into infinitesimally short current elements of length dz' and of current strength $\vec{I}(z')$, and then add up all solutions for them given by Eq. (3.24a) and (3.24b) in order to obtain the total radiated field. This procedure is cumbersome in the near field. In the far field, the solution considerably simplifies as shown in the following section.

3.12.2 Solution in the Far Field

Consider an infinitesimal current element of length dz' and constant current strength $\vec{I}(z')$ located at z' in Figure 3.6. We can write $\vec{I}(z') = \vec{a}_z I(z')$. As applied to the far field, Eq. (3.24a) and (3.24b) are reduced to

$$dE_\theta = \frac{j\eta k I(z') dz' \sin \theta}{4\pi |\vec{r}'|} \exp\left(-jk|\vec{r}'|\right), \quad E_r = 0, \quad E_\phi = 0, \quad (3.27a)$$

$$d\mathbf{H}_\varphi = \frac{jk\mathbf{I}(z')dz' \sin \theta}{4\pi |\vec{r}'|} \exp(-jk|\vec{r}'|), \quad \mathbf{H}_r = 0, \quad \mathbf{H}_\theta = 0, \quad (3.27b)$$

$$|\vec{r}'| = \sqrt{|\vec{r}|^2 + z'^2 - 2 \cos(\theta)z'|\vec{r}|} \quad \text{law of cosines.} \quad (3.27c)$$

In the far field, i.e. at $|\vec{r}| \gg z'$, Eq. (3.27c) simplifies to

$$|\vec{r}'| \approx |\vec{r}| - z' \cos \theta \quad (3.27d)$$

or eventually to

$$|\vec{r}'| \approx |\vec{r}|. \quad (3.27e)$$

We plug Eq. (3.27d) into the phase terms (which require a more precise treatment) and Eq. (3.27e) into the amplitude terms (which require a less precise treatment), and obtain

$$d\mathbf{E}_\theta = \left[\frac{j\eta k \sin \theta \exp(-jk|\vec{r}|)}{4\pi |\vec{r}|} \right] \mathbf{I}(z') \exp(jkz' \cos \theta) dz', \quad (3.28a)$$

$$d\mathbf{H}_\varphi = \left[\frac{jk \sin \theta \exp(-jk|\vec{r}|)}{4\pi |\vec{r}|} \right] \mathbf{I}(z') \exp(jkz' \cos \theta) dz'. \quad (3.28b)$$

The terms in square brackets in Eq. (3.28a) and (3.28b) do not depend on the position of the small radiation current element. Adding up the contributions of all such infinitesimal dipoles, one has for the total radiated field

$$\mathbf{E}_\theta = \left[\frac{j\eta k \sin \theta \exp(-jk|\vec{r}|)}{4\pi |\vec{r}|} \right] \int_{-l_A/2}^{+l_A/2} \mathbf{I}(z') \exp(jkz' \cos \theta) dz', \quad (3.29a)$$

$$\mathbf{H}_\varphi = \left[\frac{jk \sin \theta \exp(-jk|\vec{r}|)}{4\pi |\vec{r}'|} \right] \int_{-l_A/2}^{+l_A/2} \mathbf{I}(z') \exp(jkz' \cos \theta) dz'. \quad (3.29b)$$

The last step is to plug the current distribution given by Eq. (3.26) into Eq. (3.29a) and (3.29b). Due to symmetry of $\mathbf{I}(z')$, we end up with a single integrand of the type $\cos(kz' \cos \theta) \sin\left(k\left[\frac{l_A}{2} - |z'|\right]\right)$. The corresponding integral is found analytically and the final result becomes rather simply, i.e.

$$\mathbf{E}_\theta = \left[\frac{j\eta \exp(-jk|\vec{r}|)}{2\pi |\vec{r}|} \mathbf{I}_a \right] \left\{ \frac{\cos\left(\frac{kl_A}{2} \cos\theta\right) - \cos\left(\frac{kl_A}{2}\right)}{\sin\left(k\frac{l_A}{2}\right) \cdot \sin\theta} \right\}, \quad (3.30a)$$

$$\mathbf{H}_\varphi = \frac{\mathbf{E}_\theta}{\eta}. \quad (3.30b)$$

Eq. (3.30a) and (3.30b) are valid everywhere in the far field, i.e. at any direction of the radiated wave.

The factor in curly brackets in Eq. (3.30a) determines the direction of dipole radiation. It depends on the elevation angle. It also depends on antenna length and frequency of operation. It looks somewhat complicated but, as a matter of fact, produces a rather smooth *radiation pattern* of the well-known donut shape.

On the other hand, the factor in square brackets in Eq. (3.30a) defines an isotropic field decay due to geometrical divergence. It does not depend on the particular direction.

Example 3.4

In Chapter 2, the radiated dipole field \mathbf{E}_z that propagates along the x -axis was given by Eq. (2.6), i.e.

$$\vec{\mathbf{E}} = (0, 0, \mathbf{E}_z), \mathbf{E}_z = -j\eta \frac{\mathbf{I}_a}{2\pi} \frac{1 - \cos\left(\frac{kl_A}{2}\right)}{\sin\left(\frac{kl_A}{2}\right)} \frac{\exp(-jkr)}{r}. \quad (3.30c)$$

Show that this result coincides with Eq. (3.30a).

Solution: Along the x -axis, the z -component of the electric field is equal to the minus θ -component, i.e. $\mathbf{E}_z = -\mathbf{E}_\theta$ at $\theta = \pi/2$. Further, we plug $\theta = \pi/2$ into Eq. (3.30a) and obtain exactly Eq. (2.6) with taking into account the shortcut $|\vec{r}| = r$.

In order to visualize this solution and understand its importance, we will further need to calculate a *radiation pattern* of a dipole; in other words, calculate its *directivity* and *gain*.

REFERENCES

1. C. A. Balanis, *Antenna Theory: Analysis and Design*, Wiley, New York 2016, fourth edition.
2. C. A. Balanis, *Advanced Engineering Electromagnetics*, Wiley, New York, 2012, second edition.

3. S. N. Makarov, A. Puzella, and V. Iyer, "Scan impedance for an infinite dipole array: Accurate theoretical model compared to numerical software," *IEEE Antennas Prop. Magazine*, vol. 50, no. 6, pp. 132–149, December 2008, doi: 10.1109/MAP.2008.4768944.

PROBLEMS

1. Explain in detail the procedure of obtaining fields for the small radiating current dipole step by step, i.e.
 - (A) Introduce the electric scalar potential ϕ and the magnetic vector potential \vec{A} ;
 - (B) ...
 - (C) ...
 - (D) ...
2. For a small radiating current element, determine asymptotic behavior of the local wave impedance when $|\vec{r}| \rightarrow 0$ (find the main term of the asymptotic expansion).
3. (A) For a small radiating current element, how are the field components, \mathbf{H}_φ , \mathbf{E}_θ , related to each other in the far field, i.e. at $|\vec{r}| \rightarrow \infty$? **Hint:** Keep only the dominant terms in the corresponding expressions at $|\vec{r}| \rightarrow \infty$.
 - (B) What is a value of the radiated electric field \mathbf{E}_θ of a finite dipole in Eq. (3.30a) at $\theta = 0$, i.e. at zenith? **Hint:** Consider the case of small, but finite θ , and then find the limit at $\theta \rightarrow 0$.
 - (C) What is the corresponding field value at $\theta = 180^\circ$?
- 4*. 1. What is the value of the radiated electric field \mathbf{E} of a finite-length dipole?
 - (A) At $\theta = 0$, i.e. at zenith?
 - (B) At $\theta = 180^\circ$?

2. Justify your answer using the MATLAB Antenna Toolbox.
5. Derive Eq. (3.30a) using direct substitution of the sinusoidal current distribution and the following integration.
6. A geometry shown in Figure 3.7 is used to obtain *Pocklington integral equation* [1–3] for the electric current distribution along a dipole antenna.
 - (A) Express \mathbf{E}_x -component of the electric field in terms of the magnetic vector potential.
 - (B) Express the magnetic vector potential in terms of antenna current density \mathbf{J}_x directed along the x -axis.

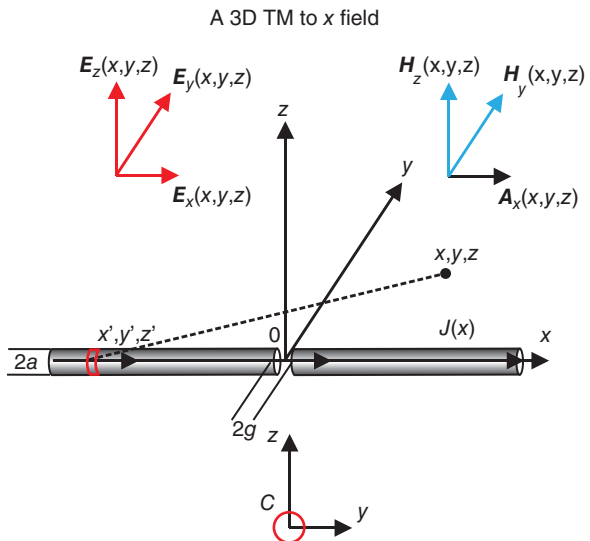


Figure 3.7 Dipole geometry for Pocklington integral equation. *Source:* S. N. Makarov, A. Puzella, and V. Iyer, “Scan impedance for an infinite dipole array: Accurate theoretical model compared to numerical software,” *IEEE Antennas Prop. Magazine*, vol. 50, no. 6, pp. 132–149, December 2008. © 2008, IEEE.

- (C) Obtain an integral equation for the antenna current using the corresponding boundary condition on the surface of a metal antenna.
- 7*. The foundations for the radiation pattern and directivity of an antenna are the electric and magnetic fields. Calculate the electric and magnetic fields for the half-wavelength dipole antenna. Use a strip dipole antenna from the MATLAB Antenna Toolbox™, with the length of 0.5 m and the width of 1 cm oriented along the z -axis and find the fields at a distance of half-wavelength along the positive x -axis. (*Hint:* Use the EHfields command for this problem. Read the help text for this.) Based on the information provided, you should be able to figure out the frequency at which the analysis is performed. Document and report your results.
- 8*. Using the dipole created in Problem 7, plot the electric field magnitude as a function of both distance and frequency along the positive x -axis.
 - (A) Compute the electric and magnetic field magnitude in dB (use 1 V/m reference) over the distance interval from $\lambda/10$ to 10λ . Turn in the plots and comment on the strength as well as the variations in the field.
 - (B) Pick a distance of 5λ along the positive x -axis. Compute the electric field at this distance for frequency band 200–400 MHz. Turn in the plot showing the field magnitude variation as a function of frequency.

- 9*.** The nature of the field regions surrounding an antenna has been described in this section. In addition to that, there is a very nice article about this subject available online: <http://m.eet.com/media/1140931/19213-150828.pdf>

Read this article and recreate Figure 3.2 from this article using the MATLAB Antenna Toolbox. Here is a sample code to help you start working on this problem:

```
f = 1e9;
c = physconst('lightspeed');
lambda = c/f;
wavenumber = 2*pi/lambda;
d = dipole;
d.Length = lambda/20;
d.Width = lambda/400;
circumference = lambda/20;
r = circumference/(2*pi);
l = loopCircular;
l.Radius = r;
l.Thickness = circumference/200;
md = mesh(d,'MaxEdgeLength',0.0003);
ml = mesh(l,'MaxEdgeLength',0.0003);
```

SECTION 4 ANTENNA DIRECTIVITY AND GAIN

3.13. Antenna Directivity	84
3.14. Antenna Gain and Realized Gain	90
3.15. Antenna Effective Aperture – Receiving Antenna as a Power Collector	92
3.16. Friis Transmission Equation	94
References	97
Problems	97

In the previous section, the dipole's near and far fields have been derived analytically. Now, it is time to convert this solution into antenna's directivity, gain, and the effective antenna aperture. The definitions of directivity, gain, and antenna aperture introduced in this section are valid not only for the simple dipole, but also for all other antennas. The antenna/array gain studied in this section is somewhat similar to the amplifier's gain; however, it depends on the direction of radiation.

3.13 ANTENNA DIRECTIVITY

3.13.1 Meaning

Antenna directivity D is defined as “the ratio of the radiation intensity in a given direction from the antenna to the radiation intensity averaged over all directions.” In other words, the directivity is the ratio of power radiated by the antenna in any direction to the power radiated in the same direction by a hypothetical isotropic source of the same total power. The antenna directivity is only meaningful in the far field. It does not depend on the total radiated power.

The antenna directivity D , $D|_{\text{dB}} = 10 \log_{10} D$, has the following features:

1. The directivity of an *isotropic antenna source* (though not existing in the nature) is one (or 0 dB).
2. If the antenna directivity is two (3 dB) in one direction and one (0 dB) in another direction, the antenna-radiated (received) power in the first direction is two times greater.
3. If the antenna directivity is 16 (12 dB) in one direction and one (0 dB) in another direction, the antenna-radiated (received) power in the first direction is 16 times greater, etc.
4. The antenna directivity cannot be greater than one (or greater than 0 dB) in all directions simultaneously. If it is greater than one in one particular direction, then it must be less than one (or become negative in dB) in some other directions.

The antenna directivity is essentially the angle-dependent “gain” of an antenna as compared to the isotropic radiator/receiver. In this sense, the antenna becomes an amplifier in certain directions while compared to the isotropic radiator/receiver.

3.13.2 Definition of Radiation Density

Average power per unit area radiated by an antenna in free space is given by the (always real-valued) *Poynting vector*

$$\vec{P} = \frac{1}{2} \operatorname{Re} (\vec{E} \times \vec{H}^*) \quad (3.31)$$

with the units of W/m^2 ($\text{V/m A/m} = \text{W/m}^2$). The cross product in Eq. (3.31) assures the correct direction of the radiated power (from the antenna) everywhere in space as shown in Figure 3.8. Eq. (3.31) looks very similar to the corresponding scalar result for AC circuits – compare Eq. (2.3):

$$P = \frac{1}{2} \operatorname{Re} (\mathbf{V} \cdot \mathbf{I}^*). \quad (3.32)$$

Everywhere in the far field, the radiated wave is a *local* plane wave, that is

$$\vec{H} = \frac{\vec{n} \times \vec{E}}{\eta}, \quad (3.33)$$

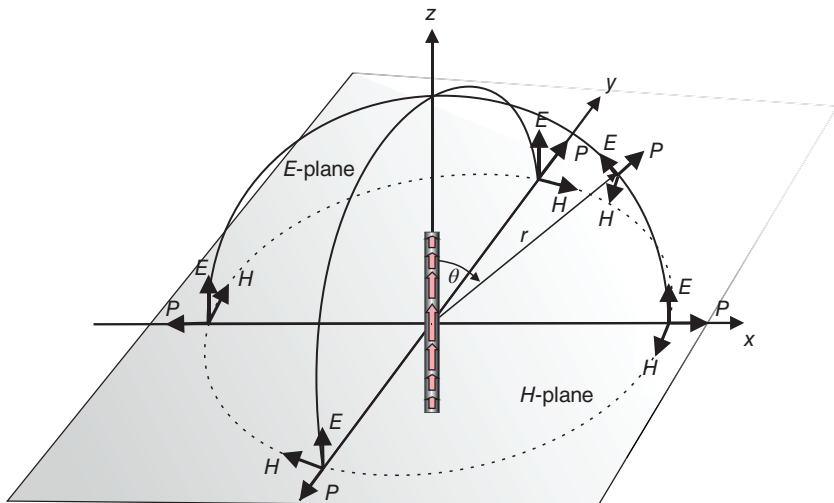


Figure 3.8 Schematic distribution of the E- and H-fields, and of the Poynting vector in space for a dipole antenna.

where \vec{n} is the unit vector in the direction from the antenna center to the observation point (in the direction of a radiated wave). Substituting Eq. (3.33) into Eq. (3.31) and using the vector identity

$$\vec{A} \times (\vec{B} \times \vec{C}) = (\vec{A} \cdot \vec{C})\vec{B} - (\vec{A} \cdot \vec{B})\vec{C}$$

along with the condition that both fields are perpendicular to \vec{n} , yields

$$\vec{P} = \frac{1}{2\eta} \operatorname{Re} (\vec{E} \cdot \vec{E}^*) \vec{n} = \frac{1}{2\eta} \vec{E} \cdot \vec{E}^* \vec{n} = \frac{1}{2\eta} |\vec{E}|^2 \vec{n} = P \vec{n}, \quad P = \frac{1}{2\eta} |\vec{E}|^2 \geq 0 \quad (3.34)$$

so that only the electric field is needed in order to find the radiated power and the antenna directivity. Such a field for the dipole antenna has already been determined in the previous section. The Poynting vector, P , in the far field is called the *radiation density*.

3.13.3 Definition of Radiation Intensity

Using the Poynting vector itself is not very convenient since, according to the energy conservation law, its magnitude decreases as $1/r^2$ when the distance r from the antenna increases. Therefore, one introduces the *radiation intensity* given by the Poynting vector magnitude, P , times distance square, that is

$$U = r^2 P \geq 0. \quad (3.35)$$

The radiation intensity is literally the *power radiated per unit solid angle*; it is measured in watts per steradian. One steradian is a solid angle covering the sphere surface equal to r^2 where r is the sphere radius.

Since the solid angle does not change when the radius r of a sphere surrounding the antenna increases, the radiation intensity remains *constant* irrespective of the radius of the particular observation sphere.

3.13.4 Definition of Directivity

The radiation intensity is not yet the antenna directivity. A problem is that the intensity depends on the voltage applied in the antenna feed and on the power delivered to the antenna. On the other hand, the antenna directivity should be independent of the feeding mechanism; it must be the property of the antenna itself, similar to the antenna's input impedance.

Thus, in order to construct the *antenna directivity*, D , we simply divide the intensity given by Eq. (3.35) by an intensity U_0 of the isotropic source with the same total power as for the antenna itself, i.e.

$$D = \frac{U}{U_0}, \quad D|_{\text{dB}} = 10 \log_{10} \frac{U}{U_0}. \quad (3.36)$$

One might call the first expression in Eq. (3.36) by *dimensionless directivity* and the second expression by *directivity in dB* (or, which is the same, *directivity in dB* where “*i*” stands for “isotropic”). If the antennae were an isotropic radiator, then D would be equal to one or 0 dB everywhere in space. Clearly, $U_0 = P_a/4\pi > 0$, where $P_a > 0$ is the *total power radiated by the antenna* and 4π is the total solid angle of the sphere. Therefore, one has

$$D = \frac{4\pi U}{P_a}, \quad (3.37)$$

which is a quite useful result. It is important to mention that the directivity Eq. (3.36) and (3.37) may be rewritten in terms of the Poynting vector magnitude of the antenna at any point in space, i.e.

$$D = \frac{P}{P_0}, \quad D|_{\text{dB}} = 10\log_{10} \frac{P}{P_0}, \quad P_0 = \frac{P_a}{4\pi r^2} \quad (3.38)$$

3.13.5 Radiation Pattern. E- and H-Planes. Polarization

Directivity D plotted in polar coordinates in one plane, i.e. as a function of the elevation or azimuthal angle, is called the *radiation pattern of an antenna*. Examples of radiation patterns are given below.

While the antenna impedance could be contemplated as a front of the antenna’s “business card,” the antenna directivity or radiation pattern is its “back.” Both these parameters do not depend on the specific mechanism of antenna excitation. An antenna is thus fully characterized by its impedance as well as directivity/radiation patterns. No other parameters are necessary.

Example 3.5

Explain the meaning of an *E-plane* and an *H-plane* in Figures 3.4, 3.6, and 3.8 of this chapter and the meaning of antenna polarization.

Solution: The *E*-plane is any plane in Figure 3.8 (and Figures 3.4 and 3.6) that contains the *E*-vector of the radiated field. In particular, this may be any plane containing the dipole itself. Similarly, the *H*-plane is a plane that contains the *H*-vector of the radiated field. The *H*-plane is the *xy*-plane in Figure 3.8. Radiation patterns are quite often plotted in the *E*- and *H*-planes, respectively.

The (*linear*) *antenna polarization* is simply the direction of the electric field in the radiated wave. The radiated field in the *xy*-plane in Figure 3.8 is said to be *linearly polarized* along the *z*-axis.

Generally, the polarization is a curve that is traced by the electric field vector at a certain point in space. One distinguishes between *linear* (dipole), *circular* (a GPS antenna such as crossed dipole or *turnstile dipole*), and *elliptical* (an intermediate case) polarizations.

Example 3.6

Determine directivity of a half-wave dipole antenna oriented along the z -axis in any E -plane in Figure 3.8. Plot the corresponding radiation pattern.

Solution: The dipole's radiated electric field is given by Eq. (3.30a) of the previous section, that is

$$\mathbf{E}_\theta = \left[\frac{j\eta \exp(-jk|\vec{r}|)}{2\pi|\vec{r}|} \mathbf{I}_a \right] \frac{\cos(k\frac{l_A}{2}\cos\theta) - \cos(k\frac{l_A}{2})}{\sin(k\frac{l_A}{2}) \cdot \sin\theta}, \quad (3.39a)$$

where $|\vec{r}| = r$ is a distance from the antenna center, θ is the elevation angle measured from zenith ($z \rightarrow \infty$ in Figure 3.8), and l_A is the antenna length. Eq. (3.39a) does not involve the azimuthal dependence; the radiation pattern will therefore be the same for *any azimuthal angle*.

According to Eq. (3.34) and (3.35) the radiation intensity of the dipole antenna after substitution of Eq. (3.39a) becomes

$$U(\theta, \varphi) = \frac{1}{2\eta} |\mathbf{E}_\theta|^2 |\vec{r}|^2 = \left[\frac{\eta}{8\pi^2} |\mathbf{I}_a|^2 \right] \left(\frac{\cos(k\frac{l_A}{2}\cos\theta) - \cos(k\frac{l_A}{2})}{\sin(k\frac{l_A}{2}) \cdot \sin\theta} \right)^2 \geq 0. \quad (3.39b)$$

The total power radiated by the dipole antenna is then

$$P_a = \int \int_{\Omega} U d\Omega = \int_0^{2\pi} \int_0^{\pi} U(\theta, \varphi) \sin\theta d\theta d\varphi, \quad (3.40)$$

where Ω is the total solid angle. We can find the total radiated power by substituting Eq. (3.39b) into Eq. (3.40) and performing either numerical or analytical integration. The numerical integration in MATLAB is probably the most straightforward way. After the total radiated power is found, the antenna directivity is evaluated according to Eq. (3.37), i.e.

$$D(\theta, \varphi) = \frac{4\pi U(\theta, \varphi)}{P_a}. \quad (3.41)$$

A MATLAB script that follows performs the above task. The result for $l_A = \lambda/2$ (half-wave dipole) is shown in Figure 3.9. The maximum directivity occurs in the H-plane; it is equal to 2.15 dB (the decibel scale) or 1.64 (the linear scale). This is the classic antenna result, and is, simultaneously, a figure of merit for the half-wave dipole.

The antenna radiation is zero at zenith, i.e. the dipole radiates nothing in the direction of its axis. The entire radiation pattern very much resembles a "donut," with the radial symmetry in the azimuthal plane. In other words, the dipole radiates equally well for any azimuthal direction. Such a pattern is called an *omnidirectional pattern*; the dipole itself is therefore an *omnidirectional antenna*.

The corresponding MATLAB script follows. The MATLAB polar plot cannot accept negative values; we therefore need to subtract 10 dB from the final result post factum.

```
% PATTERN1 Radiation pattern and effective aperture of a dipole antenna
% with a sinusoidal current distribution
clear all;
% EM data
epsilon = 8.85418782e-012;      % Vacuum, F/m
mu = 1.25663706e-006;          % Vacuum, H/m
c = 1/sqrt(epsilon*mu);         % Vacuum, m/s
eta = sqrt(mu/epsilon);         % Vacuum, Ohm
% Dipole antenna data
f = 1e9;                      % Frequency, Hz
lambda = c/f;                  % Wavelength, m
k = 2*pi/lambda;               % Wavenumber, m
Ia = 1;                        % Feed current, A
lA = 0.15;                     % Dipole length, m
% Pattern data
kl = k*lA;
theta = [1:360]/180*pi;        % Elevation angle, rad
U = eta*Ia^2/(8*pi^2)*((cos(kl/2*cos(theta)) -
cos(kl/2))./(sin(kl/2)*sin(theta))).^2;
% Radiation intensity, W/steradian
% Total radiated power (integrate)
Prad = 2*pi*sum(U(1:180).*sin(theta(1:180)))*(pi/length(theta(1:180)));
% Total radiated power, W
U0 = Prad/(4*pi);             % Radiation intensity of the
% Isotropic source,
% W/steradian
D = U/U0;                     % Directivity, dimensionless
D = 10*log10(D);              % Directivity, dB
D = D + 10;                   % Offset, dB
D(find(D<0)) = 0;
polar(theta-pi/2, D);
title('dipole directivity D, dB in the E-plane (subtract 10 dB)');
xlabel('theta, deg')
```

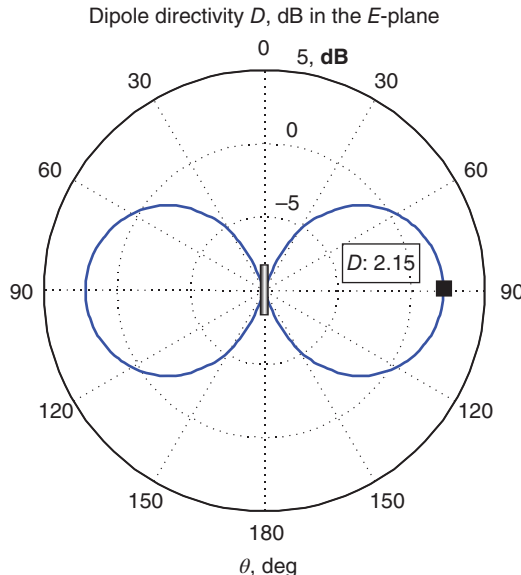


Figure 3.9 Omnidirectional directivity pattern in decibel of a half-wave dipole in any E-plane. The maximum directivity is 2.15 dB. The dipole is an *omnidirectional antenna*.

Using the same MATLAB script as in Example 3.6, one could estimate the directivity pattern not only for half-wave dipoles, but also for small dipoles. As an example, Figure 3.10 shows a comparison between the patterns of a $\lambda/2$ half-wave dipole (solid curve) and a $\lambda/20$ small dipole (dashed curve). The pattern is slightly changed, but generally its donut shape remains *the same*. The maximum directivity decreases from 2.15 to 1.76 dB. We can conclude that the patterns of small dipoles are generally similar to the radiation patterns of the half-wave dipole although their impedance characteristics will be drastically different.

3.14 ANTENNA GAIN AND REALIZED GAIN

The *antenna gain* is the antenna directivity deteriorated due to antenna loss, i.e. (not in dB)

$$G = D \frac{P_a}{P_{\text{accepted by the antenna}}} \leq D, \quad (3.42)$$

where P_a is the radiated antenna power.

Emphasize that for *lossless antennas*, the gain and the directivity *coincide*. Any project in the MATLAB Antenna Toolbox or in Ansys HFSS with a lossless antenna will give us identical values for the gain and the directivity, respectively.

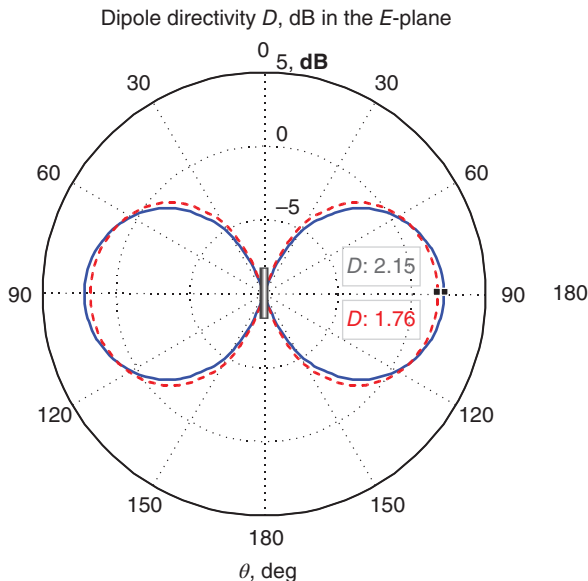


Figure 3.10 Directivity pattern in decibel of a $\lambda/2$ half-wave dipole (solid curve) versus the directivity of a $\lambda/20$ small dipole (dashed curve). The maximum directivity decreases from 2.15 to 1.76 dB.

The *realized antenna gain* (or *absolute antenna gain*) is the antenna gain further deteriorated due to the antenna impedance mismatch factor – see Chapter 1, i.e. (not in dB)

$$G_{\text{realized}} = D \frac{P_a}{P_{\text{accepted by the antenna}}} \left[1 - |\Gamma|^2 \right] \leq G, \quad (3.43)$$

where $|\Gamma|$ is the magnitude of the antenna reflection coefficient defined previously.

The realized gain is perhaps the most important antenna radiation parameter for a practical antenna. It shows how much power will the antenna radiate in the given direction once all losses in the TX circuit and in the TX antenna itself are taken into account.

Note: The realized gain is the antenna gain vs. the gain of an isotropic ideally matched radiator with no loss. For example, the realized gain of small (non-matched) dipoles may attain large negative values in decibel. It can be much lower than the gain of the half-wave dipole despite the fact that the directivities are nearly the same.

3.15 ANTENNA EFFECTIVE APERTURE – RECEIVING ANTENNA AS A POWER COLLECTOR

3.15.1 General

Although the directivity and the gain are two parameters that are predominantly used for antenna modeling and characterization, another parameter that is easy to visualize and understand is the *antenna effective aperture* or *antenna effective area*. Consider a plane wave incident upon a receiving antenna. At the antenna's location, this plane wave has a certain power flux density, P , in space, with the units of W/m^2 . The receiving antenna essentially collects or captures that power from a certain area A and then delivers this collected power to a load. How large is this area compared to the antenna size?

In order to answer this question, one defines the antenna's effective aperture or area, A , as follows. For a given direction, it is “the ratio of the available power at the terminals of the receiving antenna to the power flux density of a plane wave incident on the antenna from that direction, the wave being polarization-matched to the antenna.” In other words, the effective antenna aperture times incident power P in a plane incident wave will give us the power delivered to a matched load, that is

$$AP = P_{\text{load}} \Rightarrow A = \frac{P_{\text{load}}}{P}. \quad (3.44)$$

It is usually understood that the receiving antenna is oriented for best reception with respect to the incoming wave.

3.15.2 Relation to Directivity

Although only directly proven for small dipoles [1] and for half-wave dipoles [2], the following result can be applied to the effective area and to the maximum effective area of any antenna:

$$A = \frac{\lambda^2}{4\pi} D, \quad A_{\max} = \frac{\lambda^2}{4\pi} D_{\max}, \quad (3.45a)$$

where λ is wavelength at a given frequency. Thus, the effective area generally depends on the antenna directivity and wavelength; it also varies with the direction of incidence.

Eq. (3.45a) indeed implies that there are no RX antenna losses or mismatch losses; otherwise, the (realized) gain should be used in Eq. (3.45a) instead of the directivity.

Example 3.7

What is the (maximum) effective area (aperture) for a very small dipole of length $l_A \rightarrow 0$?

Solution: We use the MATLAB script to Example 3.6 and establish that the (maximum) directivity of a small dipole with $l_A < \lambda/20$ approaches 1.50 (or 1.76 dB) with a high degree of accuracy. Then, the use of Eq. (3.45a) yields

$$A_{max} = \frac{\lambda^2}{4\pi} D_{max} = \frac{\lambda^2}{4\pi} \times 1.50 = 0.12\lambda^2. \quad (3.45b)$$

Eq. (3.45b) may be approximated as follows:

$$A_{max} \approx \frac{\lambda}{2} \times \frac{\lambda}{4}. \quad (3.45c)$$

Thus, “irrespective of its length and radius, a short perfectly conducting dipole is *capable* of collecting from a plane wave the power passing through a rectangle whose sides are equal approximately to $\lambda/4$ and $\lambda/2$ [3].” This amazing fact may be useful in practice.

Example 3.8

What is the effective area (aperture) for the half-wave dipole of length l_A ?

Solution: We modify the script of Example 3.6 by adding two lines of the MATLAB code:

```
EffAperture = lambda^2 * max(D) / (4*pi) %Effective aperture of the dipole
EffWidth    = EffAperture/lA             %Effective width of the dipole
```

For $l_A = 15$ cm (~the half-wave dipole at 1 GHz), the effective antenna area is obtained as 0.0117 m^2 . This gives us the effective area width (area divided by dipole length) of 7.8 cm, which is the almost precisely the half of the dipole length, i.e. the result of Eq. (3.45c) again. In other words, there is only little difference in the effective area of the small dipole and the half-wave dipole, respectively. The effective area of the half-wave dipole is estimated as its length times the half of its length again, i.e.

$$A_{max} \approx \frac{\lambda}{2} \times \frac{\lambda}{4} = 0.125\lambda^2. \quad (3.46)$$

Example 3.9

Does Eq. (3.46) (and Eq. (3.45a)) mean that a half-wave dipole at 500 MHz with the length of 30 cm can potentially receive four times more power than the half-wave dipole at 1000 MHz with the length of 15 cm, given that the intensity of the incident plane wave is the same?

Solution: It does! A similar example was already considered in one of the homework problems to Chapter 2.

Unfortunately, lowering the frequency increases the antenna size (both for TX and RX) and decreases the antenna absolute bandwidth (in Hz). Decreasing the antenna bandwidth decreases the bit rate of the transmitted signal. This is why we typically do not work with large antennas and with low frequencies.

Instead, higher frequencies are chosen and more power is consumed, but the antenna link setup becomes physically smaller and faster.

Example 3.10

A beginning antenna and RF engineers are interested in increasing the received power at 1 GHz. Instead of using the half-wave dipole with the length of 15 cm, they decided to use a longer dipole with the length of 50 cm at the same frequency since this antenna apparently has a larger effective aperture. Are they right?

Solution: Unfortunately, it is not. First, the pattern of the longer dipole will be differently shaped; it is no longer a donut. Therefore, the directivity may even have a null in the direction of interest. Second, the antenna mismatch may be high, which lowers the realized gain even further.

There are two meaningful ways to increase the effective antenna aperture and directivity: use a *reflector* or an antenna *array*.

3.16 FRIIS TRANSMISSION EQUATION [1]

A simple, useful, and powerful result that establishes the antenna-to-antenna power transfer function in terms of the antenna directivities is the *Friis transmission equation*. The corresponding antenna setup is shown in Figure 3.11. The antenna types and orientations may vary. In particular, the antennas do not even have to be parallel to each other. In this case, the elevation (and azimuthal) angles in their radiation patterns should be updated accordingly.

According to the definition of the directivity, the power density (magnitude of the Poynting vector) radiated by the transmitter antenna at a given distance r and in the direction $\theta_{TX}, \varphi_{TX}$ toward the receiver is given by

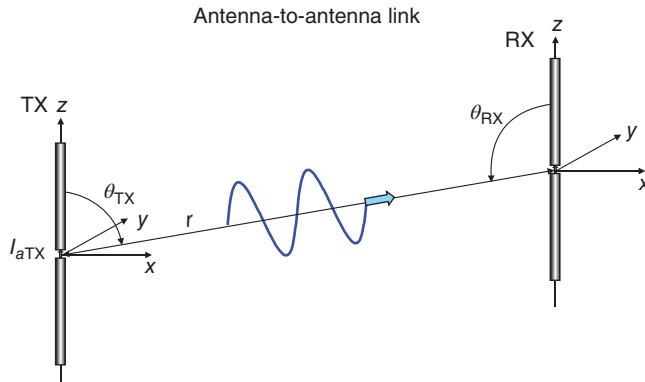


Figure 3.11 Antenna setup for Friis transmission equation. The antenna types and orientations may vary.

$$P = \frac{P_a D_{TX}(\theta_{TX}, \varphi_{TX})}{4\pi r^2}, \quad (3.47)$$

where $4\pi r^2$ is the area of the corresponding sphere and P_a is the power radiated by the transmitter antenna. On the other hand, the power received by the matched load of the RX antenna circuit is given by the product of P and the antenna effective aperture (or area), that is

$$P_{\text{load}} = AP = \frac{\lambda^2}{4\pi} D_{RX}(\theta_{RX}, \varphi_{RX}) P \quad (3.48)$$

according to Eq. (3.45a). Substitution of Eq. (3.47) into Eq. (3.48) yields the power transfer function in the form,

$$P_{\text{load}} = \underbrace{\left[D_{TX}(\theta_{TX}, \varphi_{TX}) D_{RX}(\theta_{RX}, \varphi_{RX}) \left(\frac{\lambda}{4\pi r} \right)^2 \right]}_{T_P} P_a, \quad (3.49)$$

which is the famous *Friis transmission equation*. In the present form, it is only valid for lossless matched antennas. One must emphasize that the linear directivities are used here, not the directivities in decibel. Herewith, the power transfer function T_P becomes

$$T_P = D_{TX}(\theta_{TX}, \varphi_{TX}) D_{RX}(\theta_{RX}, \varphi_{RX}) \left(\frac{\lambda}{4\pi r} \right)^2. \quad (3.50)$$

Example 3.11

Compare the Friis transmission equation with the power transfer function of two dipole antennas established in Chapter 2.

Solution: We consider Example 2.2. There, both TX and RX circuits make use of identical 15 cm long side-by-side cylindrical dipole antennas separated by 1 m. The dipoles are facing each other. The antennas are resonant (matched) at about 900 MHz, which gave us the transfer function of about -30 dB at that frequency. Note that the transfer function in Chapter 2 relates the received power at a matched load to the total transmitter power, but not to the transmitter antenna power as in Eq. (3.49) and (3.50).

On the other hand, using the linear directivities $D_{TX} = D_{RX} = 1.64$ at broadside for half-wave dipoles (see Example 3.6), we obtain from Eq. (3.50) at 900 MHz,

$$T_P \approx 0.019 \text{ or } -27.2 \text{ dB}, \quad (3.51)$$

The total transmitter power is twice the antenna power for the matched TX antenna, which is the present case. Therefore, we must further subtract $10\log_{10}2 = 3$ dB from Eq. (3.51) in order to obtain the transfer function in Chapter 2. This operation gives us -30.2 dB. This result is in a nearly perfect agreement with the transfer function value in Figure 2.4 at 900 MHz. The MATLAB script that follows solves for the transfer function given by Eq. (3.50).

```
% Friis transmission equation
clear all;
% EM data
epsilon = 8.85418782e-012; % Vacuum, F/m
mu = 1.25663706e-006; % Vacuum, H/m
c = 1/sqrt(epsilon*mu); % Vacuum, m/s
eta = sqrt(mu/epsilon); % Vacuum, Ohm
% Dipole antenna data
f = 900e6; % Frequency, Hz
lambda = c/f; % Wavelength, m
k = 2*pi/lambda; % Wavenumber, m
DTX = 1.64; % TX directivity in the direction to RX
DRX = 1.64; % RX directivity in the direction to TX
r = 1; % Distance between antenna centers, m
TF = DTX*DRX*lambda^2/(4*pi*r)^2;
TF_dB = 10*log10(TF)
```

Note: Why not to use Friis equation instead of the transfer functions introduced in Chapter 2?

Answer: The original Friis equation is only valid in free space, without the path loss. Furthermore, the original Friis equation does not straightforwardly cover the voltage transfer function, which is important for pulse radiation. Indeed, its extensions and modifications are possible.

REFERENCES

1. C. A. Balanis, *Antenna Theory. Analysis and Design*, Wiley, New York, 2016, fourth edition.
2. A. A. Oliner and R. G. Malech, "Mutual coupling in infinite scanning arrays," In *Micro-wave Scanning Antennas*, Vol. II, R. C. Hansen, Ed., Academic Press, Cambridge, 1966, Ch. 3, pp. 195–335.
3. S. A. Schelkunoff, *Antennas: Theory and Practice*, Wiley, New York, 1952, p. 36.

PROBLEMS

1. (A) How is the directivity expressed through the radiation intensity? How is it expressed in terms of the magnitude of the Poynting vector (radiation density)?
 (B) What is the radiation pattern of an antenna?
 (C) Draw an example of the E-plane and the H-plane for the dipole antenna.
 (D) What is the directivity of the half-wave dipole at *broadside* (in the direction perpendicular to the dipole axis)? Give both the dimensionless directivity and the directivity in dB. How does the directivity change when the dipole size decreases?
 (E) State differences between the antenna directivity, antenna gain, and antenna realized gain. Could the realized antenna gain be greater than the antenna directivity for a certain direction?
 (F) Describe the meaning of antenna's effective aperture or area in your own words. What is the maximum effective aperture of a half-wave dipole at 2.5 GHz? Express you result in cm^2 .
2. An antenna is suggested that has the directivity of 16 dB in the direction of the main beam and the directivity of 0.1 dB in all other directions. Could you comment on the feasibility of this design?
3. A hypothetic small isotropic antenna radiates equally well in every direction. The antenna radiated power is 1 W. What is the magnitude of the Poynting vector (show units) at the distance of 1 m from the antenna?

4. A light bulb isotropically radiates 30 W of power. What is the magnitude of the Poynting vector at the distance of 2 m from the bulb (show units)?
5. A plane wave in free space with the electric field polarized along the z -direction propagates along the y -direction in Cartesian coordinates. The amplitude of the electric field is 1 V/m.
 - (A) Sketch the wave form and show the direction of the Poynting vector in Cartesian coordinates.
 - (B) Find the magnitude of the Poynting vector (show units).
6. Rewrite Eq. (3.36) for the directivity in terms of Poynting vector instead of radiation intensity.
7. Indicate if the following cases are feasible:
 - (A) An antenna has the directivity of -100 dB in one direction.
 - (B) An antenna has the directivity of $+100$ dB in one direction.
 - (C) An antenna has the directivity of -10 dB everywhere in the lower hemisphere and of $+3$ dB everywhere in the upper hemisphere.
8. Using the MATLAB script in Example 3.6, fill out the following table:

Dipole length	Maximum directivity, linear scale	Maximum directivity, dB
$\lambda/2$		
$\lambda/10$		
$\lambda/100$		

9. The generator resistance of the TX circuit is 50Ω . Using the MATLAB script in Example 3.6 and MATLAB script `dipoleAnalytical.m` for the dipole impedance (Example 1.5), fill out the following table. Consider a lossless dipole with the radius of $\lambda/1000$. Does your result depend on the particular value of the wavelength?

Dipole length	Maximum directivity, dB	Maximum realized gain, dB
$\lambda/2$		
$\lambda/10$		
$\lambda/50$		

10. A resonant RX dipole antenna is subject to plane wave incidence at 1 GHz and at broadside. The strength of the incident electric field is 1 V/m. Approximately, how much power does the RX load of 50Ω receive?
11. Two side-by-side parallel half-wave dipoles at 2.45 GHz are separated by 50 m. The power delivered to the TX dipole is 1 W. What is the power received by the RX load of 50Ω ? The dipoles are ideal. Present the text

of the corresponding MATLAB script that solves the problem using Friis transmission equation.

- 12.** A TX antenna of a GPS satellite having an orbit at 20 200 km above mean sea level has the directivity of 13 dB and radiates 25 W of power in one linear polarization. This signal is received by an ideal polarization-aligned half-wave dipole on Earth when the satellite is at zenith. The GPS frequency is 1.575 GHz (L1 signal).
- What is the power received by the RX load of 50Ω (show units)?
 - What is the value of the transfer function in Eq. (3.50) in dB?

Present the text of the corresponding MATLAB script that solves the problem using Friis transmission Eq. (3.49).

- 13.** Repeat Problem 12 when the GPS frequency changes to 1.228 GHz (L2 signal).
- 14.** Two antennas are so positioned in Figure 3.11 that $\theta_{TX} = \theta_{RX} = 45^\circ$. The distance between antenna centers is 10 m. Both TX and RX circuits make use of identical 15 cm long thin cylindrical dipoles. The antennas are resonant. When the power delivered to the TX antenna is 1 mW, find the RX load power (to the 50Ω load) at 900 MHz.
- 15*.** Create a half-wavelength strip dipole using the MATLAB Antenna Toolbox with the total length L of 15 cm and the width W of 3 mm. Plot a *3D radiation pattern* of this antenna at 1 GHz. What is the directivity of this antenna as reported in the plot? Provide the plot along with your submission. *Hint:* Look into the *pattern* command.
- 16*.** The term “omnidirectional” is often used when referring to the half-wavelength dipole antenna or a loop antenna.
- What does this term exactly imply?
 - Investigate the omnidirectional antenna behavior by using the dipole antenna created in Problem 15. For this experiment, take slices of the 3D radiation pattern in the azimuthal plane ($elevation = 0^\circ$) and in the elevation plane ($azimuth = 0^\circ$). Use the commands *patternAzimuth* and *patternElevation* for this purpose.
 - MATLAB 2D polar plot results are interactive. They support interaction with the mouse so as to allow for right-click-based context menus and also simple point and drag capabilities. Use this property to modify azimuth and/or elevation plots from the previous step and submit extra plots that capture the pattern behavior in the clearest possible way.
- 17*.** The radiation pattern of the dipole exhibits a symmetry in both the upper and lower hemisphere. If we now introduce a conducting screen at some distance from the dipole, the free-space radiation pattern should be altered drastically. We will investigate this now:

- (A) Create a reflector by using the MATLAB Antenna Toolbox. The default reflector in the library should work at 1 GHz. Calculate the 3D pattern for this default antenna/reflector configuration. Turn in the plot and indicate the maximum antenna gain.
- (B) Use the dipole created in Problem 15 and orient it so that it lies flat in the xy plane. Use the *tilt* property of the dipole with the tilt axis of y . Plot the 3D pattern for this configuration and submit it.
- (C) Describe the differences that you observe between the plots for the reflector-backed dipole in (A) and the dipole in free space in (B).
- (D) What is the relationship between the reflector spacing and the wavelength of operation for this particular antenna (1 GHz)?
- (E) Let us characterize the maximum directivity for the reflector-backed dipole as a function of the “Spacing,” i.e. the distance of the dipole antenna from the conducting screen at 1 GHz frequency. Vary the spacing from $\lambda/10$ to $\lambda/2$ and generate 10 values for the maximum directivity. Compute the maximum directivity for each value of spacing. Make a plot of the maximum directivity value as a function of reflector spacing. At which value of the spacing does the peak value of directivity occur? How does this compare with your findings in (D)?

CHAPTER 4



Antenna Balun. Antenna Reflector. Method of Images

SECTION 1 ANTENNA BALUN

4.1. Dipole Feed in Numerical Simulations	101
4.2. Antenna Balun	102
4.3. Split-coaxial Balun	104
4.4. Dyson Balun	108
4.5. Central Tap Transformer as the Dyson Balun	110
4.6. Antenna Impedance Transformation	111
4.7. A Quick Solution	113
4.8. End-of-Section Story	113
References	113
Problems	114

In this chapter, we will start with the practical antenna design. The first candidate is indeed the wire or strip dipole. We will study how to feed the dipole using an antenna *balun*. The balun is necessary for any member of the dipole antenna family.

4.1 DIPOLE FEED IN NUMERICAL SIMULATIONS

The center-fed dipole antenna along with the current distribution is shown in Figure 4.1. If a voltage $v(t)$ is imposed in the antenna feed, then the electric field

Antenna and EM Modeling with MATLAB® Antenna Toolbox, Second Edition. Sergey N. Makarov, Vishwanath Iyer, Shashank Kulkarni, and Steven R. Best.

© 2021 John Wiley & Sons, Inc. Published 2021 by John Wiley & Sons, Inc.

Companion website: www.wiley.com/go/Makarov/AntennaandEMModelingwithMATLAB2e

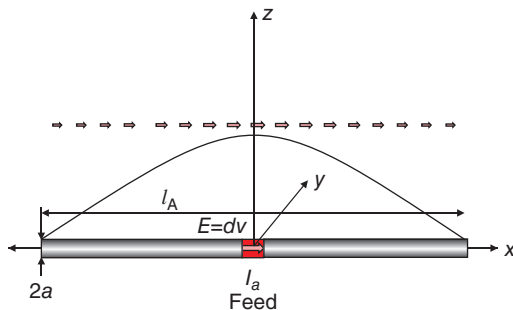


Figure 4.1 Base center-fed cylindrical dipole.

strength within the feed used for numerical modeling is simply $dv(t)$ where d is the feed width. The same result is valid in the phasor form for a harmonic excitation.

The feeding mechanism in Figure 4.1 is a convenient abstraction that may only be used to compute the input impedance of the dipole numerically. In reality, the dipole and other antennas shown in Figure 4.2 are fed through a physical coaxial cable, a microstrip line, etc. [1].

4.2 ANTENNA BALUN

Four representative feeding situations are shown in Figure 4.2, for four different antenna types. We consider the dipole connected to a coaxial cable and shown in Figure 4.2a first. For the left wing of the dipole (Figure 4.2a), the return current has two ways to flow: on the inner surface of the tubular coaxial-cable conductor, and on its outer surface, respectively. The current from the left wing will thus be separated into two distinct parts.

The current on the inner surface of the tubular coaxial-cable conductor, along with the current on the center conductor of the cable from another dipole wing, together form an expected TEM or *transverse electromagnetic wave* propagating within the coaxial cable. This wave is conventionally received by the rest of the circuit.

However, the current on the outer surface of the coaxial cable forms another undesired traveling wave signal that propagates all the way up to the first interconnection of the coaxial cable. Then, this wave may be reflected back. Simultaneously, this wave may radiate into the surrounding space or couple to nearby ground. Therefore, its useful power may be lost.

The same and even more dramatic situation may occur for transmit antennas of a high power. This fact is well known to the Amateur Radio (ham radio) operators.

A similar situation occurs for a loop antenna in Figure 4.2b, but not for the monopole antenna in Figure 4.2c, and not for the patch antenna in Figure 4.2d. As long as

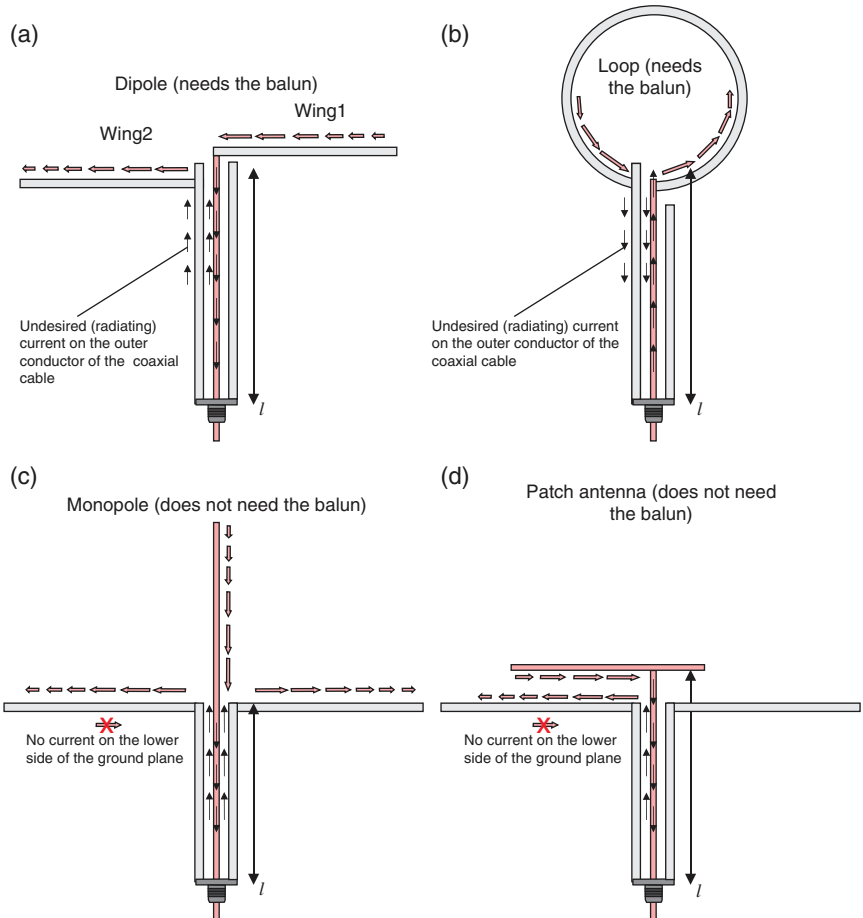


Figure 4.2 (a and b) Appearance of undesired currents on the outer surface of a coaxial feed connector; (c) and (d) no balun is necessary for those antenna types.

the ground plane is large enough, there is simply no current excited on the lower side of the ground plane which would then flow on the outer surface of the coaxial cable.

Unwanted currents on the outer surface of the coaxial cable are eliminated via a *balun*. A balun is used to “balance” systems where power flows from an unbalanced (coaxial) line to a balanced system (two symmetric dipole wings or any other symmetric antenna). Table 4.1 gives the list of antennas, which either need or do not need the balun.

The *antenna balun* (abbreviation of *balanced–unbalanced*) is generally a three-port device used to eliminate possible current flow on the outer surface of the feeding (coaxial) cable to the antenna. Those three ports are sometimes “hidden” within a certain mechanical arrangement.

TABLE 4.1 Some antenna types and balun necessity.

Antenna type	Balun required
Dipole (with or without reflector plane)	Yes
Folded dipole (with or without reflector plane)	Yes
Monopole	No
Loop (with or without reflector plane)	Yes
Half loop (with ground plane)	No
Patch antenna	No
PIFA antenna	No
Spiral antenna (with or without reflector plane)	Yes
Helical antenna (with reflector plane)	No
Horn antenna	No
Yagi-Uda antenna	Yes
Log-periodic antenna	Yes

4.3 SPLIT-COAXIAL BALUN

As a first example, we considered here the so-called *split-coaxial balun* [2] shown in Figure 4.3a. The balun is to be connected to an unfolded straight-wire dipole. This balun, in contrast to some other balun types, has a very convenient conformal geometry; it is easy to manufacture with commercial off-the-shelf tubing. It is used in both linear and circular polarization (turnstile) dipole configurations intended for communications systems [3].

The balun itself is shown in Figure 4.3a, along with the appropriate dimensions. Two dipole currents should exactly cancel each other on the outer conductor surface of the coaxial line after the split point, due to anticipated excitation symmetry [4]. On the other hand, the antenna is not shorted at the dipole feeding point due to the $\lambda/4$ short-to-open circuit transformation. According to [5], this type of balun “will give almost perfect balance over a wide frequency range if the slot width is kept small and symmetry is maintained at the strap end.” In practice, approximately a 15–20% impedance bandwidth for the split-coaxial balun supporting the dipole with a reflector has been reported.

Figure 4.3b shows a split coaxial balun “in action” modeled numerically (Ansys HFSS Electronics Desktop). The surface current density distribution (at 412 MHz) is plotted for a dipole with the split-coaxial balun (left) and for the unbalanced dipole with the same parameters (right). For the dipole with the split-coaxial balun, the current density on the outer conductor beyond the balun is at least 120–140 times smaller than the maximum current density on the dipole wings. This value multiplied with the ratio of the radii gives us the ratio of the total currents inside and outside the coaxial line as at least 40. Without the balun (Figure 4.3b-right), the ratio of the total currents reduces to approximately three.

Thus, the split-coaxial balun performs its major function: the current cancellation on the outer side of the coaxial line (22 dB or better). The *balance quality*,

which is a weak function of frequency, can be estimated based on those current density values.

A theoretical model of the split-coaxial balun has been developed based on the coupled transmission-line approach [6]. This model leads to a closed-form analytical expression for the termination impedance/transfer function of the complete antenna system that includes a dipole, balun, and a non-splitted coaxial line of a

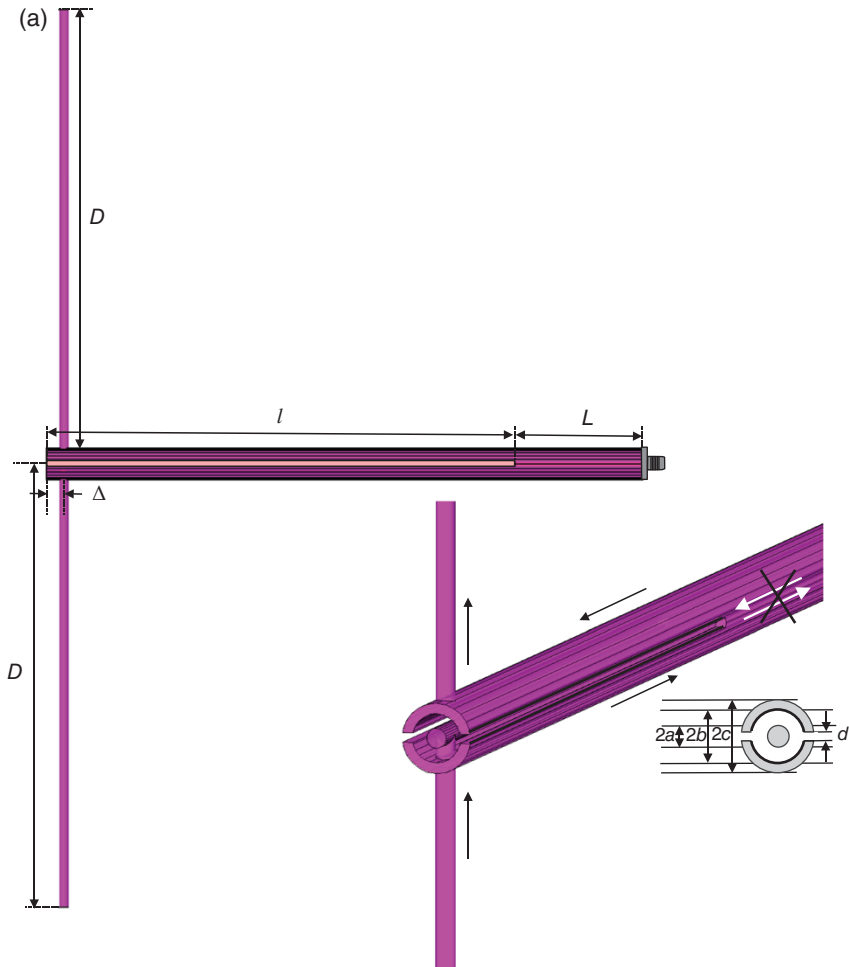


Figure 4.3 (a) Split-tube or split-coaxial balun geometry, associated dimensions, and schematic current flow. The balun uses two splits of the outer coaxial tube of length $l \approx \lambda/4$ each. (b) Surface current density distribution on the outer side of the coaxial cable for a dipole with the split-coaxial balun (left) and for the unbalanced dipole with the same parameters (right).

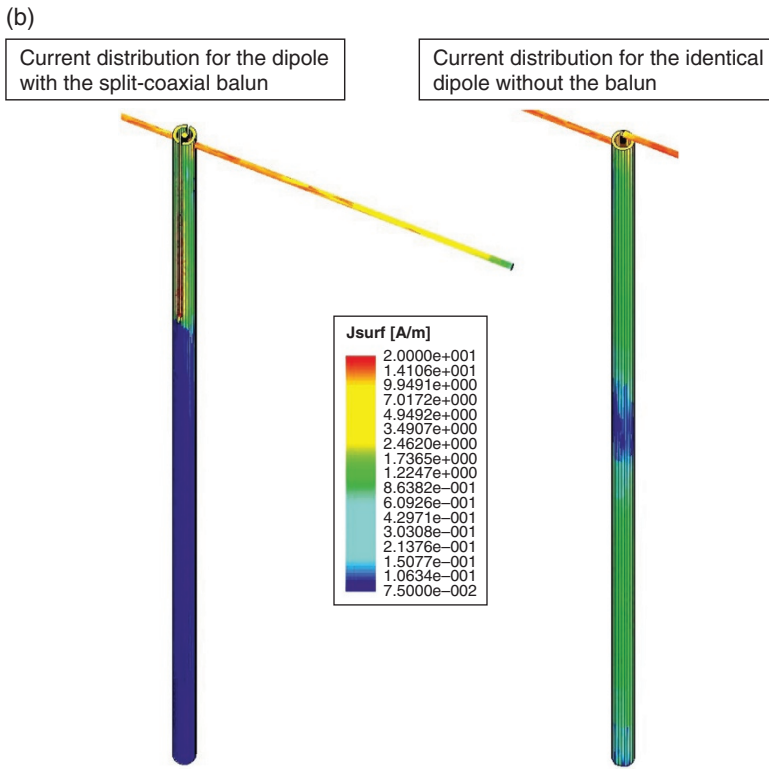


Figure 4.3 (Continued)

certain length. It accepts the impedance of a center-fed dipole as an input parameter. The model has shown an excellent agreement with full-wave simulations and enables us to optimize the impedance bandwidth of the dipole antenna. The model predicts a 12% impedance bandwidth for the resonant dipole–balun configuration and a greater than 20% bandwidth for a combined dipole, balun, and non-splitted line of a certain length L configuration in Figure 4.3a.

As an example, Figure 4.4a shows a number of dipoles manufactured with the split-coaxial balun; Figure 4.4b gives the corresponding measurement results of the reflection coefficient as compared to the theory. The antenna impedance bandwidth increases to 23% as compared to the standard dipole bandwidth of 8–12%. This is done by an optimization of the balun and the following (short) piece of the coaxial line seen in Figure 4.4a. The dipole parameters are given in Table 4.2.

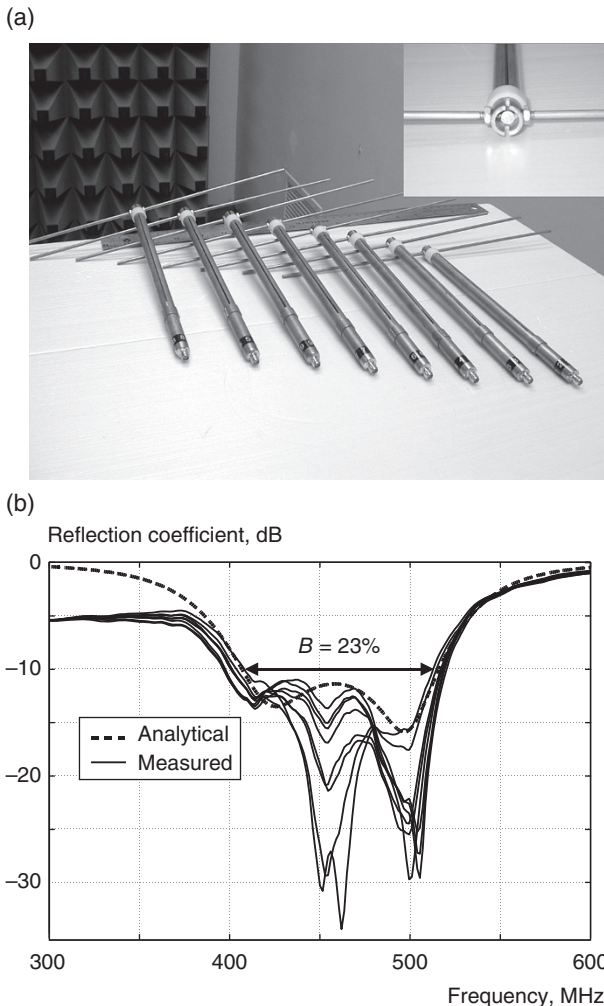


Figure 4.4 (a) Dipole prototypes built with the split-coaxial balun following Table 4.2. *Source:* Design by the authors. (b) Reflection coefficient measurements for eight 460 MHz dipole prototypes (thin curves) compared to the corresponding analytical transmission-line-based solution (thick dashed curve).

Note: Any balun is simultaneously an *impedance transformer*; this interesting fact allows us to use a variety of designs and impedance-matching techniques. The split-coaxial balun is generally a 4 : 1 transformer.

TABLE 4.2 Physical parameters of the dipole and the balun in Figure 4.4a,b optimized for a wider impedance bandwidth.

Component	Outer D (2c)	Inner D (2c)	Total length (l+L)
Outer coaxial tube	7/16"	0.3075"	9.06"
	11.1 mm	7.81 mm	230 mm
Inner rod	3/16"	—	9.06"
	4.8 mm		230 mm
Free length of dipole wing, D	1/8"	—	5.98"
	3.2 mm		152 mm
Slot length from top, l	—	—	7.09"
			180 mm
Slot width, d	—	—	47 mil 1.2 mm
Teflon tube – inner	5/16"	3/16"	Two rings: 10 mm height
Teflon tube – outer	9/16"	7/16"	One ring: 10 mm height

4.4 DYSON BALUN

The split-coaxial balun is usually relatively narrowband, even though certain efforts can be made to increase its impedance bandwidth as discussed in the previous section. So is any *resonant balun* that contains transmission-line sections of the length $\lambda/4$ or so.

Among wideband balun types [2], the most popular balun type is probably the *Dyson balun* [7, 8]. Its concept is shown in Figure 4.5. Either wing of the dipole in Figure 4.5a is fed with a separate coaxial line, sharing the same outer ground; both lines are 180° out of phase. This ensures the proper balanced current distribution along the dipole. The electric current does not exist on the outer side of coaxial conductors in Figure 4.5a. If it were, it would cancel out for two symmetric dipole wings, since the two dipoles should give us two oppositely directed current contributions there, no matter how those contributions are directed and what value do they really have.

A similar setup can also be applied to a loop antenna to be studied in the next chapter – see Figure 4.5b. The proper power division and the proper phase shift can be accomplished by the use of a 180° *power divider or splitter (phase shifter)* also shown in Figure 4.5. The ground is the case of the phase shifter. Electric currents on both lines feeding the dipole can be considered having $\pm 90^\circ$ phase shift versus the ground reference with no current.

The Dyson balun has been widely used for standard dipoles and other symmetric antennas. A particular application to the so-called “Fourpoint” antenna is of note [9–11]. For a symmetric antenna load, the Dyson balun provides equal current, voltage, and power division between the two dipole wings [12].

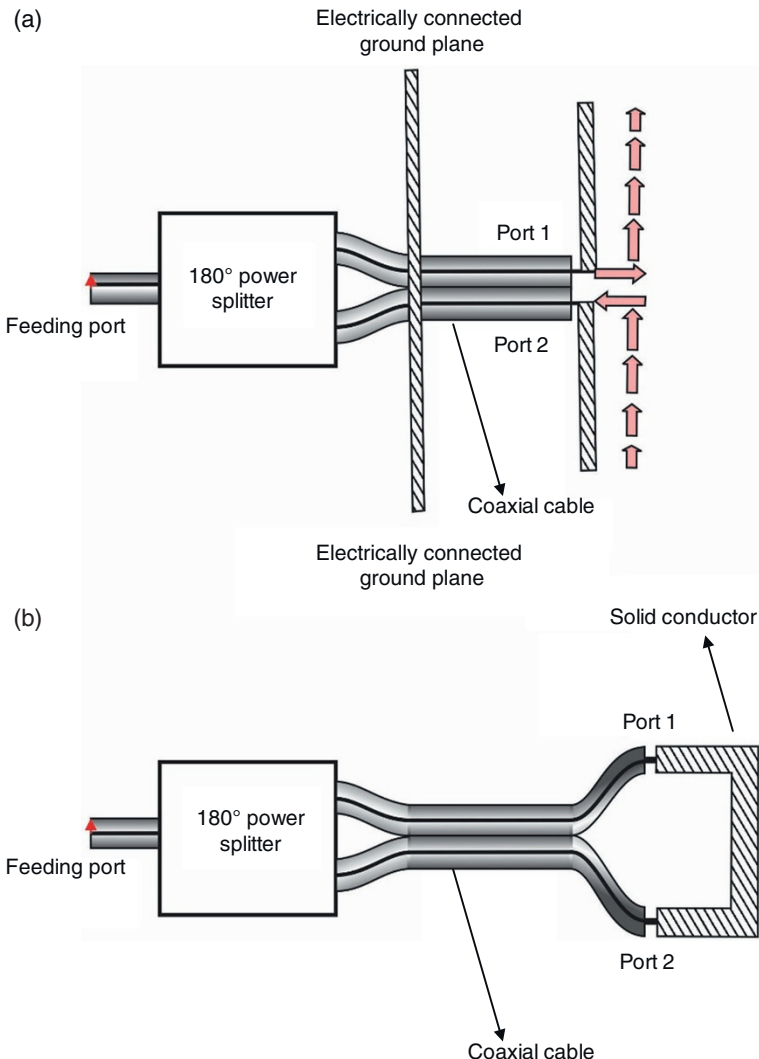


Figure 4.5 Dyson balun for (a) single-polarization dipole antenna; (b) loop antenna.

Another advantage of the Dyson balun is its direct applicability to a turnstile element with two crossed dipoles or dipole-like antennas fed with two separate hybrids. It is important that the balun inherently provides a higher isolation between two turnstile antenna elements since two pairs of feeding transmission lines are shielded. Plus, the *phase centers of two crossed dipoles* remain the same.

It was noted yet by Dyson himself [8] that the Dyson balun allows us to achieve a considerably wider bandwidth (over octave and wider) compared to the split-

coaxial balun, which bandwidth may be tuned to typically 20–25% – see the previous section.

A closest competitor to the Dyson balun, as applied to phased arrays, seems to be a *printed Marchand balun* [2, 13]. The Marchand balun is very broadband. But, at the same time, it usually requires two crossed vertical printed circuit boards (PCBs) with some slots. This might be a problem for low-cost and low-maintenance antennas.

4.5 CENTRAL TAP TRANSFORMER AS THE DYSON BALUN

A broadband (and quite versatile in the VHF or even the UHF band) 180° power divider is just a *high-frequency transformer with the central tap* shown in Figure 4.6. The commercial broadband power dividers are often based on that principle.

Two equal secondary windings, with $N_2/2$ turns each, are connected to each other and then to a virtual ground – the center tap. The center tap of the secondary coil may be physically grounded. All induced voltages $v_1(t)$, $v_2(t)$, and $v_3(t)$ in Figure 4.6 obey Faraday's law of induction. Therefore [14],

$$\frac{v_1}{N_1} = \frac{v_2}{0.5N_2} = \frac{v_3}{0.5N_2}. \quad (4.1)$$

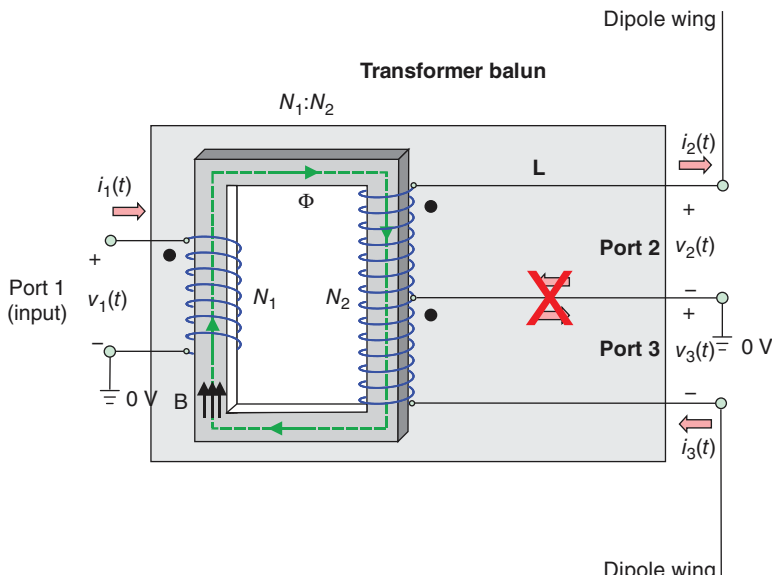


Figure 4.6 A 180° power divider on the base of an ideal transformer.

Using Ampere's law for the ideal magnetic core, we obtain [14]:

$$N_1 i_1 = 0.5 N_2 i_2 + 0.5 N_2 i_3 = 0. \quad (4.2)$$

From Eq. (4.1), one has

$$v_2(t) = v_3(t), \text{ where } v_1 = \frac{2N_1}{N_2} v_2. \quad (4.3)$$

If and only if the center-tapped transformer is connected to the two *identical* loads (antenna wings), the center tap carries *zero* current so that with reference to Figure 4.6,

$$i_2(t) = i_3(t), \text{ where } i_1 = \frac{N_2}{N_1} i_2. \quad (4.4)$$

4.6 ANTENNA IMPEDANCE TRANSFORMATION

The major point of interest is the transformed antenna impedance. The input impedance of ports 2 and 3 in Figure 4.6 is *exactly a half of the dipole impedance*. To prove this fact, we consider a dipole feeding gap with the series impedance combination, $1/2\mathbf{Z}_a + 1/2\mathbf{Z}_a$, then cutting the feeding gap in Figure 4.7 in half will result in $1/2\mathbf{Z}_a$.

To find the impedance seen at port 1, we convert the circuit in Figure 4.6 to the phasor form. Then, we obtain using Eq. (4.3) and (4.4)

$$\mathbf{Z}_1 \equiv \frac{\mathbf{V}_1}{\mathbf{I}_1} = \frac{\left(\frac{2N_1}{N_2}\right)\mathbf{V}_2}{\left(\frac{N_2}{N_1}\right)\mathbf{I}_2} = 2\left(\frac{N_1}{N_2}\right)^2 \frac{\mathbf{V}_2}{\mathbf{I}_2} = 2\left(\frac{N_1}{N_2}\right)^2 \frac{1}{2}\mathbf{Z}_a = \left(\frac{N_1}{N_2}\right)^2 \mathbf{Z}_a. \quad (4.5)$$

For a $1 : 1$ center-tap transformer, the impedance at port 1 is thus precisely the impedance of a center-fed antenna computed numerically.

In practice, there is a coaxial cable (transmission line) of length L and characteristic impedance Z_0 from each dipole wing to the power divider. The impedance of the individual antenna port, $\frac{1}{2}\mathbf{Z}_a$, is transformed to the input of the power divider in the form:

$$\frac{1}{2}\mathbf{Z}_a \rightarrow Z_0 \frac{\frac{1}{2}\mathbf{Z}_a + jZ_0 \tan kL}{Z_0 + j\frac{1}{2}\mathbf{Z}_a \tan kL}. \quad (4.6)$$

Therefore, Eq. (4.5) should be written in the form,

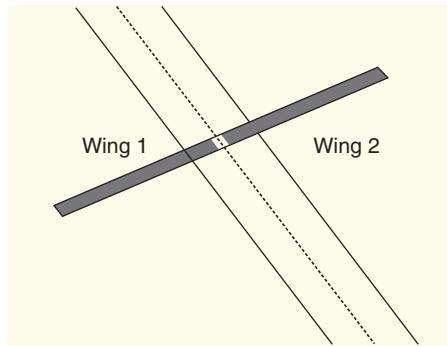


Figure 4.7 Simplified center-fed dipole model used for impedance computations.

$$\mathbf{Z}_1 \equiv 2 \left(\frac{N_1}{N_2} \right)^2 Z_0 \frac{\frac{1}{2} \mathbf{Z}_a + j Z_0 \tan kL}{Z_0 + j \frac{1}{2} \mathbf{Z}_a \tan kL}, \quad (4.7)$$

which is the final result of our study. Eq. (4.7) has been compared with accurate numerical simulations which directly modeled the Dyson balun topology including feeding transmission lines. A good agreement has been observed for both the input impedance and the radiation pattern.

Note: The length of the coaxial cable (microstrip line) from the antenna to the power divider is important for the performance of the Dyson balun over a wide band of frequencies.

Note: Many other balun types exist. A very good summary of antenna baluns is given in the Antenna Engineering Handbook [2]. Yet another highly professional reference is [3].

Note: The above example demonstrates one possible technique for evaluating the effect of a balun:

- (a) find the impedance of a center-fed symmetrical antenna numerically first;
- (b) then compute the effect of a balun via some extra analytical post-processing.

4.7 A QUICK SOLUTION

If for some reason the balun is not available, *a ferrite split snap-on core* could be used as a quick solution to suppress currents on the outer side of the feeding coaxial cable. Many such inexpensive cores are available, for different frequency bands.

4.8 END-OF-SECTION STORY

A quote from Robert C. Hansen [15] “A few years ago a large telecommunication company announced an antenna on a chip, an antenna so small that it resides in the printed circuit board. Measurements were made with the chip connected to the network analyzer by a small-diameter coax. Results were excellent. Later, when the cable was removed and the antenna was activated by the circuit board, the antenna did not operate. This was another case of an unbalanced antenna connected to a coax cable; the cable often makes an excellent radiator! All announcements on the chip antenna ceased...”

REFERENCES

1. C. A. Balanis, *Antenna Theory: Analysis and Design*, Wiley, New York, 2016, fourth edition.
2. D. F. Bowman and E. F. Kuester, In J. L. Volakis, Ed., *Antenna Engineering Handbook*, McGraw Hill, New York, 2007, fourth edition, Ch. 52, pp. 52-26–52-27.
3. T. A. Milligan, *Modern Antenna Design*, Wiley-IEEE Press, New York, 2005, second edition, pp. 231–237.
4. W. L. Stutzman and G. A. Thiele, *Antenna Theory and Design*, Wiley, New York, 2012, third edition, pp. 183–187.
5. R. C. Johnson, Ed., *Antenna Engineering Handbook*, McGraw Hill, New York, 2012, third edition.
6. S. Makarov and R. Ludwig, “Analytical model of the split-coaxial balun and its application to a wire dipole or a CP turnstile,” *IEEE Trans. Antennas Prop.*, vol. AP-56, no. 5, pp. 1909–1918, 2007.
7. J. D. Dyson, “Balanced transmission-line measurements using coaxial equipment,” *IEEE Trans. Microwave Theory Techniques*, vol. 19, no. 1, pp. 94–96, 1971.
8. J. D. Dyson, “Measurement of near fields of antennas and scatterers,” *IEEE Trans. Antennas Prop.*, vol. AP-21, no. 4, pp. 446–460, 1973.
9. Seong-Youp Suh, W. L. Stutzman, and W. A. Davis, “Low-profile, dual-polarized broadband antennas,” in *2003 IEEE Antennas and Propagation Society Int. Symp.*, vol. 2, pp. 256–259, June 2003.
10. Seong-Youp, S., W. Stutzman, W. Davis, A. Walther, K. Skeba, and J. Schiffer, “A novel low-profile, dual-polarization, multi-band base-station antenna element – the Fourpoint Antenna,” in *2004 IEEE 60th Vehicular Technology Conference*, 2004. VTC2004-Fall, vol. 1, 26–29, pp. 225–229, Sept. 2004.

11. Seong-Youp Suh, W. Stutzman, W. Davis, A. Walther, K. Skeba, and J. Schiffer, "Bandwidth improvement for crossed-dipole type antennas using a tuning plate," *2005 IEEE Antennas and Propagation Society Int. Symp.*, vol. 2A, pp. 487–490, July 2005.
12. S. McLean, "Balancing networks for symmetric antennas. I. Classification and fundamental operation," *IEEE Trans. Electromagnetic Compatibility*, vol. 44, no. 4, pp. 503–514, 2002.
13. W. R. Pickles and W.M. Dorsey, "Proposed coincident phase center orthogonal dipoles," in *2007 Antenna Applications Symposium Proc.*, Monticello, IL, pp. 106–124, Sep. 2007.
14. S. Makarov, R. Ludwig, and S. Bitar, *Practical Electrical Engineering*, Springer, New York, 2016, Ch. 12.
15. R. C. Hansen, *Electrically Small, Superdirective, and Superconducting Antennas*, Wiley, New York, 2006, p. 81.

PROBLEMS

1. 1. Describe the meaning of the antenna balun in your own words. Why do we need a balun for a dipole antenna?
 2. Do we need a balun for
 - (A) monopole antenna?
 - (B) loop antenna?
 - (C) patch antenna?
2. Does an antenna shown in Figure 4.8 need a balun?

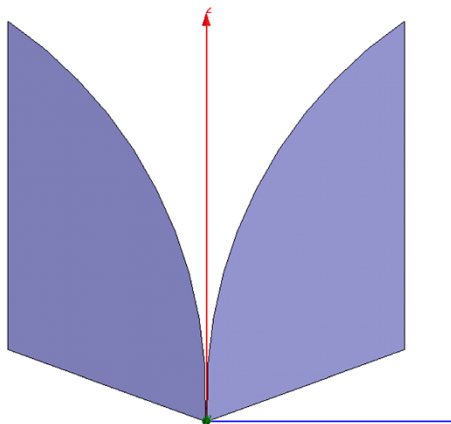


Figure 4.8 A "Vivaldi" antenna element.

- 3.** (A) Describe the construction of the Dyson balun.
(B) For the Dyson balun on the base of the center-tap transformer, present an expression for the transformed antenna impedance and describe all variable parameters.
- 4*.** A 15 cm long and 8 mm wide-strip dipole with the Dyson balun in the form of a center-tap 1 : 1 transformer is modeled. The length of a $50\ \Omega$ transmission cable from every dipole wing to the power divider is 10 cm.
(A) Using MATLAB Antenna Toolbox, determine impedance bandwidth of the center-fed dipole antenna without the balun close to its first resonance.
(B) Using previously generated MATLAB impedance data, determine impedance bandwidth of the antenna with the Dyson balun.
(C) Could you increase antenna bandwidth by varying transmission line length?
(D) Could you increase antenna bandwidth by varying transformer turns ratio?
- 5*.** Repeat Problem 4 for a 20 cm long dipole. All other geometry parameters remain the same.

SECTION 2 ANTENNA REFLECTOR

4.9. Ground Plane for an Electric Dipole. The $\lambda/4$-Rule	117
4.10. Method of Images	120
4.11. Effect of Ground Plane on Antenna Impedance	121
4.12. Effect of Ground Plane on the Radiation Pattern	122
4.13. Extensions of the Image Method: Corner Reflector	124
4.14. Finite Ground Plane – Geometrical Optics	126
4.15. Front-to-Back Ratio	127
References	130
Problems	130

Virtually every antenna may have a certain ground plane or a reflector. The primary goal of the ground plane/reflector is to shape the antenna pattern (increase directivity and gain in the desired direction) and minimize the *backlobes* or, which is the same, minimize radiation to or reception from the unwanted directions. The ground plane has also a certain effect on the antenna impedance, but this effect is typically not very profound, except for metal or dielectric surfaces located quite close to the antenna as compared to the wavelength. The design of a proper ground plane/reflector may be a significant challenge.

The most straightforward example is the ground plane of the path antenna – the PCB ground – or that of a VHF car monopole antenna – the car exterior. Similarly, for airborne antennas, the ground plane is the airplane fuselage. For other symmetric dipole-like antennas, the ground plane is typically a metal or wire conducting reflector, which should simultaneously serve as a neutral or common voltage reference for the antenna feeding circuit. For wireless communication dipoles, the ground is often represented by the Earth surface. In this section, we will review basic analytical models of solid metal ground planes and reflectors for dipole-like antennas including the edge effects and outline simple diffraction mechanisms.

There are three common analytical models that greatly help us to understand and analyze the effect of a ground plane or a reflector on the antenna, and to design an appropriate antenna ground plane. They include

- Wave reflection and *geometrical optics* (GO);
- Diffraction, *geometrical theory of diffraction* (GTD), and *uniform theory of diffraction* (UTD);
- *Physical optics* (PO)

and are commonly referred to as *high-frequency methods*.

Even today, a large ground plane and/or a large parabolic reflector present a challenge for numerical modeling of antennas as the electrical size of the complete structure increases. Hence, the value of the related analytical models greatly increases.

Interestingly, the same analytical models find their applications in a broader area of wireless communications that includes wireless channel estimation and

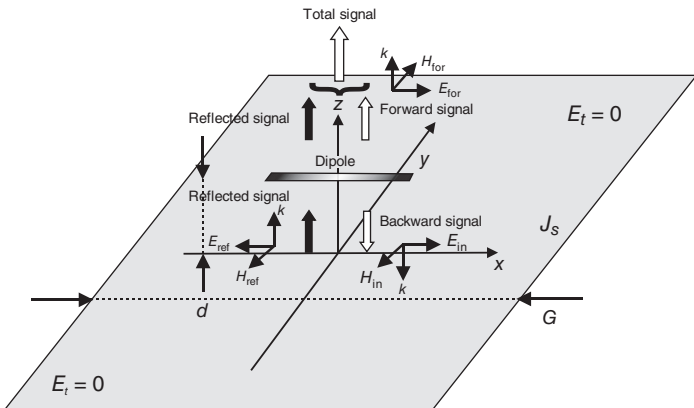


Figure 4.9 Concept of a reflecting (metal) ground plane.

path loss estimation for an indoor or outdoor environment. For example, the *ray tracing method*, which is currently widely employed for channel estimation in terrains, uses these theories.

4.9 GROUND PLANE FOR AN ELECTRIC DIPOLE. THE $\lambda/4$ -RULE

Consider a radiating dipole above a *perfect electric conductor* (PEC) ground plane as shown in Figure 4.9. We will use the GO approximation for the incident/reflected signals which is essentially the ray tracing method. We will only consider the signal in the dipole's *E-plane* which is the xz -plane in Figure 4.9. The dipole radiates two signals – the *forward wave* that propagates in the positive direction of the z -axis and the *backward wave* that is also incident upon the metal ground plane. The backward wave is then reflected from the ground plane as the *reflected wave* and is eventually added to the forward wave, with a certain phase shift. The resulting radiated field is thus a combination of the direct forward wave and the reflected wave.

Neglecting field divergence, one obtains a solution in the form of plane waves in time domain, where both forward and backward or incident wave have zero phase at $z = d$,

$$\begin{aligned} E_x^{\text{for}}(t, z) &= +E_{x0} \cos(\omega t - k_z(z-d)), \\ E_x^{\text{inc}}(t, z) &= +E_{x0} \cos(\omega t + k_z(z-d)), \\ E_x^{\text{ref}}(t, z) &= -E_{x0} \cos(\omega t - k_z(z+d)). \end{aligned} \quad (4.8)$$

The reflected wave has been selected in such a way that it satisfies the boundary condition on the metal surface at $z = 0$, i.e.

$$0 = E_{tan} = E_x = E_x^{\text{inc}}(t, z=0) + E_x^{\text{ref}}(t, z=0). \quad (4.9)$$

Note that Eq. (4.8) is the exact solution for the reflection problem given a plane wave geometry. Thus, the total forward radiated field becomes a combination of two waves. At the dipole position, the total field is given by

$$E_x^{\text{total}}(t, z = d) = E_x^{\text{for}}(t, z = d) + E_x^{\text{ref}}(t, z = d) = E_{x0}(\cos \omega t + \cos(\omega t - 2k_z d - \pi)). \quad (4.10)$$

The second cosine is phase shifted with respect to the first one by

$$\psi = 2k_z d + \pi. \quad (4.11)$$

Finding the sum of two cosine functions, one has

$$E_x^{\text{total}}(t, z = d) = 2E_{x0} \cos(\psi/2) \cos(\omega t - \psi/2). \quad (4.12)$$

Eq. (4.11) for the phase shift between the two waves is important. It says that the resulting phase shift includes two distinct contributions:

- (i) the shift of π or the E -field phase reversal due to the reflection from a PEC boundary;
- (ii) the shift $2k_z d = 4\pi d/\lambda$, which corresponds to a time delay of a reflected signal (RS) over the travel distance of $2d$.

If there were no phase reversal (e.g. a *perfect magnetic boundary* or a *perfect magnetic conductor* [PMC] was present instead of a metal boundary) then a dipole in close proximity to the ground plane would be characterized by $\psi \rightarrow 0$. According to Eq. (4.12), it will radiate forward twice the electric field (*and four times or 6 dB the power*) as compared to the dipole in free space.

When phase reversal is present (the more realistic *perfect electric boundary*), the total forward radiation becomes nearly zero according to Eq. (4.12) when $d \rightarrow 0$ ($\psi \rightarrow \pi$). So does the input resistance of the antenna. This is why the dipole close to a metal surface is a very poor antenna radiator. The physical reason for it is the appearance of surface-induced currents on the metal ground plane that are oppositely directed and radiate a field in antiphase versus the main dipole current. The antenna is thus “shorted out”; it is not functioning.

For the metal ground plane, an optimum reflector separation distance can be found based on Eq. (4.11). The maximum total radiated field is achieved when ψ in Eq. (4.11) and (4.12) is zero or a multiple of 2π , i.e. when $d = \lambda/4$, or $d = 3\lambda/4$, etc.

The separation distance between the antenna and the ground plane is thus an important design parameter, not only for the horizontal dipole above a ground plane but also in many other cases. The smallest optimum value of the separation distance, $d = \lambda/4$, corresponds to the *$\lambda/4$ rule*.

Note: The *$\lambda/4$ rule* and the one-dimensional analysis predict that the maximum dipole directivity with the plane reflector becomes the dipole directivity of 2.15 dB in free space plus $10\log_{10}(4)$ dB ~ 6 dB since the electric field doubles and the power quadruples. We will show at the end of this section that this result is actually quite close to reality.

Note: The phase reversal after the reflection from the metal boundary is responsible for a number of interesting effects. In particular, a *right-handed circularly polarized* (RHCP) signal will be reflected from a metal boundary as a *left-handed circularly polarized* (LHCP) signal, and vice versa. These polarizations will be studied in detail in Chapter 10. Here, we could immediately see a way how to eliminate or reduce multipath using circular polarization. If an antenna is intended for RHCP reception, then it will only receive the original RHCP signal but will reject all primary reflections which are LHCP.

Finally, we note that Eq. (4.12) can indeed be written in the phasor form:

$$\mathbf{E}_x^{\text{total}}(z = d) = 2E_{x0} \cos(\psi/2) \exp(-jk\psi/2) = [2j \sin(k_z d)] E_{x0} \exp(-jk_z d). \quad (4.13)$$

The term in square brackets will be recognized as an *array factor*. The term $\exp(-jk_z d)$ is of little importance to us; it only contributes to the overall solution phase.

Example 4.1

Describe another antenna (different from dipole with a ground plane) where the $\lambda/4$ rule is enforced.

Solution: As another example of the general character of the $\lambda/4$ rule, which may appear in many other situations, let us consider a feed of a standard horn that is typically given by a coaxially driven *monopole* in a rectangular cavity shown in Figure 4.10. The length of the monopole is mostly defined by the impedance matching criteria and may vary from horn to horn. However, the horn's feed separation from the side wall has to be close to $d = \lambda/4$ in order to ensure the proper reflection.

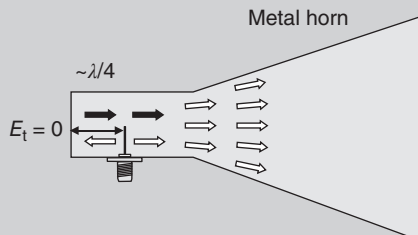


Figure 4.10 Feed placement for a horn cavity.

4.10 METHOD OF IMAGES

Now, how does the ground plane work in a general case, for all separation distances and for all radiation angles? The answer to this question cannot be given in a closed form for an arbitrary antenna above a finite ground plane. However, the exact answer does exist for an arbitrary antenna over an *infinite* ground plane using the so-called *image method* – see Figure 4.11a,b.

The idea of the image method is simple and powerful. Let us remove the PEC ground plane but add another (image) dipole at the distance $-d$ from the origin, i.e. symmetrically versus the initial ground plane position. The required boundary condition, $E_t = 0$, will be then satisfied everywhere in the imaginary ground plane due to field cancellation of two dipoles shown in Figure 4.11a.

To satisfy the PEC boundary condition, electric current in the image dipole must flow in *the opposite direction* as shown in Figure 4.11b. We remember that the radiated E -field is always directed following the antenna current. The field cancellation takes place for any point in the xy -plane. Thus, the two dipoles will

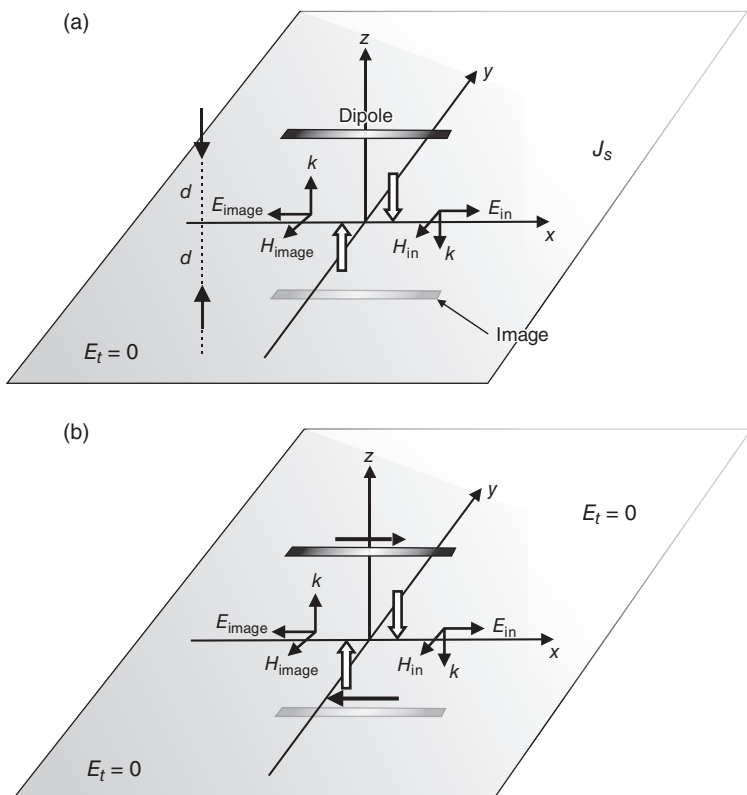


Figure 4.11 (a) Method of images for a horizontal dipole above a ground plane. The ground plane effect is mimicked by the effect of the image dipole. (b) Current and field directions for two collinear dipoles used in the method of images.

radiate in the upper hemisphere as one dipole above the ground plane since both configurations satisfy Maxwell's equations and the *identical boundary conditions*. The radiation in the lower hemisphere must be zero, but this is not the case for the image method. Therefore, the image method only works for the *exterior problem* (upper hemisphere that includes the dipole) and cannot formally provide the null in the interior (lower hemisphere).

Note: The effect of a metal ground plane on a closely spaced antenna could be nicely explained based on the image theory. When located close to each other, two oppositely directed currents radiate two oppositely directed fields that also cancel each other – one might again say that the antenna is “shorted out” and becomes a *non-radiating transmission line*.

Note: A probe-fed patch antenna above an infinite ground may be also treated using the method of images, as two patches sharing the same probe feed and with the opposite current flow.

4.11 EFFECT OF GROUND PLANE ON ANTENNA IMPEDANCE

The ground plane alters not only the radiation pattern but also the antenna impedance. The image method allows us to analyze the altered dipole impedance and the resulting radiation pattern analytically. Let us start with the impedance first. The treatment will be essentially that of Ref. [1]. Two dipoles: the original one and the image are mutually coupled through the impedance matrix (see Chapter 2)

$$\begin{bmatrix} V_1 \\ V_2 \end{bmatrix} = \begin{bmatrix} Z_{11} & Z_{12} \\ Z_{21} & Z_{22} \end{bmatrix} \begin{bmatrix} I_1 \\ I_2 \end{bmatrix}, \quad (4.14)$$

where index 1 corresponds to the original dipole and index 2 – to the image. For identical reciprocal antennas, the mutual and self- impedances are identical, i.e.

$$Z_{12} = Z_{21}, \quad Z_{11} = Z_{22}. \quad (4.15)$$

The *active impedance* of the original dipole (the impedance under the presence of the image dipole) becomes according to Eq. (4.14)

$$Z_1 \equiv \frac{V_1}{I_1} = Z_{11} + \frac{Z_{12}}{Z_{22}} \frac{I_1}{I_2} = Z_{11} - Z_{12} \quad (4.16)$$

since currents I_1, I_2 are equal in magnitude but are oppositely directed. Once Z_{12} and the impedance matrix are known, the dipole impedance above the ground plane

is Z_1 from Eq. (4.16). One special case that should be evaluated is when the separation d approaches zero. Then, $Z_{12} \rightarrow Z_{11}$ (two dipoles tend to coincide) and $Z_1 \rightarrow 0$, which again means that the original antenna is “shorted out.”

4.12 EFFECT OF GROUND PLANE ON THE RADIATION PATTERN

Now, let us proceed with the radiation pattern of a single horizontal very short dipole [2] centered at origin and oriented along the x -axis. The pattern is conveniently presented in spherical coordinates. The phasor of the electric field in the far-field region can be found, for example, from Eq. (3.24a) of Chapter 3 at $|\vec{r}| = r \rightarrow \infty$. The dipole axis is now the x -axis, but not the z -axis. The angle θ in Eq. (3.24a) is becoming an angle ψ from this x -axis to the observation point. Now, $\cos\psi = \vec{a}_x \cdot \vec{a}_r = \vec{a}_x \cdot (\vec{a}_x \sin\theta \cos\varphi + \vec{a}_y \sin\theta \sin\varphi + \vec{a}_z \cos\theta) = \sin\theta \cos\varphi$. Therefore, the result for the horizontal dipole located at the origin should be written in the far field as

$$E_\theta = j\eta \frac{kI_0 l_A \exp(-jkr)}{4\pi r} \sqrt{1 - \sin^2\theta \cos^2\varphi}. \quad (4.17)$$

We note that neither the pattern magnitude nor its polarization should change when we move the dipole (or any other antenna) by a certain finite distance, say $\pm d$, from the origin – any linear translation cannot change the pattern magnitude or add a new polarization component. What changes, however, is the phase since the signal from the dipole placed closer to the observation point will arrive earlier, no matter how large the absolute distance to that point is. Thus, for $\pm d$ translation along the z -axis, one needs to replace r in Eq. (4.17) by a new distance r' . According to the law of cosines and Figure 4.12,

$$r'^2 = r^2 + d^2 \\ \mp 2rd\cos\theta; r' = \sqrt{r^2 + d^2 \mp 2rd\cos\theta} = r \sqrt{1 + \left(\frac{d}{r}\right)^2 \mp 2\left(\frac{d}{r}\right)\cos\theta} \quad (4.18)$$

when the dipole offset from the origin is given by $\pm d$. Here, d/r is a small parameter μ , $\mu \ll 1$. Using Taylor series expansion and keeping only the dominant terms, one has

$$r' = r \sqrt{1 \mp 2\left(\frac{d}{r}\right)\cos\theta + O(\mu^2)}; r' = r \mp d\cos\theta + rO(\mu^2), \quad (4.19)$$

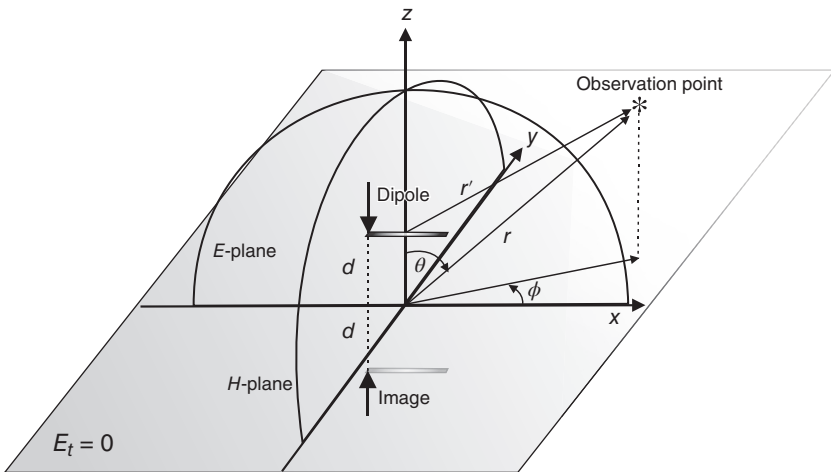


Figure 4.12 Radiation geometry in spherical coordinates. The dipole offset from the origin is given by $\pm d$.

which leads to (after substitution of r' instead of r)

$$E_\theta^{1,2} = j\eta \frac{kI_{1,2}l_A \exp(-jkr) \exp(\pm jkd \cos \theta)}{4\pi r} \sqrt{1 - \sin^2 \theta \cos^2 \varphi}. \quad (4.20)$$

Here, $E_\theta^{1,2}$ are the fields radiated by the original dipole and by the image dipole, respectively; $I_{1,2} = \pm I_0$. The total field is given by their sum, i.e.

$$E_\theta^{\text{total}}(r, \theta, \varphi) = [2j \sin(kd \cos \theta)] j\eta \frac{kI_0 l_A \exp(-jkr)}{4\pi r} \sqrt{1 - \sin^2 \theta \cos^2 \varphi}. \quad (4.21)$$

Once again we recognize the factor in square brackets as an *array factor* – one may want to compare this result to Eq. (4.13) at $\theta = 0$. One reason for using this name is that the linear pattern of two dipoles (or one dipole above the ground plane) is obtained as the single-dipole pattern Eq. (4.17) multiplied by the array factor of an array of two dipoles.

Another reason is that the array factor does not really change from antenna to antenna: if we repeat the above derivation not for the infinitesimally small dipole but for a dipole of arbitrary length, we will have exactly the same array factor in front of the (somewhat different) single-dipole pattern, etc.

However, the array factor does change if the current directions for two dipoles are not the opposite (phase shift of π) but the same (phase shift of 0). This happens, for example, for a horizontal dipole above a PMC ground plane. Another (and more important) example is that of the vertical dipole above the ground plane, when the image current flows in the same direction as the current in the actual dipole [2]. Instead of subtracting two exponential factors

$$\exp(+jkd \cos \theta) - \exp(-jkd \cos \theta) = 2j \sin(kd \cos \theta), \quad (4.22a)$$

one now adds them together in order to obtain the array factor in the form:

$$\exp(+jkd \cos \theta) + \exp(-jkd \cos \theta) = 2 \cos(kd \cos \theta). \quad (4.22b)$$

Note: Antenna arrays considered in the following text (Chapter 11) extensively use the array factor for pattern synthesis. More generic (phased) arrays usually use a certain prescribed (not necessarily 0 or π) *progressive phase shift* between the individual radiators to steer the antenna beam.

4.13 EXTENSIONS OF THE IMAGE METHOD: CORNER REFLECTOR

The method of images can be quite helpful in various antenna problems. An example is given by a corner reflector antenna shown in Figure 4.13. The dipole pattern is shaped by two finite ground planes, with a *corner (or flare) angle* α . This arrangement makes the antenna more directional, with the gain up to 12 dB. Major advantages are the construction flexibility and simplicity. The corner ground plane is usually not floating; it is connected to the outer conductor of the coaxial cable.

A solution for the corner angle of 90° is given in Figure 4.14a. It assumes three image dipoles (one for every plane plus one “balancing” image dipole). All four dipoles (the original one plus three images) form two polar dipole pairs that will cancel the tangential E -field on both corner planes. Again, the field outside the



Figure 4.13 UHF corner-reflector dipoles at 433 MHz. Source: Design by the authors.

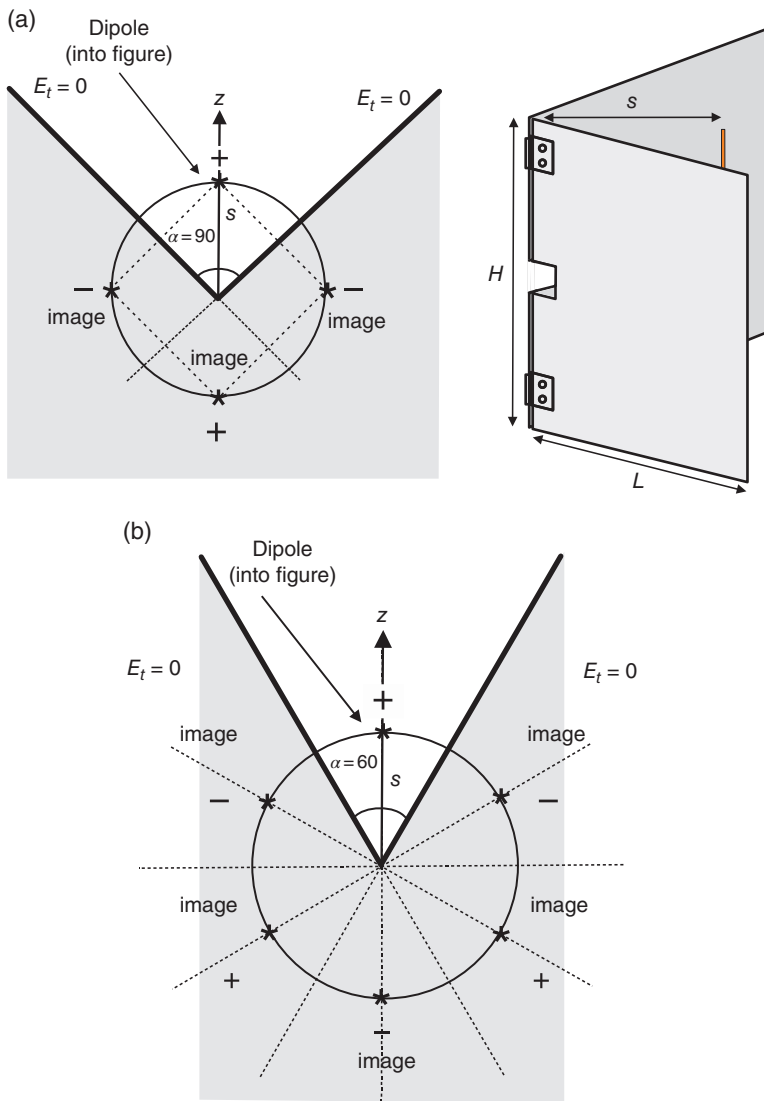


Figure 4.14 (a) The corner reflector with corner angle of 90° – top view – and the related method of images. (b) Corner reflector with corner angle of 60° – top view – and the related method of images.

corner angle is nonphysical; it should be zeroed. The method of images is a reasonable assumption when the corner plates are relatively long and wide.

A solution for the corner angle of 60° is given in Figure 4.14b. According to [3], the method of images is applicable for corner angles equal to $180^\circ/n$, where n is any positive integer. This is a well-known fact in electrostatics. Corners of 180° (flat

sheet), 90, 60, 45°, etc., can be treated by this method. The performance of corner reflectors at intermediate angles cannot be determined by this method but can be interpolated approximately from the others.

The aperture of the corner reflector (D) is usually made between one and two wavelengths ($\lambda < D < 2\lambda$) [2]. The feed-to-vertex distance (s) is usually taken to be between a third and two-thirds of the wavelength ($\lambda/3 < s < 2\lambda/3$) [2]. For each reflector, there is an optimum feed-to-vertex spacing. If the spacing becomes too small, the radiation resistance decreases and becomes comparable to the loss resistance of the system which results in an inefficient antenna. For very large spacings, the system produces undesirable multi-lobes, and it loses its directional characteristics [1, 2]. The length of the sides of the 90° corner reflector is mostly taken to be twice the distance from the vertex to the feed ($L \approx 2s$). The height (H) of the reflector is usually taken to be about 1.2–1.5 times greater than the total length of the feed element, in order to reduce radiation toward the back region from the ends.

4.14 FINITE GROUND PLANE – GEOMETRICAL OPTICS

A question of a significant practical importance relates to understanding the impact of a *finite ground plane*. The geometry of a dipole antenna above the finite ground plane is shown schematically in Figure 4.15. A first guess about the field distribution of the antenna is that of GO.

In terms of GO, the total field is a combination of rays emanating from the dipole and then reflected from the metal surface according to the Snell's law [1]

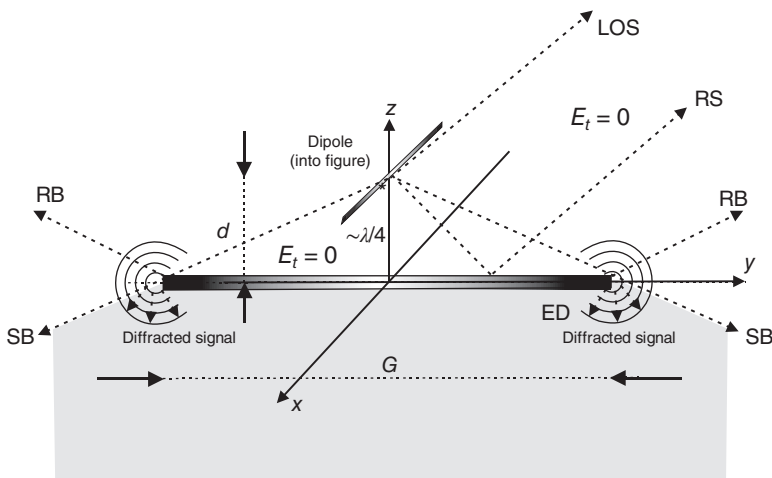


Figure 4.15 Geometrical optics approximation for a dipole above a finite ground plane.

$$\vec{n} \times (\vec{S}_2 - \vec{S}_1) = 0, \quad \vec{n} \cdot (S_2 + \vec{S}_1) = 0, \quad (4.23)$$

where \vec{S}_1 , \vec{S}_2 are the incident and reflected ray directions, respectively; \vec{n} is the unit (outer) normal vector to the reflector surface. From Eq. (4.23), one can express \vec{S}_1 through \vec{S}_2 and vice versa

$$\vec{S}_1 = \vec{S}_2 - 2(\vec{n} \cdot \vec{S}_2)\vec{n}, \quad \vec{S}_2 = \vec{S}_1 - 2(\vec{n} \cdot \vec{S}_1)\vec{n}. \quad (4.24)$$

Both expressions have an identical form due to reciprocity. According to GO, the field everywhere within the *reflection boundary* (RB) in Figure 4.15 is a combination of the incident (line-of-sight or LOS signal) and the RS (reflected signal). The field everywhere outside the RB but still above the *shadow boundary* (SB) is the LOS signal from the dipole. The field below the SB is zero. A *diffracted field* is thus ignored.

4.15 FRONT-TO-BACK RATIO

Is the field in the shadow zone really zero? If it is, then a small reflector might be completely sufficient for a dipole antenna. In practice, however, one prefers to use reflectors as large as possible, despite apparent size and weight constraints. This is because a finite ground plane does not quite follow the laws of GO [4]. It is subject to *diffraction* as schematically shown in Figure 4.15.

There is an analytical model that can provide us with an explanation of the radiation in the shadow zone of the antenna ground plane. It is based upon a famous solution for the wedge diffraction obtained by Arnold Sommerfeld some 130 years ago (in 1896) – see, for example, [5–7]. In practice, numerical simulations could be used to obtain a decisive answer.

Example 4.2

Determine the radiation pattern of a half-wave strip (or blade) dipole spaced a quarter wavelength apart from a finite square ground plane of a variable size. The geometry is shown in Figure 4.16; the dipole width is $\lambda/150$.

Solution: We will vary the ground plane size, G , as 0.5λ , 1.0λ , 1.5λ , and 2.0λ and will look at two radiation patterns: total gain in the *E*-plane of the antenna (the xz -plane) and total gain in the *H*-plane (the yz -plane). For the selected dipole geometry, total gain is close to elevation gain. The corresponding results (both rectangular and polar plots) are given in Figure 4.17. These are obtained with the MATLAB Antenna Toolbox and Ansys HFSS (ED) software. Note that, for lossless antennas, gain and directivity coincide.

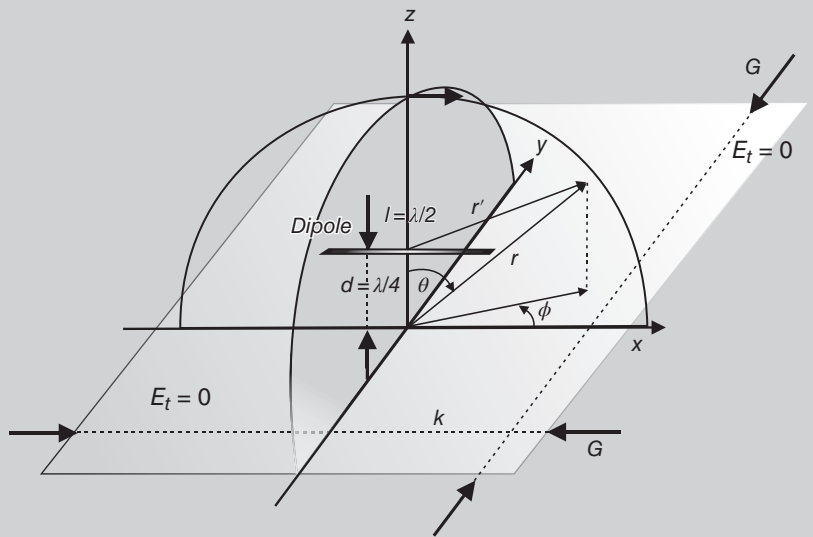


Figure 4.16 Geometry for a half-wave dipole with quarter wave separation. The xz -plane is the E -plane of the dipole; the yz -plane is the H -plane. The size of the ground plane in this figure is approximately 1.7λ .

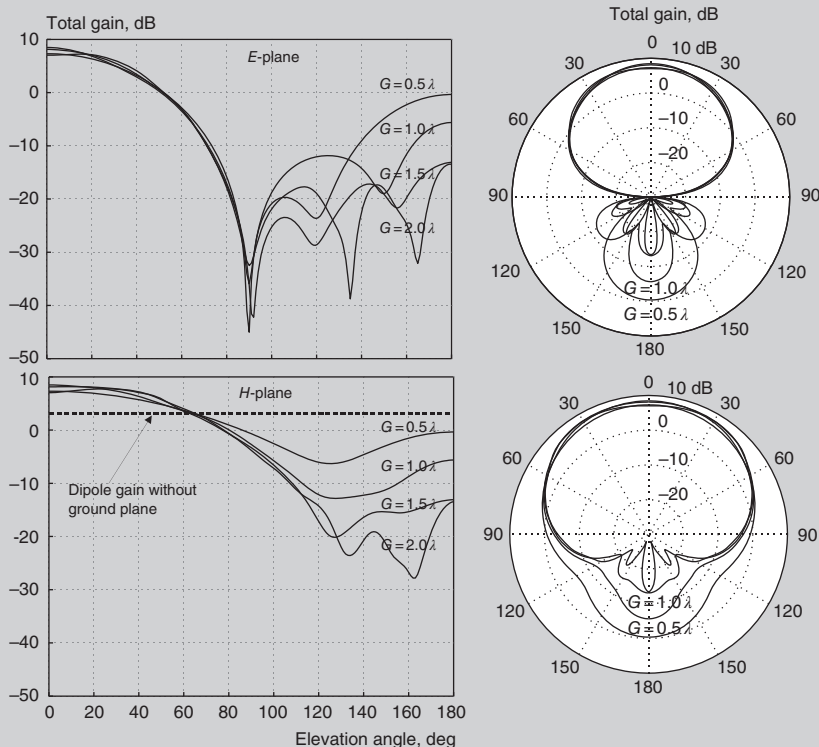


Figure 4.17 Radiation patterns of the dipole above a finite ground plane of variable size. Left – rectangular plot; right – the equivalent polar plot.

One can see from Figure 4.17 that there is in fact no complete shadow zone beneath the ground plane. Moreover, the radiation in the backward direction is quite significant. The backward radiation indeed decreases, when the ground plane size increases, but not quite monotonically.

The ratio of power gain at zenith (in the direction of maximum radiation) to the gain in the opposite direction (at nadir) is called *the front-to-back ratio*. When the gain/directivity is expressed in dB, this ratio is just a difference between the two gain values in Figure 4.17. For the present example, this ratio is given in Table 4.3.

TABLE 4.3 Front-to-back ratio for the horizontal dipole as a function of the ground plane size (square ground plane).

Ground plane size, G	Front-to-back ratio (dB)
0.5λ	~8
1.0λ	~14
1.5λ	~21
2.0λ	~21

One can see that the performance is obviously improving as the size of the ground plane increases. From the viewpoint of performance/size ratio, the most beneficial is perhaps the ground plane on the size of about 1.5λ – the incremental performance saturates after this point. Note that the full-wave numerical simulations for a large ground plane are time consuming. For antennas on large metal platforms, including aircrafts and ships, semi-analytical methods such as physical optics may be used.

Note: An interesting paradox: if the ground plane simply redirects the half of the power of the horizontal dipole up, then the gain (directivity) should increase by 3 dB, not by 6 dB as stated previously. What is the matter? The explanation uses the fact that the antenna pattern is no longer the half donut – see the dipole gain in the H-plane in Figure 4.17. The ground plane additionally zeroes the radiation with the E-field vector being parallel to the plane. In other words, it also “reshapes” the half donut and makes it more directional so that the total gain increase is 6 dB.

Note: Why is the ground plane important in general? Consider one example: a GPS base station antenna receiving signals from multiple satellites. You already know how weak the received signal could be. Now, imagine adding all the noise coming from Earth ground and surroundings. If the ground plane would not block it properly, this noise could entirely mask the useful signal.

NOTES TO PROBLEMS OF THIS SECTION GIVEN BELOW

1. This is a difficult question; integrate over azimuthal angle first and then introduce a new integration variable $t = \cos \theta$.
2. Gain in dBic refers to a circularly polarized, theoretical *isotropic* radiator of the same total power. The *realized* gain of a circularly polarized antenna is also often measured in dBic.

REFERENCES

1. T. A. Milligan, *Modern Antenna Design*, Wiley-IEEE Press, New York, 2005, second edition.
2. C. A. Balanis, *Antenna Theory. Analysis and Design*, Wiley, New York, 2016, fourth edition.
3. J. D. Kraus, “The corner reflector antenna,” *Proc. IRE.*, pp. 514–519, 1940.
4. L. Diaz and T. A. Milligan, *Antenna Engineering Using Physical Optics*, Artech House, Boston, 1996.
5. A. Sommerfeld, *Optics*, Academic Press, New York, pp. 245–265, 1964.
6. A. Ishimaru, *Electromagnetic Wave Propagation, Radiation, and Scattering*, Prentice Hall, Upper Saddle River, NJ, 1991.
7. H. Bateman, *The Mathematical Analysis of Electrical and Optical Wave Motion on the Basis of Maxwell's Equations*, Diver Publications, Inc., New York, 1955.

PROBLEMS

1. (A) Formulate the $\lambda/4$ rule for the dipole with a metal ground plane in your own words.
 (B) A dipole operates at 1 GHz. At which distance from the dipole should the ground plane be located?
 (C) What is the maximum gain for the dipole with a properly separated infinite ground plane?
 (D) Which ground plane size is most beneficial for the dipole from the viewpoint of performance/size ratio, in terms of operating wavelength λ ?
2. Results of this section give an approximation for the dipole field above a metal ground plane, i.e. above the PEC in the ideal case. One could consider an *impedance* ground plane in Figure 4.9 with a nonzero *surface impedance* (boundary condition on the reflecting surface) given by

$$\mathbf{Z}_S \equiv \frac{\mathbf{E}_x(z=0)}{\mathbf{H}_y(z=0)}, \quad \mathbf{Z}_S \neq 0. \quad (4.25)$$

- (A) Derive the dipole field above the ground when $Z_S = \infty$ ($H_y(z=0) = 0$). This case is known as PMC. Consider normal incidence only.
- (B) Find all separation values d (in terms of wavelength) necessary for the optimal separation distance (for the maximum total radiated field).
3. Repeat Problem 2 when $Z_S = j\eta$ [Ω^2] (an inductive surface impedance). Consider normal incidence only.
4. The field of an infinitesimally small dipole oriented along the x -axis above an infinite ground plane is given by Eq. (4.21).
- (A) Find analytical expression for the total radiated power in terms of the feeding current for $d = \lambda/4$.¹
- (B) Determine antenna directivity (lossless gain) in dB at zenith ($\theta = 0$).
5. The combination of two horizontal perpendicular dipoles shown in Figure 4.18 that follows is known as a *turnstile antenna*. It is commonly used for creating a dual independent polarization or a circular polarization. In this problem, we will assume infinitesimally short dipoles.
- (A) Obtain an analytical expression for the total radiated electric field of the turnstile above the ground plane assuming independent currents (phasors) in the dipole feeds I_1, I_2 and dipoles of the same length l .
- (B) Plot total normalized directivity in the xz -plane to scale when $I_1 = I_2 = I_0$ and $d = \lambda/4$, and show on the same graph directivity of only dipole #1 ($I_1 = I_0, I_2 = 0$).

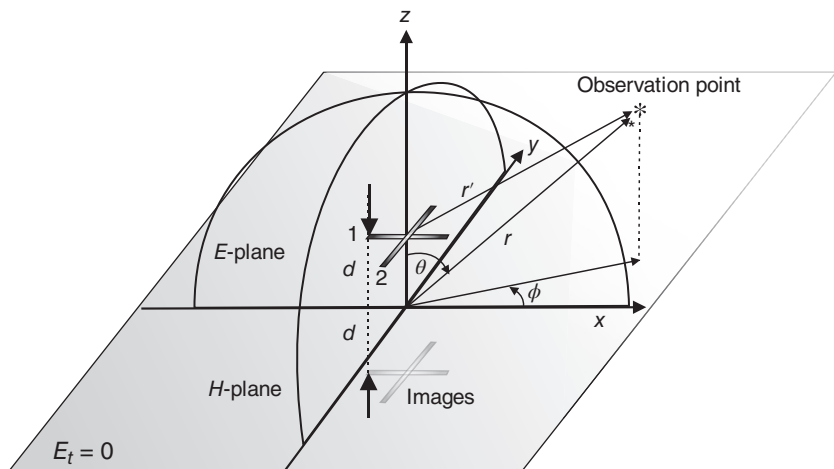


Figure 4.18 Geometry of a turnstile antenna.

6. Let us denote dipole #1 in the figure to Problem 5 as dipole X and dipole #2 as dipole Y, according to the axes of Cartesian coordinates. The total electric field, \vec{E} , of two dipoles in the H -plane of dipole X is a combination of two components (see Chapter 10)

$$\mathbf{E}_R = \frac{1}{\sqrt{2}} (\mathbf{E}_\theta + j\mathbf{E}_\phi), \quad \mathbf{E}_L = \frac{1}{\sqrt{2}} (\mathbf{E}_\theta - j\mathbf{E}_\phi). \quad (4.26)$$

These vectors determine the right-handed circular polarization (RHCP) and left-handed circular polarization (LHCP) components of the total field. From this equation, one obtains (RHCP) *polarization isolation, or cross-polarization ratio*, ρ_C , in the form $\rho_C = \frac{|\mathbf{E}_R|}{|\mathbf{E}_L|}$. Polarization isolation is generally measured in dB and shows a “quality” of circular polarization produced by an antenna. With all other data identical for both dipoles and $d = \lambda/4$,

- (A) Plot ρ_C (dB) in the *H*-plane of dipole X to scale close to zenith when $I_1 = I_0, I_2 = -jI_0$.
 - (B) Plot ρ_C (dB) in the *H*-plane of dipole X to scale close to zenith when $I_1 = jI_0, I_2 = I_0$.
 - (C) Compute and plot normalized RHCP directive gain² for either case A or B.
 - (D) Polarization isolation of a GPS RHCP antenna should be 15 dB or better. Over which beam width could this value be achieved?
 - (E) Will your result change if the *E*-plane of dipole X is considered?
 - (F) Why cannot we have a good polarization isolation over the entire hemisphere? Explain your answer. Could you suggest a possible solution?
- 7*. Figure 4.19 shows a vertical electrical dipole above a ground plane. In this problem, we will assume an infinitesimally short dipole.

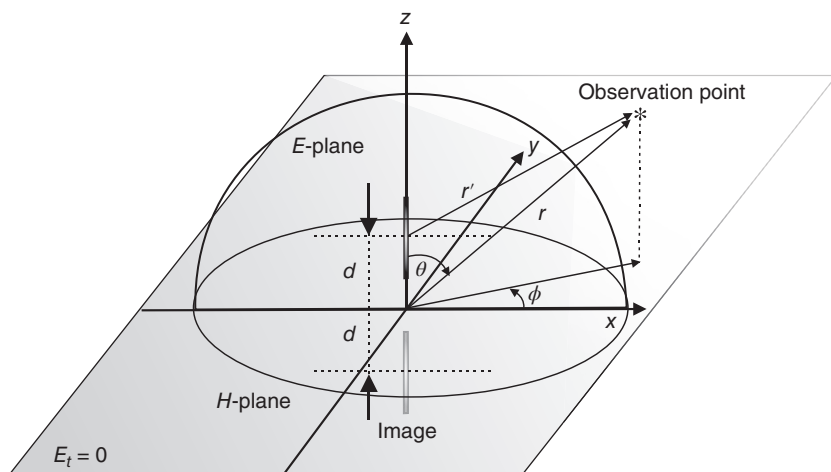


Figure 4.19 Geometry of a vertical electric dipole above a ground plane.

- (A) Obtain an analytical expression for the total radiated electric field of the vertical dipole above the ground plane assuming a very short dipole of length l .
- (B) Plot normalized directivity in the E -plane to scale, assume $d = \lambda/2$.
- (C) Repeat for directivity in the H -plane.
- (D) Justify both of your plots by performing the corresponding simulations in the MATLAB Antenna Toolbox. *Hint:* Use the `conformalArray` object in Antenna Toolbox to create the equivalent array of dipoles from the image-method analysis. The `conformalArray` object allows you to position the elements using Cartesian coordinates. Look at the documentation by using the following command in the command window `>>doc conformalArray`.
- 8***. In Sections 4.14 and 4.15, there is an introduction to the finite ground plane and its effects on the antenna. In particular, Section 4.14 introduces key concepts of the analytical technique known as GO. We will use this as inspiration for this problem. The default reflector configuration in the MATLAB Antenna Toolbox is for 1 GHz and has a half-wavelength dipole as the exciter. Create a strip dipole which is 14.1 cm long and 3 mm wide to be used as an exciter. Rotate the dipole from 0 to 90° in steps of 15° about the x -axis and for each such configuration calculate the
- (A) Impedance and maximum directivity at 1 GHz. Turn in a plot of the two results as a function of tilt angle.
- (B) Calculate the directivity at azimuth = 0, elevation = -90° for each configuration at 1 GHz. Plot the directivity as a function of the exciter's tilt angle. Comment on the variations in the plot. Put it in context of what was discussed in Section 4.14 and more specifically in Figure 4.15.
- 9.** Show how to apply the image method to a dipole-fed corner reflector antenna with corner angle of 45° . The feeding dipole is centered.
- 10.** Could we apply the image method when the corner angle is 270° ? Why yes or why not?
- 11***. Using MATLAB Antenna Toolbox and the image method, obtain and plot an H -plane radiation pattern for a dipole-fed corner reflector antenna with corner angle of 90° in Figure 4.14a. Assume a feed-to-vertex distance (s) of $\lambda/3$ and a half-wave dipole. What is the maximum directivity in dB? *Hint:* Use the `conformalArray` object in Antenna Toolbox to create the equivalent array of dipoles from the image-method analysis. The `conformalArray` object allows you to position the elements using Cartesian coordinates. Look at the documentation by using the following command in the command window `>>doc conformalArray`.
- 12.** Repeat the previous problem for a dipole-fed corner reflector antenna with corner angle of 60° in Figure 4.14b. All other parameters remain the same.

13. In this problem, we consider a vertical *monopole* over an infinite ground plane. The monopole length is not critical for the following analysis.
- Explain how does the method of images works for the vertical monopole over an infinite ground plane? Present an equivalent dipole.
 - If the impedance of an equivalent dipole is Z_a , what is the monopole impedance?
- 14*. Create a vertical *monopole* over an infinite ground plane, designed for operation at 1.7 GHz using the MATLAB Antenna Toolbox. Calculate the following:
- Monopole impedance over the frequency range 1.5–2 GHz with 100 frequency points. Turn in the plot.
 - Directivity patterns at 1.5, 1.7, and 2 GHz. Turn in the 3D plots.

Hint: To make an infinite ground plane, assign the `GroundPlaneLength/Width` to be “inf.”

15. Consider an idealized case of a tunnel environment with a dipole shown in Figure 4.20. Both 2D walls are the PEC boundaries. Is it possible to apply the image method to the present problem? Do not rush to give a negative answer.

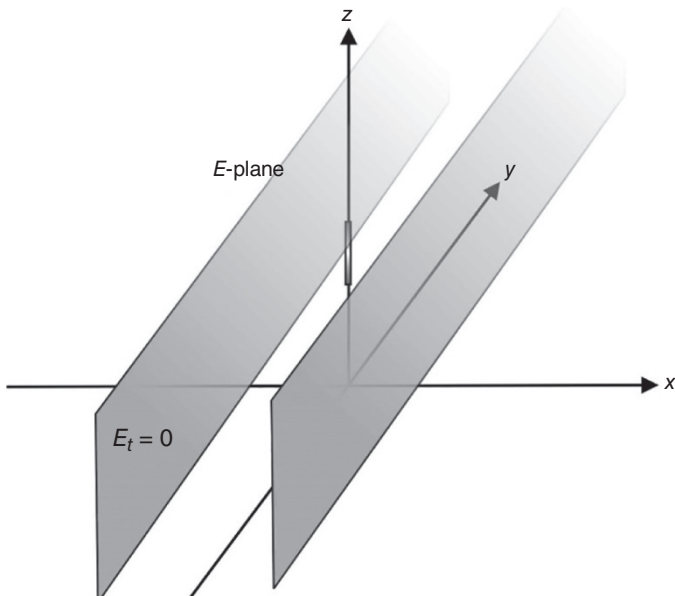


Figure 4.20 Geometry of a vertical electric dipole between two metal walls.

CHAPTER 5



Dipole Antenna Family: Broadband Antennas that Operate as Dipoles at Low Frequencies

SECTION 1 BROADBAND DIPOLES AND MONOPOLES

5.1. Dipole. Summary of Previous Results	135
5.2. Monopole	136
5.3. Broadband (Large) Dipoles	137
5.4. Canonic Dipoles and Their Performance	137
Reference	140
Problems	140

In this chapter, we will concentrate on the particular dipole-based antenna configurations. The first candidate is indeed the dipole and other dipole-like antennas.

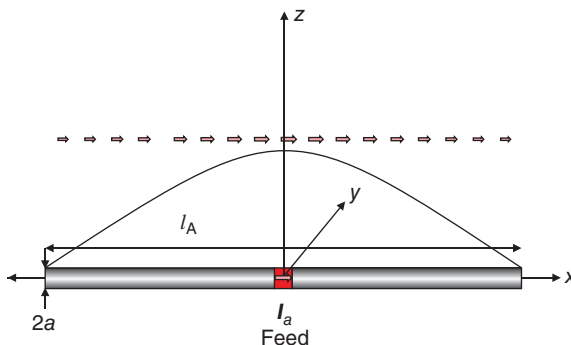
5.1 DIPOLE. SUMMARY OF PREVIOUS RESULTS

The center-fed dipole antenna is shown in Figure 5.1. The *broadside direction* of the dipole (direction of maximum radiation) now coincides with the yz -plane. The *endfire direction* is the direction along the x -axis, similar to that in Chapter 4. There is no dipole radiation in the endfire direction for a straight dipole.

Antenna and EM Modeling with MATLAB® Antenna Toolbox, Second Edition. Sergey N. Makarov, Vishwanath Iyer, Shashank Kulkarni, and Steven R. Best.

© 2021 John Wiley & Sons, Inc. Published 2021 by John Wiley & Sons, Inc.

Companion website: www.wiley.com/go/Makarov/AntennaandEMModelingwithMATLAB2e

Figure 5.1 Center-fed cylindrical dipole oriented along the x -axis.**TABLE 5.1 Impedance parameters of the center-fed wire or strip dipole.**

Dipole impedance:

l_A is the total dipole length, a is the dipole radius, $z = kl_A/2$, and

$k = \frac{2\pi}{\lambda}$, $\lambda = c_0/f$ is the wavenumber. If a strip or blade dipole of width t is considered, then $a_{eq} = t/4$ where t is the strip width [1]. Typical impedance bandwidth: 8–12%

$$Z_a = R_a(z) - j \left[120 \left(\ln \frac{l_A}{2a} - 1 \right) \cot z - X_a(z) \right]$$

$$R_a(z) \approx -0.4787 + 7.3246z + 0.3963z^2 + 15.6131z^3$$

$$X_a(z) \approx -0.4456 + 17.0082z - 8.6793z^2 + 9.6031z^3$$

(programmed in Example 1.5)

Valid at $0.05 \leq f_c/f_{res} \leq 1.2$

where $f_{res} \equiv c_0/(2l_A)$ is the resonant frequency of an idealized dipole having exactly the half-wave resonance and f_C is the center frequency of the band.

In the previous chapters, we have established a number of useful facts for the center-fed cylindrical dipole or the strip dipole including both the input impedance and the radiation patterns. The radiation patterns for the geometry shown in Figure 5.1 follow from Eq. (4.17) (short dipole); the patterns for dipoles of various lengths oriented along the z -axis follow from the results of Chapter 3. The dipole impedance results from Chapter 1 are again summarized in Table 5.1.

5.2 MONOPOLE

A *monopole* (a half of the dipole over an infinite ground plane) has the same radiation pattern as the dipole over the upper hemisphere. The pattern is zero over the lower hemisphere, indeed. However, monopole's input impedance is *exactly a half of the dipole impedance* in Table 5.1 when an infinite ground plane is considered. To prove this fact, we consider a dipole feeding gap with the series impedance combination, $1/2Z_a + 1/2Z_a$, then cutting by an infinite metal plane will leave $1/2Z_a$.

5.3 BROADBAND (LARGE) DIPOLES

After the cylindrical/strip dipole and its major features including the balun assembly have been established, the next question of practical interest is how to increase the dipole bandwidth. Since the bit transfer rate (the speed of digital wireless transmission) continuously increases, the required baseband bandwidth increases. So does the passband bandwidth, which needs to be covered by an antenna. Wideband or broadband, and possibly small antennas, are therefore the most important subject of ongoing antenna research.

The impedance bandwidth of the dipole is changed (increased) by varying its geometry [1]. Generally, one could distinguish between two types of antenna geometry variations:

- (i) those on a large scale affecting the entire antenna geometry; and
- (ii) those in the vicinity of the antenna feed only.

It will be shown later in Chapter 7 that the bandwidth of an antenna, which can be enclosed within a sphere with radius a , can be improved if the (dipole) antenna utilizes the sphere volume as efficiently as possible. On the other hand, the antenna cannot cover the entire sphere volume in a watertight manner since it would not radiate at all. Therefore, there is always a tradeoff between the specific antenna shape and the bandwidth. As a result, the dipole (and other) antenna design sometimes becomes more of an art than a science.

Another important point is a proper treatment of the dipole feed. Sometimes, a small correction of the antenna geometry close to the feed may have a significant impact on its impedance performance (but not on the radiation pattern!).

Ultimately, as long as the radiation pattern is not concerned, changing antenna geometry for impedance matching over a wider band is equivalent to putting an *impedance-matching network* in “space,” instead of doing so with an extra *impedance matching lumped circuit*. This method is traditionally preferred since it has a lower loss.

A wide variety of dipole antenna configurations exist; some of them are shown in Figure 5.2. From left to right (and then from top to bottom) one could observe

- (i) a *bowtie dipole* with a split-coaxial balun;
- (ii) a (*wide*) *blade dipole*;
- (iii) a *coaxial dipole*;
- (iv) a *droopy dipole* with a tapered printed balun.

Those are only a few selected examples; we will study other dipole configurations as well.

5.4 CANONIC DIPOLES AND THEIR PERFORMANCE

Five representative dipole-based antenna configurations are shown in Figure 5.3 along with the corresponding simulation results in Ansys Electronics Desktop. Those are: a thin dipole, a thicker cylindrical dipole, a bowtie dipole, a wide blade dipole, and a *biconical dipole*.

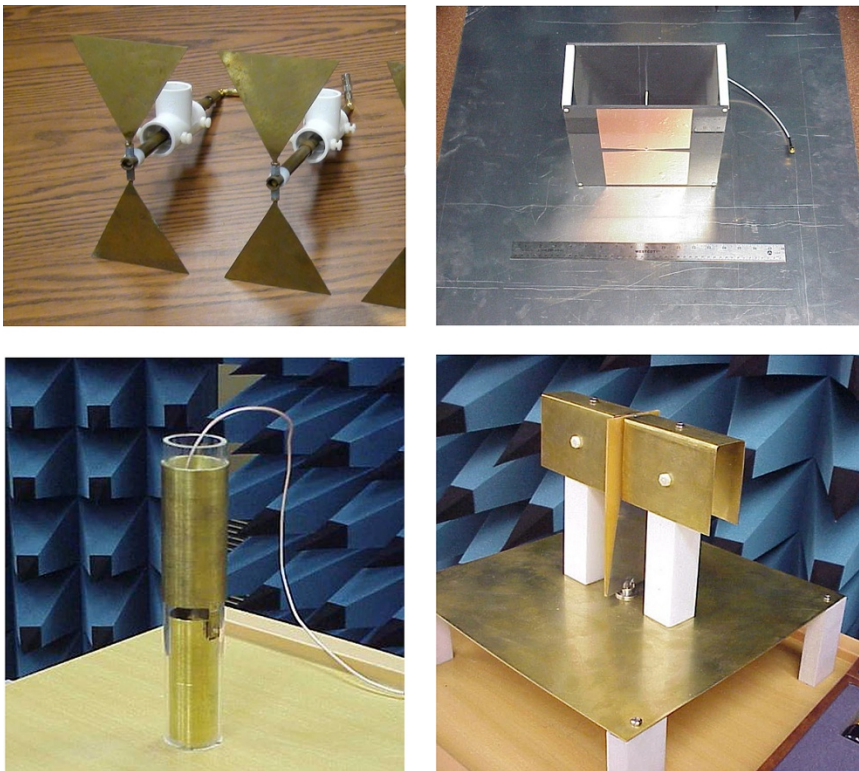


Figure 5.2 Examples of broadband dipoles. From left to right (and then from top to bottom) – bowtie dipole with a split-coaxial balun, blade dipole, coaxial dipole (does not need a balun), and a droopy dipole with a printed tapered balun. *Source:* Design by the authors.

All of those antennas utilize the dipole mode of operation and the dipole pattern either over the entire frequency band or only at lower frequencies.

We must be extra careful about the last two antennas even though they might look like the standard dipole antenna at first sight. The biconical “dipole” antenna and the wide blade “dipole” will be discussed separately later in this chapter.

All antennas in Figure 5.3 are 15 cm in length. For bowtie, wide blade, and biconical dipoles, the largest transversal dimension is 7.5 cm. Note that all antennas have different impedance bandwidths, but nearly *the same omnidirectional dipole radiation pattern* over the wide band from 0.3 to 1.2 GHz.

All antennas in Figure 5.3 are matched to 50Ω ($R_g = 50 \Omega$ for the transmitting antenna). One can see that the thin dipole has the smallest possible bandwidth of 11%, the thicker dipole has a somewhat larger bandwidth of 15%, the bowtie has the bandwidth of 18%, and the cone dipole has the bandwidth of 24%.

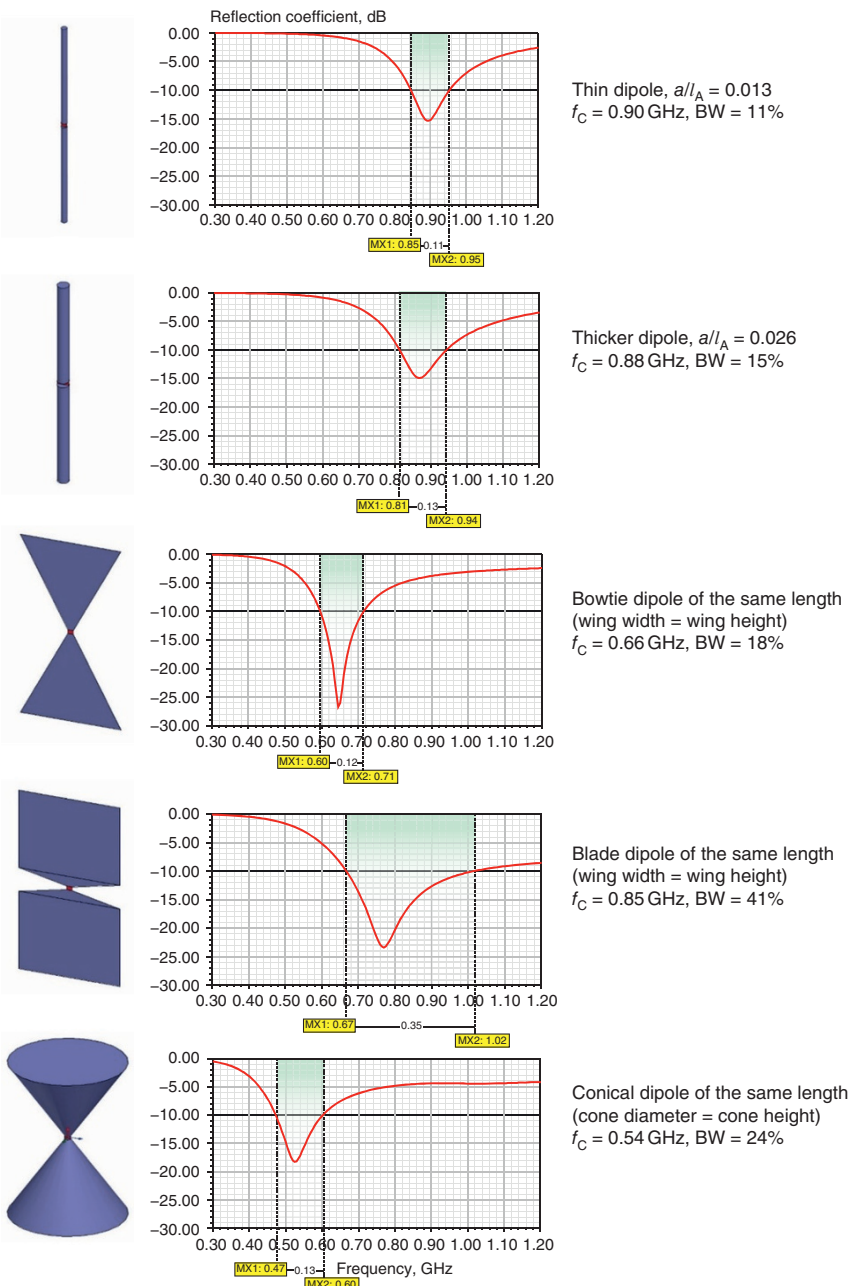


Figure 5.3 Five representative dipole antenna configurations: thin dipole, a thicker cylindrical dipole, bowtie dipole, wide blade dipole, and the biconical “dipole.” All antennas have different impedance bandwidths (when matching to $50\ \Omega$), but nearly the same omnidirectional radiation pattern over the band. All antennas are 15 cm in length.

One specifically notes the blade dipole in Figure 5.3 has the largest possible bandwidth of 41%. This bandwidth is achieved by a proper selection of the geometry of the feeding cone. Even a larger bandwidth may be achieved when this cone is optimized.

Example 5.1

It is intuitive that the biconical dipole in Figure 5.3 is expected to have the largest possible bandwidth. However, this is not the case. Maybe we have missed something?

Solution: It follows from the corresponding plot in Figure 5.3 that the biconical dipole has almost a constant reflection coefficient, after the first resonance. Such an observation usually means that the antenna is indeed well matched to a certain impedance, but this impedance is not necessarily equal to 50Ω . An analytical theory of the biconical dipole antenna will be given in the next section. This theory will support our intuitive conclusion.

REFERENCE

1. C. A. Balanis, *Antenna Theory: Analysis and Design*, Wiley, New York, 2016, fourth edition.

PROBLEMS

1. (A) Why do we often modify the dipole antenna shape? Why not to use only one “universal” cylindrical dipole shape?
(B) Name two major reasons to change the dipole antenna geometry.
2. (A) List all dipole and dipole-like antenna types that you already know.
(B) Find ratio D/λ for every dipole in Figure 5.3 where D is the largest antenna dimension and λ is the wavelength at the lower frequency of the band.

SECTION 2 BICONICAL, WIDE BLADE, AND VIVALDI ANTENNAS

5.5. Biconical "Dipole" or Biconical Antenna	141
5.6. Wide Blade Dipole: Two Antennas in One	147
5.7. Wide Dipole with One Radiating Slot – Vivaldi Antenna	149
References	153
Problems	153

5.5 BICONICAL "DIPOLE" OR BICONICAL ANTENNA [2]

The biconical antenna is a classic *broadband antenna type* [1]. Even though it might look like a dipole at first sight, its mode of operation at large sizes (higher frequencies) and large flare angles α in Figure 5.4 becomes quite different from the standard half-wave resonant dipole.

In contrast to the familiar dipole, the large biconical antenna will utilize a *traveling non-resonant wave*, not the *standing resonant wave*. This is the first *traveling-wave antenna* that we will encounter.

5.5.1 Structure of the Solution – Transmission Line Approach [2]

An *infinite* biconical dipole is considered first; its geometry (a representative cross-section in the xz -plane) is shown in Figure 5.4. Based on the geometry given, we make the following assumptions (use the solution in the phasor form):

1. Only the E_θ -component of the electric field exists; $E_\theta = E_\theta(r, \theta)$ in spherical coordinates. This assumption automatically satisfies the boundary condition on the metal surface (tangential component of the E-field is zero).
2. Only the H_φ -component of the magnetic field exists; $H_\varphi = H_\varphi(r, \theta)$ in spherical coordinates.
3. The radiated field is a locally plane wave (an outgoing *spherical TEM – transverse electromagnetic wave*) where $E_\theta = \eta H_\varphi$.

Note: Assumptions made at beginning of this section reduce the antenna radiation problem essentially to a *transmission line problem*, where the transmission line is now a *radial diverging volume* between two individual cones excited at the central point. Similar radial lines are not only used as antennas, but also as feeding networks for antenna arrays (the so-called *radial-line feed*).

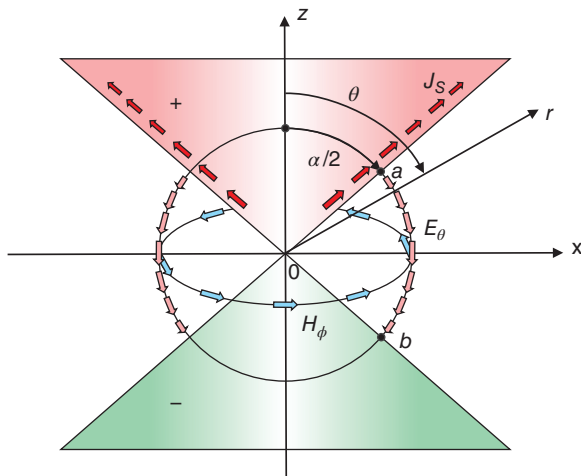


Figure 5.4 Biconical dipole geometry – the xz -plane.

Next, Ampere's law is applied in the free space where there are no currents. It is given by Eq. (3.21),

$$\vec{E} = \frac{1}{j\omega\epsilon_0} \nabla \times \vec{H} \quad (5.1)$$

where, in spherical coordinates [Eq. (3.22)],

$$\nabla \times \vec{H} = \vec{a}_r \frac{1}{rsin\theta} \left[\frac{\partial}{\partial\theta} (\mathbf{H}_\varphi sin\theta) \right] + \vec{a}_\theta \frac{1}{r} \left[-\frac{\partial}{\partial r} (r\mathbf{H}_\varphi) \right], r = |\vec{r}|. \quad (5.2)$$

Since only the elevation component of the electric field exists, we must request that, according to Eq. (5.1) and (5.2)

$$\frac{1}{rsin\theta} \left[\frac{\partial}{\partial\theta} (\mathbf{H}_\varphi sin\theta) \right] = 0 \Rightarrow \mathbf{H}_\varphi = \frac{f(r)}{sin\theta}, \quad (5.3a)$$

where $f(r)$ is an arbitrary function. Similarly,

$$\mathbf{E}_\theta = \eta \frac{f(r)}{sin\theta} \quad (5.3b)$$

according to the assumption of the outgoing spherical (or locally plane) wave. Eq. (5.3a) and (5.3b) establish the solution in a general form.

5.5.2 Radiated Fields

The yet unknown function $f(r)$ is found from the condition that both the H-field and the E-field, along with the magnetic and electric potentials, must satisfy the Helmholtz equations (wave equations in terms of phasors) in free space. One thus has,

$$\nabla^2 \vec{E} + k^2 \vec{E} = 0, \quad (5.4a)$$

$$\nabla^2 \vec{H} + k^2 \vec{H} = 0, \quad (5.4b)$$

everywhere in free space. In spherical coordinates, one obtains for the corresponding elevation component of the Laplace operator [1]:

$$\left(\nabla^2 \vec{E} \right)_\theta = \frac{1}{r^2} \frac{\partial}{\partial r} \left[r^2 \frac{\partial E_\theta}{\partial r} \right] - \frac{1}{r^2 \sin^2 \theta} E_\theta + \frac{1}{r^2} \frac{\partial^2 E_\theta}{\partial \theta^2} + \frac{\cot \theta}{r^2} \frac{\partial E_\theta}{\partial \theta}, \quad |\vec{r}| = r. \quad (5.5a)$$

Substitution of Eq. (5.3b) into this expression shows that all terms, which do not include radial derivatives, precisely cancel out, which yields

$$\left(\nabla^2 \vec{E} \right)_\theta = \frac{1}{\sin \theta} \frac{1}{r^2} \frac{\partial}{\partial r} \left[r^2 \frac{\partial f}{\partial r} \right]. \quad (5.5b)$$

Therefore, from Eq. (5.4a) written in the form $\left(\nabla^2 \vec{E} \right)_\theta + k^2 E_\theta = 0$, one has

$$\frac{1}{r^2} \frac{\partial}{\partial r} \left[r^2 \frac{\partial f}{\partial r} \right] + k^2 f = 0. \quad (5.5c)$$

Eq. (5.5c) is a wave equation in 3D with the radial symmetry. The standard solution is an *outgoing spherical wave*, i.e.

$$f(r) = f_0 \frac{\exp(-jkr)}{r}, \quad |\vec{r}| = r. \quad (5.5d)$$

The solution for the E-field is complete. The solution for the H-field has the same form.

5.5.3 Antenna Input Impedance

Voltage (phasor voltage) between two nodes *a* and *b* (transmission line voltage) in Figure 5.4 becomes

$$V_{ab} = \int_a^b \vec{E} \cdot d\vec{l}, \quad (5.6a)$$

where *l* is an arbitrary contour connecting *a* and *b*. Choosing the contour as shown in Figure 5.4, one obtains

$$V_{ab} = V(r) = \int_{\alpha/2}^{\pi-\alpha/2} E_\theta r d\theta = \eta f_0 \exp(-jkr) \int_{\alpha/2}^{\pi-\alpha/2} \frac{1}{\sin \theta} d\theta = 2\eta f_0 \exp(-jkr) \ln \left[\cot \left(\frac{\alpha}{4} \right) \right]. \quad (5.6b)$$

On the other hand, the total current on the cone surface in the vertical direction either in the cross-section *a* or in the cross-section *b* in Figure 5.4 is found from Ampere's law,

$$\mathbf{I}_a = \mathbf{I}(r) = \int_0^{2\pi} \mathbf{H}_\varphi r \sin\theta d\varphi = 2\pi f_0 \exp(-jkr). \quad (5.6c)$$

Characteristic transmission line impedance (impedance, Z , per unit length in the radial direction) is then given in the form

$$Z \equiv \frac{V(r)}{I(r)} = \frac{\eta}{\pi} \log \left[\cot \left(\frac{\alpha}{4} \right) \right] \quad (5.7a)$$

and does not depend on the distance from the origin! Clearly, the antenna impedance (line impedance at origin) has the same form, i.e.

$$Z_a = Z = \frac{\eta}{\pi} \log \left[\cot \left(\frac{\alpha}{4} \right) \right]. \quad (5.7b)$$

In other words, the impedance becomes real; it is only a function of the flare angle of the cone, and does not depend on frequency. The impedance tends to infinity when $\alpha \rightarrow 0$. Otherwise, it may have any desired value.

Note: A similar derivation method or its modifications are applicable to other antenna types such as various *horn antennas* and *tapered slot* (or *Vivaldi*) antennas.

Note: The above analysis indicates that the biconical antenna may in principle have an infinite bandwidth as long as its size is large enough. In that sense, this antenna is a member of the family of the so-called *frequency-independent antennas*. *Spiral antennas*, *log-periodic antennas*, etc., are other members of this family.

5.5.4 Matching Biconical Antenna to 50 Ω

At which value of the flare angle is the biconical antenna matched to 50Ω ? Or to another required generator resistance? An example that follows answers this question.

Example 5.2

Design a biconical antenna matched to 50Ω .

Solution: The proper value of the flare angle of the cone, α , should be determined. To do so, we simply plot the antenna impedance given by Eq. (5.7b) in MATLAB as a function of the cone angle. The corresponding MATLAB script follows:

```
% CONE1 Input impedance of the biconical antenna
clear all;
% EM data
epsilon = 8.85418782e-012;      % Vacuum, F/m
mu = 1.25663706e-006;          % Vacuum, H/m
c = 1/sqrt(epsilon*mu);         % Vacuum, m/s
eta = sqrt(mu/epsilon);         % Vacuum, Ohm
% Bicone data
alpha = [5:0.5:150];           % Cone angle, deg
Za = eta/pi*log(1./tan((alpha/180*pi)/4));
plot(alpha, Za);
title('Impedance of a large biconical antenna');
xlabel('full cone angle, deg');
ylabel('radiation resistance, \Omega');
grid on;
```

The corresponding plot of the antenna radiation resistance (impedance) is shown in Figure 5.5. The resistance approaches 50Ω when $\alpha/2 = 66.8^\circ$.

5.5.5 Antenna Competition

Equipped with the knowledge of the biconical antenna theory, we now change the biconical antenna design shown in Figure 5.3 in order to achieve the proper match to 50Ω . According to Figure 5.5, the cone angle should be increased from 54° to 133.5° . We still keep the overall antenna height equal to 15 cm.

The simulation results for two biconical antennas (the biconical antenna from Figure 5.3 and the biconical matched to 50Ω) are shown in Figure 5.6. Although the biconical dipole matched to 50Ω has indeed a larger bandwidth, its size in the lateral direction greatly increases. Sometimes, this is not desired. Therefore, a compromise should be sought between the antenna size and its bandwidth. Matching the biconical antenna to a larger generator impedance (100–200 Ω) is more beneficial and is used in practice. An impedance transformer may be employed to convert back to 50Ω .

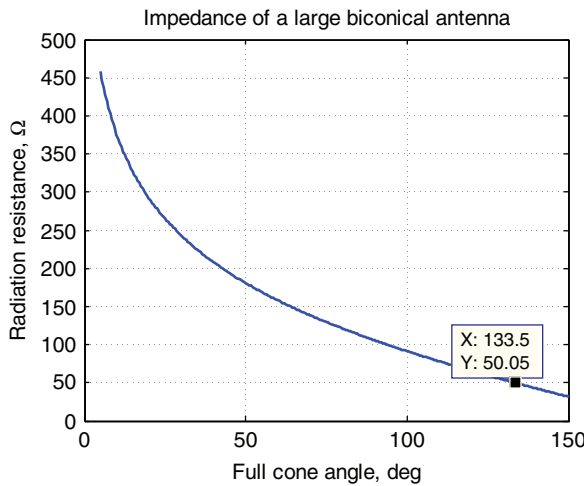


Figure 5.5 Impedance (radiation resistance) of a large biconical antenna as a function of the cone angle.

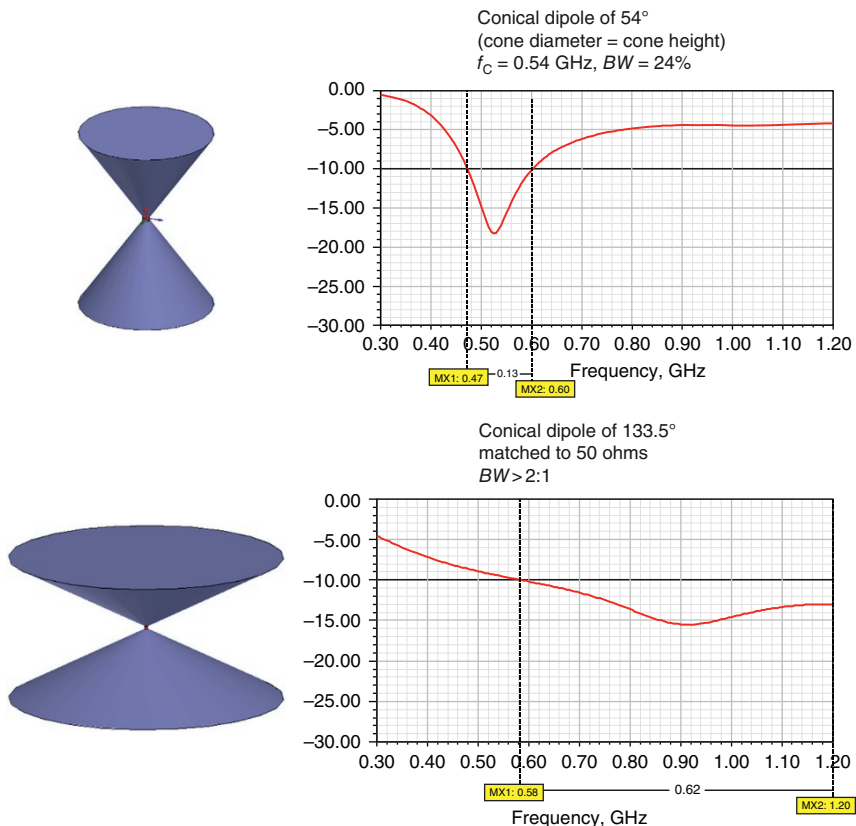


Figure 5.6 Two biconical antenna configurations: a “slender” biconical dipole from Figure 5.3 and a “fat” biconical dipole matched to 50 Ω . Both antennas (of the height 15 cm each) have different impedance bandwidths (for $R_g = 50 \Omega$), but nearly the same omnidirectional radiation pattern over the band.

Note: A finite length of the biconical dipole in Figure 5.6 is another reason why its impedance not exactly approaches $50\ \Omega$ when frequency increases. Another point of concern might be the antenna feed.

5.5.6 Wire Bicone

Having a solid cone dipole is impractical. Quite often, it is replaced by a wire skeleton sketched in Figure 5.7, which has a similar performance. A denser wire mesh may be used instead of the mesh shown in Figure 5.7. As long as the wire mesh is dense, the analysis is performed similarly.

5.6 WIDE BLADE DIPOLE: TWO ANTENNAS IN ONE

Among other dipole types, the wide-blade dipole shown in Figure 5.3 could have an exceptionally large bandwidth, such as 10 : 1 and even larger, while still maintaining a relatively small size [3]. However, the radiation pattern may be distorted. Figure 5.8 provides a qualitative explanation of the large bandwidth. The point is that the blade dipole effectively contains two different antennas in one geometrical setup.

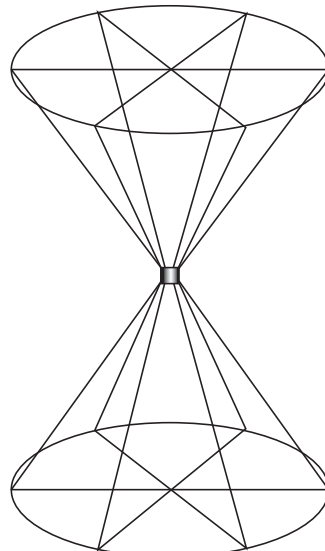


Figure 5.7 A wire-wound biconical dipole.

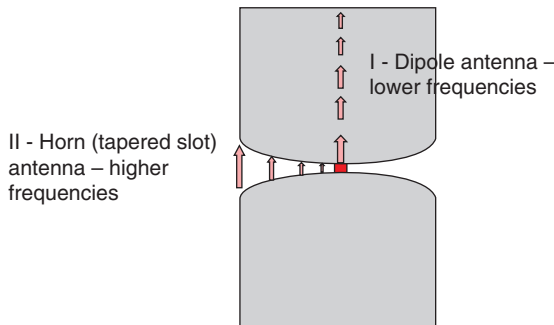


Figure 5.8 Blade dipole – two antennas in one geometry setup.

At lower frequencies, the dipole itself (antenna I in Figure 5.8) plays the major role and produces the familiar dipole pattern. The feeding gap is less important.

At higher frequencies, the feeding slots in Figure 5.8 start to play the major role – they operate as a *notch antenna* or *Vivaldi antenna*. The dipole wings play the role of two ground planes.

The Vivaldi antenna is essentially a *planar horn*, which utilizes a nonresonant traveling wave. Its analysis is conceptually similar to the analysis just performed in the previous section for the conical dipole. It has a very large impedance bandwidth that is covering the upper frequency band of the blade antenna.

As a result, the antenna bandwidth improves at high frequencies, but the true wide dipole will still perform well at low frequencies.

Various dipole antenna variations in Figure 5.8 are possible, for example, with only one radiating slot as shown in Figure 5.9, etc.

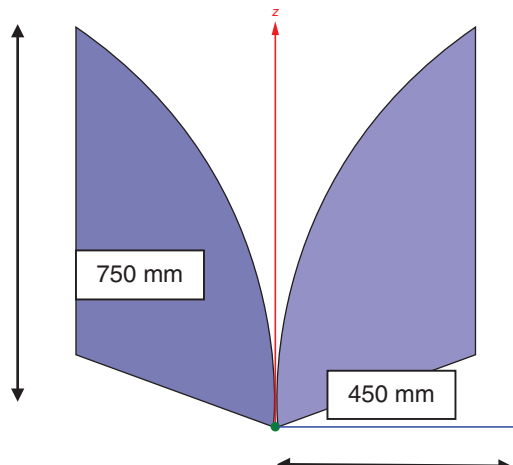


Figure 5.9 Blade dipole with one radiating slot – two antennas in one setup – the Vivaldi antenna. The antenna may be scaled; only relative dimensions count.

5.7 BLADE DIPOLE WITH ONE RADIATING SLOT – VIVALDI ANTENNA

5.7.1 Matching to 100 Ω

Figure 5.9 shows an example of the antenna geometry which may be scaled to operate at different frequencies. The total dipole height (or rather length in Figure 5.9) is 900 mm. In contrast to Figure 5.8, the dipole has two blades but one radiating slot. Figure 5.10 reports VSWR of the antenna matched to 100 Ω and the broadside gain computed numerically.

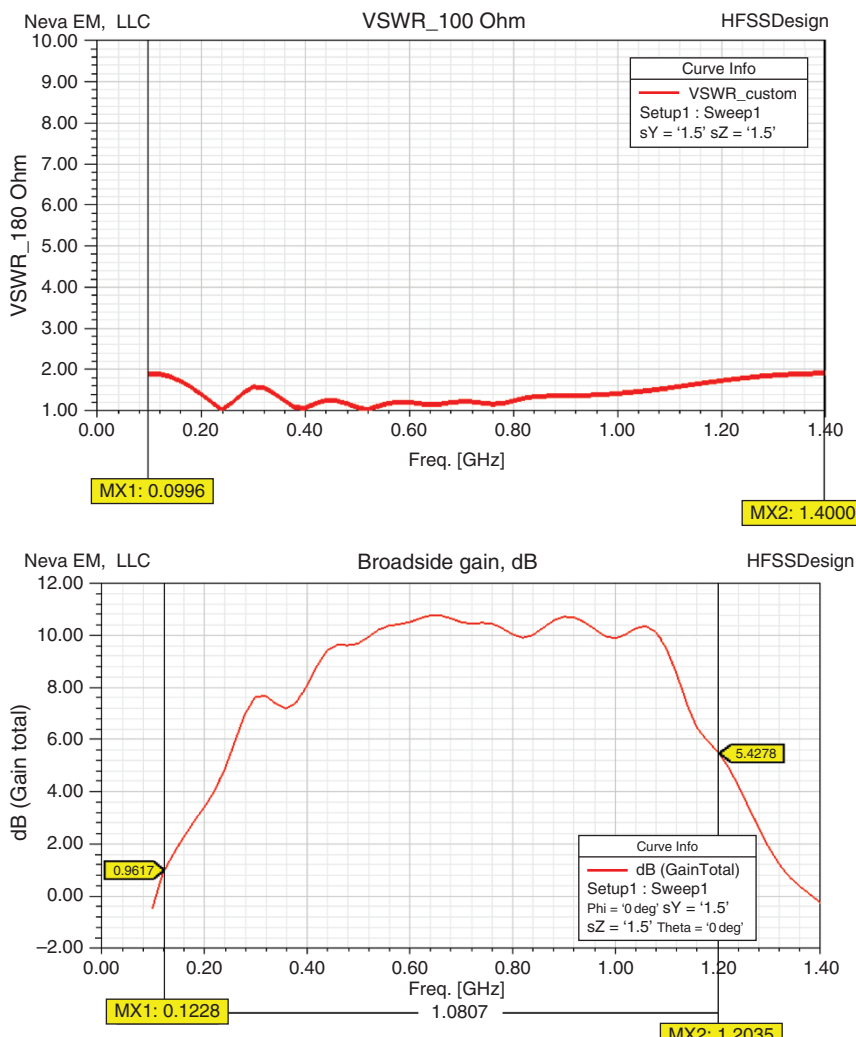


Figure 5.10 VSWR of the antenna in Figure 5.9 and its broadside gain.

Remarkably, the antenna has at least a 14 : 1 impedance bandwidth, from 100 MHz to 1.4 GHz, seen in Figure 5.10. The largest antenna dimension, D , versus the lower band frequency (or better versus wavelength λ at the lower frequency of the band equal to 100 MHz) may be estimated using inequality

$$\frac{D}{\lambda} = \frac{0.9 \text{ m}}{3 \text{ m}} = 0.3. \quad (5.8)$$

Thus, the antenna is still smaller than a $\lambda/2$ dipole. The broadside gain (gain in the direction of the vertical z -axis in Figure 5.9) is high at the band center, but it drops down significantly at the band edges. Antenna gain at high frequencies might be improved by using an exponential taper instead of a three-point arc in Figure 5.9. Note that the antenna in Figure 5.9 must be used with a balun.

Note: The antenna shown in Figure 5.9 covers most of the digital TV bands (400–1000 MHz) with the gain of about 10 dB. Its disadvantage is a bulky shape affected by wind.

5.7.2 Matching to 50Ω

Often, especially for a low-cost design, matching to exactly 50Ω , but not to 100Ω as for the antenna in Figure 5.9, is required. Indeed, an impedance transformer may accomplish this task, but such a transformer operating over a 10 : 1 frequency band of interest might be lossy and costly.

A variation of the antenna in Figure 5.9 that is matched to 50Ω without the transformer is shown in Figure 5.11. This is a “double” blade dipole antenna, which resembles an open book. The antenna impedance halves, much as for the monopole antenna compared to the dipole antenna.

Figure 5.12 shows antenna performance results for the following dimensions in Figure 5.11: $L = 1119 \text{ mm}$, $H = 1200 \text{ mm}$, $\alpha = 20^\circ$, $g = 20 \text{ mm}$. The antenna has a 12 : 1 bandwidth and an exceptionally low VSWR over the band of interest. However, its size is considerably larger than the size of the antenna in Figure 5.9.

Antenna gain at high frequencies in Figure 5.12 could be improved by using an exponential taper instead of a three-point arc in Figure 5.11. The *antenna backlobe gain*, which is shown in Figure 5.12 along with the broadside gain, is often the *most significant feature* of the antenna pattern degradation. The backlobe gain shown in Figure 5.12 may be substantial at high frequencies.

5.7.3 Other Broadband Designs

Figure 5.13 demonstrates some other possible designs with broadband blade dipoles. Figure 5.13a gives a modification of the blade dipole in Figure 5.9. This modification only keeps the outer rim of the solid blade and is less affected by

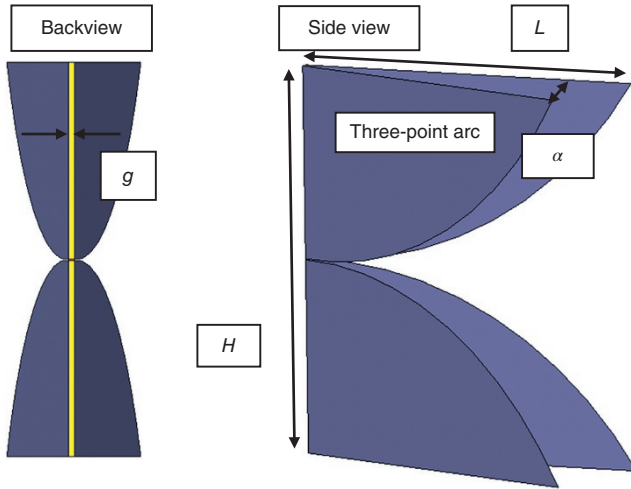


Figure 5.11 Double blade dipole with a Vivaldi slot directly matched to 50Ω .

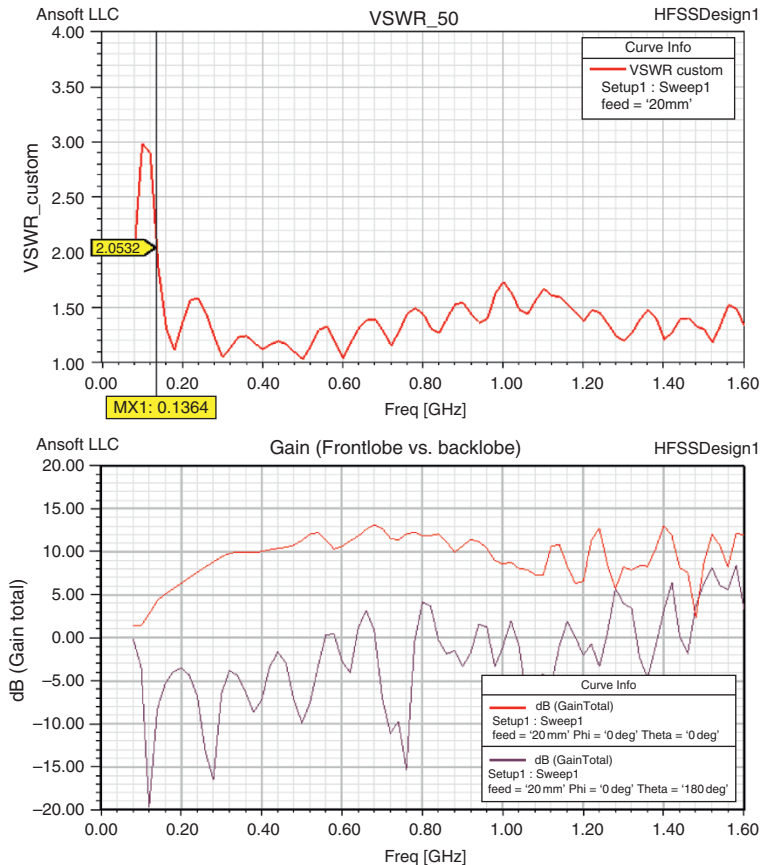
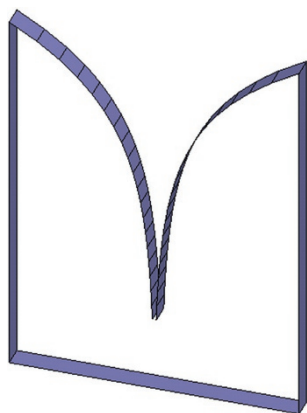
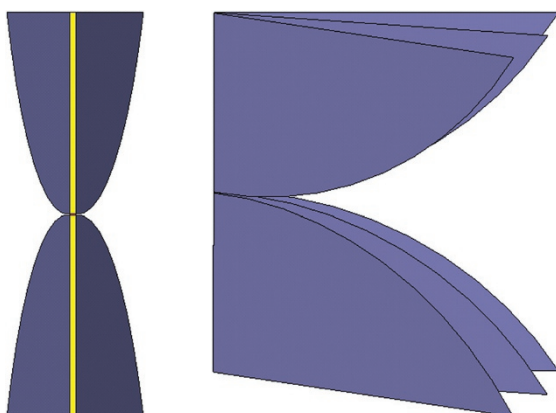


Figure 5.12 VSWR of the antenna in Figure 5.11 and its broadside gain along with the antenna backlobe.

(a)



(b)



(c)

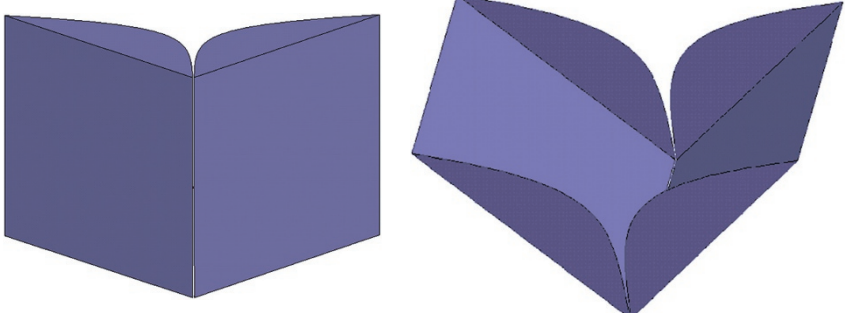


Figure 5.13 Other shapes of broadband dipoles combining the dipole and horn geometries.

wind. Unfortunately, its performance degrades compared to the antenna shown in Figure 5.9. Figure 5.13b gives a modification of the blade dipole in Figure 5.11, which improves both the gain and the bandwidth. The antenna thus more and more resembles a horn antenna. Finally, Figure 5.13c shows a blade dipole which could perhaps be called a “whale mouth.” The size of this antenna type could be made quite small.

REFERENCES

1. C. A. Balanis, *Antenna Theory: Analysis and Design*, Wiley, New York, 2016, fourth edition.
2. S. A. Schelkunoff, *Electromagnetic Waves*, Van Nostrand, New York, 1943, Ch. 11.
3. D. Benzel. “Private communications and joint research with the authors,” *Lawrence Livermore National Laboratory*. 2008–2012.

PROBLEMS

1. (A) Give an expression for the input impedance of a large biconical antenna as a function of the cone angle, α .
(B) A large biconical antenna is to be matched to 100Ω . What cone angle should be chosen for that purpose?
(C) A large conical *monopole* antenna is to be matched to 100Ω . What cone angle should be chosen for that purpose?
(D) An infinite biconical antenna is called a frequency-independent antenna. Why do you think is it so?
(E) Name one straightforward reason why the analysis of this section cannot be applied to an arbitrary cone, e.g. to a cone with the exponential profile.
2. A dipole antenna with two center-fed wide disks is shown in Figure 5.14. Analytically derive the input impedance to the antenna assuming that the disk radii are very large (infinite).

Hint: The present geometry is equivalent to the *radial-line transmission line*.

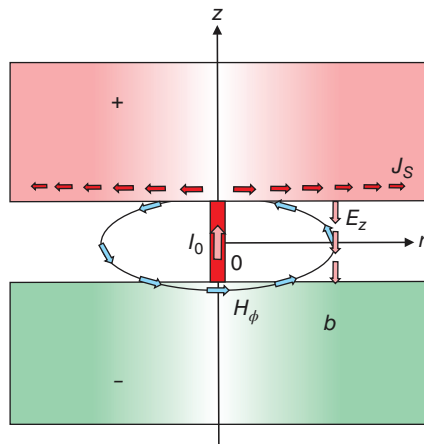


Figure 5.14 Dipole antenna in the form of two disks.

3. (A) Explain in your own words why the blade dipole may have a very large bandwidth?
 (B) How would the dipole in Figure 5.8 radiate? At low frequencies? At high frequencies? Qualitatively sketch the corresponding radiation patterns.
- 4*. Does the Antenna Toolbox have a template for the Vivaldi antenna analysis? If so, present one antenna example including reflection coefficient and pattern plots.

CHAPTER 6



Loop Antennas

SECTION 1 LOOP ANTENNA VS. DIPOLE ANTENNA

6.1. Concept	155
6.2. Analytical Results	161
6.3. Full-wave Simulation Results	165
6.4. Why Loop Antenna?	168
References	169
Problems	169

6.1 CONCEPT

The construction of a loop antenna is simple: this is a loop of wire with a feeding gap. The antenna balun would be necessary. When a high-frequency current flows through the loop (on its surface), it radiates. The loop antenna is a competitor to the dipole. Similarly, the half-loop above a ground plane is a competitor to the monopole antenna. A UHF loop antenna is shown in Figure 6.1.

Note: Antennas in Figure 6.1 do not yet have the balun. According to Chapter 4, the loop antenna does need the balun for the proper operation; so does the dipole antenna.

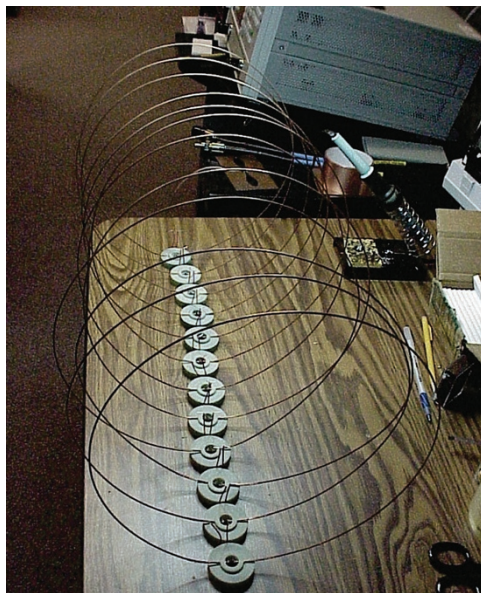
Loop antennas ($D = 11.5''$)

Figure 6.1 Loop antennas with the diameter of $11.5''$ (thick copper wire with a dielectric support) used for student experimentation. *Source:* Design by the authors. The balun is not yet included.

Table 6.1 that follows lists comparative characteristics of the small radiating current element from Chapter 3 (small *electric dipole*) and a small loop of constant current (small *magnetic dipole*) [1]. One can see that both antennas are “dual” to each other: the near field of the small loop antenna may be obtained from the near field of the small dipole antenna using *electromagnetic duality*, i.e. interchanging the electric and magnetic fields, respectively.

Similarly, both antennas have a very similar donut-type pattern, but the polarizations of the electric and magnetic fields will change by 90° .

The following properties of the dipole and loop antennas are of note:

1. The small dipole is *capacitive* while the small loop is *inductive*. This distinction is critical from the viewpoint of matching the small loop antenna or the small dipole antenna. It is generally easier to match the small loop antenna.
2. With reference to Figure 6.2a,b, the small loop/dipole antenna pattern is nearly the same (the donut) in either case. However, the dipole antenna has the *vertical polarization* whereas the loop antenna has a *horizontal polarization*. The type of polarization significantly affects signal propagation along the Earth ground (or sea water). Vertical polarization is more beneficial.
3. At higher frequencies (when approaching the first resonance and above it), the loop changes its radiation pattern from a donut (the so-called *normal*

TABLE 6.1 Comparative Characteristics of Dipole and Loop Antennas.

Dipole (feed current I_0)	Loop (feed current I_0)
$l_A \ll \lambda$ ($l_A \leq \lambda/6$)	$C_A = 2\pi a \ll \lambda$ ($C_A \leq \lambda/4$)
$E_r = \frac{\eta I_0 l_A \cos \theta}{2\pi r^2} \left(1 + \frac{1}{jkr} \right) \exp(-jkr)$	$H_r = \frac{I_0 k a^2 \cos \theta}{2r^2} \left(1 + \frac{1}{jkr} \right) \exp(-jkr)$
$E_\theta = \frac{j\eta k I_0 l_A \sin \theta}{4\pi r} \left(1 + \frac{1}{jkr} - \frac{1}{k^2 r^2} \right) \exp(-jkr)$	$H_\theta = -\frac{(ka)^2 I_0 \sin \theta}{4r} \left(1 + \frac{1}{jkr} - \frac{1}{k^2 r^2} \right) \exp(-jkr)$
$E_\phi = 0, H_r = 0, H_\theta = 0$	$H_\phi = 0, E_r = 0, E_\theta = 0$
$H_\phi = \frac{j\eta k I_0 l_A \sin \theta}{4\pi r} \left[1 + \frac{1}{jkr} \right] \exp(-jkr)$	$E_\phi = \frac{\eta (ka)^2 I_0 \sin \theta}{4r} \left[1 + \frac{1}{jkr} \right] \exp(-jkr)$
Small dipole – impedance $R + jX$	Small loop – impedance $R + jX$
$R = \frac{2\pi\eta}{3} \frac{l_A^2}{\lambda^2}$	$R = \frac{2\pi\eta}{3} \frac{(kS)^2}{\lambda^2}, S = \pi a^2$
$X = -\frac{1}{\omega} \left[\frac{2}{3} \frac{1}{\epsilon_0 l_A} \left(\ln \frac{l_A}{2a} - 1 \right) \right] (a - \text{wire radius})$	$X = +\omega \left[\mu_0 a \left(\ln \left(\frac{8a}{b} \right) - 2 \right) \right] (b - \text{wire radius})$

(Continued)

TABLE 6.1 (Continued)

Dipole (feed current I_0)	Loop (feed current I_0)
Dipole far field and pattern (sinusoidal current)	For the N -turn loop, $R = N^2 R_{\text{one loop}}$ Small loop far field and pattern (const. current)
$\mathbf{E}_\theta = \left[\frac{j\eta \exp(-jkr)}{2\pi r} I_0 \right] \frac{\cos\left(\frac{kl_A}{2} \cos\theta\right) - \cos\left(\frac{kl_A}{2}\right)}{\sin\left(k \frac{l_A}{2}\right) \sin\theta} \quad (6.5a)$	$\mathbf{E}_\phi = \left[\frac{k\eta \exp(-jkr)}{2r} I_0 \right] J_1(k a \sin\theta) \quad (6.5b)$
First resonance (series) $l_A \approx 0.5\lambda$ (6.6a)	(J_1 – Bessel function of first order) First resonance (parallel) $C_A = 2\pi a \approx 0.5\lambda$ (6.6b) Resonance (series) $C_A = 2\pi a \approx 1.1\lambda$ to 1.2λ (6.6c)

Sources: C. A. Balanis, *Antenna Theory: Analysis and Design*, Wiley, New York, 2016, fourth edition.; G. S. Smith, "Loop Antennas," In *Antenna Engineering Handbook*, J. L. Volakis, Ed., McGraw Hill, New York, 2007, fourth edition, Ch. 5, pp. 5-1–5-25.

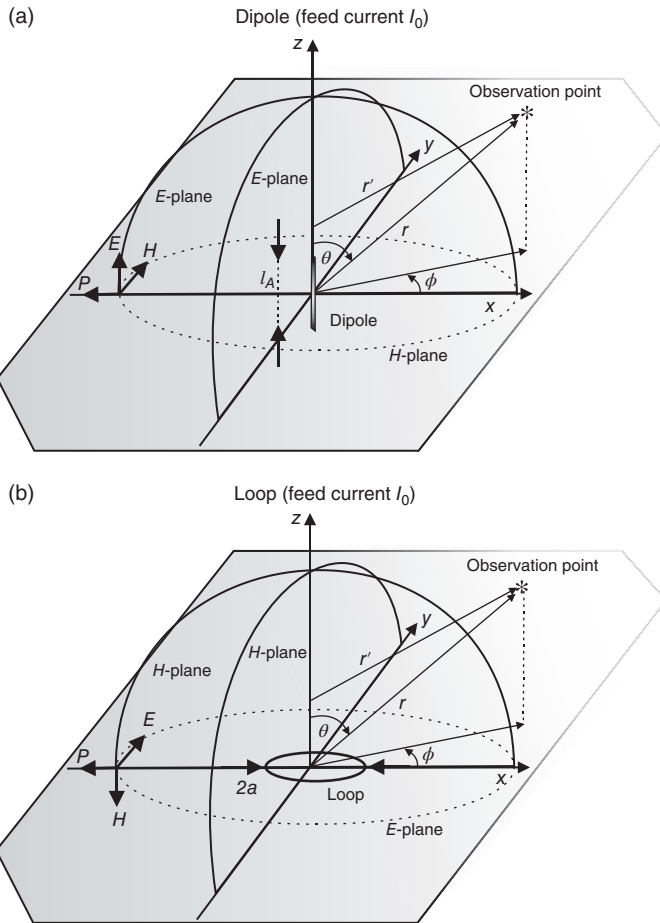


Figure 6.2 (a) Small dipole of constant current I_0 – (the derivation is given in Chapter 3).
(b) Small loop of constant current I_0 – (the same derivation as in Chapter 3).

mode of loop antenna) to the radiation in the direction of its axis (the so-called *axial mode of loop antenna*). The dipole radiation pattern is much more stable than the radiation pattern of the loop antenna.

4. The dipole's first resonance is at

$$\frac{l_A}{\lambda} \approx 0.5, \quad (6.1a)$$

see Eq. (6.6a) in Table 6.1. This is the *series resonance* (corresponding to a *series RLC lumped circuit*). Antenna reactance becomes zero, antenna resistance is close to $60\text{--}75 \Omega$. The loop's first resonance is at

$$\frac{C_A}{\lambda} = \frac{2\pi a}{\lambda} = ka = \frac{2\pi a f}{c_0} \approx 0.5, \quad (6.1b)$$

where C_A is the loop circumference. This is a *parallel resonance* (corresponding to a *parallel RLC lumped circuit*). Antenna reactance still becomes zero at exactly the resonant frequency, but peaks nearby and has a very steep slope. Resonant antenna resistance becomes very large: typically in excess of 2–100 kΩ depending on the conductor thickness. The loop's second resonance is at

$$\frac{C_A}{\lambda} = \frac{2\pi a}{\lambda} = ka = \frac{2\pi a f}{c_0} \approx 1.1 \text{ to } 1.2. \quad (6.1c)$$

This is the *series resonance*. Antenna reactance becomes zero; antenna resistance is close to 160–170 Ω. Those variations in the resonant frequency are due to different conductor thicknesses for the wire loop.

Comprehensive theory of loop antennas is developed in Ref. [2].

Note: The meaning of the parallel half-wave resonance for the loop antenna is quite clear: the current arrives at the second antenna terminal with the phase shift of 180° (half-wave circumference), which effectively cancels the overall current flow through the antenna – this means a very large antenna resistance.

So is the meaning of the series full-wave resonance: the current arrives at second antenna terminal with no phase shift (for the approximately full-wave circumference). The only resistance is that due to current radiation in free space while traveling along the loop circumference.

Note: In contrast to the dipole antenna, the loop antenna cannot be matched to 50 Ω directly, neither at the first resonance nor at the second resonance. Therefore, an impedance-matching network (a transformer) has to be employed for this purpose.

Example 6.1

For a loop antenna with the radius of 10 cm, determine resonant frequencies for the first (parallel) and second (series) resonance.

Solution: We apply Eq. (6.1b) and (6.1c), and obtain:

First (parallel) resonance:

$$\frac{C_A}{\lambda} = \frac{2\pi a f}{c_0} \approx 0.5 \Rightarrow f \approx \frac{0.5 c_0}{2\pi a} = 239 \text{ MHz.} \quad (6.1d)$$

Second (series) resonance:

$$\frac{C_A}{\lambda} = \frac{2\pi a f}{c_0} \approx 1.15 \Rightarrow f \approx \frac{1.15 c_0}{2\pi a} = 549 \text{ MHz.} \quad (6.1e)$$

Those results may slightly vary in every particular case depending on different wire thicknesses.

6.2 ANALYTICAL RESULTS

In this section, we present some analytical results for a small (and only small!) loop antenna related to its pattern and polarization.

Example 6.2

Determine directivity of a small loop antenna in the *H*-plane (a vertical plane passing through the loop axis) in Figure 6.2b. The loop axis in Figure 6.2b coincides with the *z*-axis.

Solution: The electric field radiated by a loop antenna is given by Eq. (6.5b), that is

$$\mathbf{E}_\phi = \left[\frac{k a \eta \exp(-jkr)}{2r} I_0 \right] J_1(ka \sin \theta), \quad (6.7a)$$

where $|\vec{r}| = r$ is the distance from the antenna center, θ is the elevation angle measured from zenith ($z \rightarrow \infty$ in Figure 6.2), and a is the loop radius. J_1 is the Bessel function of the first kind of order 1. These Bessel functions are straightforwardly found using MATLAB (function `besselj`) at any value of the argument. Eq. (6.7a) does not involve the azimuthal dependence; the pattern will therefore be the same for any azimuthal angle – similar to the dipole’s donut pattern.

According to Eq. (3.34) and (3.35), the radiation intensity of the loop antenna after substitution of Eq. (6.7a) becomes

$$U(\theta, \varphi) = \frac{1}{2\eta} |\mathbf{E}_\phi|^2 |\vec{r}|^2 = \left[\frac{\eta a^2 k^2}{8} |I_0|^2 \right] (J_1(ka \sin \theta))^2 \geq 0. \quad (6.7b)$$

The total power radiated by the loop antenna is then given by

$$P_a = \int \int_{\Omega} U d\Omega = \int_0^{2\pi} \int_0^{\pi} U(\theta, \phi) \sin \theta d\theta d\phi, \quad (6.8)$$

where Ω is the total solid angle. We could find the total radiated power by substituting Eq. (6.7b) into Eq. (6.8) and performing either numerical or analytical integration.

After the total radiated power is found using straightforward numerical integration, the antenna directivity is evaluated according to Eq. (3.37), i.e.

$$D(\theta, \phi) = \frac{4\pi U(\theta, \phi)}{P_a}. \quad (6.9)$$

MATLAB script that follows performs the above task. The result for $C_A = 2\pi a = \lambda/4$ (*quarter-wave-circumference loop*) is shown in Figure 6.3. The maximum directivity occurs in the *E*-plane (the loop plane); it is 1.75 dB (dB scale) or 1.50 (linear scale). This is the classic result and simultaneously a figure of merit for the loop antenna. The antenna radiation is zero at zenith. In other words, the small loop radiates nothing in the direction of its axis, similar to the dipole.

Loop directivity (dashed) versus dipole directivity (solid),
dB in a vertical plane in Figure 6.2

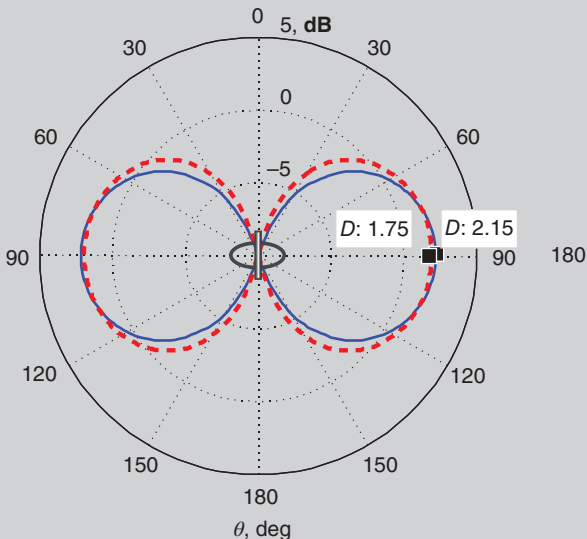


Figure 6.3 Directivity pattern of a quarter-wave-circumference loop versus the half-wave dipole pattern in any vertical plane in Figure 6.2. The maximum loop directivity is 1.75 dB. The dipole antenna and the loop antenna are both *omnidirectional antennas*.

The entire radiation pattern very much resembles a “donut,” with the radial symmetry in the azimuthal plane. In other words, the small loop radiates equally well for any azimuthal direction. Such a pattern is called an *omnidirectional pattern*; the loop antenna is therefore another *omnidirectional antenna*, along with the dipole antenna.

The MATLAB script for the present example follows. The MATLAB polar plot cannot accept negative values; we therefore subtract 10 dB or so from the final result.

```
% PATTERN1 Radiation pattern and effective aperture of a loop antenna
% with a constant current distribution
clear all
% EM data
epsilon = 8.85418782e-012;      % Vacuum, F/m
mu = 1.25663706e-006;          % Vacuum, H/m
c = 1/sqrt(epsilon*mu); % Vacuum, m/s
eta = sqrt(mu/epsilon); % Vacuum, Ohm
% Loop antenna data
f = 1e9;                      % Frequency, Hz
lambda = c/f;                  % Wavelength, m
k = 2*pi/lambda;               % Wavenumber, m
Ia = 1;                        % Feed current, A
a = lambda/(2*pi); % Loop radius, m
% Pattern data
ka = k*a
theta = [1:360]/180*pi;        % Elevation angle, rad
U = eta*ka^2*Ia^2/8*(besselj(1, ka*abs(sin(theta)))).^2;
% Radiation intensity, W/steradian
Prad = 2*pi*sum(U(1:180).*sin(theta(1:180)))*(pi/length(theta(1:180)));
% Total radiated power, W
U0 = Prad/(4*pi);              % Radiation intensity of the equivalent
% isotropic source, W/steradian
D = U/U0;                      % Directivity, dimensionless
EffAperture = lambda^2*max(D)/(4*pi) % Effective aperture of the loop
EffRadius = sqrt(EffAperture/pi)/a
% Relative effective radius of the loop
D = 10*log10(D); % Directivity, dB
D = D + 10; % Offset, dB
D(find(D<0)) = 0;
polar(theta-pi/2, D);
xlabel('theta, deg');
title('loop directivity D, dB in the E-plane (subtract 10 dB)');
```

Loop directivity for $C_A = \lambda/4$ (dashed curve) versus
loop directivity for $C_A = \lambda/10$ (dotted curve),
in a vertical plane in Figure 6.2

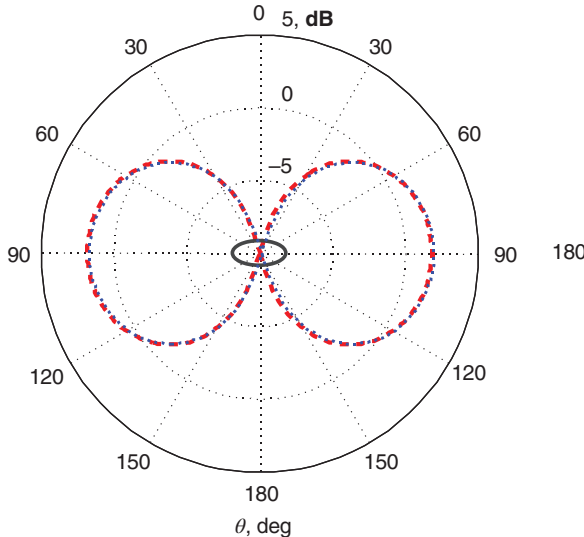


Figure 6.4 Directivity pattern of a quarter-wave-circumference loop (dashed curve) versus the directivity pattern of a one-tenth-wave-circumference loop (dotted curve). The constant loop current is assumed. The maximum directivity is 1.75 dB versus 1.76 dB, respectively. Two patterns are nearly identical.

Using the same script as in Example 6.2, one could estimate the directivity pattern not only of the quarter-wave-circumference loop, but also for *any* small loop. As an example, Figure 6.4 shows a comparison between the directivity pattern of the quarter-wave-circumference loop (dashed curve) and a one-tenth-wave-circumference loop (dotted curve). The maximum directivity is 1.75 dB versus 1.76 dB, respectively. The pattern shape remains nearly identical.

Note: The MATLAB script for Example 6.2 simultaneously calculates the *effective radius* of the loop antenna, which is the radius of its effective aperture – see Chapter 3. For the quarter-wave-circumference loop, the effective radius is 4.9 times greater than the physical loop radius:

$$a_{\text{eff}} \approx 4.9a \quad (6.10a)$$

whereas for the one-tenth-wave-circumference loop, the effective radius is 12.2 times (!) greater than the loop radius,

$$a_{\text{eff}} \approx 12.2a. \quad (6.10b)$$

In other words, the small loop antenna still has a large effective aperture, many times greater than its size. Unfortunately, it is not matched. A similar observation is valid for the dipole (cf. Chapter 3).

6.3 FULL-WAVE SIMULATION RESULTS

Figure 6.5 shows two competing antennas used for comparison: a 15 cm long dipole (resonating at approximately 1 GHz) versus a 30 cm long loop (with the first parallel resonance at about 500 MHz). The wire radius is 2 mm in both cases.

The loop antenna has been created by creating a torus in Ansys HFSS and subtracting a rectangular feeding gap. An alternative is to create a circle first (torus cross section) and then sweep it around the vertical axis.

6.3.1 Antenna Impedance

Figure 6.6 gives the impedance curves for both antenna types. The dipole's curves are more attractive in general – they are more “smooth,” which implies a wider bandwidth and better impedance matching. Furthermore, it is clearly seen that the loop antenna cannot be matched to $50\ \Omega$ directly.

On the other hand, the loop has a larger radiation resistance at low frequencies: it is $6.4\ \Omega$ at 300 MHz in Figure 6.6-center versus dipole's $4.7\ \Omega$ at 300 MHz in Figure 6.6-top.

Figure 6.6-bottom indicates that the loop antenna's resistance at the first resonance becomes very large – in excess of $10\ k\Omega$.

6.3.2 Radiation Pattern – Note of Caution

It is very important to emphasize that, in contrast to the dipole, the loop pattern changes drastically when frequency increases, even below the first resonance.

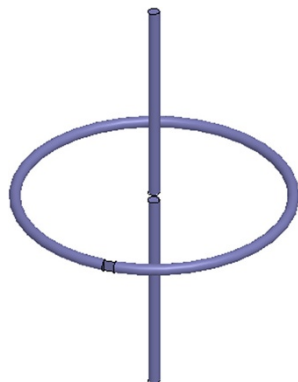


Figure 6.5 A 15 cm long dipole versus a 30 cm long loop to scale.

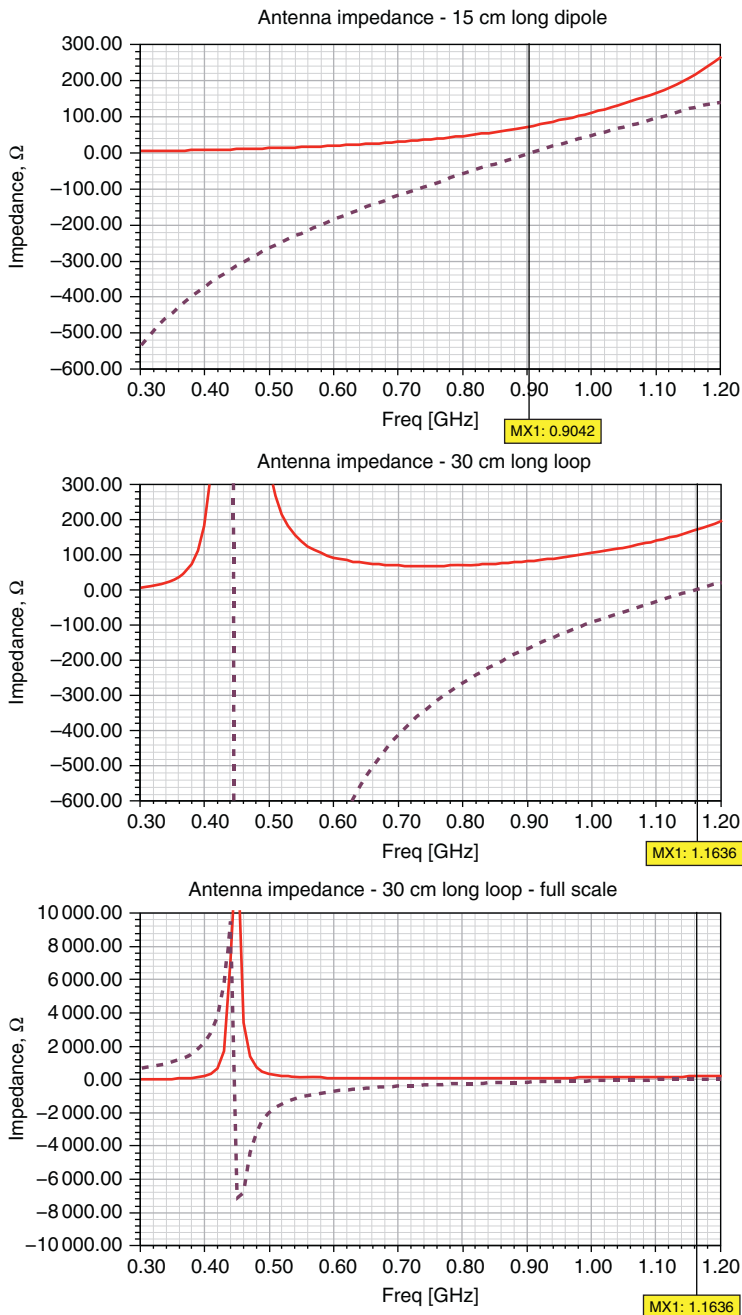


Figure 6.6 Input impedance of the 15 cm long dipole (Figure 6.6-top) versus input impedance of the 30 cm long loop (Figure 6.6-center). Figure 6.6-bottom shows the full-scale loop impedance swing.

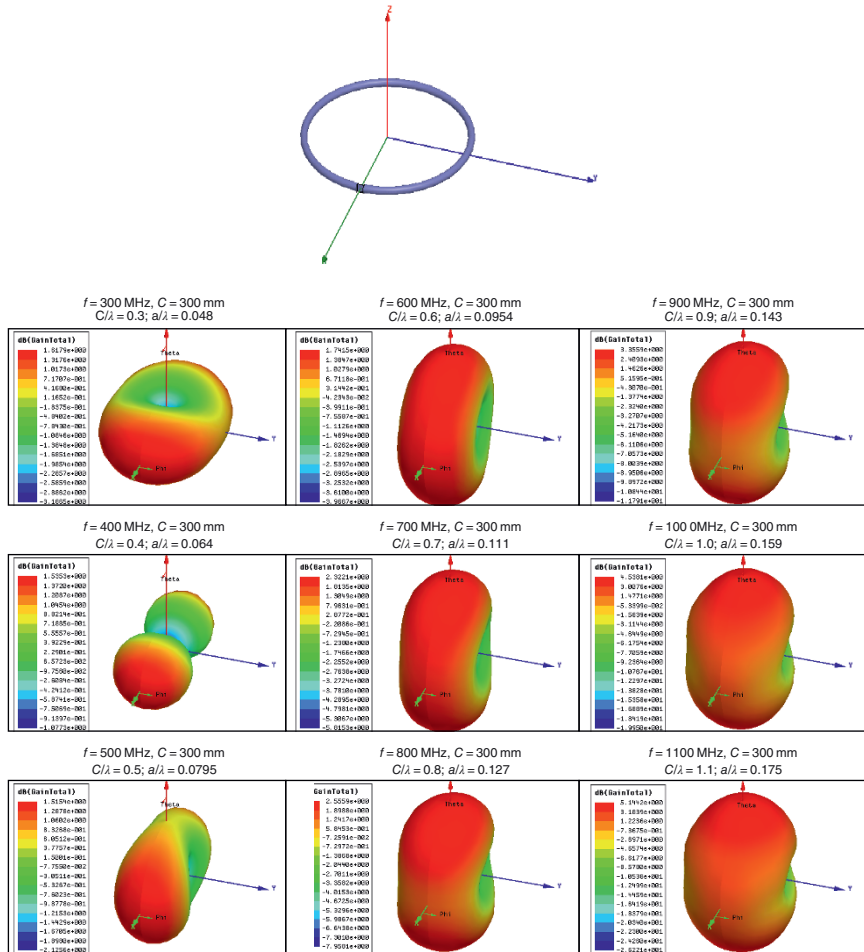


Figure 6.7 Radiation patterns (total gain) of the loop antenna with the length of 30 cm and wire radius of 2 mm at different values of the dimensionless parameter $\frac{C_A}{\lambda} = ka$ computed numerically.

Figure 6.7 shows radiation patterns (total gain) of the loop antenna with the length of 30 cm and the wire radius of 2 mm at different values of the dimensionless parameter $\frac{C_A}{\lambda} = ka$. The pattern already starts to deviate from the donut shape when $C_A/\lambda = 0.3$, and then approaches the *axial mode of radiation*, with the maximum radiation at zenith.

Note: Theory results for the loop patterns given in Constantine Balanis' textbook (C. A. Balanis, *Antenna Theory: Analysis and Design*, Wiley, New York, Ch. 5 Loop antennas, Section 5.3) are based on the analytical expressions from Table 6.1. Those expressions are only valid for the uniform loop current, i.e. for very small loops. Comparison with Figure 6.7, which covers nearly the same range of the dimensionless parameter $\frac{C_A}{\lambda} = ka$, indicates that those results may have a large error.

6.4 WHY LOOP ANTENNA?

Why use the loop antenna if the dipole antenna has presumably much better impedance characteristics and the better pattern stability with regard to frequency variations? Well, there are at least a few distinct and inviting features of the loop antenna that stimulate its wide use. Some of them are listed below.

1. For an N -turn loop (a helical coil antenna), the radiation resistance is approximately the radiation resistance of the single loop times the number of turns squared, i.e. $R = N^2 R_{\text{one loop}}$ – see Table 6.1. Therefore, by using a small coil antenna with multiple turns at low frequencies, we could achieve much *higher* radiation resistances than for the *small* dipole. Unfortunately, this method does not work for a half loop above the ground plane.
2. The further miniaturization of the coil antenna implies the use of a *magnetic core*, which makes the antenna size smaller, similar to the dielectric loading of the dipole/monopole. The antenna so constructed (the popular AM radio antenna) is called the *loopstick antenna*.
3. Quite important, the small loop is inductive. Therefore, it can be matched with a capacitor in parallel (or a capacitive network); see Chapter 7. This is in contrast to the small dipole or monopole, which itself is capacitive and is therefore usually matched with an inductor in parallel (or an inductive network); see Chapter 7. While it is perfectly fine to use an inductor in a larger circuit, an on-chip matching circuit does not benefit from the use of bulky inductors since the inductor of an appreciable inductance cannot be made really small.
4. Therefore, in a tiny on-chip matching circuit such as in a *passive RFID tag*, we prefer using a loop-based antenna rather than the dipole antenna since it is easier (and less expensive) to match it with an integrated capacitor. On the other hand, in a larger circuit, such as in an *active RFID tag*, we may use a dipole since the inductor size is not a problem.
5. A loop antenna is less strongly affected by a dielectric loading, e.g. close to human body. Therefore, loop antennas are frequently used as on-body antennae.

REFERENCES

1. C. A. Balanis, *Antenna Theory: Analysis and Design*, Wiley, New York, 2016, fourth edition.
2. G. S. Smith, "Loop Antennas," In *Antenna Engineering Handbook*, J. L. Volakis, Ed., McGraw Hill, New York, 2007, fourth edition, Ch. 5, pp. 5-1–5-25.

PROBLEMS

1. (A) For the loop antennas shown in Figure 6.1, determine resonant frequencies for the first (parallel) and second (series) resonances, respectively.
 (B) A loop antenna is needed with the first (parallel) resonance at 500 MHz. Estimate its diameter.
2. A small loop antenna is given which has the circumference equal to the length of a small dipole.
 (A) Which antenna has a higher radiation resistance if the loop antenna uses one turn?
 (B) Which antenna has a higher radiation resistance if the loop antenna uses hundred turns (is a coil antenna)?
3. (A) At which value of the dimensionless parameter $\frac{C_A}{\lambda} = ka$ does the loop antenna pattern start to deviate from the theoretical donut shape established for very small loops? What is the major reason for such deviation?
 (B) Does the loop antenna have any potential advantages compared to the dipole? If so, list one of them, which is most important in your opinion.
- 4*. Using a loop antenna model (`loopCircular`) of the MATLAB Antenna Toolbox
 (A) Generate Figure 6.6c (Figure 6.6 bottom) of this section.
 (B) Generate Figure 6.7 of this section.
 Include figures so generated into your report.
- 5*. Create a circular loop in Antenna Toolbox – the default is fine for this exercise. Do the following:
 (A) Calculate the impedance over the frequency band 10–120 MHz. Use 100 points.
 (B) Identify the series and parallel resonance frequencies.
 (C) Provide a qualitative description of the series and parallel resonances (determine values of antenna resistance at the resonance).

- (D) In your opinion is there a frequency at which it is easier to match this antenna to 50Ω ?
- (E) Create 3D directivity plots at 10, 40, 80, and 120 MHz. Comment on the results.
- (F) Repeat the previous task for the 2D radiation patterns in the E- and H- planes of the loop, respectively. Label the corresponding figures.

CHAPTER 7



Small Antennas

SECTION 1 FUNDAMENTAL LIMITS ON ANTENNA BANDWIDTH

7.1. Antenna Size Estimate	171
7.2. Bandwidth of a Small Antenna	172
7.3. Fundamental Limits on the Bandwidth of a Small Antenna	175
7.4. One Hidden Problem with a Small Antenna	178
References	182
Problems	182

7.1 ANTENNA SIZE ESTIMATE

In Chapter 5, we have studied resonant dipole antennas of different shapes and bandwidths. Let us define the size, D , of any such antenna as its longest dimension. Then, for every antenna (resonant cylindrical dipole, bowtie, etc.) the following inequality approximately holds

$$D \geq \frac{\lambda}{4}. \quad (7.1)$$

Here, λ is the wavelength at the lowest frequency of the band (the longest wavelength). In other words, the resonant dipole-like antenna size was always approaching or exceeding $\lambda/4$.

Antenna and EM Modeling with MATLAB® Antenna Toolbox, Second Edition. Sergey N. Makarov, Vishwanath Iyer, Shashank Kulkarni, and Steven R. Best.

© 2021 John Wiley & Sons, Inc. Published 2021 by John Wiley & Sons, Inc.

Companion website: www.wiley.com/go/Makarov/AntennaandEMModelingwithMATLAB2e

What if the antenna size has to be much less than this value? As a simple example, let us consider an unmanned vehicle or an unmanned aircraft with the largest dimension of 1 m. An antenna is required for a 30 MHz band (low VHF). Then, if a monopole-like antenna (a half of the dipole above the ground plane) is chosen, the antenna size may be estimated as (a factor of $\frac{1}{2}$ is inserted for the monopole compared to the dipole in Eq. (7.1))

$$D \geq \frac{\lambda}{8} = \frac{10m}{8} = 1.25m, \quad (7.2)$$

which is greater than the size of the vehicle or the aircraft itself! Therefore, a *small antenna* should be used.

Typically, an *electrically small antenna* is characterized by the size, $D < \lambda/10$. *Electrically short antenna* (an intermediate case) is often characterized by $\lambda/10 < D < \lambda/4$.

Even though the small antenna cannot perform as good as the large antenna, the size requirements may be most critical.

7.2 BANDWIDTH OF A SMALL ANTENNA

7.2.1 Small Antennas

A small antenna is usually a dipole/monopole-based antenna, or a loop-based antenna, or a patch/microstrip-based antenna. Generally, the following observations are valid:

1. For the small dipole, the antenna resistance is small (much less than 50Ω) while the antenna reactance is large and negative (large capacitance).
2. For the small loop, the antenna resistance is also very small, but the antenna reactance is large and positive (large inductance).
3. For the small patch antenna, the antenna resistance is very small, and the antenna reactance is positive (inductance), but is not necessarily large.

Therefore, any small antenna cannot be directly matched to a 50Ω generator resistance no matter what its specific geometry is.

The Method of Moments (the boundary element method) used in Antenna Toolbox is ideally suited for modeling small antennas since it is not affected by artificial boundaries around the computational volume. As a result, more realistic values can be obtained for the extremely small radiation resistances of small antennas.

7.2.2 Test Circuit for a Small Antenna

How do we define the small antenna bandwidth then? Does the small antenna have a bandwidth at all? To answer the last question, let us consider a test

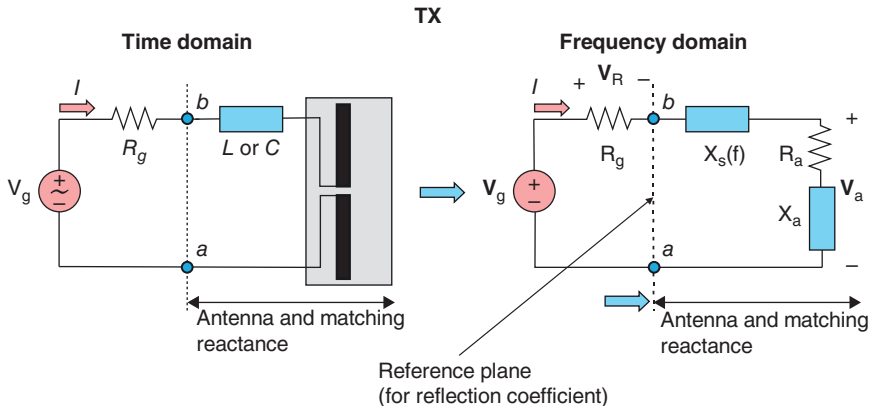


Figure 7.1 TX circuit with a small antenna.

antenna-generator circuit shown in Figure 7.1. Here, a yet unknown *matching reactance* is additionally introduced in series with the antenna.

Let us assume that the antenna itself has the complex impedance $Z_a(f) = R_a(f) + jX_a(f)$. For the small TX antenna, the antenna circuit will now include not only the antenna impedance $Z_a(f)$ itself, but also a *matching lumped reactance* $X_s(f)$.

Such an extra lumped reactance (capacitor or inductor in series with the antenna, for example) constitutes a simple *matching circuit*. The extra reactance must be chosen positive (inductor in series) for the small dipole antenna and negative (capacitor in series) for the small loop antenna. It is chosen in such a way as to exactly cancel the antenna's reactance at a given center band frequency, f_C . In other words, one has

$$\begin{aligned} X_a(f_C) > 0 \Rightarrow X_s(f) &= -\frac{1}{2\pi f C}, \quad C = \frac{1}{2\pi f_C X_a(f_C)} \\ X_a(f_C) < 0 \Rightarrow X_s(f) &= +2\pi f L, \quad L = -\frac{X_a(f_C)}{2\pi f_C}. \end{aligned} \quad (7.3)$$

Next, the generator resistance R_g should be chosen to be exactly equal to the antenna's radiation resistance (for a lossless antenna) at the given center band frequency, f_C , i.e.

$$R_g = R_a(f_C). \quad (7.4)$$

7.2.3 Small Antenna Bandwidth Definition [1, 2]

The TX circuit so defined has the reflection coefficient, Γ , in the reference plane ab in Figure 7.1 in the form [see Eq. (1.16) and (1.17)]:

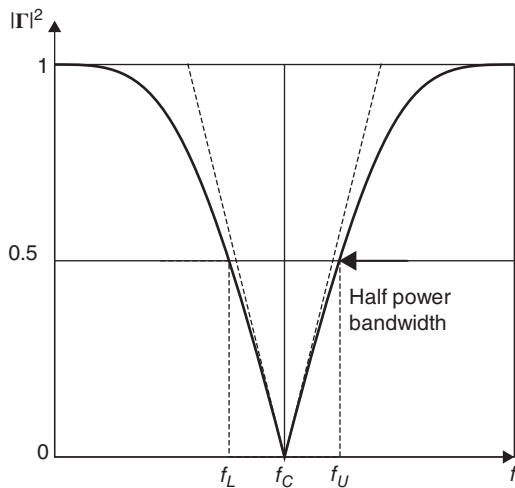


Figure 7.2 Half-power small-antenna bandwidth and its approximation.

$$\frac{P_{avg}}{P_{avg \text{ max available}}} = 1 - |\Gamma|^2, \quad \Gamma(f) = \frac{R_a(f) - R_a(f_C) + j(X_a(f) + X_s(f))}{R_a(f) + R_a(f_C) + j(X_a(f) + X_s(f))}. \quad (7.5)$$

Here, P_{avg} is the *accepted antenna power* (or power delivered to the antenna).

The reflection coefficient in Eq. (7.5) is equal to zero at the center frequency of the band since the reactances exactly cancel out at the center frequency. In other words, the small antenna is now *ideally matched* at its center frequency. Simultaneously, Eq. (7.3)–(7.5) will determine the reflection coefficient behavior over the entire band of frequencies. The *half-power small-antenna bandwidth*, BW , may then be defined as a frequency domain or band around f_C where the magnitude square of the reflection coefficient does not exceed 0.5 (the *3 dB rule*) as shown in Figure 7.2. In other words, the antenna-accepted power should be at least 50% of the maximum available antenna power for the given circuit,

$$BW = f_U - f_L, \quad |\Gamma(f_U)|^2 = |\Gamma(f_L)|^2 = \frac{1}{2}. \quad (7.6)$$

The fractional bandwidth, FBW , is given by

$$FBW = \frac{f_U - f_L}{f_C}. \quad (7.7)$$

Note: The bandwidth in Eq. (7.7) can also be called *fraction matched VSWR bandwidth* [1].

Note: The condition $|\Gamma|^2 \leq 1/2$ corresponds to $|\Gamma|^2|_{\text{dB}} \leq -3 \text{ dB}$ in decibel. For large resonant antennas considered in the previous chapters, the bandwidth threshold has been more demanding: it was equal to -10 dB (maximum 10% but not 50% of power is lost).

Note: While adding a conjugate-matched reactance in series with the small antenna is straightforward, decreasing generator's internal resistance for the purposes of antenna resistance matching is difficult to achieve in practice since this operation would require very large generator currents.

How do we match to the 50Ω -generator then? The answer is that *often we do not*. Therefore, the reflection loss factor, $1 - |\Gamma|^2$, has to be added to the antenna gain as in Chapter 3, which will yield the *realized antenna gain*. This extra power loss may be so significant that the realized antenna gain becomes, say, -20 dB , versus the expected $+2.15 \text{ dB}$ for the half-wave dipole. And yet, even such a low gain value may be acceptable. Therefore, in many small-antenna specifications (especially for tunable antennas) the small antenna performance is determined in terms of the realized (and negative!) antenna gain.

7.2.4 Analytical Approximation of the Small Antenna Bandwidth [1]

Using Taylor series expansion for $|\Gamma(f)|^2$ about f_C with $|\Gamma(f_C)|^2 = 0$, an analytical approximation of the antenna bandwidth in Eq. (7.7) may be obtained using Eq. (7.5), that is

$$FBW \approx \frac{4R_a(f_C)}{f_C \left| \frac{d(\mathbf{Z}_a(f) + jX_s(f))}{df} \right|_{f=f_C}}. \quad (7.8)$$

This analytical approximation is shown schematically in Figure 7.2 by a dashed cone.

7.3 FUNDAMENTAL LIMITS ON THE BANDWIDTH OF A SMALL ANTENNA [1–6]

7.3.1 Antenna Q-Factor

The fundamental limit on antenna bandwidth is primarily written in terms of a *Q-factor* or a *quality factor of an antenna*. What is the *Q-factor* of an antenna? It is very similar to the *Q-factor* of an *electromagnetic resonator* since many antennas are essentially *open resonators*. Such a *Q-factor* is equal to [1, 7, 8]

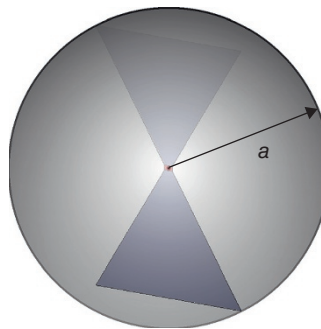


Figure 7.3 A base sphere surrounding a small antenna.

$$Q = \omega \frac{W_{avg}}{P_{avg}}, \quad (7.9)$$

where W_{avg} is the average stored energy in the antenna and antenna's surrounding space and P_{avg} is the average antenna's accepted power. P_{avg} is the total power going into the antenna, which is equal to the power being radiated plus dissipated.

Note that Eq. (7.9) has a clear physical interpretation if we recognize that P_{avg}/f is the energy loss per cycle. When the total stored energy is large compared to its loss per cycle, the Q -factor is large and vice versa. The Q -factor may be established numerically using full-wave computational electromagnetics (CEM) simulations [1].

Consider now Figure 7.3 where a small antenna of arbitrary shape is enclosed into a sphere of radius a . The *Wheeler–Chu limit* (Wheeler, 1947 [3]; Chu 1948 [4]) says that the *lowest possible Q-factor* (or quality factor) of an antenna is given by

$$Q = \frac{1}{ka} + \frac{1}{(ka)^3}. \quad (7.10)$$

Here, $k = 2\pi/\lambda$ is the wavenumber at the center frequency f_C . Emphasize again that Eq. (7.10) gives the lowest achievable Q , when the antenna maximally efficiently occupies the space of a sphere with the radius a .

7.3.2 Relation Between Small Antenna Q-Factor and Small Antenna Bandwidth

The half-power bandwidth (7.7) for small antennas may be expressed through the Q -factor by [1]

$$FBW \approx \frac{2}{Q} \quad (7.11a)$$

or, in the equivalent form,

$$BW = f_U - f_L \approx \frac{2f_c}{Q} \quad (7.11b)$$

provided that the fractional bandwidth is small enough. Eq. (7.11a) and (7.11b) give the *maximum bandwidth ever possible*, when the antenna maximally efficiently occupies the sphere space in Figure 7.3.

When the sphere radius, a , in Figure 7.3 is small compared to the wavelength, the second term on the right-hand side of Eq. (7.10) becomes large; so does the Q -factor. As a result, the antenna bandwidth becomes very small, which prevents using the small antenna for a sufficiently fast data transfer, even in the tunable mode.

All investigated small antennas have the bandwidth below the Wheeler–Chu limit. One of the best candidates is the so-called *Goubau antenna* [5] (a loop-dipole combination), which approaches about 70% of the predicted limit. For a small straight dipole, the achievable bandwidth is 20–30% of the predicted limit.

Example 7.1

What is the theoretical limit on the half-power bandwidth for a short dipole of arbitrary shape with the total length (the largest antenna dimension) of 1 cm at 1 GHz center frequency?

Solution: First, the radius of the surrounding sphere is 0.5 cm. Second, the wavenumber is $k = \frac{2\pi}{\lambda} = \frac{2\pi}{30 \text{ cm}} = 0.21 \text{ cm}^{-1}$. Therefore, $ka = 0.105$. The Q -factor of the antenna, according to Eq. (7.10) is given by $Q = 873.4$. Therefore, the maximum possible half-power bandwidth, according to Eq. (7.11a) is given by $BW = 2/Q = 0.22\%$. The –10 dB bandwidth would be much smaller.

Example 7.2

What is the theoretical limit on the half-power bandwidth for a printed dipole antenna “Taoglas 433 MHz” shown in Figure 7.4? The antenna size is $75 \times 45 \times 0.1 \text{ mm}$.

Solution: We should first note that the printed dipole shown in Figure 7.4 has a complicated shape. This shape is usually so designed that the antenna’s reactance at the resonant frequency of 433 MHz is equal to zero.

However, even if the manufacturer claims in the datasheet that the antenna matching resistance is 50Ω , we must be quite careful with this value. It is very difficult (saying less diplomatically – rather impossible) to reach the antenna radiation resistance of 50Ω with such a small antenna size (about $\lambda/10$) and

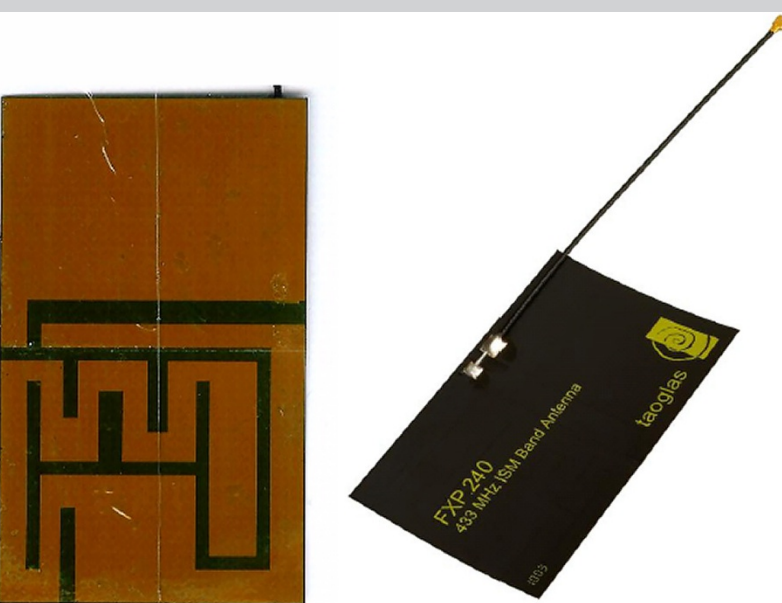


Figure 7.4 Commercial printed flexible dipole antenna “Taoglas 433 MHz.” The overall antenna size is $75 \times 45 \times 0.1$ mm.

such a small occupied volume. Therefore, we must carefully examine this value.

The radius of the surrounding sphere is 3.75 cm. Next, the wavenumber is $k = 2\pi/\lambda = 2\pi/69.3$ cm = 0.09 cm⁻¹. Therefore, $ka = 0.34$. The *Q*-factor of the antenna, according to Eq. (7.10) is given by $Q = 28.4$. Therefore, the maximum half-power bandwidth, according to Eq. (7.11a), is given by $BW = 1/Q = 7\%$. The -10 dB bandwidth would be much smaller.

7.4 ONE HIDDEN PROBLEM WITH A SMALL ANTENNA

The theoretical limit of 7% fractional half-power bandwidth for the Taoglas printed dipole established in the previous section could be compared to manufacturer’s datasheet. Figure 7.5 shows the measured reflection coefficient of the antenna from the datasheet, where we have additionally imposed the -3 dB bandwidth window. The measured bandwidth is thus 22 MHz. This gives us the measured fractional bandwidth of

$$FBW = \frac{22}{433} \times 100\% = 5.1\%. \quad (7.12)$$

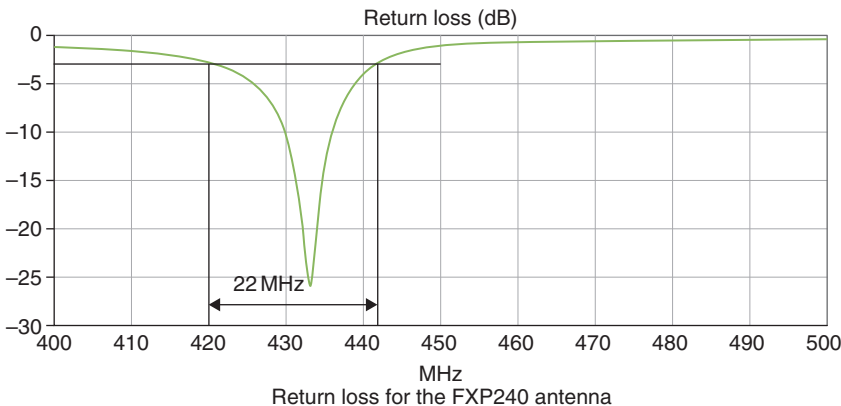


Figure 7.5 Reflection coefficient (called return loss here) for printed flexible dipole antenna “Taoglas 433 MHz” reported in the datasheet.

This value closely approaches the ever possible theoretical limit of 7%! On the other hand, it is frequently reported in the literature that even approaching the Wheeler–Chu limit constitutes a hardly solvable problem. According to Constantine Balanis, “this limit is only approached but is never exceeded or even equaled” [6]. What is the matter? Did we discover a new ultimate antenna?

In order to resolve this paradox, one may turn to MATLAB Antenna Toolbox or to Ansys HFSS Electronics Desktop simulations or use other numerical antenna software of your choice and examine the antenna in detail.

The antenna in Figure 7.4 was scanned; its geometry was then parameterized into 13 rectangles and exported to Ansys HFSS. The resulting numerical model is shown in Figure 7.6. It consists of:

1. The metal shape – a printed dipole including a matching network. The metal sheet is modeled by an ideal conductor (PEC) of zero thickness.
2. A flexible substrate – a dielectric film with the thickness of 0.2 mm and with $\epsilon_r = 2$. Loss tangent, $\tan\delta$, of the dielectric substrate may vary.
3. Plastic support – the ABS material (suggested in the datasheet) with the thickness of 2.0 mm and with $\epsilon_r = 3$. The size of the ABS sheet is 400×400 mm. Loss tangent of the ABS material, $\tan\delta$, may vary.
4. A radiation box.

The solution runs at the center frequency of 433 MHz, uses 10 passes, requires final meshes with about 25 000 tetrahedra, and is using the fast frequency sweep.

Figure 7.7 shows the simulated reflection coefficient of the printed dipole at different values of the dielectric loss tangent of both the substrate and the plastic support: $\tan\delta = 0.00$, 0.05, and 0.10. When there is no loss, the simulation correctly

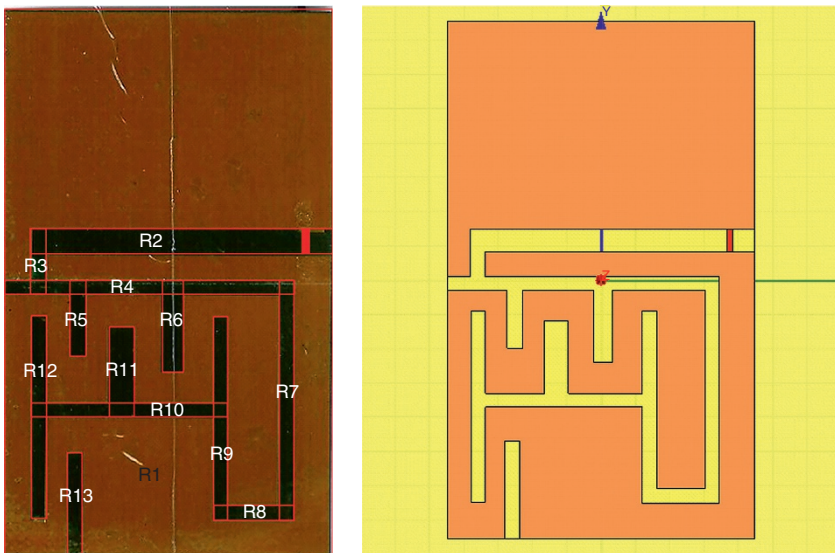


Figure 7.6 Antenna metal foil – the printed dipole – modeled in Ansys HFSS.

predicts the resonant frequency, but gives no bandwidth. When the loss tangent increases, the result starts to approach Figure 7.5 of the datasheet.

Thus, the above antenna is “matched” to $50\ \Omega$ and has an exceptionally large bandwidth only because it is very lossy. One reason for such high losses is perhaps the presence of the lossy dielectric in close proximity to the multiple waveguides cut in the antenna body. These waveguides could convey most of the signal/power created by the feed and promote rapid field decay. It seems that losses in the adhesive and in the flexible film material covered with the adhesive may further decrease efficiency and provide even better “matching” and even wider “wider” bandwidth.

This problem is well known in the antenna community. High losses make an antenna looking good while losing most of the TX power. In fact, the calculated radiation resistance, R_r , of the non-lossy Taoglas antenna at 433 MHz is about $4\ \Omega$, but not $50\ \Omega$. It means that the rest of the antenna resistance ($46\ \Omega$) necessary for the nearly ideal match in Figure 7.5 is likely the series loss resistance, R_L , that is probably coming due to dielectric losses. Therefore, the radiation efficiency of the antenna in the form of the ratio of two powers – the radiated power and the total power delivered to the antenna – becomes

$$E = \frac{P_{\text{radiated}}}{P_a} = \frac{1}{1 + R_L/R_r} = 0.08 \text{ or } 8\%. \quad (7.13)$$

In other words, 92% of power is lost. We expect the real power efficiency to be slightly higher than this value, due to an approximate character of the present estimates.

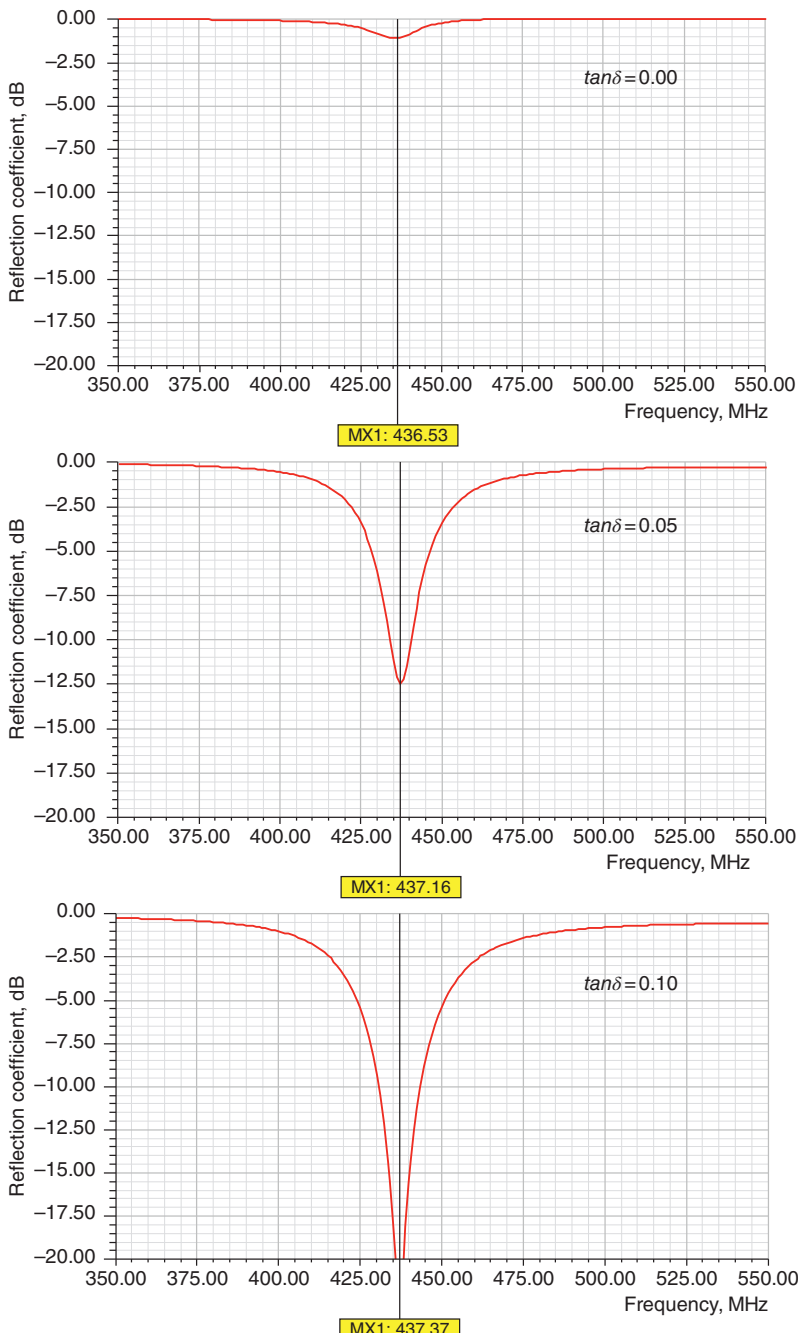


Figure 7.7 Reflection coefficient Γ of the printed dipole versus 50Ω at different values of the dielectric loss tangent of the substrate/plastic support.

REFERENCES

1. A. D. Yaghjian and S. Best, "Impedance, bandwidth, and Q of antennas," *IEEE Trans. Antennas Prop.*, vol. 43, no. 4, pp. 1298–1324, 2005.
2. R. C. Hansen, *Electrically Small, Superdirective, and Superconducting Antennas*, Wiley, New York, 2006, pp.10–17.
3. H. A. Wheeler, "Fundamental limitations of small antennas," *Proc. IRE*, vol. 35, no. 12, pp. 1479–1484, 1947. doi: <https://doi.org/10.1109/JRPROC.1947.226199>.
4. L. J. Chu, "Physical limitations of omni-directional antennas," *J. Appl. Phys.*, vol. 19, no. 12, pp. 1163–1175, 1948.
5. R. C. Hansen, "Fundamental limitations in antennas," *Proc. IEEE*, vol. 69, no. 2, pp. 170–182, 1981.
6. C. A. Balanis, *Antenna Theory: Analysis and Design*, Wiley, New York, 2016, fourth edition.
7. D. R. Jackson, "Microstrip Antennas," In *Antenna Engineering Handbook*, J. L. Volakis, Ed., McGraw Hill, New York, 2007, fourth edition.
8. S. A. Schelkunoff, *Electromagnetic Waves*, Van Nostrand, New York, 1943, Ch. 6.

PROBLEMS

1. (A) Describe in your own words how do we define the bandwidth of a small antenna?
 (B) Which units does the Q -factor of an antenna have?
 (C) What is an inherent absolute limit on the bandwidth of a small antenna?
 (D) What is the theoretical limit on the half-power bandwidth for a short dipole of arbitrary shape with the total length (the largest antenna dimension) of 5 cm at 300 MHz?
 (E) What does the antenna loss do:
 - (i) Decreases the bandwidth?
 - (ii) Increases the bandwidth?
 (F) Which quick test may you suggest to check if the small antenna has a significant ohmic loss?
2. Derive Eq. (7.8) for the bandwidth of a small antenna.
3. Establish an analytical expression for the bandwidth of a small dipole antenna as a function of its parameters and frequency f , using an approximation for the dipole impedance given by (cf. Chapter 1)

$$Z_a = R_a(z) - j \left[120 \left(\ln \frac{l_a}{2a} - 1 \right) \cot z - X_a(z) \right],$$

$$R_a(z) \approx -0.4787 + 7.3246z + 0.3963z^2 + 15.6131z^3,$$

$$X_a(z) \approx -0.4456 + 17.0082z - 8.6793z^2 + 9.6031z^3.$$

Here, l_A is the total dipole length, a is the dipole radius, $z = kl_A/2$, and $k = 2\pi f/c_0$. Assume $z \ll 1$ and keep only the leading terms of the corresponding asymptotic expansions.

4. Establish an analytical expression for the bandwidth of a small loop antenna as a function of its parameters and frequency f , using an approximation for the small loop impedance given by (cf. Chapter 6)

$$R = \frac{2\pi\eta_0}{3} \frac{(kS)^2}{\lambda^2}, X = +\omega \left[\mu_0 a \left(\ln \left(\frac{8a}{b} \right) - 2 \right) \right],$$

where b is the wire radius and a is the loop radius; $S = \pi a^2$.

- 5*. One of the ways of reducing the size of an antenna is to build up internal reactance (capacitive or inductive). We will use the *top-hat monopole* structure to study this. Create a top-hat monopole and monopole by using the Antenna Toolbox. We will use the monopole as a reference. Set the ground plane length and width at 4 m in both cases. Use the default monopole/top-hat monopole height of 1 m and all other default parameters. Set the frequency band for analysis to be from 10 to 100 MHz. Choose 101 frequency points. Do the following:

- (A) Calculate the impedance of the monopole and the top-hat monopole for their default geometry parameters. Label the first resonance frequency for each antenna on the plot (using a marker on the plot).
- (B) Is the first resonance a series or parallel resonance?
- (C) In steps of 25 cm, change the length and width of the top hat in the top-hat monopole antenna and recalculate the impedance. Do this till the top hat size is 1×1 m. For each change to the top-hat configuration, recalculate the impedance of the top-hat monopole. Turn in a plot of the resistance and reactance on separate plots for each change to the top-hat. Note: you will have to use the `impedance` command with the left-hand argument specified. In addition, you will have to store the values of impedance for each configuration and use the `plot` command in MATLAB to make these plots. Label all axes appropriately and include legends.
- (D) Provide a table of the top-hat size vs. first resonance frequency starting with the default monopole top-hat geometry.
- (E) Between the monopole and the top-hat monopole, which one has the higher resonance frequency? What is the relationship between the first resonance frequency of the monopole and all the top-hat

resonance frequencies expressed as a fraction of the monopole's resonance frequency?

- (F) Provide a table of the monopole and top-hat monopole resonance frequencies and the impedance at each of those resonance frequencies (to within the margin of error for the frequency discretization). What trend do you notice?
- (G) What is the relationship between the electrical size of the vertical radiator of the monopole and top-hat monopole and each of their first resonance frequencies? Express it as a function of wavelength?
- (H) Based on your overall findings, would it be accurate to state that, at the lowest resonance frequency, the top-hat monopole is electrically small or electrically short? If not, why not? If yes, you have designed an *electrically small resonant antenna*, which is a significant achievement.

SECTION 2 PRACTICAL ANTENNA MATCHING AND TUNING FOR A PREDEFINED ($50\ \Omega$) IMPEDANCE

7.5. Double Tuning – Inductive (Small Loop) Antenna 185

7.6. Double Tuning – Capacitive (Small Dipole or Monopole) Antenna 190

References 193

Problems 193

Practical antenna tuning implies the generator's matching impedance of $50\ \Omega$ or another large prescribed impedance. All results for the antenna bandwidth remain valid in this case too.

7.5 DOUBLE TUNING – INDUCTIVE (SMALL LOOP) ANTENNA

7.5.1 Problem Statement [1, 2]

Figure 7.8 shows the problem statement for the TX or RX configuration, respectively. The loop antenna is represented by its equivalent impedance – an inductance in series with a resistance. The loop antenna is electrically small – its reactance is positive and large (inductance) while the resistance is small.

The goal is to tune the loop antenna to $50\ \Omega$ or to another real impedance at a desired frequency of interest, which we will still call f_{res} . This frequency is the center band frequency of the antenna. For tuning, it does not really matter whether the antenna is in the transmitting or in the receiving mode.

7.5.2 Double Tuning

The tuning procedure is done with two capacitors: the series capacitor C_1 with the impedance Z_1 and the parallel capacitor C_2 with the impedance Z_2 . Very qualitatively then, the series capacitor essentially cancels the series inductance whereas the parallel capacitor increases the output resistance to $50\ \Omega$.

The lumped-circuit analysis uses the standard impedance transformations known from the steady-state AC circuit theory. We need to find the equivalent impedance of the antenna Z_{out} with the tuner when looking into terminals a and b in Figure 7.8. From Figure 7.8,

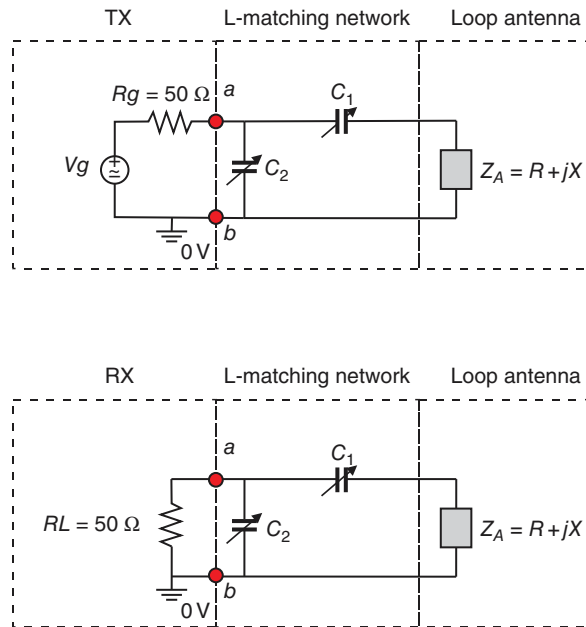


Figure 7.8 Double tuning the loop antenna in the TX or RX mode.

$$\begin{aligned}
 \mathbf{Z}_{out} &= \mathbf{Z}_2 | (\mathbf{Z}_1 + jX + R) = \frac{\mathbf{Z}_2(\mathbf{Z}_1 + jX + R)}{\mathbf{Z}_1 + jX + R + \mathbf{Z}_2} = \frac{\frac{1}{j\omega C_2} \left(\frac{1}{j\omega C_1} + jX + R \right)}{\frac{1}{j\omega C_1} + \frac{1}{j\omega C_2} + jX + R} \rightarrow \\
 \mathbf{Z}_{out} &= \frac{\frac{1}{j\omega C_2}(R + jB)}{R + jB + \frac{1}{j\omega C_2}}, \quad B = X - \frac{1}{\omega C_1}.
 \end{aligned} \tag{7.14}$$

We need to find the real and imaginary parts of \mathbf{Z}_{out} , respectively. Multiplying both the numerator and the denominator by the complex conjugate of the denominator, one has

$$\mathbf{Z}_{out} = \frac{\frac{1}{j\omega C_2}(R + jB)\left(R - j\left[B - \frac{1}{\omega C_2}\right]\right)}{R^2 + \left[B - \frac{1}{\omega C_2}\right]^2} = \frac{\frac{R}{\omega C_2} \left(\frac{1}{\omega C_2} \right) - \frac{j}{\omega C_2} \left(R^2 + B\left[B - \frac{1}{\omega C_2}\right] \right)}{R^2 + \left[B - \frac{1}{\omega C_2}\right]^2}. \tag{7.15}$$

Therefore,

$$\begin{aligned} \operatorname{Re}(\mathbf{Z}_{out}) &= \frac{\frac{R}{\omega^2 C_2}}{R^2 + \left[B - \frac{1}{\omega C_2}\right]^2}, & \operatorname{Im}(\mathbf{Z}_{out}) &= \frac{-\frac{1}{\omega C_2} \left(R^2 + B \left[B - \frac{1}{\omega C_2}\right]\right)}{R^2 + \left[B - \frac{1}{\omega C_2}\right]^2}. \end{aligned} \quad (7.16)$$

Clearly, $\operatorname{Re}(\mathbf{Z}_{out}) > 0$. The condition of zero output reactance and 50Ω output resistance yield

$$R^2 + B \left[B - \frac{1}{\omega C_2}\right] = 0, \quad \frac{\frac{R}{\omega^2 C_2}}{R^2 + \left[B - \frac{1}{\omega C_2}\right]^2} = 50. \quad (7.17)$$

7.5.3 Solution

Two unknowns in Eq. (7.17) are B and C_2 . We denote $1/(\omega C_2)$ by Y . Eq. (7.17) is transformed in the form:

$$R^2 + B^2 = BY, \quad \frac{RY^2}{R^2 + B^2 - 2YB + Y^2} = 50. \quad (7.18)$$

Further transformation gives

$$R^2 + B^2 = BY, \quad \frac{RY^2}{Y^2 - YB} = 50 \quad (7.19)$$

or, which is the same,

$$R^2 + B^2 = BY, \quad RY = 50(Y - B). \quad (7.20)$$

We substitute and transform

$$\begin{aligned} Y &= AB, \quad A = \frac{50}{50-R} \\ R^2 + B^2 = AB^2 &\Rightarrow B = \pm \sqrt{\frac{R^2}{A-1}} = \pm \sqrt{R(50-R)} \Rightarrow Y = \pm 50 \sqrt{\frac{R}{(50-R)}}. \end{aligned} \quad (7.21)$$

Using the definition of Y , we see that the sign + must be chosen in Eq. (7.21). Using the equality $B = X - \frac{1}{\omega C_1}$, we finally obtain

$$X - \frac{1}{\omega C_1} = \sqrt{R(50-R)} \Rightarrow \frac{1}{\omega C_1} = X - \sqrt{R(50-R)}, \quad \frac{1}{\omega C_2} = +50\sqrt{\frac{R}{(50-R)}}.$$

(7.22)

The solution is complete. It can be rewritten it in the form:

$$C_1 = \frac{1}{\omega(X - \sqrt{R(50-R)})} [F], \quad C_2 = \frac{1}{50\omega} \sqrt{\frac{(50-R)}{R}} [F]. \quad (7.23)$$

Example 7.3

A small (relative to wavelength) loop antenna with the radius of 10 cm is to be matched to 50Ω at 96.1 MHz (FM radio, Worcester, MA). Discuss the matching procedure and find the necessary capacitance values.

Solution: The corresponding MATLAB script follows:

```
% EM data
const.epsilon = 8.85418782e-012; % ANSYS HFSS value
const.mu      = 1.25663706e-006; % ANSYS HFSS value
const.c       = 1/sqrt(const.epsilon*const.mu);
const.eta     = sqrt(const.mu/const.epsilon);

% Loop parameters
Rad      = 0.1/(2*pi);    % Radius in m
C        = 2*pi*Rad;      % Circumference, m
A        = pi*Rad^2;       % Area, m^2
a        = 0.003;           % Wire radius, m
fc       = 96.1e6;          % Center frequency in Hz
omega   = 2*pi*fc;
lambda  = const.c/fc;     % Wavelength
disp(strcat('circumference over lambda=' , num2str(C/lambda)));
% Input impedance (analytical, see Chapter 6)
Rloss   = 0.5;             % Loss resistance, Ohm
R        = 100*(pi*const.eta/6)*(C/lambda)^4 + Rloss;
L        = 100*const.mu*Rad*(log(8*Rad/a)-2);
X        = 2*pi*fc*L;

% Exact values
Rg      = 50;
C10    = 1./((omega*(X-sqrt(R*(Rg-R)))))    % C1 in F;
C20    = 1./((Rg*omega)*sqrt(Rg-R)/sqrt(R)) % C2 in F;

% Frequency sweep
f       = [0.95*fc:0.0001*fc:1.05*fc];
omega  = 2*pi*f;
Z1     = 1./((j*omega*C10));
Z2     = 1./((j*omega*C20));
imp_   = R + j*X;
impm  = (imp_ + Z1).*Z2./((imp_ + Z1 + Z2));
```

```

Gamma = (impm - Rg)./(impm + Rg);
RL = 20*log10(abs(Gamma));
plot(f, RL, 'k', 'LineWidth', 2);
title(strcat('Reflection coeff; matching to Rg= ',num2str(Rg)));
xlabel('frequency, Hz'); grid on; axis([min(f) max(f) -30 0]);

```

The resulting capacitance values are $C_1 = 0.786 \text{ pF}$ and $C_2 = 0.323 \text{ nF}$. The -3 dB (half power) bandwidth is approximately 100 kHz . The matched antenna simultaneously operates as a *bandpass filter*.

7.5.4 Single Tuning

It is seen from the above example that the double-tuning solution works, but it might become unstable due to the small capacitance values to be used. In many other situations, we still have the stable solution, indeed.

Instead of the double tuning procedure, we could now employ simple matching with the only one parallel capacitor C_2 . We match for zero input reactance. In other words, $C_1 = \infty$ (the short circuit). In this case, $B = X - \frac{1}{\omega C_1} = X$ and first Eq. (7.17) yields

$$R^2 + X \left[X - \frac{1}{\omega C_2} \right] = 0. \quad (7.24)$$

The solution is

$$C_2 = \frac{X/\omega}{R^2 + X^2} \quad (7.25)$$

and the resistance of the antenna with the matching capacitor becomes

$$\operatorname{Re}(\mathbf{Z}_{out}) = \frac{\frac{R}{\omega^2 C_2^2}}{R^2 + \left[B - \frac{1}{\omega C_2} \right]^2} = \frac{R \frac{(R^2 + X^2)^2}{X^2}}{R^2 + \frac{R^4}{X^2}} = \frac{R^2 + X^2}{R}. \quad (7.26)$$

Example 7.4

A small (relative to wavelength) loop antenna with the radius of 10 cm is to be matched at 96.1 MHz (FM radio) with a single capacitor in parallel. Determine the output resistance of the matched configuration.

Solution: The corresponding MATLAB script follows:

```

% EM data
const.epsilon = 8.85418782e-012; % ANSYS HFSS value
const.mu      = 1.25663706e-006; % ANSYS HFSS value
const.c       = 1/sqrt(const.epsilon*const.mu);
const.eta     = sqrt(const.mu/const.epsilon);

% Loop parameters
Rad      = 0.1/(2*pi);    % Radius in m
C        = 2*pi*Rad;      % Circumference, m
A        = pi*Rad^2;       % Area, m^2
a        = 0.003;          % Wire radius, m

fc       = 96.1e6;         % Center frequency in Hz
omega   = 2*pi*fc;
lambda  = const.c/fc;    % Wavelength
disp(strcat('circumference over lambda=' , num2str(C/lambda)));
% Input impedance (analytical, see Chapter 6)
Rloss   = 0.5;            % Loss resistance, Ohm
R        = (pi*const.eta/6)*(C/lambda)^4 + Rloss;
L        = const.mu*Rad*(log(8*Rad/a)-2);
X        = 2*pi*fc*L;

% Exact values
C20     = X/(omega)/(R^2+X^2); % C2 in F;
C10     = 1;                  % C1 (very large)
Rmatched = (R^2+X^2)/R;      % Obtained resistance

% Frequency sweep
f        = [0.95*fc:0.0001*fc:1.05*fc];
omega   = 2*pi*f;
Z1      = 1./ (j*omega*C10);
Z2      = 1./ (j*omega*C20);
imp_    = R + j*X;
impm   = (imp_ + Z1).*Z2./ (imp_ + Z1 + Z2);
a       = figure;
Gamma   = (impm - Rmatched)./(impm + Rmatched);
RL      = 20*log10(abs(Gamma));
plot(f, RL, 'k', 'LineWidth', 2);
title(strcat('Refl coeff; matching to Rg= ', num2str(Rmatched)));
xlabel('frequency, Hz'); grid on; axis([min(f) max(f) -30 0]);

```

The resulting output resistance is 891Ω . The resulting bandwidth is quite large.

7.6 DOUBLE TUNING – CAPACITIVE (SMALL DIPOLE OR MONOPOLE) ANTENNA

7.6.1 Double Tuning [2]

Figure 7.9 shows the tuning concept for a monopole antenna. Instead of two capacitors, we are now using two inductors.

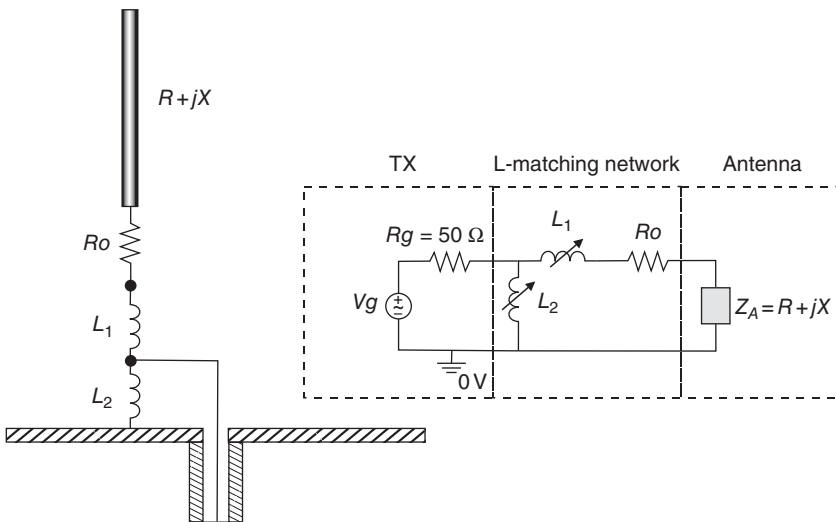


Figure 7.9 Double tuning a small monopole antenna in the TX mode. The dipole tuning is done in the same way. Parasitic resistance R_0 of the tuning circuit will be neglected.

The same derivation holds as for the small loop antenna due to duality. The following substitutions are to be made:

$$1/(\omega C_1) \rightarrow -\omega L_1, \quad 1/(\omega C_2) \rightarrow -\omega L_2. \quad (7.27)$$

Also, the sign minus should now be chosen in Eq. (7.21). This yields the solution in the form (note that the reactance, X , is now negative):

$$\begin{aligned} -\omega L_1 &= X + \sqrt{R(50-R)} \Rightarrow \omega L_1 = -X - \sqrt{R(50-R)}, \\ -\omega L_2 &= -50 \sqrt{\frac{R}{(50-R)}} \Rightarrow \omega L_2 = 50 \sqrt{\frac{R}{(50-R)}}. \end{aligned} \quad (7.28)$$

Example 7.5

A short (compared to wavelength) dipole antenna with the total length of 60 cm is to be matched to 50Ω at 96.1 MHz (FM radio). Discuss the matching procedure and find the necessary inductance values.

Solution: The corresponding MATLAB script follows:

```
% EM data
const.epsilon = 8.85418782e-012;
```

```

const.mu          = 1.25663706e-006;
const.c          = 1/sqrt(const.epsilon*const.mu);
const.eta        = sqrt(const.mu/const.epsilon);
% Dipole parameters
lA    = 0.6;           % Dipole length, m
a     = 0.003;          % Dipole wire radius, m
fc    = 96.1e6;         % Center frequency in Hz
omega = 2*pi*fc;
lambda = const.c/fc;   % Wavelength
disp(strcat('dipole length over lambda=',num2str(1/lambda*(lA))));
% Input impedance (analytical, see Chapters 1 and 2)
Rloss  = 0.5;           % Loss resistance, Ohm
lambda = const.c/fc;
R      = (pi*const.eta/6)*(0.5*lA/lambda)^2 + Rloss;
X      = -(const.eta/pi^2)*(log(0.5*lA/(2*a))-1)*lambda/(0.5*lA);
% Exact values
Rg    = 50;
L20   = (Rg/omega)*sqrt(R/((Rg-R)))*1.00 % L2 in H;
L10   = (1/omega)*(-X-sqrt(R*(Rg-R)))*1.00% L1 in H;
% Frequency sweep
f      = [0.95*fc:0.0001*fc:1.05*fc];
omega = 2*pi*f;
Z1    = j*omega*L10;
Z2    = j*omega*L20;
imp_  = R + j*X;
impm = (imp_ + Z1).*Z2./((imp_ + Z1 + Z2));
Gamma = (impm - Rg)./(impm + Rg);
RL   = 20*log10(abs(Gamma));
plot(f, RL, 'k', 'LineWidth', 2);
title(strcat('Reflection coeff; matching to Rg= ',num2str(Rg)));
xlabel('frequency, Hz'); grid on; axis([min(f) max(f) -30 0]);

```

The resulting inductance values are $L_1 = 1.90 \mu\text{H}$ and $L_2 = 18.3 \text{nH}$. The -3 dB (half power) bandwidth is approximately 760 kHz. This matched antenna simultaneously operates as a *bandpass filter*.

7.6.2 Single Tuning

The single tuning is made with the inductor L_2 in parallel. The inductance L_1 is exactly zero. Instead of Eq. (7.24), one now has

$$R^2 + X[X + \omega L_2] = 0. \quad (7.29)$$

The solution is

$$L_2 = \frac{R^2 + X^2}{-X\omega} \quad (7.30)$$

and the resistance becomes ($B = X$ as long as L_1 is zero)

$$\operatorname{Re}(\mathbf{Z}_{out}) = \frac{R\omega^2 L_2^2}{R^2 + [B + \omega L_2]^2} = \frac{R\omega^2 L_2^2}{R^2 + [X + \omega L_2]^2} = \frac{R(R^2 + X^2)^2}{(R^2 + R^4/X^2)X^2} = \frac{R^2 + X^2}{R}. \quad (7.31)$$

Remarkably, this result is the same as in Eq. (7.26).

REFERENCES

1. C. A. Balanis, *Antenna Theory: Analysis and Design*, Wiley, New York, 2016, fourth edition.
2. M. M. Weiner, *Monopole Antennas*, Marcel Dekker, New York, 2003.

PROBLEMS

1. A 0.5 m long wire dipole antenna with the wire radius of 2 mm is used to receive the 96.1WSRS FM Radio Station (from Worcester, MA). The antenna ohmic loss is 0.5Ω .
For both single tuning and double tuning (to 50Ω) procedures, estimate:
 - The value of the tuning inductor(s).
 - Tuned antenna bandwidth (-10 dB).
 - The effect of $\pm 1\%$ variation in tuning inductance(s).
 - Value of the matched resistance for the maximum power transfer (for single tuning).
2. A 0.2 m long wire *monopole antenna* with the wire radius of 3 mm is used to receive the 96.1WSRS FM Radio Station (from Worcester, MA). The antenna ohmic loss is 0.5Ω . Using the MATLAB script for the double tuning procedure from this section estimate:
 - The value of two tuning inductors.
 - Tuned antenna half-power bandwidth (half power or -3 dB).
 - The effect of $\pm 1\%$ variation in either inductance.
3. In Problem 2, a loop antenna of 0.5 m circumference with the wire radius of 3 mm is chosen as an alternative to the monopole. Does it have a larger bandwidth after double tuning?
4. A 0.5 m diameter wire loop antenna with the wire radius of 2 mm is used to receive the 96.1WSRS FM Radio Station (from Worcester, MA). The antenna ohmic loss is 0.1Ω .
 1. For the single tuning procedure, estimate:

- (a) The value of the tuning capacitor.
 - (b) The effect of $\pm 1\%$ variation in capacitance.
 - (c) The value of the matched resistance for the maximum power transfer.
2. For the double tuning procedure, estimate:
- (a) The value of two tuning capacitors.
 - (b) Tuned antenna bandwidth (-10 dB).
 - (c) The effect of $\pm 1\%$ variation in either capacitance.

Which antenna (dipole or loop) would you prefer if the space (or aesthetic) constraints were not very critical?

- 5***. Create an electrically small dipole, loop, and equiangular spiral antennas with the help of the Antenna Toolbox using the following starter code:

```
f = 1e9;
c = physconst('lightspeed');
lambda = c/f;
wavenumber = 2*pi/lambda;
%% Small dipole
d = dipole;
d.Length = lambda/8;
d.Width = lambda/400;
%% Small loop
circumference = lambda/8;
r = circumference/(2*pi);
l = loopCircular;
l.Radius = r;
l.Thickness = circumference/200;
%% Small spiral
s = spiralEquiangular;
s.OuterRadius = .006;
%%
md = mesh(d,'MaxEdgeLength',0.001);
ml = mesh(l,'MaxEdgeLength',0.001);
ms = mesh(s,'MaxEdgeLength',0.001);
```

Tabulate the impedance for these antennas at 101 frequency points over the frequency range 900 MHz–1.1 GHz. Submit the resistance of the three antennas overlaid on a single plot and the reactance overlaid on a separate plot. Make sure to include a legend in the plots and also use appropriate scaling on the axis to make it easy to read (use GHz for scaling on the frequency axis, no multipliers of 10^9 , etc.). Answer the following:

1. Among the three antennas, which one might be easier to cancel the reactance of?
 2. What would be the type of a series element to connect for canceling the reactance for each antenna?
 3. Your boss tells you to match these antennas for $50\ \Omega$ input impedance. What is the minimum number of passive components needed to do so?
- 6***. For the three electrically small antennas created in Problem 5, compute the far-field directivity and submit the plots for each. Aside from the differences in the pattern, what is common to the directivity of these plots qualitatively?
- 7***. For this problem, we will study the antenna-to-antenna transfer function by using a resonant dipole as a transmitting antenna and the three electrically small antennas created earlier in Problem 5 as receiving antennas. Create a resonant dipole for operation at 1 GHz by using the Antenna Toolbox. Choose length as 0.47λ and width of $\lambda/400$. Create a transmit–receive system by positioning the transmitting antenna (the dipole) at the origin and the receiving antenna at 5λ . Do the following:
- (A) Comment on the receiving antenna orientation you have chosen for each case. Use your judgment based on the findings from the previous problem.
 - (B) Calculate the S-parameters for each configuration, i.e. dipole–dipole, dipole–loop, and dipole–spiral. Before calculating the S-parameters, mesh the array with a maximum edge length of 1 mm.
 - (C) On a single plot, show the S_{21} of the three configurations in decibels.
 - (D) What could explain the differences in the S_{21} between the three configurations?

CHAPTER 8



Patch and PIFA Antennas

SECTION 1 PATCH ANTENNAS

8.1. Concept	197
8.2. Fields	198
8.3. CAD Formulas for Patch Antenna	199
8.4. CAD Formulas for the Patch Antenna Efficiency	203
8.5. Patch Antenna Example: Cross-Polarization and Near Fields	206
8.6. Patch Antenna Family	215
References	215
Problems	215

8.1 CONCEPT

The dipole antenna is a $\lambda_0/2$ (half-wave) resonator – a piece of the wire with the length approximately equal to half wavelength, $\lambda_0/2$, in air. The patch antenna is also a half-wave resonator, but on the basis of a transmission line. This is usually a wide microstrip line as shown in Figure 8.1. The patch antenna is simply a $\lambda_g/2$ open–open section of a microstrip transmission line that is cut out as shown in Figure 8.1. Here, $\lambda_g \leq \lambda_0$ is the transmission line wavelength. It is different from λ_0 (smaller than or equal to λ_0) due to the presence of a dielectric.

Antenna and EM Modeling with MATLAB® Antenna Toolbox, Second Edition. Sergey N. Makarov, Vishwanath Iyer, Shashank Kulkarni, and Steven R. Best.

© 2021 John Wiley & Sons, Inc. Published 2021 by John Wiley & Sons, Inc.

Companion website: www.wiley.com/go/Makarov/AntennaandEMModelingwithMATLAB2e

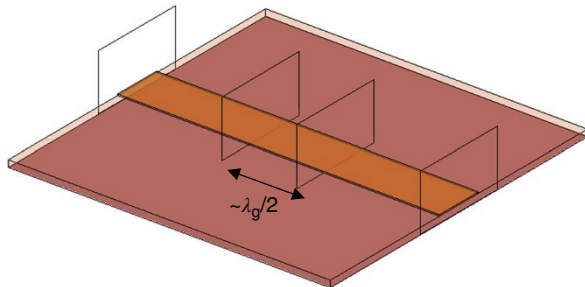


Figure 8.1 A metal patch antenna as a $\lambda_g/2$ open–open section on the base of a microstrip transmission line that is cut out in the figure.

The patch antenna is a competitor to the dipole or monopole-like antenna when a low-profile antenna with a broadside radiation pattern is necessary.

8.2 FIELDS

The fields inside and outside the patch antenna resonator are quite different. Figure 8.2a shows a very simplified yet functioning version of the patch antenna – a wide $\lambda_0/2$ -long section of an *air-filled* parallel-plate waveguide. The electric field

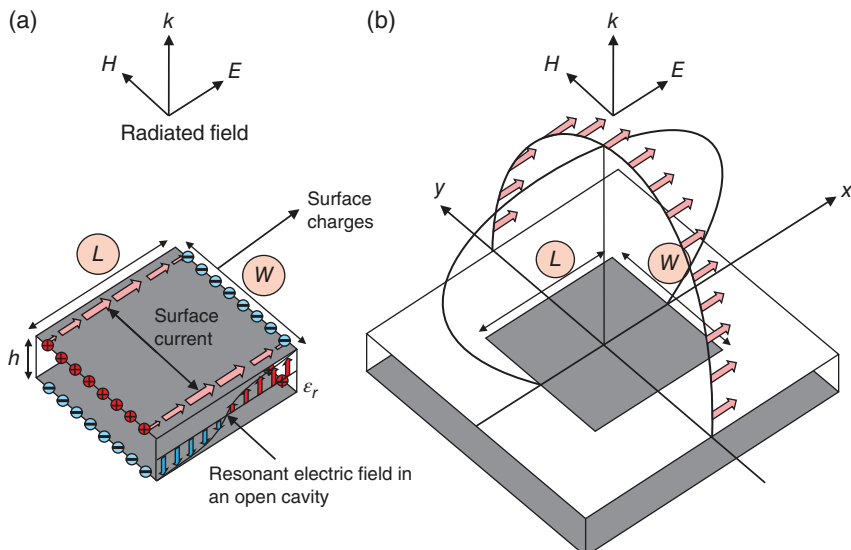


Figure 8.2 Left – Fields, charges, and currents for the simplified patch antenna geometry. Right – construction and outline of the radiation pattern.

within the antenna oscillates along the length, L , of the antenna where $L \approx \lambda_0/2$ as shown by vertical arrows in Figure 8.2a.

The field behavior may then be described as follows:

1. Oscillations of the electric field *within* the resonator volume in Figure 8.2a are accompanied by electric charges of oscillating polarity concentrated close to two patch edges along its length – the *radiating edges of the patch* – see the same figure. The charge polarity changes with every oscillation cycle.
2. The electric charges will be distributed not only on the inner surface of the metal patch, close to its edges, but also partially on the outer surface in the vicinity of the patch edges.
3. Those charges on the surface of the patch create oscillating surface currents as shown in Figure 8.2a. The currents flow from left to right and vice versa in Figure 8.2a. They concentrate closer to two other patch antenna edges – see Figure 8.2a.
4. The currents (and the associate charges) radiate as shown in Figure 8.2b. The radiated E-field in Figure 8.2b has the same direction as the patch currents in Figure 8.2a.
5. As a result, the radiation pattern of the patch antenna becomes similar to the pattern of a horizontal dipole above the metal ground plane. A larger ground plane in Figure 8.2b redirects the radiation into the upper hemisphere.
6. The above qualitative description corresponds to the well-known analytical model for a patch antenna as a combination of two radiating slots in a resonant cavity [1].

Note: The most critical parameter of the patch antenna is its length, L , shown in Figure 8.2. The length (dimension along which field oscillations occur) of the patch determines its resonant frequency. On the other hand, the width of the patch, W , only slightly affects the resonant frequency, but more significantly – the antenna bandwidth.

8.3 CAD FORMULAS FOR PATCH ANTENNA

All CAD formulas for a patch antenna referenced below have been obtained on the base of approximate analytical solutions of Maxwell's equations.

Two basic patch antenna designs – two conventional patch antenna configurations with linear polarization – are shown in Figure 8.3. The antenna can be fed via a microstrip feed (Figure 8.3a) or via a coaxial probe feed (Figure 8.3b). A slot

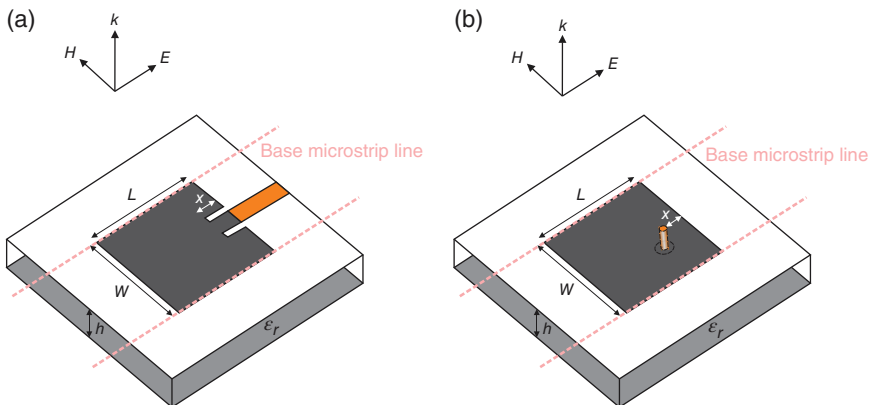


Figure 8.3 Patch antenna geometry for linear polarization: (a) with a microstrip feed; (b) with a probe feed.

excitation is also possible that is characterized by a significantly larger (up to 50% and even more) bandwidth [2].

The patch itself has the width W and the length L . A ground plane is located at a distance h underneath the patch (h is the patch thickness), separated by a dielectric with relative dielectric constant ϵ_r . Note that the ground plane must extend beyond the edges of the patch to ensure the antenna radiation into upper half space – see Figure 8.2b. Typically, the dimensions of the ground plane are 1.4–2 times larger than those of the patch itself.

The antenna's resonant mode of operation is the microstrip mode in the direction of the antenna length. The microstrip patch always functions as a half-wave open–open resonator. In Figure 8.3, the location of the feed with respect to the radiating edge of the patch is characterized by an inset distance x . The following features of the patch antenna feed are of note:

1. The feed must be maintained symmetrically with respect to the width in order to prevent excitation of a parasitic resonant mode in the perpendicular direction (direction of the antenna width).
2. The feed located exactly in the middle of the patch will give us the input impedance of zero since the electric field (voltage) is zero there – see Figure 8.2a.
3. The feed located exactly at the edge of the patch will typically give us a too high value of the input impedance on the order of 200–500 Ω .
4. Therefore, for the direct 50 Ω match, the feed must be located somewhere in between the patch center and its edge and on the patch centerline.

Both antennas in Figure 8.3 radiate almost identical and predominantly vertically – see Figure 8.2b. The radiated electric field E is polarized along the dimension L (length) of the patch as shown in Figures 8.3 and 8.2b. Therefore,

the conventional patch antenna is always a *linearly polarized antenna*, similar to the dipole.

The maximum patch antenna directivity at zenith is typically 4–7 dB. The antenna (realized) gain may have a much lower value due to dielectric and metal loss(es) as was already shown in Chapter 1.

The following subsections briefly describe the relationship between the physical properties of the patch antenna and its performance parameters [1–4].

Resonant frequency: At a give length, the resonant or center frequency of the rectangular patch antenna is approximately estimated as [1] ($c_0 = 3 \times 10^8$ m/s is the velocity of light in vacuum)

$$f_{\text{res}} = \frac{0.49c_0}{\sqrt{\epsilon_r}L}. \quad (8.1a)$$

A fairly more accurate result obtained taking into account the microstrip line theory has the form [3, 4]:

$$\begin{aligned} f_{\text{res}} &= \frac{0.5c_0}{\sqrt{\epsilon_r}(L + 2\Delta L)}, \\ \Delta L &= h \frac{0.412(\epsilon_{\text{eff}} + 0.3) \left(\frac{W}{h} + 0.264 \right)}{(\epsilon_{\text{eff}} - 0.258) \left(\frac{W}{h} + 0.8 \right)}, \\ \epsilon_{\text{eff}} &= \frac{\epsilon_r + 1}{2} + \frac{\epsilon_r - 1}{2} \frac{1}{\sqrt{1 + 10 \frac{h}{W}}}. \end{aligned} \quad (8.1b)$$

Antenna resistance(impedance): The inset parameter x in Figure 8.3 determines the microstrip antenna radiation resistance: when $x = 0$, the impedance is of order 200–500 Ω ; when $x = L/2$, the resistance approaches zero. The best match to 50 Ω is achieved at an intermediate value of x which can be determined in a predictable fashion from computational electromagnetics (CEM) simulation of the antenna geometry.

Bandwidth: The fractional bandwidth percentage ($\text{VSWR} < 2$) for a *low-loss conventional patch antenna* is estimated as a function of the antenna geometry and the antenna resonant frequency f_{res} in the form [3] (at $\epsilon_r \geq 2$):

$$B = 3.77 \frac{\epsilon_r - 1}{\epsilon_r^2} \frac{W}{L} \frac{h}{\lambda_0} \times 100\%, \quad \lambda_0 = \frac{c_0}{f_{\text{res}}}. \quad (8.2a)$$

The bandwidth in Hz is given by

$$B = 3.77 \frac{\epsilon_r - 1}{\epsilon_r^2} \frac{W}{L} \frac{h}{\lambda_0} f_{\text{res}} \quad (8.2b)$$

TABLE 8.1 Design Criteria for a Simple Patch Antenna Configuration.

Dimension	Design criteria
L	Determined by the required resonant frequency f_{res} (which is simultaneously the center frequency of the band) and relative dielectric constant of the substrate
W	Choose $W \leq L$ to avoid potential parasitic resonances
X	Choose $0 < x < L/2$ to meet the 50Ω input impedance match
h	Determined by the desired bandwidth B

with taking into account Eq. (8.1a) or Eq. (8.1b).

Eq. (8.2a) and (8.2b) indicate that the bandwidth increases with increasing W ; this is due to lowering the Q -factor of the microstrip resonator (see Chapter 7). If a wider antenna bandwidth is desired, it appears that increasing W would be an option to be considered. In practice, however, it is not recommended to increase W above the limit $W = L$ in order to avoid potential excitation of the parasitic perpendicular resonant mode. For a lossy patch antenna, the bandwidth increases inversely proportional to the efficiency.

Simplified design process: Given the relationships in Eq. (8.1a), (8.1b), (8.2a), and (8.2b), the simplified process for designing a patch antenna proceeds as indicated in Table 8.1.

Example 8.1

A MATLAB script given below estimates the resonant frequency and the bandwidth of a 94 mm long by 100 mm wide patch antenna on a 4.67 mm or $3/16''$ thick acrylic ($\epsilon_r \approx 3.0$ in average) substrate:

```

clear all
L      = 94e-3;          % Antenna length, m
W      = 100e-3;         % Antenna width, m
h      = 4.67e-3;        % Antenna height, m
epsr  = 3.0;
c0    = 3e8;             % Speed of light, m/s
epseff = (epsr+1)/2+(epsr-1)/2/sqrt(1+10*h/W);
dL    = h*0.412*(epseff+0.300)*(0.264+W/h)/...
        ((epseff-0.258)*(0.800+W/h));
fres  = 0.5*c0/(sqrt(epsr)*(L+2*dL))/1e6 % Resonant frequency, MHz
B     = 0.91*(epsr-1)/epsr^3*W*h*c0/L^3/1e6 % Bandwidth, MHz

```

and outputs 879, and 11.4 MHz, respectively. The above antenna has the calculated efficiency of approximately 90% (see the next example) since the substrate dielectric loss is low.

8.4 CAD FORMULAS FOR THE PATCH ANTENNA EFFICIENCY

Any patch antenna is a half-wave open–open quasi-transverse electromagnetic mode (TEM) resonator with two supporting metal conductors (the patch itself and the ground plane) and a (lossy) dielectric filler. Its efficiency is to be estimated based on the general approach summarized in [3–5]. This approach implies the use of the quality or Q -factors for every particular radiation and/or loss process.

The general definition of the Q -factor was introduced in Chapter 7. For every particular i -th loss/radiation process, one introduces a *partial quality factor* in the same form, namely [5]

$$Q_i = \omega \frac{W}{P_i}, \quad (8.3a)$$

where W is the average electromagnetic energy stored in the antenna and P_i/f is the energy outflow per period due to this particular process.

The total patch antenna Q -factor is given by a parallel combination of the partial Q -factors

$$Q^{-1} = Q_{sp}^{-1} + Q_{sw}^{-1} + Q_d^{-1} + Q_c^{-1}, \quad (8.3b)$$

where Q_{sp} , Q_{sw} , Q_d , Q_c are the *space-wave (radiation)*, *surface-wave*, *dielectric loss*, and *conductor loss* Q -factors [5].

Note: Though dimensionless, the corresponding Q -factors are inversely proportional to the corresponding equivalent resistances. For example, if Q_c is equal to infinity (no conduction loss), then the corresponding conduction loss resistance (a part of the total antenna loss resistance, R_L) is zero. In view of this, Eq. (8.3b) is equivalent to

$$R = \underbrace{R_r}_{\text{radiation resistance inversely proportional to } Q_{sw}} + \underbrace{R_{sw} + R_d + R_c}_{\text{total loss resistance } R_L} \quad (8.3c)$$

where R is the total antenna's resistance including radiation resistance and all kinds of loss resistances. Here, the surface-wave loss is included into the loss resistance although it might also be associated with the radiation resistance itself.

The antenna's radiation efficiency, E , is then expressed in the form

$$E = \frac{P_{\text{radiated}}}{P_a} = \frac{Q}{Q_{sp}}, \quad Q = \omega \frac{W}{P_a}, \quad Q_{sp} = \omega \frac{W}{P_{\text{radiated}}} \quad (8.4)$$

since every partial Q -factor is inversely proportional to the corresponding (radiated or dissipated) partial power, respectively. Here, P_{radiated} is the radiated power and P_a is the total power delivered to the antenna (average accepted power).

The partial Q -factors may be found by tracking energy radiated or dissipated in the half-wave resonator due to a specific loss mechanism per unit time. We briefly recall those Q -factors. We consider a half-wave rectangular patch with the length $L \approx \lambda_0 / (2\sqrt{\epsilon_r})$ where index 0 denotes the free-space wavelength and ϵ_r is the relative dielectric constant. One has:

1. The Q -factor of the radiated field is approximately written as (see Refs. [4, 5])

$$Q_{sp} \approx \frac{3}{32} \sqrt{\epsilon_r} \frac{\lambda_0^2}{hW}, \quad (8.5)$$

where h is the patch antenna height and W is the patch antenna width.

2. A conductor loss Q -factor (metal loss) is expressed in terms of the skin layer depth, δ (see Refs. [4, 5]),

$$Q_c \approx \frac{\eta_0 k_0 h}{2 R_s^{av}}, R_s^{av} = \frac{1}{\sigma \delta} \quad (8.6)$$

with R_s^{av} being the average surface resistance of the patch and the ground plane, respectively, and σ (S/m) being the corresponding volume conductivity of the conductor. In a good conductor (metal), the skin layer depth is given by $\delta = \sqrt{\frac{2}{\omega \mu_0 \sigma}}$. The general expression for the skin layer depth, δ , in a nonmagnetic material is [6]

$$\delta = \text{skin depth} = \left(\frac{1}{2} \left[\sqrt{1 + (\sigma/\omega\epsilon)^2} - 1 \right] \right)^{-1/2} (\omega \sqrt{\mu_0 \epsilon})^{-1}, \quad (8.7)$$

where μ_0 is the magnetic permeability of vacuum.

3. The dielectric (channel) loss factor is given by

$$Q_d = 1 / \tan \delta, \tan \delta = \sigma_i / (\omega \epsilon_r \epsilon_0), \quad (8.8)$$

where σ_i is the effective conductivity of the dielectric layer.

4. The surface-wave loss (loss into the outgoing surface waves) is often assumed to be rather small or reduced using potentially well-known means (see Ref. [4]). We will neglect this factor in future.

Example 8.2

For a half-wave perfectly conducting patch antenna on a lossy dielectric substrate, the ratio of two resistances (the loss resistance and the radiation resistance), R_L/R_r , is approximately given by (see Ref. [5], pp. 7–12 to 7–14.)

$$\frac{R_L}{R_r} = \frac{Q_{sp}}{Q_d} = \frac{3}{32} \sqrt{\epsilon_r} \frac{\lambda_0^2 \tan \delta}{hW}, \quad (8.9)$$

where h is the patch antenna thickness or height, W is the patch antenna width, $\lambda_0 = c_0/f$ is the wavelength in free space at frequency f in Hz, ϵ_r is the relative dielectric constant of the substrate, and $\tan \delta$ is the loss tangent of the substrate. Determine the antenna efficiency if $f = 930$ MHz, $W = 7$ cm, and the substrate is a low-cost 62 mil FR4 with $\epsilon_r = 4.2$ and $\tan \delta = 0.02$.

Solution: A simple MATLAB script given below programs Eq. (8.9) and outputs $R_L/R_r = 3.62$ and, according to Eq. (1.10),

$$E = \frac{P_{\text{radiated}}}{P_a} = \frac{R_r I^2}{(R_r + R_L) I^2} = \frac{R_r}{(R_r + R_L)} = \frac{1}{1 + R_L/R_r} = 0.22 \text{ or } 22\%. \quad (8.10a)$$

The same value is indeed obtained in terms of the Q -factors, i.e.

$$E = \frac{Q}{Q_{sp}} = \frac{1}{1 + Q_{sp}/Q_d} = 0.22 \text{ since } Q = \frac{Q_{sp} Q_d}{Q_{sp} + Q_d}. \quad (8.10b)$$

This result is remarkably discouraging; it says that 78% of power supplied to the (already matched) antenna is lost in the antenna substrate itself whereas only 22% of the supplied power is really radiated! Better dielectric substrates with lower loss (and typically of higher cost) must be used in order to reduce power loss to an acceptable level.

```
clear all;
epsilon      = 8.85418782e-012;          % Vacuum, F/m
mu          = 1.25663706e-006;          % Vacuum, H/m
c           = 1/sqrt(epsilon*mu);        % Vacuum, m/s
eta          = sqrt(mu/epsilon);          % Vacuum, Ohm
h            = 62/1000*2.54e-2;          % Patch antenna thickness, m
W            = 0.07;                      % Patch antenna width, m
eps_r        = 4.2;                      % Rel. diel. constant, FR4
tand         = 0.02;                      % Loss tangent, FR4
f             = 930e6;                    % Frequency, Hz
lambda0      = c/f;                      % Wavelength in vacuum
Ratio        = 3/32*sqrt(eps_r)*lambda0^2*tand/(h*W)
E            = 1/(1 + Ratio)
```

8.5 PATCH ANTENNA EXAMPLE: CROSS-POLARIZATION AND NEAR FIELDS

The conventional patch antenna is a half-wavelength open-cavity resonator. The patch length along the resonant dimension and the dielectric constant of the substrate determine the resonant frequency following Eq. (8.1a) and (8.1b). The feed position determines which mode is exactly excited (along which patch dimension) and is also responsible for the proper impedance matching. The probe feed thickness slightly tunes the resonant frequency (toward lower values when thickness increases). The antenna bandwidth [see Eq. (8.2b)] is determined by the substrate thickness, substrate's dielectric constant, the patch shape, and, maybe, by the presence of a superstrate.

Among a number of the analytical CAD formulas listed above, none is exact. Moreover, a good analytical formula for the antenna feed position does not seem to be in place. Therefore, numerical analysis remains the major engineering tool for practical patch antenna design and the only reliable tool for broadband patch antenna design. In this section, we present an analysis of a narrowband patch antenna using two different methods: Method of Moments (MoM) in MATLAB Antenna Toolbox versus the corresponding Ansys HFSS (Ansys Electronics Workbench) simulation (finite-element method or FEM).

8.5.1 Geometry

This example describes a linearly polarized patch antenna at 2.37 GHz on a Rogers RT/duroid® laminate with $\epsilon_r = 2.33$ and the thickness of 1.57 mm. The antenna geometry is shown in Figure 8.4. The loss tangent of the Rogers substrate is small; it is therefore set to zero for simplicity.

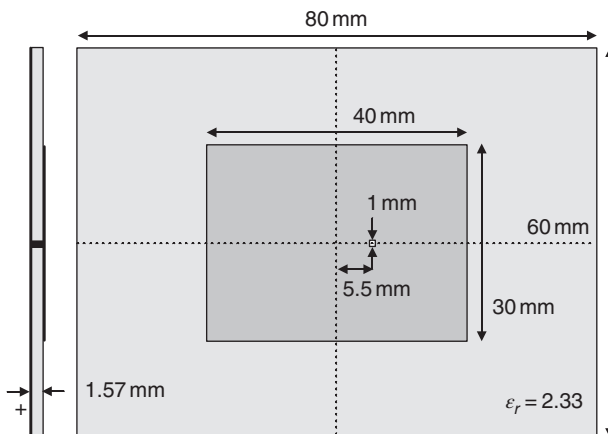


Figure 8.4 Rectangular-patch antenna at 2.37 GHz on a low- ϵ RT/duroid® laminate.

The antenna in Figure 8.4 has the following features:

1. The ground plane is finite but is relatively large. Therefore, the antenna is expected to have a good *front-to-back ratio* – the ratio of front lobe and back lobe directivities.
2. The corresponding metal-dielectric resonator (that includes the volume between the patch and the ground plane) is excited in the fundamental resonant mode (half wavelength), along the longer patch dimension. The dielectric constant of the substrate is rather small but the dielectric substrate is very thin. Therefore, the antenna is expected to have a small bandwidth (due to a high *Q*-factor) and a relatively large size.

The probe feed conductor will be offset by 5.5 mm from the patch center in order to achieve proper impedance matching. The feed is a rectangular or cylindrical metal conductor of 1 mm in width/diameter.

8.5.2 Antenna Mesh

In order to apply a numerical method, a *mesh subdivision* of the patch antenna volume into tetrahedra and a subdivision of the patch antenna surface into triangles are necessary. Figure 8.5 shows one such imprinted mesh created in MATLAB Antenna Toolbox via extrusion. Special attention is paid to an accurate mesh around the feed.

8.5.3 Input Impedance

The antenna input impedance $Z_a = R_{in} + jX_{in}$ is calculated numerically. Figure 8.6 shows the comparison of the impedance data obtained via the MoM in Antenna Toolbox versus the corresponding Ansys HFSS simulation.

The antenna resonance occurs when the reactance X_{in} becomes zero at a certain frequency. The resonant frequency is close to 2.37 GHz in Figure 8.6. The magnitude of the antenna reflection coefficient vs. $50\ \Omega$ in dB is given by

$$|\Gamma|_{dB} = +20 \log_{10} \left(\left| \frac{Z_a - 50}{Z_a + 50} \right| \right); \quad Z_a = \frac{V_a}{I_a}. \quad (8.11)$$

The voltage standing wave ratio (VSWR) is defined by

$$\text{VSWR} = \frac{1 + |\Gamma|}{1 - |\Gamma|} \geq 1. \quad (8.12)$$

The impedance bandwidth (for a narrowband antenna, e.g. for the patch antenna) is estimated as the frequency band where the reflection coefficient falls below $-10\ \text{dB}$. The estimation for the present antenna gives us the value of about 1.0% versus antenna's center (resonant) frequency of 2.37 GHz.

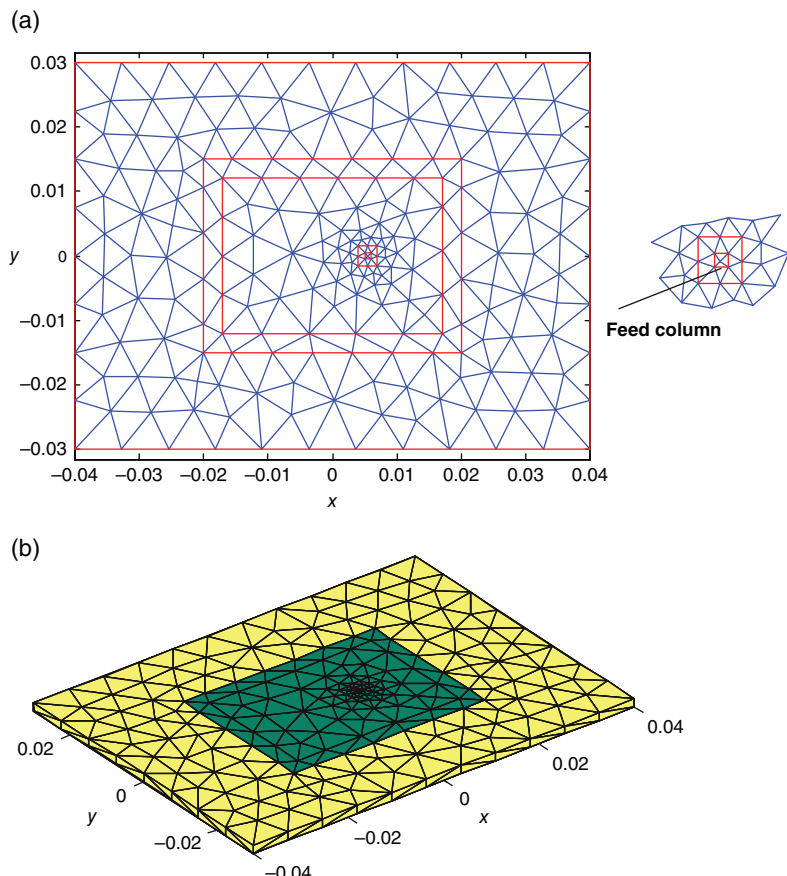


Figure 8.5 (a) Surface mesh for a patch antenna. (b) Tetrahedral volume mesh for a patch antenna obtained by extrusion.

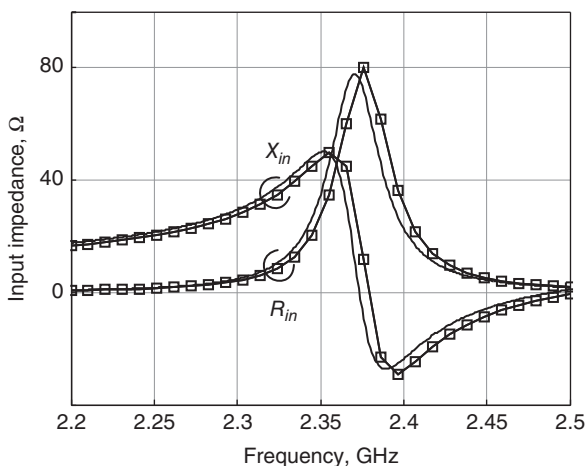


Figure 8.6 Input impedance curves for the patch antenna shown in Figure 8.4. Curves with squares – MoM MATLAB solution for the resistance/reactance; plain solid curves – Ansys HFSS FEM solution.

8.5.4 Radiation Pattern – Total Directivity and Gain

The radiation characteristics are calculated numerically, from the known field distributions. The fields are first calculated over a large sphere of radius R in order to find the total radiated power, P_{radiated} , expressed through local Poynting vector \vec{P} (see Chapter 3):

$$P_{\text{radiated}} = \int_S \vec{P} \cdot \vec{n} \, ds, \quad \vec{P} = \frac{1}{2} \operatorname{Re} [\vec{E} \times \vec{H}^*], \quad \vec{P} = \frac{1}{2\eta} |\vec{E}|^2 \vec{n} \quad \text{when } R \rightarrow \infty$$
(8.13)

Herein, \vec{P} is the time-averaged Poynting vector, \vec{n} is the outer normal to the sphere surface. This value can be compared to the previously computed antenna feed power, $P_a = \frac{1}{2} \operatorname{Re} (\mathbf{V} \cdot \mathbf{I}^*)$. The ratio of these two powers characterizes the antenna radiation efficiency, E ,

$$E = \frac{P_{\text{radiated}}}{P_a},$$
(8.14)

which characterizes the antenna loss. Since a lossless dielectric and a perfect metal conductor have been used, the relative difference between the two powers is expected to be small in a numerical solution. The MATLAB MoM method predicts a difference of 0.9% in the present case so that the efficiency is 100% to within 1%.

Next, the total or absolute logarithmic directivity, D , on the sphere surface of radius R is found in the form:

$$D(\vec{r}) = 10 \log_{10} \left(\frac{4\pi R^2 \vec{P}(\vec{r}) \cdot \vec{n}(\vec{r})}{P_{\text{radiated}}} \right).$$
(8.15)

For the antenna gain, G , the radiated power, P_{radiated} in Eq. (8.15) should be replaced by total power accepted by the antenna in the feed, P_a . For the lossless antenna, $G = D$. The directivity plot over the sphere surface for the present antenna is shown at the resonance in Figure 8.7.

The directivity and gain plots do not change significantly when frequency deviates a little ($\pm 10\text{--}20\%$ or so) from the resonant frequency.

RADIATION PATTERN – CO-POLAR AND CROSS-POLAR COMPONENTS. POLARIZATION ISOLATION

For the elevation radiation patterns (patterns containing the z-axis in Figure 8.7), one may use the elevation angle over the interval $\theta \in [0, \pi]$ as an independent variable. Then, the xz - and yz -planes are described by

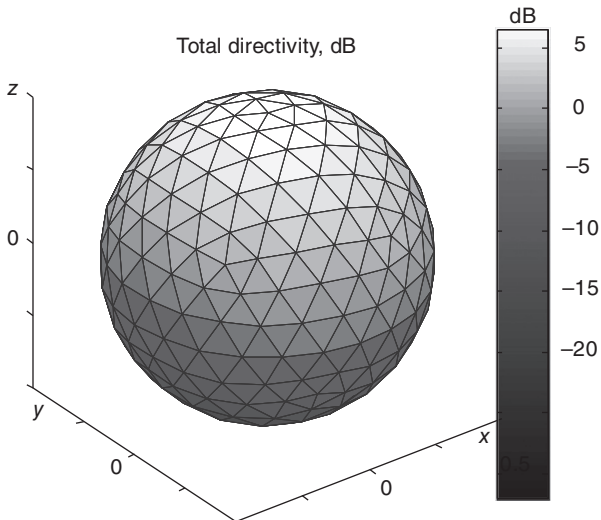


Figure 8.7 Total directivity for the patch antenna shown in Figure 8.4 at resonance – MoM simulations in MATLAB. The maximum directivity (maximum gain in this lossless case) is approximately 7 dB at broadside.

$$\varphi = 0 \text{ for the } xz\text{-plane}$$

$$\varphi = \frac{\pi}{2} \text{ for the } yz\text{-plane} \quad (8.16)$$

in spherical coordinates

$$x = r \sin \theta \cos \varphi, \quad y = r \sin \theta \sin \varphi, \quad z = r \cos \theta. \quad (8.17)$$

Instead of the Cartesian components of the electric field, one will need its spherical components given by

$$E_\theta = E_x \cos \theta \cos \varphi + E_y \cos \theta \sin \varphi - E_z \sin \theta, \quad (8.18)$$

$$E_\varphi = -E_x \sin \varphi + E_y \cos \varphi. \quad (8.19)$$

Then, the *co-polar directivity* (directivity of the major electric field component) or simply the *co-polarization* in the *H*-plane (the *yz*-plane in our case – cf. Figure 8.2b) is

$$D(\vec{r}) = 10 \log_{10} \left(\frac{4\pi R^2 P}{P_{\text{rad}}} \right), \quad P = \frac{1}{2\eta} |E_\varphi|^2 \quad (8.20)$$

for any fixed large radius R . Similarly, the cross-polar directivity (directivity of the minor or perpendicular electric field component) or the *cross-polarization* in the H -plane gives (cf. Figure 8.2b)

$$D(\vec{r}) = 10 \log_{10} \left(\frac{4\pi R^2 P}{P_{\text{rad}}} \right), \quad P = \frac{1}{2\eta} |\mathbf{E}_\theta|^2. \quad (8.21)$$

Eq. (8.20) and (8.21) are only valid for the elevation radiation patterns in the H -plane.

Note: In a general case of a linearly polarized antenna, the co-polar directivity is always the directivity of the *dominant component of the electric field* in a plane (E- or H-planes). The cross-polar directivity is always the directivity of the *minor (orthogonal) component of the electric field* in a plane (E- or H-planes).

The two radiation patterns (co-pol and cross-pol) for the present antenna in the H -plane (the yz -plane in our case) are shown in Figure 8.8. This particular antenna has a very small cross-polarization component and a good *cross-polarization isolation*, which is simply the difference between the two patterns in decibel.

In Figure 8.8, a comparison is also given of the MATLAB MoM method with the corresponding Ansys HFSS FEM radiation patterns. One can see a reasonably good agreement.

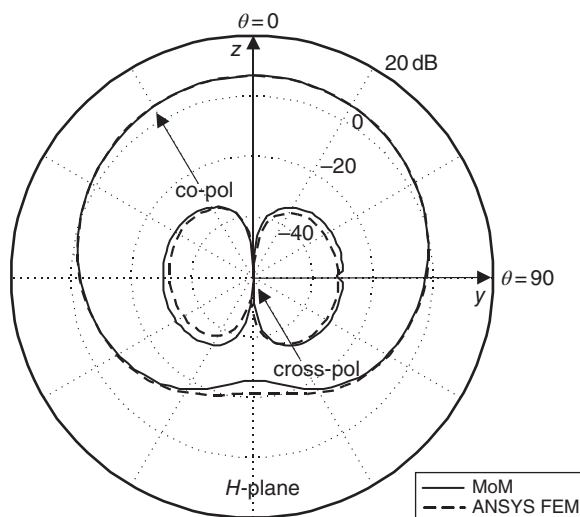


Figure 8.8 Directivity of the co-polar and cross-polar fields vs. elevation angle for the patch antenna in Figure 8.4 at the resonant frequency, in the H -plane. The MoM solution is shown by a solid curve; the Ansys solution is given by a dashed curve.

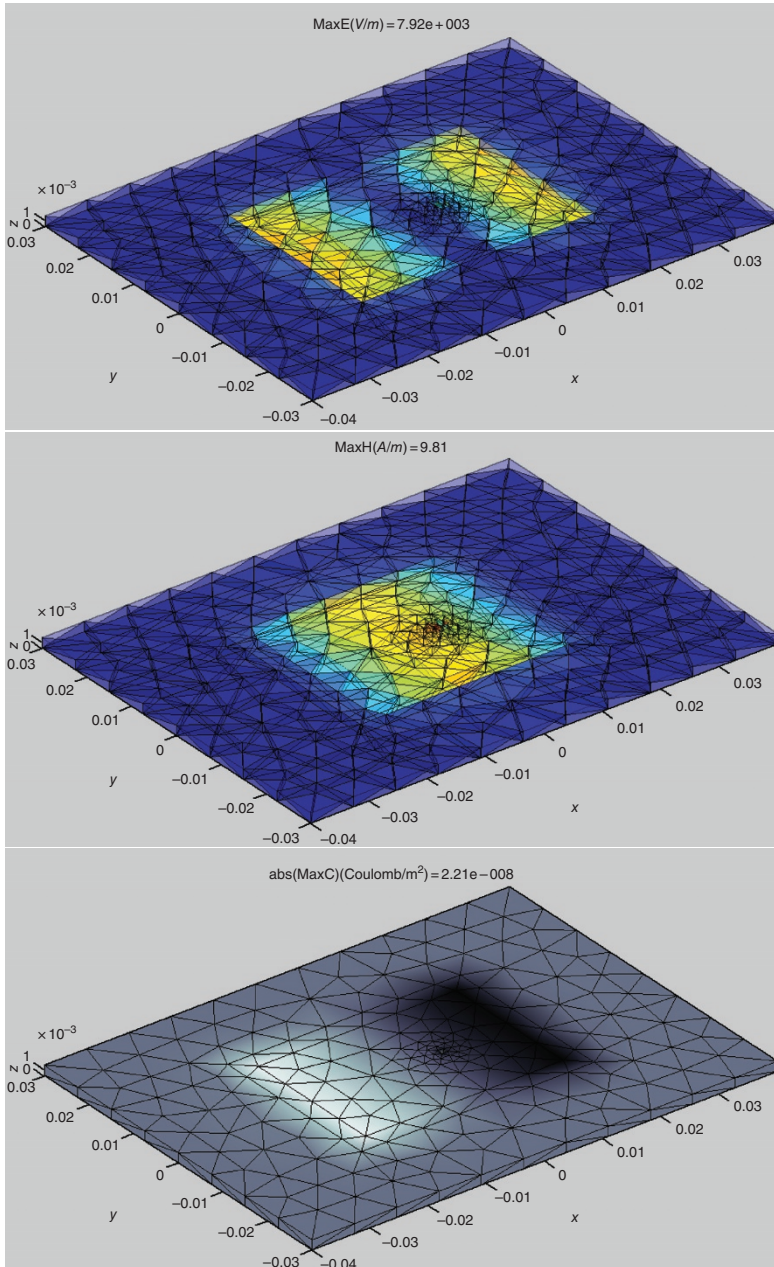


Figure 8.9 Fields within the patch antenna at the resonant frequency. Top – electric field (magnitude distribution) within the dielectric tetrahedra. Redder hues correspond to the larger field magnitudes. Center – magnetic field (magnitude distribution) within the dielectric tetrahedra. Bottom – bound charge density on the surface of the dielectric substrate– the patch side. Light colors correspond to the positive charges, dark colors – to the negative charges.

8.5.5 Near Fields

It is also instructive to inspect the near-field distributions in the antenna volume or on the antenna surface. Figures 8.9 and 8.10 show these distributions for the patch antenna obtained with the MATLAB Antenna Toolbox.

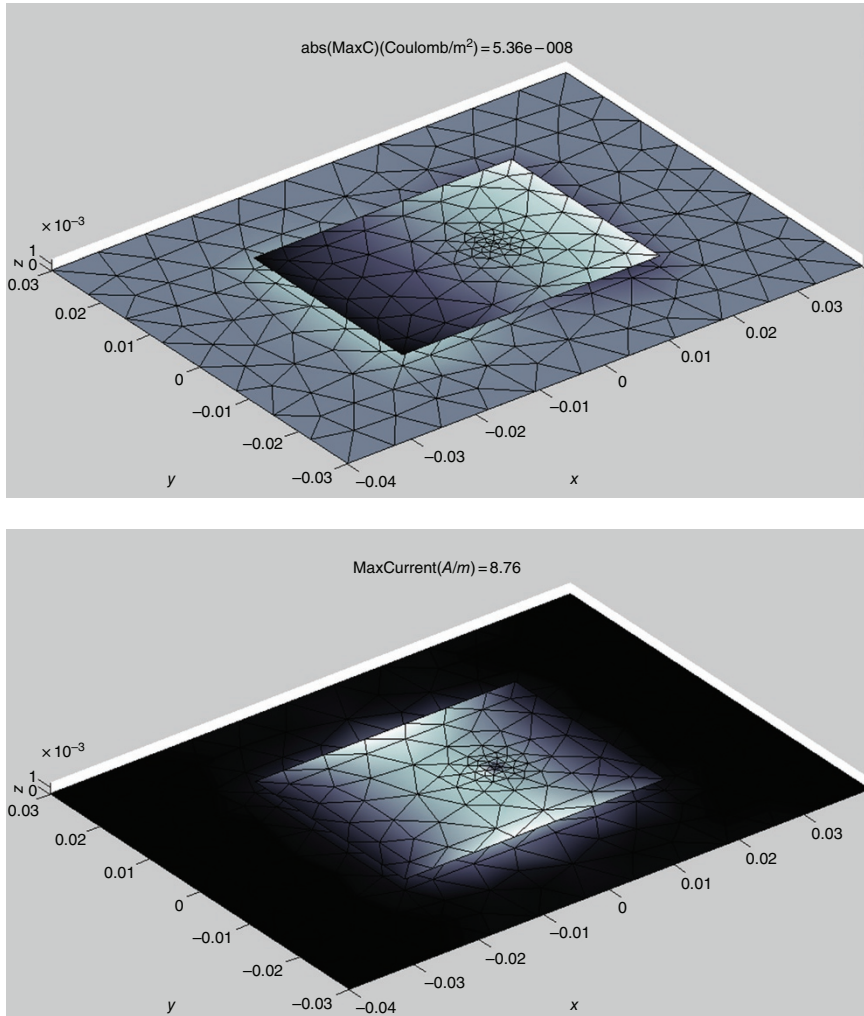


Figure 8.10 Top – free surface charge density on the metal surface. Light colors correspond to the positive charges, dark colors to the negative charges. Bottom – the surface current magnitude distribution on the metal surface. Lighter colors correspond to larger current magnitudes.

Thus, the typical half-wave resonator behavior is observed in Figures 8.9 and 8.10 for the resonant mode of the patch cavity, with the quasi-TEM mode resonating in the xz -plane (the E -plane of the antenna).

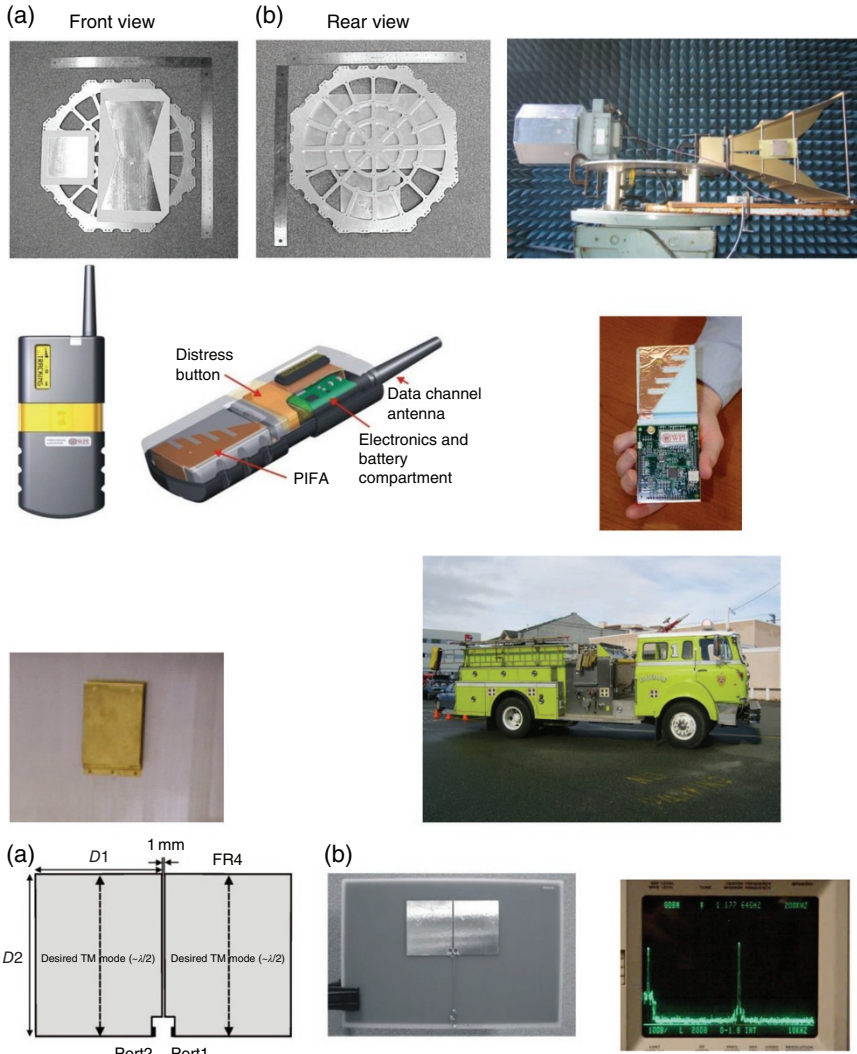


Figure 8.11 First row – VHF/UHF downlink/uplink patch antennas at 146/437 MHz on a satellite prototype measured at Hanscom AFB facility (Hanscom MA); second row – quarter-wave patch – PIFA antenna for a 550–700 MHz UHF radio; third row – patch antennas on a firefighter truck at 550–700 MHz; fourth row – an *active patch antenna-based oscillator* or *active antenna* at 0.9–1.8 GHz. *Source:* Design by the authors.

8.6 PATCH ANTENNA FAMILY

A patch antenna model is not limited to the narrowband design studied in this section. A wide variety of patch antenna designs may be found in the literature and on the market, with the bandwidth as large as 50% and even higher, and often with different functional features and shapes. Figure 8.11 shows some examples of patch antennas.

REFERENCES

1. C. A. Balanis, *Antenna Theory: Analysis and Design*, Wiley, New York, 2016, fourth edition.
2. D. M. Pozar, "Microstrip antennas," *Proc. IEEE*, vol. 80, no. 1, pp. 79–91, 1992, doi: <https://doi.org/10.1109/5.119568>.
3. K. R. Carver and J. W. Mink, "Microstrip antenna technology," *IEEE Trans. Antennas Prop.*, vol. AP-29, pp. 2–24, 1981.
4. D. R. Jackson and N. G. Alexopoulos, "Simple approximate formulas for input resistance, bandwidth, and efficiency of a resonant rectangular patch," *IEEE Trans. Antennas Prop.*, vol. 39, pp. 407–410, 1991.
5. D. R. Jackson, "Microstrip Antennas," In *Antenna Engineering Handbook*, J. L. Volakis, Ed., McGraw Hill, New York, 2007, fourth edition.
6. C. A. Balanis, *Advanced Engineering Electromagnetics*, Wiley, New York, 2012, second edition.

PROBLEMS

1. (A) Why do we use a patch antenna? Why not to use the dipole/monopole only?
(B) Does the patch antenna need a ground plane?
(C) A patch antenna has the following parameters:
 - (a) Length of 20 mm.
 - (b) Width of 20 mm.
 - (c) Thickness of 2 mm.
 - (d) Relative dielectric constant of the substrate equal to 10.0.
Estimate antenna's resonant frequency and antenna's bandwidth assuming ideal efficiency.
(D) State if the following statements are true:
 - (a) Patch antenna bandwidth increases with increasing its height (thickness).
 - (b) Patch antenna bandwidth increases with increasing its width.

- (c) Patch antenna bandwidth increases with increasing the relative dielectric constant of the substrate, ϵ_r .
2. A *square* patch antenna printed on a very large (infinite) substrate is required which resonates at 1 GHz with the bandwidth of 2%. The substrate is Rogers RT/duriod® laminate with $\epsilon_r = 2.33$. Theoretically design the antenna, i.e. present one possible set of two values:
- Patch length, L .
 - Patch antenna thickness or height, h .
3. A patch antenna has the following parameters:
- Length of 20 mm.
 - Width of 20 mm.
 - Thickness of 2 mm.
 - Relative dielectric constant of the substrate equal to 10.0 and substrate's loss tangent equal to 0.01.

Estimate antenna's efficiency assuming perfect metal surfaces.

- 4*. This problem studies a linearly polarized patch antenna on a high-frequency PTFE laminate with $\epsilon_r = 2.55$ and the thickness of 1.50 mm. The antenna geometry is shown in Figure 8.12. The loss tangent of the substrate is assumed to be 0.001.

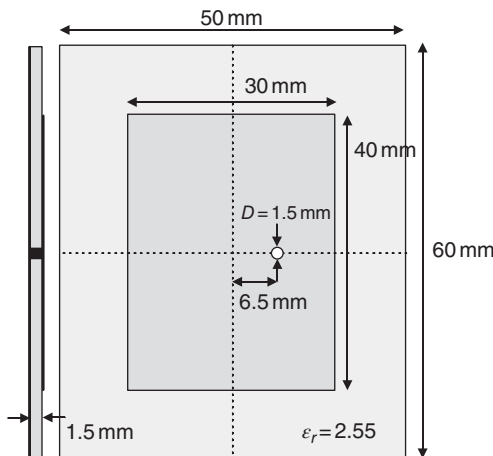


Figure 8.12 Patch antenna geometry.

- Obtain and plot antenna's input impedance from 2 to 3 GHz. Design the antenna using functions `dielectric` and `patchMicrostrip` of the MATLAB Antenna Toolbox.
- Determine antenna's impedance bandwidth.
- Plot the total directivity in dB (a 3D polar plot) at the resonant frequency.

5*. This problem studies a linearly polarized patch antenna on a high-frequency Rogers laminate with $\epsilon_r = 9.29$ and the thickness of 3.82 mm. The antenna geometry is shown in Figure 8.13. The loss tangent of the substrate is assumed to be 0.001.

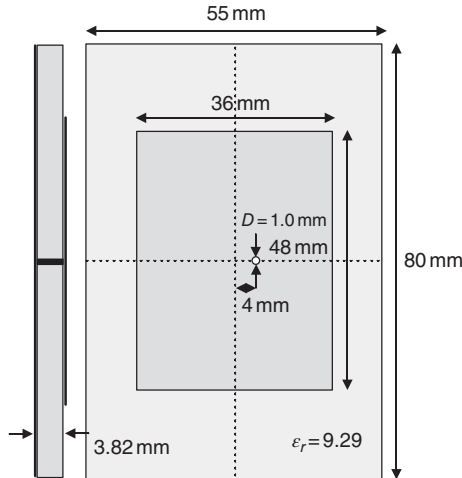


Figure 8.13 Patch antenna geometry.

- (A) Approximately determine antenna's resonant frequency.
- (B) Obtain and plot antenna's input impedance. To do so, design the antenna using functions `dielectric` and `patchMicrostrip` of the MATLAB Antenna Toolbox.
- (C) Determine antenna's impedance bandwidth.
- (D) Plot the total directivity in dB (a 3D polar plot) at the resonant frequency.

- 6*.** Create a probe-fed microstrip patch antenna at 2.4 GHz. To do so, use the `design` function in the MATLAB Antenna Toolbox (`p=design(patchMicrostrip, 2.4e9)`). Do the following:
 - (A) Calculate the impedance at 2.4 GHz.
 - (B) Calculate the 3D pattern and plot it at 2.4 GHz.
 - (C) Reduce the width of the patch and make it equal to the length. Recalculate the impedance at 2.4 GHz.
 - (D) Adjust the feed offset and achieve as best a match as possible to 50Ω .
 - (E) Plot the 3D pattern for the modified patch at 2.4 GHz.
 - (F) Plot the current at 2.4 GHz for the modified patch structure. Comment on the current behavior in the plot. Use the color bar on the right to adjust the displayed colors. This is an interactive color bar which allows you to drag directly on the color or the values.

- 7*. For the patch antenna designed in Problem 6, make the feed offset to be 0 for both dimensions (x , y). Calculate impedance for this configuration. In an approximate sense, does this imply a short- or an open-circuit condition at this position for the feed? Can you suggest a way to convert this structure into a PIFA (next section)?
- 8*. This problem introduces a *circularly polarized* patch antenna shown in Figure 8.14.

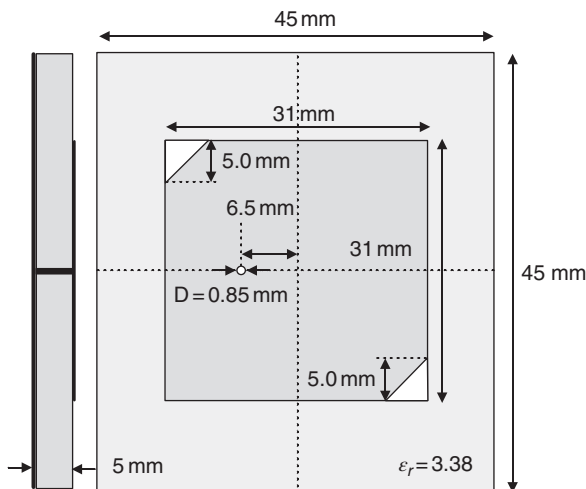


Figure 8.14 Patch antenna geometry.

- (A) Attempt to model this antenna using the MATLAB Antenna Toolbox.
Describe your approach.
- (B) Justify the circular polarization.

**SECTION 2 PLANAR INVERTED F (PIFA) ANTENNA.
BANDWIDTH ESTIMATIONS**

8.7. Concept	219
8.8. PIFA Types. Behavior of Input Impedance	220
8.9. PIFA Modeling	223
8.10. Bandwidth Results	226
8.11. Comparison with Other Data	227
8.12. Summary	230
References	230
Problems	231

The motivation for the organization of this section was a request from a local company to estimate the bandwidth of a PIFA antenna for a passive RFID tag chip operating at 915 MHz as a function of antenna height. The PIFA is less dependent on the platform than the design for conventional printed dipoles. Hence, it may be used in close proximity to metal objects or to objects with a high dielectric constant. Furthermore, the PIFA is smaller than a patch antenna, which makes it more attractive for tag miniaturization. The antenna height can be made reasonably small; a small height may be a critical requirement from the production point of view.

8.7 CONCEPT

The patch antenna is a half-wave resonator on the base of a transmission line. The conventional *planar inverted F antenna (PIFA)* is simply a half of the patch antenna, a *quarter-wave resonator* obtained from shorting the patch exactly in the middle, where the electric field already becomes zero.

This operation reduces the size of the antenna by approximately a factor of two, but simultaneously alters the radiation pattern and polarization isolation. The last circumstance may be less important for cell-phone-type antennas working in the multipath environment or for *radio-frequency identification (RFID)* tag antennas. Today, the PIFA is one of the leading cellphone antennas. The PIFA was first invented in 1986–1987 (T. Taga, K. Tsunekawa, and A. Sasaki, “Antennas for detachable mobile radio units,” *Review of the ECL, NTT*, Japan, vol. 35, no. 1, pp. 59–65 Jan. 1987).

In this section, the resonant impedance bandwidth of four basic types of small rectangular PIFAs will be estimated as a function of the antenna height. It will be shown that the relative or fractional *half-power bandwidth B* (small antennas are investigated) for all investigated antenna types is described by the inequality

$$0.5 \frac{h}{\lambda} < B < 3 \frac{h}{\lambda}, \quad (8.22)$$

where h is the antenna height and $\lambda = \lambda_0$ is the free-space wavelength at the antenna's center frequency. The upper estimate for the bandwidth ($B = 3 \frac{h}{\lambda}$) corresponds to a shunt–shunt PIFA with a top-located feed, optimized for maximum impedance bandwidth. The lower estimate ($B = 0.5 \frac{h}{\lambda}$) belongs to a shunt–open planar inverted L-antenna (PILA), also optimized for maximum impedance bandwidth.

We will show that the majority of collected literature data for the PIFAs with real or complex input impedances are within this range. This suggests a simple estimate for the achievable bandwidth of a low-profile PIFA.

A significant body of work on RFID tag PIFA antennas exists (cf. [1–6]). Data can also be obtained for standard PIFAs that are used for communication purposes and whose typical input impedance is typically 50Ω [7–9]. A problem is that different PIFA antennas have very different geometries and are designed for different (and generally reactive) matching impedances that are chip-dependent (and not equal to 50Ω).

In order to obtain the chip-independent results, we suggest estimating the *resonant half-power impedance bandwidth* of a PIFA antenna, very similar to the bandwidth of small antennas defined in Chapter 7. The resonant impedance bandwidth is obtained vs. resonant antenna resistance that may itself have different values. If necessary, the reactance is matched using the conjugate matching.

Such estimates provide us with the exact bandwidth for a real matching impedance that is equal to that of the antenna and a good approximation for a complex matching impedance if the reactance of an antenna is a linear function of frequency near the resonance. The latter behavior (a series RLC circuit) may be typical for (printed) RFID tag dipoles and some PIFA antennas. To simplify the analysis, we only considered *air-filled* PIFAs *without a dielectric medium*.

8.8 PIFA TYPES. BEHAVIOR OF INPUT IMPEDANCE

8.8.1 Transmission Line Model

Figure 8.15 shows three possible PIFA modifications that have been tested. The first antenna is a conventional PIFA. Instead of the most common probe feed, a slot feed or another kind of capacitive/inductive coupling could be employed. This antenna configuration is mostly used in mobile communications. The second antenna (PIFAI) implies a top-located voltage feed without a circuit-board via; such an antenna is called PILA [10]. It is more convenient for the RFID tag chips; the chip itself can be located on the top layer. The third antenna (PIFAII) is the PILA with a shorted patch.

The antenna input impedance in Figure 8.15 is given by $Z_{in} = \frac{V^*}{I^*}$, where V^* and I^* are the phasor voltage and phasor current recorded at the antenna terminals – see Figure 8.15. Here, the superscript star simply labels the antenna terminal parameters, but not the complex conjugate. To qualitatively describe the input

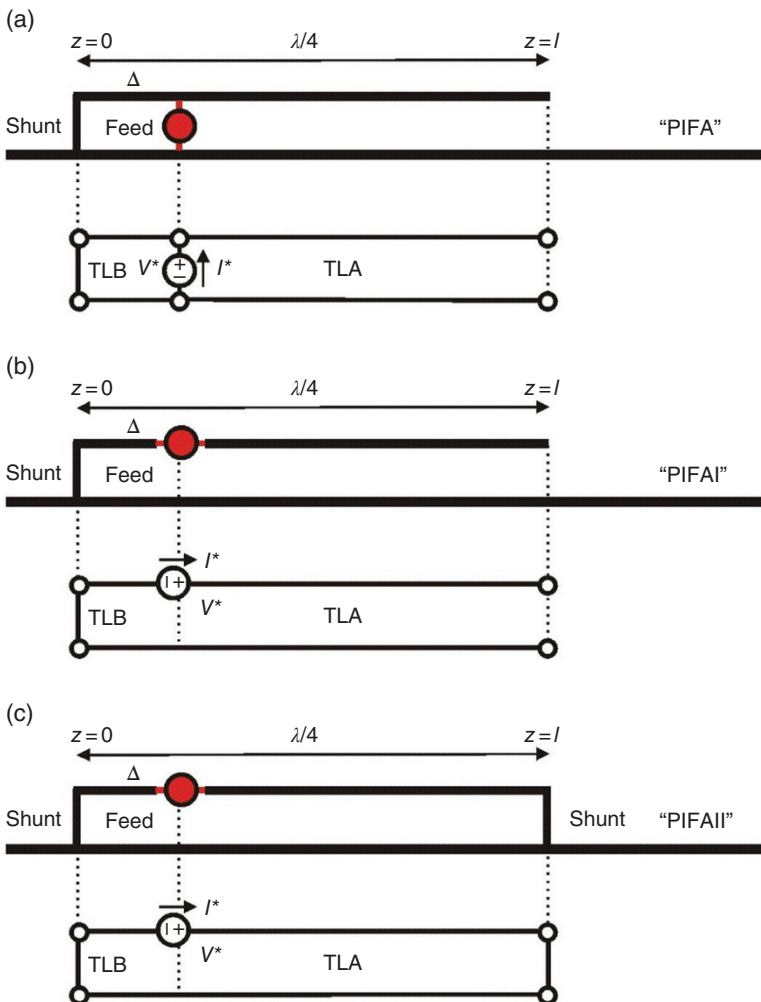


Figure 8.15 Three variations of PIFA: (a) Conventional PIFA. (b) PIFA with a top-located feed (PIFAI). (c) The same as (b) but with a shunted $\lambda/4$ resonator.

impedance of the antenna, it is suggested to use a transmission line model where its loss per unit length, α , could also approximately describe both the radiation loss and the ohmic loss of the corresponding antenna.

Every antenna in Figure 8.15 includes two transmission line stubs labeled as TLA and TLB, respectively. The input impedance is given by a parallel or series combination of the stub impedances Z_A and Z_B , respectively. In terms of

- (i) the line propagation constant γ ;
- (ii) the real characteristic impedance Z_0 of the transmission line; and
- (iii) the real load impedance Z_L (short or open)

one finds for two terminal line impedances in the feed reference plane,

$$l = \frac{\lambda}{4}, \gamma = \alpha + jk, Z_A = Z_0 \frac{Z_L + Z_0 \tan h\gamma(l - \Delta)}{Z_0 + Z_L \tan h\gamma(l - \Delta)}, Z_B = jZ_0 \tan k\Delta, \quad (8.23)$$

where $k = 2\pi/\lambda$ is the wavenumber. We will consider this model using two inequalities

$$\alpha l \ll 1, k\Delta \ll 1, \quad (8.24)$$

which assume relatively low losses (a high Q -factor) and a relatively short offset length Δ , respectively.

8.8.2 PIFA

The case of a conventional PIFA is shown in Figure 8.15a. To find the input impedance, one combines two transmission lines TLA and TLB *in parallel*. By taking into account Eq. (8.23) and (8.24) and to within the first order of approximation, one has for antenna's input impedance Z_a ,

$$Z_A = Z_0(\alpha l - jk\Delta), Z_B = jZ_0 k\Delta \\ Z_a = Z_A \parallel Z_B = Z_0 \frac{(k\Delta)^2}{\alpha l} + jZ_0 k\Delta, Z_a \approx Z_0 \frac{(k\Delta)^2}{\alpha l} \quad \text{if } k\Delta \gg \alpha l. \quad (8.25)$$

The presence of an imaginary part of the input impedance at $l = \lambda/4$ in Eq. (8.25) is expected. The nonzero reactance is present because the PIFA does not resonate at exactly $l = \lambda/4$. The reactance may be eliminated by a slight deviation of the PIFA resonant length from $\lambda/4$.

The PIFA, similar to the patch antenna, indicates a *parallel RLC resonator behavior* – the magnitude of the input impedance has a local maximum at the resonance. This fact is established using original Eq. (8.23). The radiation resistance of the resonant PIFA can vary widely – the control of the resistance is achieved by the feed shift Δ . Also note that the PIFA bandwidth depends on the size of the shunt stub.

8.8.3 PIFAI or PILA

The case of PILA is shown in Figure 8.15b. To evaluate the input impedance, one now combines two transmission lines TLA and TLB *in series*. One has

$$Z_A = Z_0(\alpha l - jk\Delta), Z_B = jZ_0 k\Delta \quad Z_a = Z_A + Z_B = Z_0 \alpha l. \quad (8.26)$$

In contrast to the PIFA, the PILA indicates a *series RLC resonator behavior* – the magnitude of the input impedance has a minimum at the resonance. This fact is again established using complete Eq. (8.23). The resonance is achieved at exactly $l = \lambda/4$. The resistance of the resonant PILA is generally small (on the order of 0.1–10 Ω); its control may be partially achieved by changing Z_0 ; increase in Z_0 (decrease in line capacitance) leads to larger values of the resistance.

8.8.4 PIFAI^I

This case is shown in Figure 8.15c. For the input impedance, one again combines two transmission lines TLA and TLB in series. This yields

$$\begin{aligned} Z_A &= \frac{Z_0}{\alpha l - jk\Delta}, \quad Z_B = jZ_0 k\Delta \\ Z_a = Z_A + Z_B &= Z_0 \frac{1 + jk\Delta\alpha l + (k\Delta)^2}{\alpha l - jk\Delta}, \quad Z_a \approx Z_0 \frac{1}{\alpha l} \quad \text{if } k\Delta \ll \alpha l. \end{aligned} \quad (8.27)$$

This antenna indicates a parallel RLC resonator behavior similar to the PIFA. The resistance of the resonant antenna is generally large (on the order of 100–100 000 Ω); its control may be partially achieved by changing Z_0 ; decrease in Z_0 (increase in line capacitance) leads to smaller values of the resistance. The conventional PIFA in Figure 8.15a can be further subdivided into two slightly different antenna configurations – see Figure 8.16 below.

The results are summarized in Table 8.1. A problem with the transmission-line approach discussed above is a proper definition of the loss factor, α , which should also include radiation loss (the space wave). It is not a straightforward task. Therefore, numerical modeling is employed.

8.9 PIFA MODELING

The conventional PIFA shown in Figure 8.15a may have different bandwidths depending on the width of the shunt. Therefore, we further subdivide this case (case a in Figure 8.15) and consider not three, but rather four basic PIFA configurations as shown in Figure 8.16. The initial antenna parameters are as follows:

$$\begin{aligned} a &= 300 \text{ mm}, \quad b = 200 \text{ mm}, \quad l = 100 \text{ mm}, \quad d = 5:15:275 \text{ mm}, \\ h &= 1, 2, 5, 10 \text{ mm} \\ f &= 250:0.1:1200 \text{ MHz}; \quad \% \text{centered antenna}, \end{aligned}$$

where the ground plane has the size $a \times b$. For antenna simulations, the parametric sweeper of Ansys HFSS was primarily used and then controlled by a slightly faster MoM solver of the MATLAB Antenna Toolbox. Both methods gave similar results.

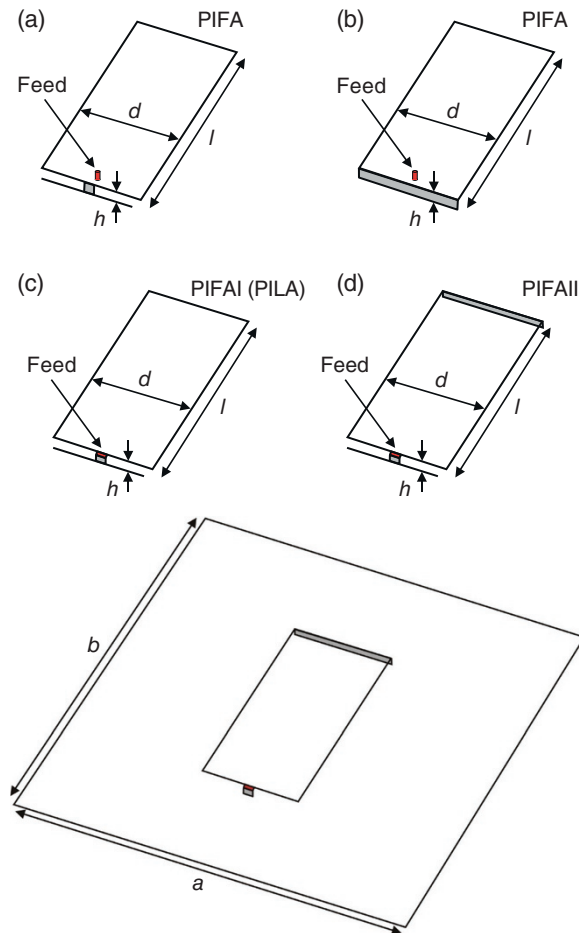


Figure 8.16 Top – Four different base PIFA configurations: (a) PIFA with a narrow shunt; (b) PIFA with a wide shunt; (c) PIFAI (PILA); (d) PIFAI_{II}. Bottom – Ground plane and the centered PIFA used in the simulations. (Simulations were carried out for off-center antennas too. The results were generally similar.)

An antenna resonance was found for every geometry configuration, and every antenna geometry set was then rescaled to a 915 MHz resonant frequency. Note that antenna PIFA b in Figure 8.16b still has an inductive reactance component at the parallel resonance, which increases with increasing the width, d . Therefore, this antenna was matched with a series capacitance to achieve the proper resonant behavior and to be consistent with the others. Table 8.2 lists some antenna impedance characteristics.

TABLE 8.2 Resonant behavior of four PIFA antennas and optimal antenna width, d .

Antenna	Resonance type	Resonant d for maximum bandwidth	Typical resonant Z_a at 915 MHz without an impedance matching network	Typical real part of Z_a with 100 Ω inductance
PIFA (a)	Parallel RLC	$\sim 0.4\text{--}0.5\lambda$ then saturated	Arbitrary	—
PIFA (b)	Parallel RLC with a series inductor	$\sim 0.07\lambda$	Arbitrary (with a series matching capacitor)	—
PIFAI or PILLA	Series RLC	$\sim 0.07\lambda$	0.001 Ω ($h = 1.0$ mm) 1.0 Ω ($h = 10$ mm)	5–10 Ω ($h = 10$ mm)
PIFAII	Parallel RLC	$\sim 0.4\text{--}0.5\lambda$ then saturated	250 Ω ($h = 10$ mm) 150 k Ω ($h = 1.0$ mm)	—

8.10 BANDWIDTH RESULTS

Figure 8.17 shows the values of the half-power resonant impedance bandwidth for four antennas extracted from simulations, all as a function of the normalized antenna height. A linear behavior of the bandwidth is observed for all antennas except PIFA b) (with a matching capacitor) where a weak nonlinearity becomes apparent.

The results for PIFAII at $d = 0.5\lambda$ (such a large width is probably interesting only theoretically and is hardly justified in practice) almost perfectly follow the linear dependence of the fractional bandwidth percentage on antenna height,

$$B = 300 \frac{h}{\lambda} [\%] \quad (8.28)$$

with the standard deviation of 1.1%. The results for PIFAII at $d = 0.4\lambda$ (this width is interesting only theoretically and is also hardly justified in practice) follow the dependence

$$B = 270 \frac{h}{\lambda} [\%] \quad (8.29)$$

with the standard deviation of 1.6%. The results for PIFA a) ($d \sim 0.07\lambda$ – optimized for a maximum bandwidth) follow

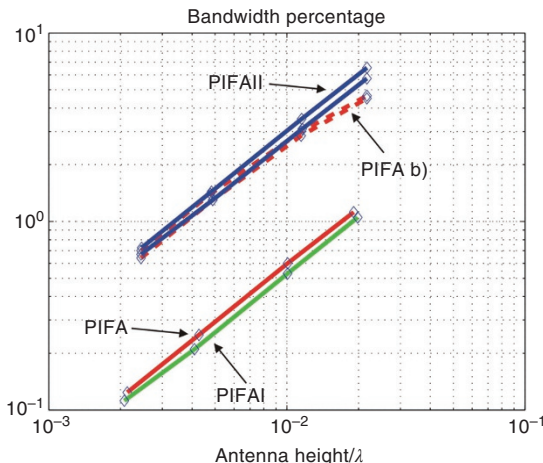


Figure 8.17 Half-power antenna bandwidth vs. normalized antenna height for four PIFA configurations shown in Figure 8.16a-d). Two PIFAII curves correspond to $d = 0.5\lambda$ (upper) and $d = 0.4\lambda$ (lower), respectively. The same is valid for two PIFA b) antennas ($d = 0.5\lambda$ (upper) and $d = 0.4\lambda$ (lower)) shown by dashed curves.

$$B = 59 \frac{h}{\lambda} [\%] \quad (8.30)$$

with the standard deviation of 1.1%. Finally, the results for PIFAII ($d \sim 0.07\lambda$ – optimized for a maximum bandwidth) follow the dependence

$$B = 53 \frac{h}{\lambda} [\%] \quad (8.31)$$

with the standard deviation of 2.0%.

All intermediate results are confined between the curves for PIFAII and PIFAI. Thus, one approximately has for the relative bandwidth (not percentage)

$$0.5 \frac{h}{\lambda} < B < 3 \frac{h}{\lambda}. \quad (8.32)$$

8.11 COMPARISON WITH OTHER DATA

Table 8.3 lists some collected literature data. Only the RFID tag-related references are included into the table. The original PIFA design suggested by Taga et al. [7] is also included. We did not pay special attention to the size of the ground plane and used the reported bandwidth irrespective of the variable ground plane size. When several ground planes have been used, the largest value of the bandwidth was usually retained. It is known that the impedance bandwidth generally increases with increasing the ground plane size [9].

The bandwidth for different PIFA antennas is then plotted as a function of the dimensionless antenna height in Figure 8.18, similar to Figure 8.17. In Figure 8.18, we simultaneously plot two extreme curves from Figure 8.17: the results for PIFAII optimized for maximum bandwidth and given by Eq. (8.28) and the result for PIFAI again optimized for maximum impedance bandwidth and given by Eq. (8.31). It can be seen that the majority of the collected literature data for the PIAs with real or complex input impedances are within the domain bounded by two curves that follow Eq. (8.28) and (8.31), respectively. The combined inequality is Eq. (8.32).

This is a remarkable observation that suggests a simple impedance-independent estimate for the achievable bandwidth of the low-height PIFA. However, the antenna “position” within the allowed domain is impedance-dependent.

One exception seems to be reference [1] in Figure 8.18, which predicts a considerably larger impedance bandwidth than the others. Note that this reference suggests a PIFA with two closely spaced resonances, in contrast to some other antennas. A similar design of a wearable foam-based PIFA for communication purposes at 440 MHz [11] also indicated a large half-power impedance bandwidth.

TABLE 8.3 Some UHF PIFA/patch RFID antennas in 915 MHz and 869 MHz bands. The effect of the finite ground plane is not separately investigated; the highest bandwidth value for multiple ground planes is used wherever possible.

Refs.	Type	Center frequency	Required antenna impedance ¹	Size	Height	Half-power bandwidth (VSWR<6; Γ <0.5)
[1]	Three-layer ² PIFA; three shunts	915 MHz	$Z_a=(6+j127) \Omega$	Patch: 74.5 × 24.5 mm GP: 400 × 400 mm ³	3 mm	51–57 MHz
[2]	Two-layer ⁴ PIFA (PIFAII)	869 MHz	$Z_a=(7+j170) \Omega$	Patch: 45 × 45 mm GP: 59 × 59 mm	3 mm	~16 MHz
[3]	Three-layer patch with EBG	916 MHz	$Z_a=1200 \Omega$	Patch: 49 × 47 mm GP: 100 × 100 mm	6.4 mm	~20 MHz
[4]	Two-layer slotted PIFA	915 MHz	$Z_a=(7+j197) \Omega$	Patch: 82 × 46 mm GP: 90 × 54 mm	5 mm	~26 MHz
[5]	Two coupled two-layer PIFAs (PIFAII)	915 MHz	$Z_a=(10+j150) \Omega$	Patch: 46 × 54 mm GP: NA	3 mm	~17 MHz
[6]	Three-layer slotted PIFA	914 MHz	$Z_a=(77+j100) \Omega$	Patch: 46 × 46 mm GP: NA	3.25 mm	~8 MHz

¹Chip impedance to be matched to is a complex conjugate of this value.

²Antenna with three layers, each of which includes metal stubs.

³Dual-resonance antenna with the large ground plane.

⁴Antenna with only two layers containing metal stubs.

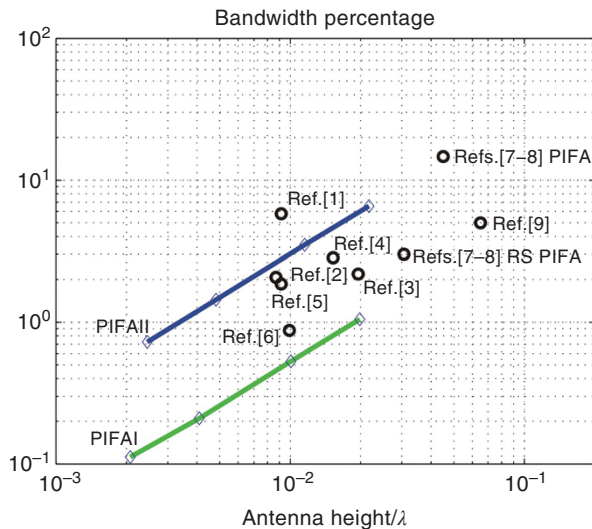


Figure 8.18 Some literature data on the PIFA bandwidth. References [1–6] correspond to RFID tag PIFA/patch antennas; References [7–9] correspond to conventional PIAs. In Ref. [9], the ground plane is $0.5\lambda \times 0.5\lambda$.

However, this antenna had a significant relative height. The present study is limited to the low-profile antennas with $h/\lambda < 0.05$.

Example 8.3

A PIFA antenna for a GSM 850 MHz uplink band

```
% GSM850u = [824 849]; % uplink
```

is needed. Using Eq. (8.32), estimate the approximate antenna height, which may be required.

Solution: From Eq. (8.32), we obtain two estimates for the maximum and minimum value of the antenna height, respectively

$$0.5 \frac{h}{\lambda} < B < 3 \frac{h}{\lambda} \Rightarrow h_{max} = \frac{B\lambda}{0.5}, h_{min} = \frac{B\lambda}{3}. \quad (8.33)$$

A simple MATLAB script that follows

```
clear all;
```

```

fL = 824e6;
fU = 849e6;
fC = (fL+fU ) /2;
B = (fU-fL)/fC;
lambda = 3e8/fC;

hmax =B*lambda/0.5
hmin =B*lambda/3.0

```

solves the problem and yields

$$h_{\max} = 21 \text{ mm}, \quad h_{\min} = 3.6 \text{ mm.} \quad (8.34)$$

Note: The *uplink channel* is the channel from a terminal (cellphone) to the base station. Sometimes it is called the *reverse channel*.

The *downlink channel* is the channel from a base station to the terminal (cellphone). Sometimes it is called the *forward channel*.

8.12 SUMMARY

In this section, the resonant impedance bandwidth of four basic types of rectangular PIFAs has been estimated as a function of antenna height. Extensive numerical simulations have been performed over a representative domain of the antenna height and antenna length/width ratio. It was found that the relative bandwidth for all antenna types is described by the inequality $0.5 \frac{h}{\lambda} < B < 3 \frac{h}{\lambda}$ where h is the antenna height. The upper estimate for the bandwidth ($B = 3 \frac{h}{\lambda}$) corresponds to a shunt–shunt PIFA with a top-located feed, optimized for maximum impedance bandwidth. The lower estimate ($B = 0.5 \frac{h}{\lambda}$) belongs to a shunt–open PILA, also optimized for maximum impedance bandwidth. It was found that the majority of collected literature data are within those limits. This observation suggests a simple impedance-independent estimate for the achievable bandwidth of a low-profile PIFA. PIFA antennas matched to a large real impedance seem to have a larger bandwidth (and simultaneously larger length and width) compared to the nonresonant antennas with the inductive reactance on the order of approximately 100Ω .

REFERENCES

1. H.W. Son, J. Yeo, G.Y. Choi, and C.S. Pyo, “A low-cost, wideband antenna for passive RFID tags mountable on metallic surfaces,” in *Proc. IEEE Antennas and Propagation Society Int. Symp.*, Albuquerque , NM, 2006, pp. 1019–1022, July 2006.

2. M. Hirvonen, P. Pursula, K. Jaakkola, and K. Laukkanen, "Planar inverted-F antenna for radio frequency identification", *Electron. Lett.*, vol. 40, no. 14, pp. 848–850, 2004.
3. L. Ukkonen, L. Sydänheimo, and M. Kivikoski, "Patch antenna with EBG ground plane and two-layer substrate for passive RFID of metallic objects", in *2004 IEEE Antennas and Propagation Society International Symposium*, Monterey, CA, vol. 1, pp. 93–96, July 2004.
4. S.-J. Kim, B. Yu, H.-J. Lee, M.-J. Park, F. J. Harackiewicz, and B. Lee, "RFID tag antenna mountable on metallic plates," in *Microwave Conference Proceedings*, 2005. APMC 2005. Asia-Pacific Conference Proceedings, vol. 4, 4–7 Dec. 2005.
5. B. Yu, S.-J. Kim, B. Jung, F. J. Harackiewicz, M.-J. Park, and B. Lee, "Balanced RFID tag antenna mountable on metallic plates," in *Proc. IEEE Antennas and Propagation Society Int. Symp.*, Albuquerque, NM, 2006, pp. 3237–3240, July 2006.
6. W. Choi, H. W. Son, J.-H. Bae, G. Y. Choi, C. S. Pyo, and J.-S. Chae, "An RFID tag using a planar inverted-F antenna capable of being stuck to metallic objects," *ETRI J.*, vol. 28, no. 2, pp. 216–218, 2006.
7. T. Taga, K. Tsunekawa, and A. Sasaki, "Antennas for detachable mobile radio units," *Review ECL, NTT*, vol. 35, no. 1, pp. 59–65, 1987.
8. R. Bancroft, *Microstrip and Printed Antenna Design*, Noble Publishing, Atlanta, GA, 2004.
9. M.-C. Huynh and W. Stutzman, "Ground plane effects on planar inverted-F antenna (PIFA) performance," in *IEE Proceedings on Microwaves, Antennas and Propagation*, vol. 150, no. 4, 8 Aug. 2003, pp. 209–213.
10. K. Boyle, "Radiating and balanced mode analysis of PIFA shorting pins," in *Proc. IEEE Antennas and Propagation Society Int. Symp.*, San Antonio, TX, 2002, pp. 508–511, June 2002.
11. S. Kulkarni and S. Makarov, "A compact dual-band foam-based UHF PIFA," in *Proc. IEEE Antennas and Propagation Society Int. Symp.*, Albuquerque, NM, 2006.

PROBLEMS

1. (A) Draw the schematic of a patch antenna.
 (B) Draw the schematic of a conventional PIFA antenna and indicate the difference between the two antenna types.
2. (A) An air-filled PIFA for a GSM 850 MHz downlink band

% GSM850d = [864:894]; % downlink

is needed. Using Eq. (8.32), estimate the approximate antenna height which may be required.

- (B) An air-filled PIFA for an ISM 900 MHz band

% ISM = [902:928]; % ISM 900 MHz

is needed. Using Eq. (8.32), estimate the approximate antenna height which may be required.

- 3*.** Create an air-filled PIFA with the following parameters: $L = W = \lambda/4$, $h = 0.05 * \lambda$ using the MATLAB Antenna Toolbox. The ground plane is $\lambda/2 \times \lambda/2$. Center the PIFA at $[-\lambda/10, \lambda/8]$ and create the initial feed at the feed offset of $[-\lambda/8, \lambda/8]$. Make the short pin width to be $W/8$. Hint: use `pifa` function of the MATLAB Antenna Toolbox. Do the following:
- (A) Calculate the impedance of the PIFA at 2.4 GHz.
 - (B) Find a feed offset that can bring the radiation resistance to as close as possible to 50Ω .
 - (C) Vary the shorting pin width to be $W/8$, $W/4$, $W/2$, $0.75 * W$, and W , and tabulate the effect of pin width on the impedance.
 - (D) For the PIFA with a shorting pin width of $W/8$ and W , plot the directivity patterns (in both E- and H-planes) at 2.4 GHz. Turn in the plots.
- 4*.** Repeat Problem 3 for the antenna center frequency of 915 MHz.

CHAPTER 9



Traveling Wave Antennas

SECTION 1 LONG WIRE ANTENNA AND YAGI-UDA ANTENNA

9.1. Concept	233
9.2. Features and Modeling	234
9.3. Modeling with Antenna Toolbox	237
9.4. Yagi-Uda Antenna	238
9.5. Traveling Wave Formation Along Yagi-Uda Antenna	238
References	239
Problems	239

9.1 CONCEPT

Almost all antennas considered so far were *open resonators*: either half-wave (dipole, patch) or quarter wave (monopole, PIFA antenna). The resonator antennas utilize *standing waves* and inherently have a limited bandwidth since they operate close to the corresponding resonant frequency.

Antennas can be designed which utilize *traveling* (over relatively long distances) *current and voltage waves*, that do not experience significant reflections from antenna terminations. One example of such an antenna is a biconical antenna operating at higher frequencies and studied in Chapter 5.

Another simple yet important example is given by a *long wire antenna* shown in Figure 9.1. A generator creates a voltage and current wave that propagates along a

Antenna and EM Modeling with MATLAB® Antenna Toolbox, Second Edition. Sergey N. Makarov, Vishwanath Iyer, Shashank Kulkarni, and Steven R. Best.

© 2021 John Wiley & Sons, Inc. Published 2021 by John Wiley & Sons, Inc.

Companion website: www.wiley.com/go/Makarov/AntennaandEMModelingwithMATLAB2e

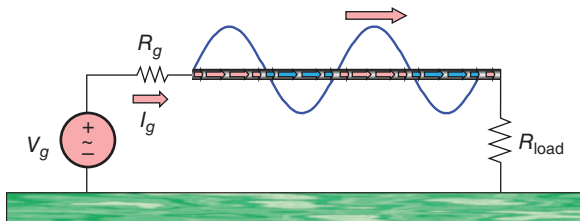


Figure 9.1 Long wire antenna with a generator and a termination resistance (impedance).

transmission line formed by a long wire and a ground conductor, for example, Earth. When the wave meets a termination resistance (impedance), R_{load} , no reflection occurs if R_{load} is equal to the *characteristic impedance of the transmission line* formed by the wire and the ground plane. Values of R_{load} in the range 200–300 Ω are typical [1].

While propagating along the (widely open) transmission line, the high-frequency voltage wave radiates into free space. This is a simple *traveling wave antenna*.

9.2 FEATURES AND MODELING

The radiation pattern of the long wire antenna in the presence of the ground could be modeled as an antenna in free space plus its image below the ground [1]. The corresponding approach was described in Chapter 4. Therefore, it is sufficient to model a stand-alone long wire antenna of length l_A as shown in Figure 9.2. We will assume that the antenna axis is now the z -axis.

According to the approach of Chapter 3, the antenna radiation in the far field is given by a sum (later converted to an integral) of the contributions of individual infinitesimally short current elements $d\vec{z}'$. From Eq. (3.28a), the contribution of every such individual element to the dominant radiated field component E_θ is given by (the phasor form)

$$dE_\theta = \left[\frac{j\eta k \sin \theta \exp(-jk|\vec{r}|)}{4\pi |\vec{r}|} \right] \mathbf{I}(z') \exp(jkz' \cos \theta) dz' \quad (9.1)$$

so that the entire far field of the long wire antenna becomes (Eq. (3.29a))

$$E_\theta = \left[\frac{j\eta k \sin \theta \exp(-jk|\vec{r}|)}{4\pi |\vec{r}|} \right] \int_{-l_A/2}^{+l_A/2} \mathbf{I}(z') \exp(jkz' \cos \theta) dz'. \quad (9.2)$$

We assume that the phase speed on the line is the same as in vacuum (a metal ground plane). A more general situation is considered in [1–3]. Thus, a traveling current wave along the long wire has the form:

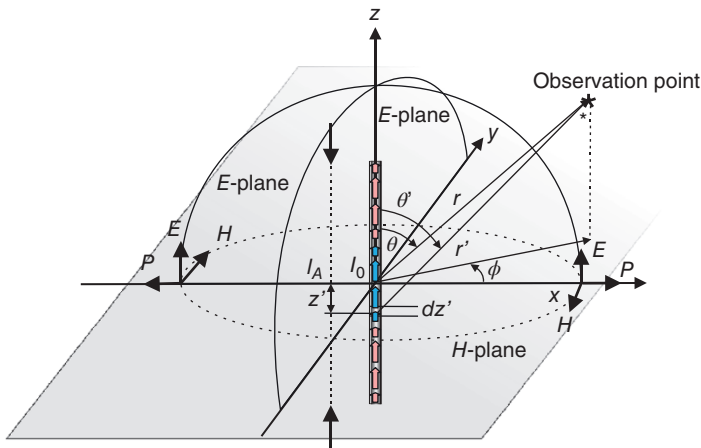


Figure 9.2 Geometry for computing radiation pattern of the long wire antenna.

$$\mathbf{I}(z') = I_0 \exp(-jkz'). \quad (9.3)$$

Substitution of Eq. (9.3) into Eq. (9.2) yields

$$\mathbf{E}_\theta = I_0 \left[\frac{j\eta k \sin \theta \exp(-jk|\vec{r}|)}{4\pi |\vec{r}|} \right] \int_{-l_A/2}^{+l_A/2} \exp(j[k(\cos \theta - 1)]z') dz'. \quad (9.4)$$

Integral Eq. (9.4) is the integral of the cosine function (since sine contribution is equal to zero due to symmetry), which yields

$$\mathbf{E}_\theta = I_0 \left[\frac{j\eta k l_A \sin \theta \exp(-jk|\vec{r}|)}{4\pi |\vec{r}|} \right] \frac{\sin(x)}{x}, x = \frac{kl_A}{2(\cos \theta - 1)}. \quad (9.5)$$

The function $\sin c(x) \equiv \sin \pi x / (\pi x)$ is called the *sinc function*. This function is widely used in signal processing. The time-average power density (Poynting vector magnitude) is given by Eq. (3.34), i.e.

$$P = \frac{1}{2\eta} |\mathbf{E}_\theta|^2 \geq 0. \quad (9.6)$$

This function, normalized by the Poynting vector magnitude of an equivalent isotropic source, gives us the antenna directivity.

When $\theta = 0$ (at zenith), the radiation pattern of the long wire antenna has a null due to the factor of $\sin \theta$ in Eq. (9.5). When θ increases, multiple nulls and lobes will occur.

Example 9.1

The radiation pattern of a long dipole also has multiple nulls and lobes. What is the advantage of the long wire traveling wave antenna?

Solution: First and foremost, the antenna impedance only weakly depends on the frequency (cf. [1]). Second, let us plot the radiation pattern in the E-plane normalized to the maximum directivity according to Eq. (9.5) and (9.6):

```
clear all;
f      = 1e9;          % Frequency
k      = 2*pi*f/3e8;
lA     = 0.9;          % Antenna length
N      = 100;           % Pattern nodes
theta  = linspace(pi/N, pi-pi/N, N);
x      = k*lA/2*(cos(theta) - 1);
U      = (sin(theta).*sin(x)./x).^2;
U      = 100*U/max(U); % The offset should be removed
U(U>1) = 1;
U      = 10*log10(U);
polar(theta, U); grid on;
```

and arrive at Figure 9.3 after eliminating pattern offset (MATLAB polar plots cannot handle negative values), rotating, and mirroring (the effect of ground plane). We can see that the antenna is now becoming more directional. In particular, the maximum directivity of a 3λ long wire antenna is approximately 10 dB [2].

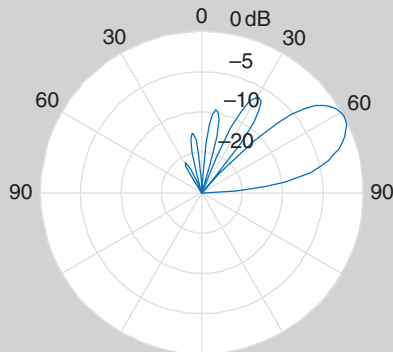


Figure 9.3 Normalized directivity pattern of the long wire (“beverage”) antenna with the length equal to three wavelengths. Obtained from the code of Example 9.1 after eliminating pattern offset (MATLAB polar plots cannot handle negative values), rotating, and mirroring (the effect of ground plane is considered).

9.3 MODELING WITH ANTENNA TOOLBOX

The long wire antenna above a finite metal ground plane, with or without dielectric filling, could be modeled using the *pcbStack* object. The following example describes a way of doing so for a long wire antenna in air. After running this example, we will see quite significant differences as compared to the ideal-case pattern in Figure 9.3. The two chief reasons are likely the effect of a finite ground plane and the deviation of Eq. (9.3) from reality.

Example 9.2

Model a long wire antenna of total length 3λ at 1 GHz and with the height above the ground plane of 10 cm. The radiation pattern is sought. The termination resistance is 250Ω .

Solution: The solution is given by the following MATLAB script:

```
f = 1e9; lambda = physconst('lightspeed')/f;
a = antenna.Rectangle; a.Length = 3*lambda;
a.Width = lambda/50; a.NumPoints = 2;

g = antenna.Rectangle; g.Length = a.Length + lambda;
g.Width = lambda; g.NumPoints = 2;

%% Create the antenna
p = pcbStack;
p.Name = 'Beverage antenna';
p.BoardShape = g;
% Thickness will be equal to the height of the radiating wire
p.BoardThickness = 10e-2;
% First shape is the radiating wire and the second is ground
p.Layers = {a,g};
% Drive this antenna at the end along the negative x-axis
p.FeedLocations = [-a.Length/2 0 1 2];
p.FeedDiameter = a.Width/2;
% Terminate the opposite end of the line into a short
p.ViaLocations = [a.Length/2 0 1 2];
p.ViaDiameter = p.FeedDiameter;
figure; show(p)
%% Load:add terminating resistive load at the non-driven end
loadR = lumpedElement;
loadR.Impedance = 250;
loadR.Location = [a.Length/2,0,0,0];
p.Load = loadR;
%% Mesh the structure
% Choose a 1/10th of lambda to mesh the structure
mesh(p,'MaxEdgeLength',lambda/10);
z = impedance(p, f)
%% Field pattern
```

```

figure; pattern(p, f, 'Type', 'Efield')
%% Directivity pattern
figure; Q = PatternPlotOptions; Q.MagnitudeScale = [-5 10];
AZ = [-180:5:180]; EL = [-90:5:90];
pattern(p, f, AZ, EL, 'patternOptions', Q);

```

Maximum directivity is about 6.3 dB. The antenna's input impedance is obtained using command `impedance(p, f)`; and yields the value of $176-j73 \Omega$.

Variations of the long wire antenna include a *V-antenna* and a *rhombic antenna* [1–3]. All those antennas are indeed electrically large structures, on the order of several wavelengths.

Conceptually similar traveling wave antenna types also include a *corrugated-rod antenna* and a *dielectric-rod antenna* [2].

9.4 YAGI-UDA ANTENNA

One problem with the long wire antenna is the null in the endfire direction (at horizon in Figure 9.3). A Yagi-Uda antenna [1–3] overcomes this difficulty. It uses mutual coupling between standing-wave current elements to produce a traveling wave unidirectional pattern [2]. It usually includes the following elements shown in Figure 9.4:

Reflector (a shorted dipole).

Feed (an ordinary feeding dipole or folded feeding dipole).

Multiple directors – shorted dipoles (#1, 2, 3, 4, etc. They form *the traveling wave path*).

Conducting or non-conducting support (a boom).

The antenna gain of the main beam is determined by the number of directors; such number may reach 10–15 and the corresponding gain value may approach 20 dB. Reflector, feed, and directors all have a length varying around 0.5λ . The spacing along boom axis may vary from 0.20λ to 0.85λ .

Yagi-Uda antennas could be constructed with loops instead of the dipoles [2].

9.5 TRAVELING WAVE FORMATION ALONG YAGI-UDA ANTENNA

Movie clip *Yagi_10dB.mp4* computed in Ansys HFSS and showing the traveling wave formation along a Yagi-Uda antenna is included into supplementary materials to this chapter.

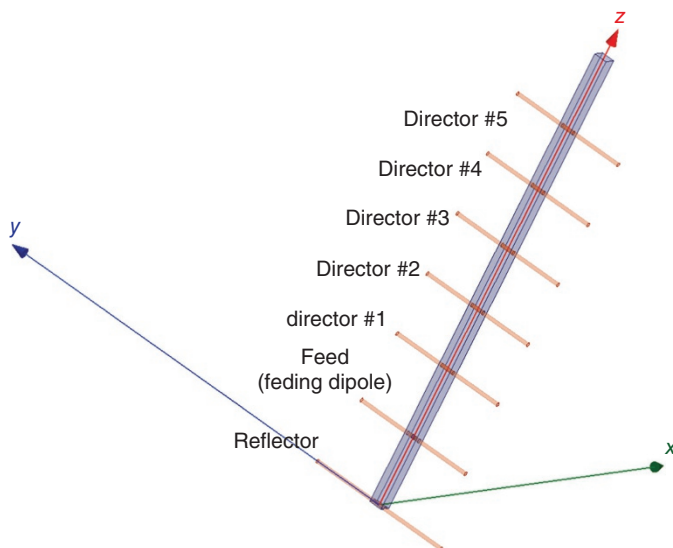


Figure 9.4 Construction of Yagi-Uda antenna.

REFERENCES

1. C. A. Balanis, *Antenna Theory: Analysis and Design*, Wiley, New York, 2016, fourth edition.
2. T. A. Milligan, *Modern Antenna Design*, Wiley, New York, 2005, second edition.
3. R. C. Johnson, Ed., *Antenna Engineering Handbook*, McGraw Hill, New York, 1993, third edition, pp. 43-23–43-27.

PROBLEMS

1. Derive an expression for the radiating E-field of a long wire antenna (similar to Eq. (9.5)) when the phase speed on the line is a constant, but is not the same as in vacuum. Express your result in terms of the dimensionless parameter $K = \lambda_0/\lambda_{\text{line}}$.
2. Compare Eq. (9.5) with the corresponding result of Ref. [1] (Eq. (10.2)). Why are they different?
- 3*. Investigate if the long wire antenna from Example 9.2 could be matched to 50Ω (or to a comparable real impedance) by varying the antenna height in steps of 5 mm and antenna width in steps of 3 mm.
- 4*. In the online examples related to Yagi-Uda antennas:
 - (A) *Radiation Pattern Optimization of a Six-element Yagi-Uda Antenna*

- (B) *Analysis of Biquad Yagi for WIFI Applications*
- (C) *Surrogate-Based Optimization Design of a Six-element Yagi-Uda Antenna*

of the Antenna Toolbox, what is the antenna's input impedance at the design frequency? Give the value for every example and comment on their variations.

SECTION 2 HELICAL AND SPIRAL ANTENNAS

- 9.6. Helical Antenna: Normal Mode of Operation 241**
- 9.7. Helical Antenna: Axial Mode of Operation 242**
- 9.8. Modeling with Antenna Toolbox 243**
- 9.9. Spiral Antenna: Archimedean Spiral 243**
- 9.10. Modeling with Antenna Toolbox 245**
- 9.11. Principle of Operation 245**
- 9.12. Equiangular Spiral Antenna 246**
- References 247**
- Problems 247**

9.6 HELICAL ANTENNA: NORMAL MODE OF OPERATION

In the *normal model of operation* (or T_0 mode [1, 2]), a helical antenna shown in Figure 9.5a is usually small compared to the wavelength. It is *not* the traveling wave antenna, but rather a combination of small dipole elements S and loop elements D as shown in Figure 9.5b. This combination radiates at broadside, like the standard dipole or a loop [1–3].

When the overall length of the helix is small compared to the wavelength, the current distribution for dipoles/loops is nearly uniform. The far-field of the small dipole of length S with constant-current I_0 follows Eq. (9.1) at $z' = 0$,



Figure 9.5 (a) Small helical antenna connected to a passive RFID tag at 433 MHz (antenna height is about 3 cm). *Source:* Design by Dr. S. Sabah and the authors; (b) approximation of the small helix by several small dipoles/loops. *Source:* Antenna design by the authors.

$$\mathbf{E}_\theta = j\eta k I_0 S \frac{\exp(-jk|\vec{r}|)}{4\pi|\vec{r}|} \sin\theta. \quad (9.7)$$

The far-field of the constant-current small loop of diameter D follows from Eq. (6.2b) in the form:

$$\mathbf{E}_\phi = \pi\eta(kD/2)^2 I_0 \frac{\exp(-jk|\vec{r}|)}{4\pi|\vec{r}|} \sin\theta. \quad (9.8)$$

The two components are in quadrature, which is an indication of the possible *circular polarization*. We introduce the ratio

$$R = \frac{|\mathbf{E}_\theta|}{|\mathbf{E}_\phi|} = \frac{4S}{\pi k D^2}, \quad \mathbf{E}_\phi = -j\frac{1}{R}\mathbf{E}_\theta \quad (9.9)$$

and the *right-handed circular polarization* (RHCP) and *left-handed circular polarization* (LHCP) polarization components $\mathbf{E}_R, \mathbf{E}_L$ in the form (for the detailed discussion, please see Chapter 10):

$$\begin{aligned} \mathbf{E}_R &\equiv \frac{1}{\sqrt{2}}(\mathbf{E}_\theta + j\mathbf{E}_\phi) = \frac{1}{\sqrt{2}}\mathbf{E}_\theta \left(1 + \frac{1}{R}\right) \\ \mathbf{E}_L &\equiv \frac{1}{\sqrt{2}}(\mathbf{E}_\theta - j\mathbf{E}_\phi) = \frac{1}{\sqrt{2}}\mathbf{E}_\theta \left(1 - \frac{1}{R}\right). \end{aligned} \quad (9.10)$$

Furthermore, the *axial ratio* is defined in the form:

$$\text{axial ratio} = \frac{|\mathbf{E}_R| - |\mathbf{E}_L|}{|\mathbf{E}_R| + |\mathbf{E}_L|} = \frac{2\frac{1}{R}}{2} = \frac{1}{R}. \quad (9.11)$$

When $R = 1$, we obtain the sole RHCP precisely, with the axial ratio being equal to one. However, such an antenna may be quite *narrow* in the bandwidth.

9.7 HELICAL ANTENNA: AXIAL MODE OF OPERATION

In this mode (or T_1 mode [2]), the helix radiates a circularly polarized endfire pattern on its axis. This is the true traveling wave antenna. The circumference of the helical antenna should be about one wavelength and the spacing, S , about quarter wavelength [1]. In low-gain applications, the antenna works over a 1.7 : 1 bandwidth which decreases as gain increases [2]. The terminal impedance of the helix is nearly resistive with the values between 100 and 200 Ω .

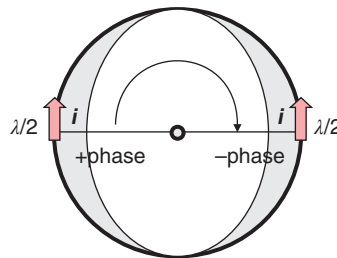


Figure 9.6 Illustration of circularly polarized or rotating current (and field) distribution for an idealized full turn of the helical antenna with circumference equal to one wavelength.

The pattern of the helical antenna is obtained analytically as a summation of the single-turn (but not just the loop!) contributions for each consecutive turn with the corresponding spatial phase correction, similar to an *antenna array*.

The single-turn helical antenna already creates circular polarization as illustrated in Figure 9.6, due to the nature of the traveling wave. Addition of more turns does not improve the polarization ratio of the main beam any further, but it decreases the beam width (increases the gain of the main beam) and increases the front-to-back ratio [2].

9.8 MODELING WITH ANTENNA TOOLBOX

Antenna Toolbox has a special function to create a helical antenna with a ground plane, that is

```
hx = helix('Radius',radius,'Width',width,'Turns',turns,...  
'Spacing',spacing,'GroundPlaneRadius',radiusGP);
```

Further simulations are done similar to the other antenna types.

9.9 SPIRAL ANTENNA: ARCHIMEDEAN SPIRAL

Spiral antennas consist of a thin metal foil spiral pattern etched on a substrate, usually fed from the center, and usually located over a cavity. The etching contains a symmetric pattern of at least two arms. The two-arm spiral-antenna version can be fed using a simple balanced line requiring a balun.

An *Archimedean spiral* antenna in polar coordinates (r, θ) can be described by the equation

$$r = a + b\theta^{1/x} \quad (9.12)$$

with some real numbers a and b . The normal Archimedean spiral occurs when $x = 1$. Changing the parameter a will widen the spiral, while b controls the distance between successive turns. The normal Archimedean spiral is distinguished from the *logarithmic spiral* by the fact that successive turns of the spiral have a constant separation distance (equal to $2\pi b$), while in a logarithmic spiral these distances form a geometric progression. Note that the Archimedean spiral has two arms; one for $\theta > 0$ and one for $\theta < 0$. The two arms are smoothly connected at the origin.

Example 9.3

Create an Archimedean spiral antenna structure using MATLAB.

Solution: The solution is given by the following MATLAB script. This script, for a given spiral, outputs the discrete 2D curve points (arranged in a two-column array) into two text files, one for each arm of the spiral. This format is appropriate for export to other CEM software packages.

```
clear all
N      = 3;          % Number of full turns
step   = pi/12;       % Discretization step
b      = 1;           %  $2\pi b^{(1/n)}$  - separation between turns
a      = b*step/(1-cos(step)); % Offset from center in mm
n      = 1;           % Power

theta  = [0:step:2*pi*N];
r      = a + b*theta.^^(1/n);
x      = r.*cos(theta);
y      = r.*sin(theta);

theta  = theta + pi;
r1     = a + b*theta.^^(1/n);
x1    = r.*cos(theta);
y1    = r.*sin(theta);

plot(x,    y, 'b', 'LineWidth', 2); grid on; hold on;
plot(x1,  y1, 'r', 'LineWidth', 2); grid on; hold on;
axis('equal'); title('Units - mm')
z = [x' y'];
save('spiral1.txt','z','-ASCII');
z = [x1' y1'];
save('spiral2.txt','z','-ASCII');
```

9.10 MODELING WITH ANTENNA TOOLBOX

Antenna Toolbox has a special function to create an Archimedean spiral antenna with or without cavity backing, that is

```
sa = spiralArchimedean('Turns',5, 'InnerRadius',1e-3, 'OuterRadius',40e-3); show(sa)
```

The above line of the code generates the spiral shown in Figure 9.7. The width of the spiral wings is equal to spacing between them.

9.11 PRINCIPLE OF OPERATION

The simple geometry of the Archimedean spiral antenna affords an opportunity to explain an important mechanism in many frequency-independent antennas. This is the *band description of radiation* that is characterized by an *active antenna region* responsible for radiation [4]. The description will be done in several steps.

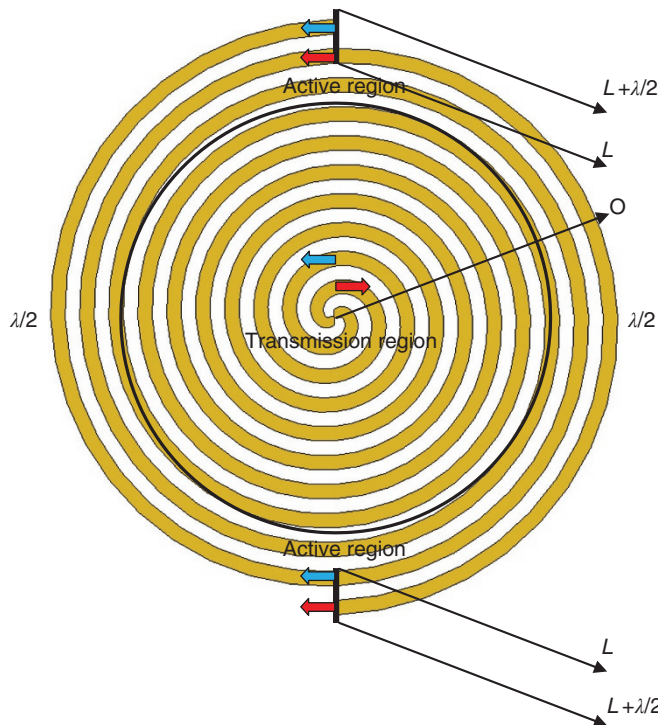


Figure 9.7 Geometry of a two-arm Archimedean spiral antenna and the band radiation concept.

1. Between the feed point and the active region in Figure 9.7, there is a *transmission region*. The currents on two arms are canceling each other (so are the radiated fields). Therefore, there is little radiation from this region. The traveling wave propagates without essential radiation.
2. The active region occurs on that portion of the antenna that is *one length in circumference*. The currents (two red arrows or two blue arrows) in the same arm on top and bottom of Figure 9.7 will be *in phase* since the travel distance is now $\lambda/2$ (the phase shift of 180°). This effect is very similar to that in Figure 9.6 for the helical antenna.
3. Moreover, in the active region, the currents on two distinct spiral arms will be *also in phase* since the travel distances (lengths) for the feed will differ by exactly $\lambda/2$ (the phase shift of 180°).
4. Thus, we have coincident current phases everywhere in the active region so that the entire region radiates a circularly polarized wave similar to Figure 9.6.
5. Beyond the active region, currents are small, having lost power to radiation in the active region. The antenna effectively behaves as if it is infinite in extent. Often, resistive loads are added to the ends of the spiral to prevent reflection of the remaining traveling waves.
6. Of course, the active region moves away from the antenna center with changing (decreasing) frequency. Therefore, the spiral antennas may inherently have a very large bandwidth. However, the input impedance is on the order of $100\text{--}200 \Omega$.
7. A cavity-backed spiral antenna is normally used; cavity backing constitutes a significant design problem.

9.12 EQUIANGULAR SPIRAL ANTENNA

An equiangular spiral antenna is modeled in Antenna Toolbox using the function

```
se = spiralEquiangular('GrowthRate', 0.35, 'InnerRadius', 0.65e-3, ...
'OuterRadius', 40e-3); show(se)
```

It could have a smaller number of turns than the Archimedean spiral antenna. The input impedance is again on the order of $100\text{--}200 \Omega$. The radiation patterns for both antenna types are similar. Spiral antennas and other frequency-independent antennas are thoroughly studied and described in detail in Ref. [5].

Some useful facts about the spiral antennas are:

1. Spiral antennas are inherently broadband radiators ($5:1$ or even $10:1$ impedance bandwidth is common). Bandwidth is determined by
 - (a) *At low frequencies – by the overall spiral size* [5]. The spiral size is about 0.4λ at the lowest band frequency. This value approximates the size of an-air filled patch antenna radiating at the same frequency or the size of a straight dipole.
 - (b) *At high frequencies – by the fine precision of the feeding region* [5].
2. Spiral antennas are inherently circularly polarized radiators, with a relatively constant pattern over a wide frequency range. To create two independent orthogonal polarizations, a four-arm spiral may be used [5].
3. The minimum number of arms needed for single-mode broadband operation is two [5].
4. The feeding techniques include the standard baluns (such as Marchand, Dyson, etc.), including the printed baluns [5].
5. A planar spiral antenna radiates bidirectionally. For unidirectional radiation, cavity-backing needs to be used (with or without an absorber), with the depth of the cavity being equal to a significant fraction of wavelength [5]. The large size of the cavity does not usually allow us to build a compact planar unidirectional spiral antenna.

REFERENCES

1. C. A. Balanis, *Antenna Theory: Analysis and Design*, Wiley, New York, 2016, fourth edition.
2. T. A. Milligan, *Modern Antenna Design*, Wiley, New York, 2005, second edition.
3. R. C. Johnson, Ed., *Antenna Engineering Handbook*, McGraw Hill, New York, 1993, third edition, pp. 43-23–43-27.
4. W. L. Stutzman and G. A. Thiele, *Antenna Theory and Design*, Wiley, New York, 2012, third edition.
5. D. S. Filipovic and T. T. Cencich, “Frequency-independent Antennas,” In *Antenna Engineering Handbook*, J. L. Volakis, Ed., McGraw Hill, New York, 2007, fourth edition, pp. 13-1–13-67.

PROBLEMS

- 1***. In the online example, *Helical Antenna Design* of the Antenna Toolbox, establish the axial ratio of the helical antenna in the main beam (at zenith) at 1.6 GHz.

- 2*.** Create a helical antenna with the following specifications for operation at 1.65 GHz. Use the `helix` element from Antenna Toolbox™.

Conductor radius = 0.3 mm

Helix diameter = 56 mm

Number of turns = 17.5

Pitch = 11.2°.

Diameter of ground-plane = 600 mm

Do the following:

- Create the helix and display the geometry.
- Calculate the directivity pattern at 1.65 GHz.
- Write a program to calculate the peak directivity of this helix as a function of frequency. Choose a frequency range that spans from 1.2 to 2.1 GHz with a frequency step of 0.1 GHz.
- What kind of polarization does this antenna have?
- Is this statement correct? “This antenna operates in the normal mode.” Justify your answer.

- 3*.** Using the Antenna Toolbox, create an Archimedean spiral with the following parameters:

Outer radius = 50 mm

Inner radius = 5.5 mm

Number of turns = 4

Do the following:

- Based on the dimensions, it is possible to determine the frequency range over which to calculate the impedance so that you can capture the resonances typical to such structures at the lower frequency (f_{\min}) and the stable impedance behavior at higher frequencies (f_{\max}). Use any resource necessary (e.g. [5]) to find analytical expressions that will help you in your efforts.
- Test out your result from (a) for the f_{\min} and f_{\max} by computing the impedance of the spiral. Choose a sufficiently fine discretization so that impedance variations are captured accurately.
- Assuming a matched condition based on the real part of the impedance being stable, compute the reflection coefficient and the bandwidth estimate for this antenna.
- Determine at the lowest, highest, and the middle of the frequency band the radiation pattern of this antenna.
- Is the axial ratio better at the lower frequencies as compared to the higher frequencies? Provide your arguments regarding the axial ratio result.

- 4***. Create an equiangular spiral by using the Antenna Toolbox. Use the following geometry parameters:

Inner Radius = 1.97 mm

Outer Radius = 5.68 mm

Growth Rate = 0.3

Do the following:

- (a) Plot the impedance of this antenna over the frequency band 3–10 GHz.
- (b) Assuming a matched condition, what is the impedance bandwidth of this antenna?
- (c) How would you classify this antenna in terms of the bandwidth: narrowband, wideband, ultra-wideband?
- (d) Provide a backing to this antenna in the form of an infinite ground plane. Create a separate antenna for this problem. Recalculate the impedance over the same frequency band specified in (a). Explain the difference when compared to (a). Also, recalculate the impedance bandwidth for this case.
- (e) Compute the axial ratio for both spirals, with and without the reflector, over the frequency band 3–10 GHz at boresight.

CHAPTER 10



Antenna Designer Including Circularly Polarized Antennas

SECTION 1 FAST ANALYSIS AND DESIGN OF INDIVIDUAL ANTENNAS

10.1. Antenna Designer	251
10.2. Using Pre-optimized Antenna Geometry	252
10.3. Performing Geometry Optimization on the Fly	252
10.4. Design Example	256
10.5. Antenna Preselection for a Given Task	257
Reference	258
Problems	258

10.1 ANTENNA DESIGNER

The Antenna Designer app [1] lets us design, visualize, and analyze basic antenna types in the MATLAB Antenna Toolbox library interactively. Using this app, we can:

Antenna and EM Modeling with MATLAB® Antenna Toolbox, Second Edition. Sergey N. Makarov, Vishwanath Iyer, Shashank Kulkarni, and Steven R. Best.

© 2021 John Wiley & Sons, Inc. Published 2021 by John Wiley & Sons, Inc.

Companion website: www.wiley.com/go/Makarov/AntennaandEMModelingwithMATLAB2e

- Select antennas based on general properties or antenna performance.
- Visualize antennas based on frequency and frequency range.
- Analyze antennas based on radiation pattern, polarization, and bandwidth.
- Change antenna parameters.
- Add cavity backing, or reflector backing to the antennas.
- Export selected and designed antennas as variables to MATLAB workspace, and export a script with the commands.

10.2 USING PRE-OPTIMIZED ANTENNA GEOMETRY

To open the Antenna Designer app, in the Apps tab, under Signal Processing and Communications, click the app icon as shown in Figure 10.1. Alternatively, you may run the Antenna Designer using command

```
>>antennaDesigner
```

directly from the Command Window. Click “New” in the canvas toolbar to choose the antenna you want to analyze. The corresponding menu is shown in Figure 10.2. This menu currently (2020) features approximately 60 different antennas grouped by various families such as the patch, monopole, dipole, etc., and continues to grow. As an example, let us choose a PIFA antenna from the “patch” family. Select the design frequency as 915 MHz and press the “Accept” button. You will obtain antenna dimensions *pre-optimized* for the given center frequency.

Using buttons:

- Impedance
- S Parameter
- Current (on the antenna surface)
- 3D Pattern
- AZ/EL Pattern

one could analyze both terminal and radiation antenna parameters in a matter of seconds.

10.3 PERFORMING GEOMETRY OPTIMIZATION ON THE FLY

As an example, run the default antenna setup for the PIFA antenna at 915 MHz. Compute impedance, S-parameter data, and a 3D pattern. *Tile* the resulting analysis figure windows in the app as shown in Figure 10.3. This layout allows you to see all four plots (antenna geometry, impedance, S-parameter, and the radiation pattern) simultaneously. Change the default value of the feed offset from -5 to -8 mm in

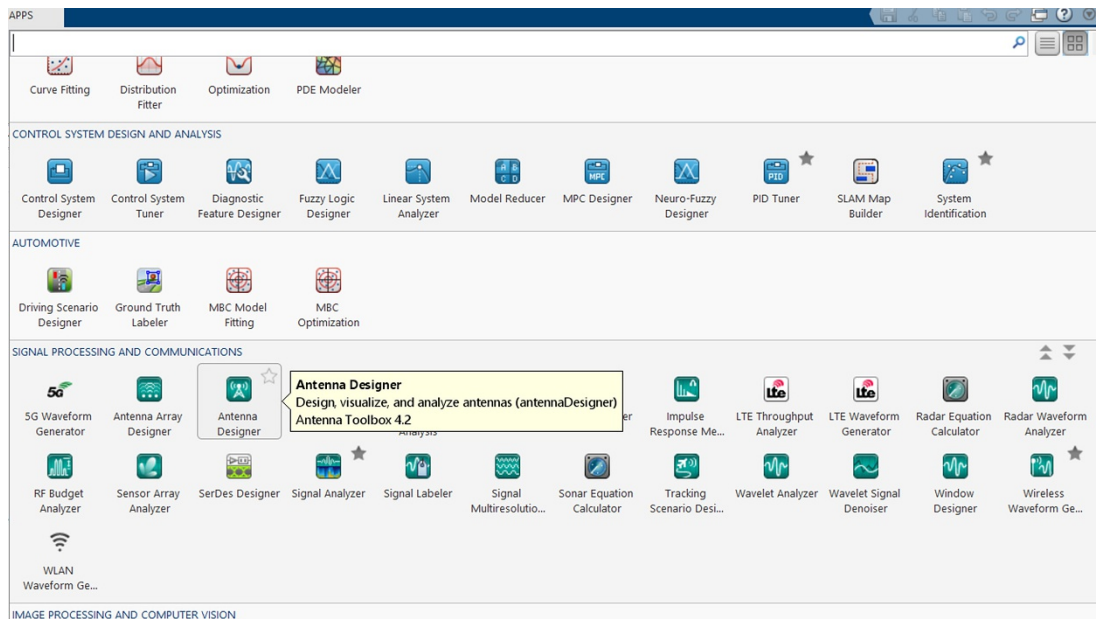


Figure 10.1 Opening Antenna Designer app in MATLAB 2020a. *Source:* The MathWorks, Inc.

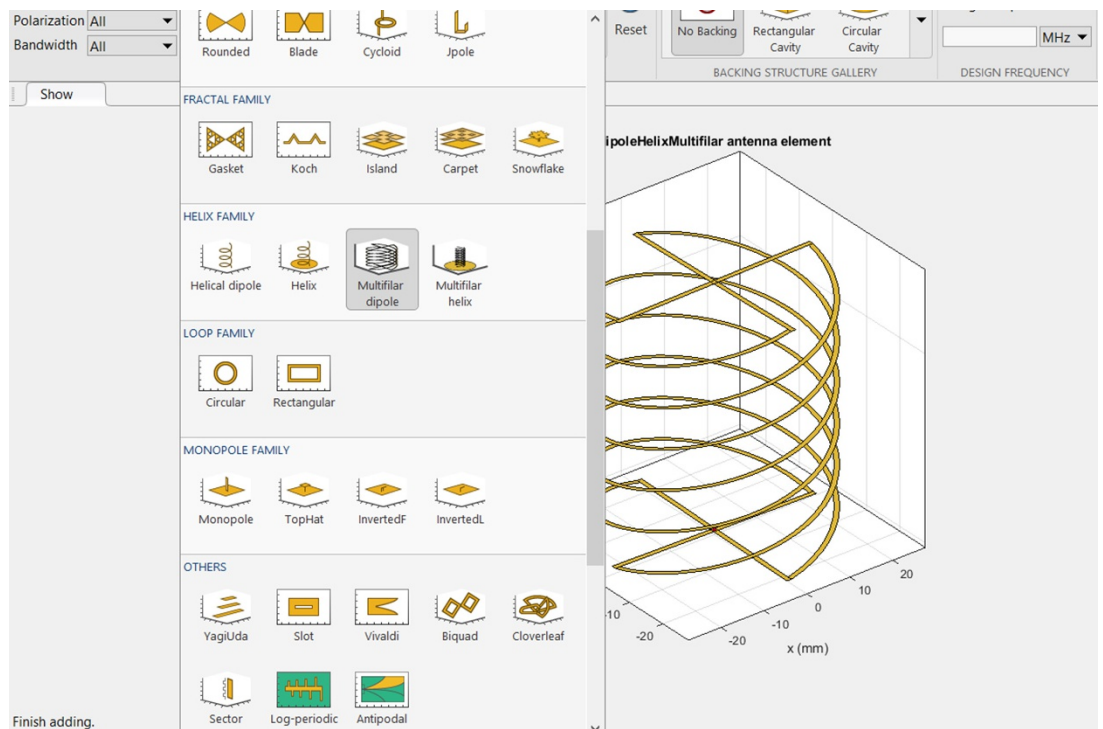


Figure 10.2 Set of available antenna topologies in MATLAB 2020a. *Source:* The MathWorks, Inc.

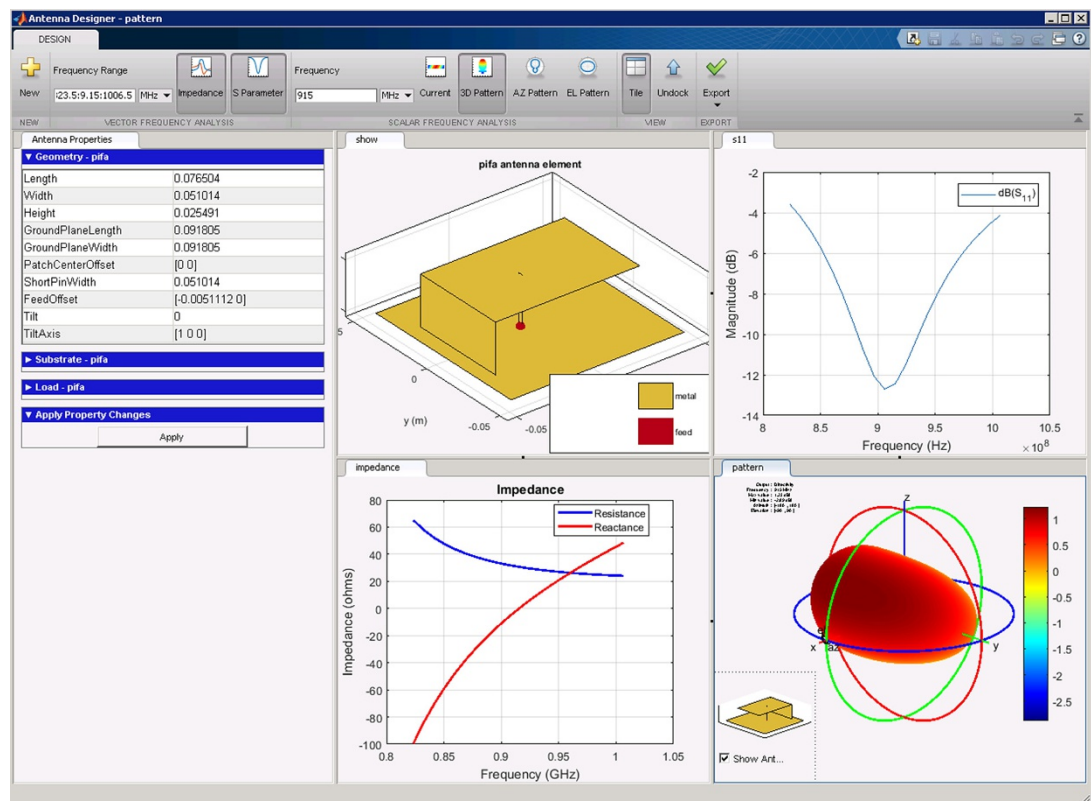


Figure 10.3 Geometry and simulation data for the PIFA radiator. *Source:* The MathWorks, Inc.

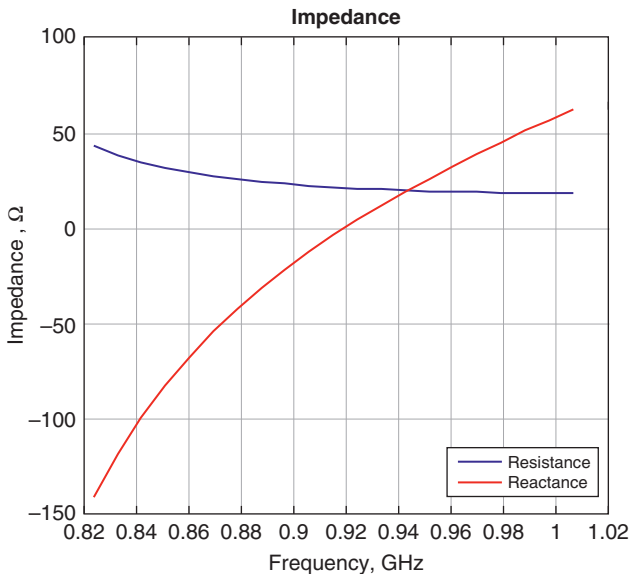


Figure 10.4 Input impedance for the default inverted-F antenna configuration at 915 MHz.

the *Antenna Properties* section. The “Apply” button is used to push the changes into the geometry. Observe how the antenna’s center frequency changes due to changes in the feed position. By changing the feed position, we could tune the antenna resonance. The analysis selections are enabled and therefore all plots get updated as soon as a change is made to the geometry.

10.4 DESIGN EXAMPLE

We will now analyze the PIFA in the Antenna Designer as an example, at the center frequency of 915 MHz. The default pre-optimized antenna geometry yields impedance data shown in Figure 10.4. Although the antenna is resonant close to its center frequency, its radiation resistance only approaches approximately $20\ \Omega$.

Example 10.1

Investigate matching the inverted-F antenna with the input impedance shown in Figure 10.4 to a $15\ \Omega$ generator.

Solution: We could now obtain the impedance data in the MATLAB workspace by running the command

```
f=823.5e6:9.15e6:1006.5e6;
Z= impedance(invertedF_antennaDesigner, f)
```

directly in the command window where variable f is the frequency array copied and pasted from the app and multiplied by 10^6 . Further, we form the reflection coefficient for a $15\ \Omega$ generator in the form

```
S11 = (Z-15)./(Z+15); S11dB = 20*log10(abs(S11)); plot(f, S11dB)
```

and obtain an impedance bandwidth of approximately 3%.

10.5 ANTENNA PRESELECTION FOR A GIVEN TASK

The Antenna Designer app also has another mode of operation; one which allows you to narrow down the antenna possibilities based on some simple input parameters. As an example, open the Antenna Designer app and choose the following design parameters:

- Radiation: All
- Polarization: Circular
- Bandwidth: Octave (or 2 : 1 bandwidth).

The result of this search shown in Figure 10.5 will lead us to three potential candidates, which may satisfy all three requirements:

- Archimedean spiral antenna
- Equiangular spiral antenna
- Rectangular spiral antenna



Figure 10.5 Three antenna candidates for the selected antenna task. *Source:* The MathWorks, Inc.

REFERENCE

1. Antenna Designer. Online: <https://www.mathworks.com/help/antenna/ref/antennadesigner-app.html>

PROBLEMS

- 1*. Perform antenna design for a default PIFA antenna with and without the cavity backing at 915 MHz. How does the antenna bandwidth change?
- 2*. Perform antenna design for a default PIFA antenna at 915 MHz matched to $35\ \Omega$. How does the antenna bandwidth change?
- 3*. Design a PIFA antenna at 433 MHz matched to $50\ \Omega$. Present antenna dimensions. Report the impedance bandwidth and the 3D radiation pattern.
- 4*. Please report any flaw (or your improvement suggestion) for the Antenna Designer interface that you have encountered so far by contacting MathWorks Technical Support (filling out an online form).

SECTION 2 MEANING OF CIRCULAR POLARIZATION AND PROPER ANTENNA ORIENTATION

- 10.6. Antenna Phase Shift or Delay 259**
- 10.7. Circularly Polarized RX/TX Antennas and Their Required Orientations in Space 259**
- 10.8. Separation of Radiated Field Into Two Circular Polarization Components 262**
- 10.9. Quantitative Measures of Circular Polarization 264**
- 10.10. Circularly Polarized Turnstile Antenna 266**
- 10.11. Circularly Polarized Patch Antenna 266**
- References 267**
- Problems 268**

10.6 ANTENNA PHASE SHIFT OR DELAY

One useful tool for understanding a *circularly polarized transmit/receive antenna pair* operation is an analog phase shifter that is shown schematically in Figure 10.6. Such phase shifter (a transmission line of length $\lambda/4$ in the simple case) always adds a phase shift of $-\pi/2$ to the incoming signal, no matter what direction does the signal go, in a transmit or in the receive mode. We also assume wave propagation in the form $\cos(\omega t - ky)$ from input at $y = 0$ to output at $y = \lambda/4$. One can see that the transmit/receive operations of an antenna with the phase shifter shown in Figure 10.6 are antisymmetric, i.e. one has signal from generator = $\cos \omega t$ → signal transmitted by antenna = $\cos(\omega t - \pi/2) = \sin \omega t$ signal received by antenna = $\sin \omega t$ → signal to receiver = $\sin(\omega t - \pi/2) = -\cos \omega t$.

10.7 CIRCULARLY POLARIZED RX/TX ANTENNAS AND THEIR REQUIRED ORIENTATIONS IN SPACE

The next step is to consider operation of a *right-handed circularly polarized (RHCP)* antenna schematically shown in Figure 10.7. Let us assume that, in the transmit mode, the input current (signal) $I = 2 \cos \omega t$ is equally split between two orthogonal dipoles (or other linearly-polarized antennas) in the xy -plane, called TX and TY. The y -oriented dipole (TY) has a $-\pi/2$ phase shift. The x -oriented dipole (TX) has no phase shift.

The radiated electric field for either dipole is proportional to the current. This yields for the radiated field,

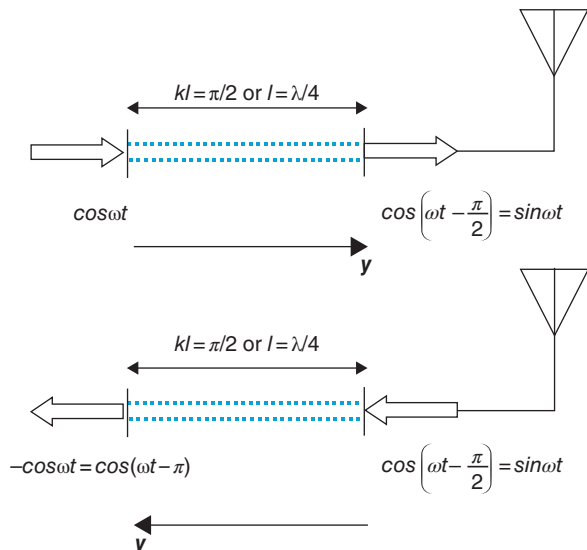


Figure 10.6 Asymmetry of the phase shifting operation in the TX/RX mode at the same time instant.

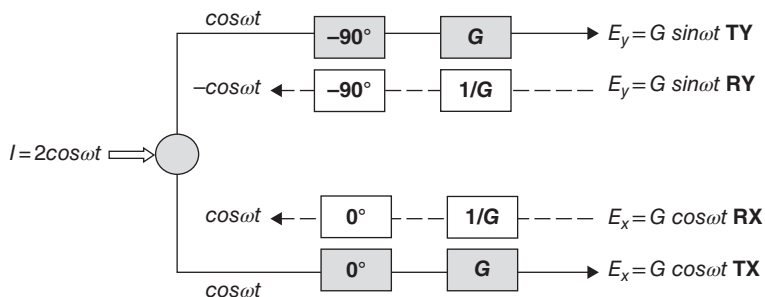


Figure 10.7 Operation of the RHCP antenna.

$$\vec{E} = [E_x, E_y] = G \times [\cos \omega t, \sin \omega t] \quad (10.1)$$

since $\cos(\omega t - \pi/2) = \sin \omega t$. Here, G is a constant. Eq. (10.1) predicts a clockwise rotation of the electric field around a circle in the xy -plane when looking into the positive z -direction – the propagation direction. This is a definition of the RHCP signal.

Example 9.2

Visualize circular polarization in MATLAB.

Solution: The following MATLAB script illustrates the rotation of the electric field for the right-handed circular polarization:

```
clear all;
T      = 0.1;
f      = 1/T;
t      = 0:1e-3+1e-6:2*T;
omega  = 2*pi*f;
E1    = 1;
a = figure; hold on; grid on;
axis([- 2 2 - 2 2]); axis equal;
xlabel('X-AXIS'); ylabel('Y-AXIS');
title('Z-axis is directed out of the screen; right-handed...
Cartesian system')
for m = 1:length(t)
    Ex = E1*cos(omega*t(m));
    Ey = E1*cos(omega*t(m) - pi/2);
    X = [0 Ex]; Y = [0 Ey];
    plot(Ex, Ey, 'o', 'MarkerSize', 25, 'MarkerEdgeColor', 'g',...
'MarkerFaceColor', 'm')
    line(X, Y, 'Color', 'y', 'LineWidth', 4);
    drawnow
    pause(0.05);
end
```

However, if we consider the receiving mode and feed exactly the same signal (10.1) back to the same RHCP antenna, we will finally obtain the *zero* total received current, due to the accumulating phase shift. Such an operation is shown in Figure 10.7 by dashed lines. This result does not change when a constant phase shift is added to both E -field components, due to a finite propagation distance. In other words, two identically oriented RHCP antennas shown in Figure 10.8-II will not generate any power transmission, if one of them is working as a transmitter and another – as a receiver.

On the other hand, two RHCP antennas facing each other as shown in Figure 10.8-II, will have zero polarization loss factor (full transmitted power) due to the fact that the direction of the y-oriented dipole is opposite and one more minus sign is added. It means that $E_y = -G \sin \omega t$ in Figure 10.7 in the receiving mode.

Two other cases shown in Figure 10.8, which include the *LHCP antennas* (counterclockwise rotation of the E-field when looking into the positive z -direction), are treated in the same way.

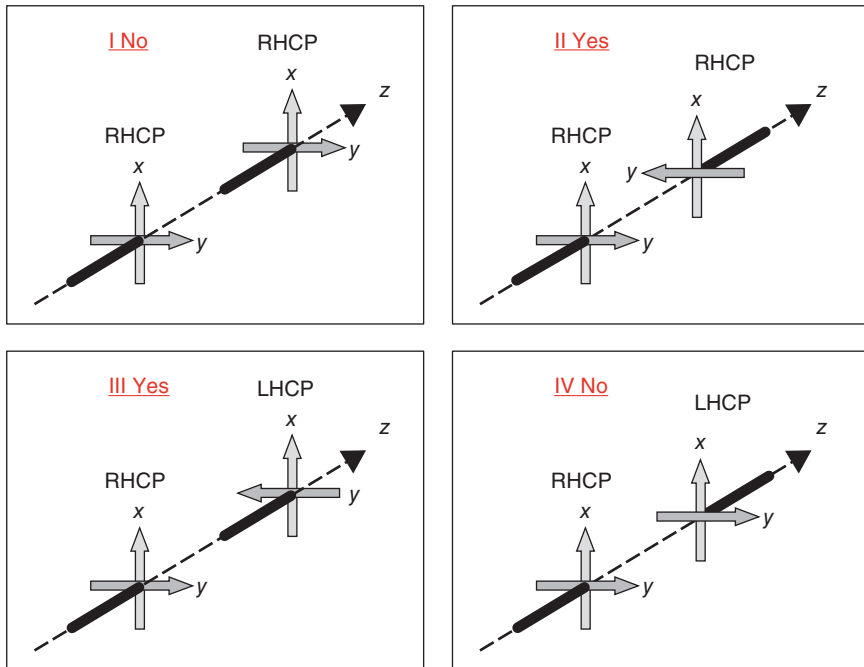


Figure 10.8 RHCP/LHCP antenna orientations and the corresponding transmission conditions. Antenna handle is shown.

10.8 SEPARATION OF RADIATED FIELD INTO TWO CIRCULAR POLARIZATION COMPONENTS [1-3]

We handle all polarization problems by using vector operations in a local *two-dimensional* plane (*x* and *y*) using the far-field radial vector as the normal vector to the plane. The spherical wave in the far field has only θ and φ components, i.e.

$$\vec{E} = E_\theta \hat{\theta} + E_\phi \hat{\phi}. \quad (10.2)$$

Given a local Cartesian *xyz*-coordinate system associated with an observation point in the far field shown in Figure 10.9, we arrive at

$$\hat{\theta} = \hat{x}, \hat{\phi} = \hat{y}, E_\theta = E_x, E_\phi = E_y \quad (10.3)$$

and

$$\vec{E} = E_x \hat{x} + E_y \hat{y}. \quad (10.4)$$

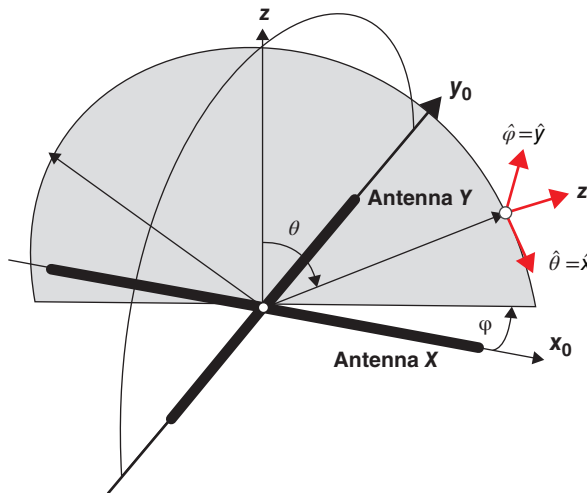


Figure 10.9 Local coordinate system for explaining circular polarization.

According to Eq. (10.1), in order to achieve the “perfect” RHCP, we should assume

$$E_x(t) = E_0 \cos \omega t, \quad E_y(t) = E_0 \sin \omega t = E_0 \cos(\omega t - \pi/2) \quad (10.5)$$

or in the phasor form,

$$\mathbf{E}_x = E_0, \quad \mathbf{E}_y = E_0 \exp(-j\pi/2) = -jE_0. \quad (10.6)$$

The phasor vector electric field therefore becomes

$$\vec{\mathbf{E}} = \mathbf{E}_x \hat{x} + \mathbf{E}_y \hat{y} = E_0 \hat{x} - jE_0 \hat{y} = E_0 \vec{\mathbf{R}}, \quad \vec{\mathbf{R}} = \hat{x} - j\hat{y}. \quad (10.7)$$

Similarly, in order to achieve the “perfect” LHCP, we should assume

$$\vec{\mathbf{E}} = E_0 \vec{\mathbf{L}}, \quad \vec{\mathbf{L}} = \hat{x} + j\hat{y}, \quad (10.8)$$

where $\vec{\mathbf{R}}$ and $\vec{\mathbf{L}}$ are two *orthogonal* ($\vec{\mathbf{R}} \cdot \vec{\mathbf{L}}^* = 0$) *polarization vectors*. These vectors are not yet normalized. In order to do so, we should choose

$$\vec{\mathbf{R}} = \frac{1}{\sqrt{2}}(\hat{x} - j\hat{y}) \Rightarrow \vec{\mathbf{R}} \cdot \vec{\mathbf{R}}^* = 1, \quad \vec{\mathbf{L}} = \frac{1}{\sqrt{2}}(\hat{x} + j\hat{y}) \Rightarrow \vec{\mathbf{L}} \cdot \vec{\mathbf{L}}^* = 1. \quad (10.9)$$

The entire E-field at the observation point is thus expressed as a sum of two orthogonal polarization components,

$$\vec{E} = \vec{E}_R \vec{R} + \vec{E}_L \vec{L}, \quad (10.10)$$

where

$$\vec{E}_R = \vec{E} \cdot \vec{R}^*, \quad \vec{E}_L = \vec{E} \cdot \vec{L}^*. \quad (10.11)$$

Complex scalars E_R and E_L determine the “amount” of every polarization (RHCP and LHCP) in the total radiated field. Returning back to the spherical coordinates and using Eq. (10.3), we finally obtain

$$E_R = \frac{1}{\sqrt{2}} (E_\theta + jE_\phi), \quad E_L = \frac{1}{\sqrt{2}} (E_\theta - jE_\phi). \quad (10.12)$$

Thus, if we know both complex far-field components, E_θ, E_ϕ , then the circular polarization content and amount can be uniquely established.

10.9 QUANTITATIVE MEASURES OF CIRCULAR POLARIZATION

We introduce *axial ratio* for circular polarization in the form:

$$\text{axial ratio} = \frac{|E_R| - |E_L|}{|E_R| + |E_L|}, \quad \text{axial ratio}_{dB} = 20 \log_{10} \frac{|E_R| - |E_L|}{|E_R| + |E_L|}. \quad (10.13)$$

For the ideal RHCP, the axial ratio is 1 or 0 dB; for a linearly polarized plane wave, the axial ratio tends to 0 or to $-\infty$ dB. Thus, the axial ratio behaves similar to the reflection coefficient for the antenna. Therefore, we could also define *polarization bandwidth* as a band of frequencies where the axial ratio in the direction(s) of interest goes below a certain value, say below -6 dB.

Often, a complex *circular polarization ratio* is also considered in the form:

$$\rho_C = \frac{E_L}{E_R}. \quad (10.14)$$

When the LHCP is sought instead of the RHCP, all indexes in Eq. (10.13) and (10.14) should be interchanged. Some examples of circularly or *dual-polarized* (two independent polarizations) antennas are shown in Figure 10.10 that follows.

Why do we need the circular polarization? The answer is a great immunity against noise. For example, the RHCP wave will be reflected from a metal surface as an LHCP wave so that the reflected signal will not be received by an anticipated RHCP RX antenna.



Figure 10.10 Examples of circularly polarized antennas (turnstile dipoles). Top row – bowtie turnstile; second row – dipole turnstile with an on-antenna phase shifter; third row – bowtie turnstile with a corrugated ground plane; last row – asymmetric wideband variations. *Source:* Design by the authors.

10.10 CIRCULARLY POLARIZED TURNSTILE ANTENNA

The *crossed-dipole antenna* or the *turnstile antenna* invented in 1936 by G. H. Brown [4] is a valuable tool to create a circularly polarized pattern (RHCP or LHCP). Since the invention much efforts have been made to design efficient built-in phase shifting networks [5–9], achieve a wider impedance bandwidth [7], nearly hemispherical coverage with droopy dipoles [10–15], and a good axial-ratio bandwidth [7, 9, 16].

The turnstile antenna has either an external quadrature hybrid as a 90° power divider/combiner [7, 16] or an internal built-in phase shifting network [7]. The latter is briefly described below. The internal network may be based on

- (i) a narrowband $\lambda/4$ transmission line connecting two dipoles in parallel [7];
- (ii) the use of two electrically different dipoles with complex conjugate impedances connected by a very short transmission line [5–7];
- (iii) the use of another transmission line section by partially folding one dipole [8] (cf. also the second row of Figure 10.10);
- (iv) the use of a turnstile *waveguide* network [9].

A popular internal network seems to be a combination of two electrically non-equal dipoles, either due to a different load [5, 6] or due to a different geometrical length [7]. A figure of merit is 41.5% impedance bandwidth and a 16.4% 6-dB axial-ratio bandwidth reported by T. A. Milligan [7] for this particular combination. On the other hand, R. K. Zimmerman [9] reports an approximately 15% wide impedance bandwidth and a 28% 6-dB axial-ratio bandwidth for the turnstile-type feeding network that also incorporates a balun.

The use of a partially folded dipole is less common and was reported in only one reference [8], where a 6-dB axial-ratio bandwidth in excess of 16% has been found. The most common balun type used for the turnstile antenna is perhaps a split-coaxial balun [7, 10]; cf. also [17, 18].

10.11 CIRCULARLY POLARIZED PATCH ANTENNA

A two-feed design for a circularly polarized patch antenna is shown in Figure 10.11. Both feeding signals should be in quadrature (a 90° phase shift). Other designs are possible, which excite two resonant orthogonal microstrip modes in quadrature with a single feed (cf. Problem 8 of Section 1 of Chapter 8).

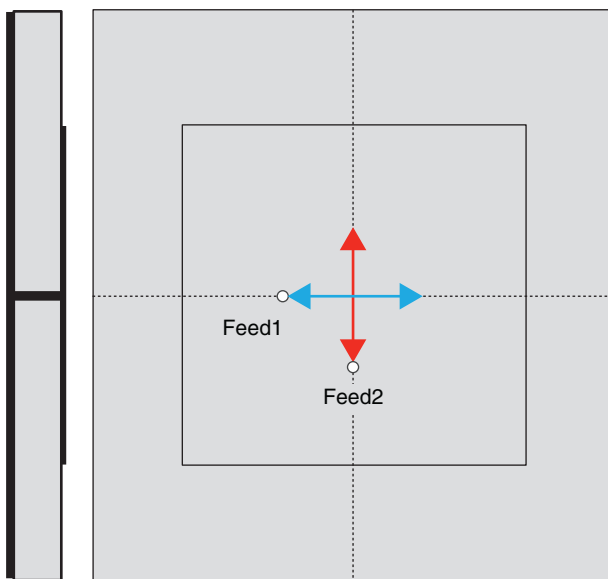


Figure 10.11 A circularly polarized patch antenna with two separate feeds exciting two orthogonal microstrip modes in quadrature.

REFERENCES

1. W. L. Stutzman and G. A. Thiele, *Antenna Theory and Design*, Wiley, New York, 2012, third edition.
2. T. A. Milligan, *Modern Antenna Design*, Wiley, New York, 2005, second edition.
3. C. A. Balanis, *Antenna Theory: Analysis and Design*, Wiley, New York, 2016, fourth edition.
4. G. H. Brown, “The ‘turnstile’ antenna,” *Electronics*, vol. 48, pp. 14–17, 1936.
5. G. H. Brown, “A pretuned turnstile antenna,” *Electronics*, vol. 18, pp. 102–107, 1945.
6. J. D. Kraus, *Antennas*, McGraw Hill, New York, 2001, third edition.
7. See Ref [2] above, pp. 231–237.
8. K. Maamria and T. Nakamura, “Simple antenna for circular polarization,” *IEE Proc. Microwaves Antennas Prop.*, vol. 139, no. 2, pp. 157–158, 1992.
9. R. K. Zimmerman, “Crossed dipoles fed with a turnstile network,” *IEEE Trans. Microwave Theory Techniques*, vol. 46, no. 12, pp. 2151–2156, 1998.
10. M. S. Gatti and D. J. Nybakken, “A circularly polarized crossed drooping dipole antenna,” in *1990 IEEE Antennas and Propagation Society International Symposium*, vol. 1, 1990, pp. 254–257.
11. C. -N. Hu, C. -S. Chuang, D. -C. Chou, K. -J. Liu, and C. -I. Hung, “Design of the cross-dipole antenna with near-hemispherical coverage in finite-element phased array by using genetic algorithms,” in *2000 IEEE International Conference on Phased Array Systems and Technology*, May 2000, pp. 303–306.

12. A. Kerkhoff and S. Ellingson, "A wideband planar dipole antenna for use in the long wavelength demonstrator array (LWDA)," in *2005 IEEE Antennas and Propagation Society International Symposium*, vol. 1B, 2005, pp. 553–556.
13. S. Ellingson and A. Kerkhoff, "Comparison of two candidate elements for a 30-90 MHz radio telescope array," in *2005 IEEE Antennas and Propagation Society International Symposium*, July 2005, vol. 1A, pp. 590–593.
14. J. A. MacDonald, D. M. McPherson, and M. J. Devine, "Axial ratio optimization of an array of crossed-dipoles using phasing posts," in *1994 IEEE Antennas and Propagation Society International Symposium*, June 1994, vol. 2, pp. 1252–1255.
15. V. Ovsyanikov, A. L. Olshevsky, A. V. Reuta, K. V. Rodin, E. D. Romanenko, and E. R. Beznosova, "Dual-frequency turnstile antenna with impedance elements," in *2002 12th International Conference Microwave and Telecommunication Technology*, Sep. 2002, pp. 339–340.
16. D. E. Ping, J. T. Shaffer, L. U. Brown, and R. B. Dybdal, "A broadband rolled edged cavity antenna," in *2004 IEEE Antennas and Propagation Society International Symposium*, June 2004, vol. 1, pp. 787–790.
17. R. A. Burberry, *VHF and UHF Antennas*, Peter Peregrinus Ltd., London, 1992, pp. 242–245.
18. R. C. Johnson, Ed., *Antenna Engineering Handbook*, McGraw Hill, New York, 2018, fifth edition.

PROBLEMS

1. (A) Express a linearly polarized electric field, $\mathbf{E} = E_x \hat{x}$, as a sum of two polarization vectors $\vec{\mathbf{R}}$ and $\vec{\mathbf{L}}$ from Eq. (10.9).
 (B) Derive Eq. (10.12).
 (C) Express the axial ratio in terms of the circular polarization ratio.
- 2*. Using a *Crossed-Dipole (Turnstile)* Antenna example of the MATLAB Antenna Toolbox,
 - (A) Design an *RHCP* turnstile antenna operating at 1575 MHz (L1 GPS band). Present all lines of your code.
 - (B) Plot the axial ratio in dB at the center frequency as a function of the elevation angle at two different azimuthal angles: 0 and 90°, respectively.
 - (C) Why do you think the axial ratios are somewhat different? Where is the best axial ratio achieved?
- 3*. Design a *monofilar helix antenna* (made of one helical wire) with a ground plane for operation in the band 1.4–2 GHz. Choose the parameters to achieve LHCP operation over the band. Compute the achieved directivity at zenith as well as the realized gain. Are you able to achieve more than 12 dBi in both cases?

- 4*.** Design a equiangular spiral antenna backed by a reflector for operating in the 3–10 GHz frequency range. Use the `design` function for this.
- (A) Plot the impedance over that frequency range. Sample the frequency range every 100 MHz.
 - (B) Plot the RHCP and LHCP radiation patterns in 3D at 5 GHz in separate figures. Use the `pattern` function for this exercise.
 - (C) Based on the plots, which kind of polarization is dominant for this antenna?
 - (D) Look at the `Exciter` property in the reflector antenna object as follows: `s = r.Exciter` Which property would you say contributes to the dominant polarization being radiated by this antenna? How would you make this antenna radiate the alternate polarization option? To investigate, make the change to `s`, and reassign it back to the reflector antennas as shown: `r.Exciter = s`

CHAPTER 11



Antenna Arrays

SECTION 1 ARRAY TYPES. ARRAY FACTOR. CONCEPT OF A SCANNING ARRAY

11.1. Array Types	271
11.2. Basic Array of Two Dipoles	275
11.3. Array Factor for Identical Radiators	277
11.4. Array Radiated Power and Array Directivity	280
11.5. Directivity of the Array and Directivity of the Array Factor	282
11.6. Concept of a Scanning Array	282
References	284
Problems	285

11.1 ARRAY TYPES

All antenna arrays are roughly subdivided into two groups: *scanning arrays* and *non-scanning arrays*. The non-scanning (simpler) arrays are used for various directional-power applications; they compete with the reflector antennas considered previously. Compared to the reflector antennas, the non-scanning arrays might have the following potential advantages:

1. Low-profile design – using patch arrays – for example, in a directional Wi-Fi link.

Antenna and EM Modeling with MATLAB® Antenna Toolbox, Second Edition. Sergey N. Makarov, Vishwanath Iyer, Shashank Kulkarni, and Steven R. Best.

© 2021 John Wiley & Sons, Inc. Published 2021 by John Wiley & Sons, Inc.

Companion website: www.wiley.com/go/Makarov/AntennaandEMModelingwithMATLAB2e

2. Low-cross-section design – using log-periodic arrays for TV reception and other tasks.
3. Higher gain as compared to the reflector of the same cross section (directional-power applications).

As an example, Figures 11.1–11.3 show some non-scanning arrays. Figure 11.1 illustrates a 4 GHz directional-power 4×4 non-scanning patch antenna array with a *corporate feed*. The array gain is 16.5 dB.

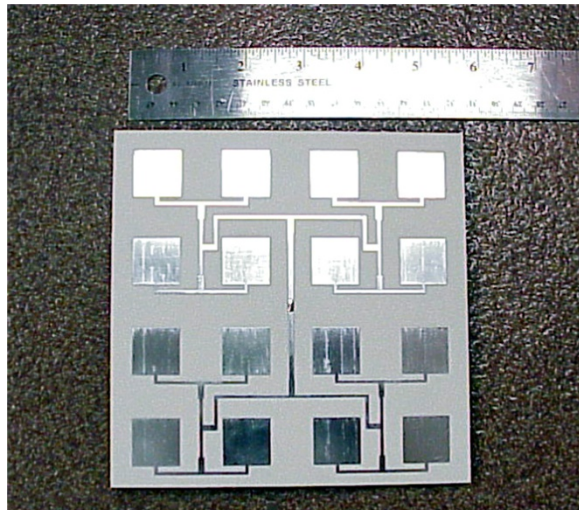


Figure 11.1 A 4 GHz directional-power 4×4 patch antenna array with the corporate feed. The array gain is 16.5 dB. *Source:* Design by the authors.



Figure 11.2 A 500 MHz–1 GHz directional-power dipole antenna array with the corporate feed (multiple Wilkinson power dividers). The array gain is 21–22 dB. *Source:* Design by the authors.

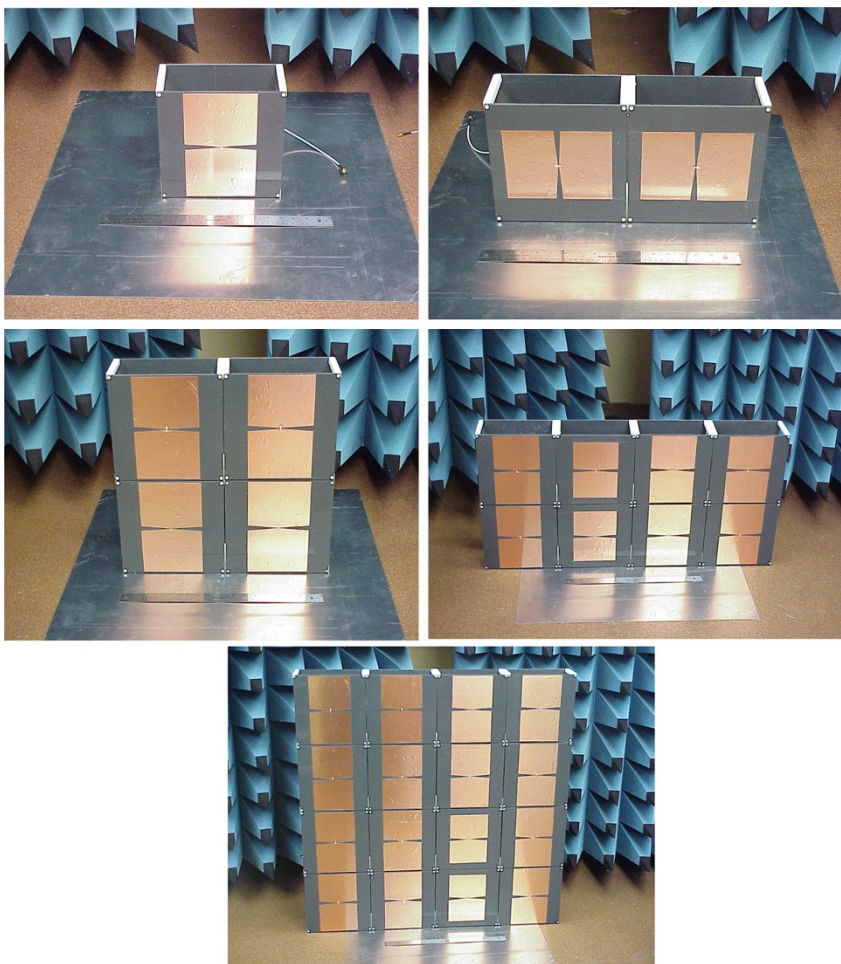


Figure 11.3 A 500 MHz–1 GHz directional-power blade-dipole *modular* antenna array with the corporate feed. *Source:* Design by the authors.

Figure 11.2 shows a 500 MHz–1 GHz directional-power 8×8 dipole antenna array with the corporate feed and a substantial input power. The array gain is 21–22 dB.

Figure 11.3 demonstrates a non-scanning 500 MHz–1 GHz *modular* array of wide-blade dipoles with a ground plane, which could be combined using specially optimized individual cells in various arrangements, e.g. 2×1 , 2×2 , 4×4 , etc.

The scanning arrays, on the other hand, have an ability to *steer the main beam electronically*, in contrast to mechanical scanning with the reflector antennas. Furthermore, they possess a high-fidelity angular resolution and a direction-finding capability when every array element is fed independently. As an example,



Figure 11.4 A 500–750 MHz coaxial-dipole antenna array with the independent feed for every array element. *Source:* Design by the authors.

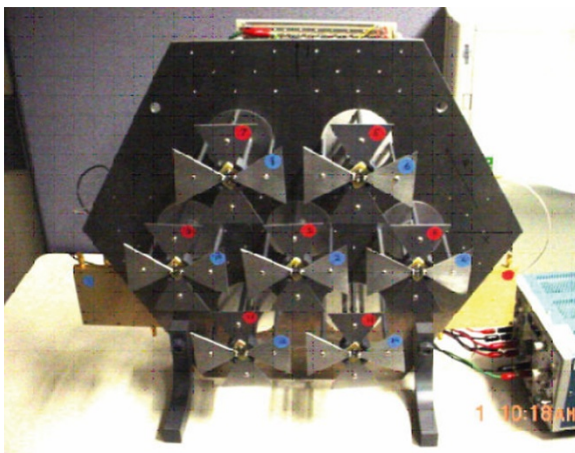


Figure 11.5 A small-size scanning 920 MHz bowtie dipole array with dual linear polarization (14 independent radiators). *Source:* Design by the authors.

Figures 11.4–11.5 show some scanning arrays. Figure 11.4 shows a 500–750 MHz coaxial-dipole antenna array with an independent feed for every element. The array has an omnidirectional pattern that stays unchanged in the desired frequency range. This array has been designed for some geolocation purposes. Next, Figure 11.5 shows a small-size scanning 920 MHz bowtie dipole array with dual linear polarization. This array includes built-in baluns, electronic phase shifters, power combiners, and post-processing software operating in real time. The array resolves

motion of an ISM 900 MHz source in two planes, and is intended for scanning over the angles of $\pm 45^\circ$ from its axis in both planes. The source may have arbitrary polarization (vertical, horizontal, or mixed).

11.2 BASIC ARRAY OF TWO DIPOLES

11.2.1 Array of Two Dipoles

Understanding the array operation starts with understanding the operation of an array with only two radiating elements shown in Figure 11.6. In Chapter 4, Section 2, a simple array – the dipole and its image versus a metal ground plane – has been in fact studied. Both the dipole and the image radiated in antiphase. In this section, the corresponding analysis will be repeated and expanded. However, we will assume that both radiators are in phase.

First, let us recall the radiation pattern of a single horizontal infinitesimally small dipole in free space [1]. The dipole is centered at the origin and is now oriented along the x -axis rather than along the z -axis. The pattern is conveniently presented in spherical coordinates shown in Figure 11.6. The phasor of the electric field has the form [1], cf. also Eq. (4.17),

$$E_\theta = j\eta \frac{kI_0 l \exp(-jkr)}{4\pi r} \sqrt{1 - \sin^2 \theta \cos^2 \phi}. \quad (11.1)$$

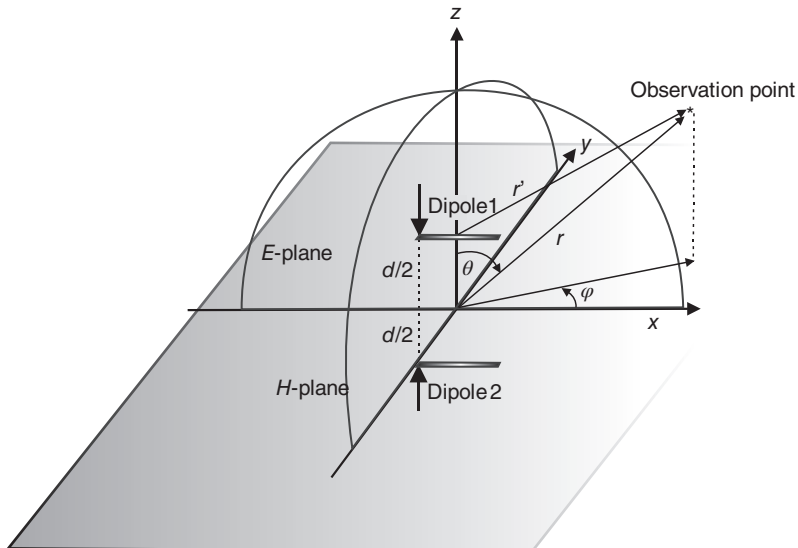


Figure 11.6 Radiation geometry of two dipoles in spherical coordinates. The dipole offset from the origin is given by $\pm d/2$.

We know that, for the resonant $\lambda/2$ dipole, the radiation pattern would be approximately the same.

It is clear that neither the pattern magnitude nor its polarization should change when we move the dipole (or any other antenna) by a certain finite distance, say $\pm d/2$, from the origin. This is because any linear translation cannot change the pattern magnitude or add a new polarization component.

What changes, however, is the phase since the signal from the dipole spaced closer to the observation point will arrive earlier, no matter how large the absolute distance to that point is. Thus, for a $\pm d/2$ translation along the z -axis, one needs to replace r in the phase factor $\exp(-jkr)$ in Eq. (11.1) by a new distance r' . Assume that the upper dipole (dipole #1) and the lower dipole (dipole #2) in Figure 11.6 are identical. According to the law of cosines and with reference to Figure 11.6, one has

$$\begin{aligned} r'^2 &= r^2 + (d/2)^2 \mp 2r(d/2)d\cos\theta; r' = \sqrt{r^2 + (d/2)^2 \mp 2r(d/2)\cos\theta} \\ &= r\sqrt{1 + \left(\frac{d/2}{r}\right)^2 \mp 2\left(\frac{d/2}{r}\right)\cos\theta} \end{aligned} \quad (11.2)$$

with d/r being a small parameter μ , $\mu \ll 1$. Using Taylor series expansion and keeping only dominant terms, one has

$$r' = r\sqrt{1 \mp \left(\frac{d}{r}\right)\cos\theta + O(\mu^2)}; \quad r' = r \mp d/2\cos\theta + rO(\mu^2) \approx r \mp d/2\cos\theta, \quad (11.3)$$

which leads to (after substitution of r' (11.3) instead of r in Eq. (11.1))

$$E_\theta^{1,2} = j\eta \frac{kI_{1,2}l_A \exp(-jkr) \exp(\pm jkd/2\cos\theta)}{4\pi r} \sqrt{1 - \sin^2\theta \cos^2\phi}, \quad (11.4)$$

where $E_\theta^{1,2}$ are the fields radiated by dipole #1 and by dipole #2, respectively. Next, we assume that $I_{1,2} = +I_0$, which is in phase radiation. The total field is finally given by the sum of two dipole fields, i.e.

$$E_\theta^{\text{total}}(r, \theta, \phi) = [2\cos(kd/2\cos\theta)]j\eta \frac{kI_0l_A \exp(-jkr)}{4\pi r} \sqrt{1 - \sin^2\theta \cos^2\phi}. \quad (11.5a)$$

11.2.2 Array Factor and Pattern Multiplication Rule

The factor in square brackets in Eq. (11.5a) is called the *array factor* or *AF*, i.e.

$$AF(\theta) = [2\cos(kd/2\cos\theta)]. \quad (11.5b)$$

One reason for emphasizing the value of array factor is that the linear pattern of an array of two dipoles is obtained as a single dipole pattern multiplied by the array factor – cf. Eq. (11.5a) and (11.1), respectively.

Another reason is that the array factor does not really change from antenna to antenna. If we repeat the above derivation not for the small dipole but for a dipole of arbitrary length or for a loop antenna, we will have exactly the same array factor in front of the corresponding electric field, $E_\theta^0(r, \theta, \phi)$, radiated by a single antenna. The same observation is valid for other antenna types: patches, Vivaldi antennas, etc. Therefore, we could write

$$E_\theta^{\text{total}}(r, \theta, \phi) = AF(\theta)E_\theta^0(r, \theta, \phi) \quad (11.5c)$$

for the radiated electric field of an array consisting of arbitrary antenna elements. Eq. (11.5c) is known as a *pattern multiplication rule* or a *pattern multiplication theorem*.

At the same time, the array factor would change if the electric current directions in two dipoles were not the same (phase shift of 0) but the opposite (which would correspond to a relative phase shift of π). This happened, for example, for a horizontal dipole above a PEC ground plane in Chapter 4. Instead of adding two exponents in the case of the same current flow,

$$\exp(+jkd/2\cos\theta) + \exp(-jkd/2\cos\theta) = 2\cos(kd/2\cos\theta) \quad (11.6)$$

one should subtract them when there is a phase shift of π , which results in a different array factor in the form (cf. also Section 2 of Chapter 4):

$$\exp(+jkd/2\cos\theta) - \exp(-jkd/2\cos\theta) = 2j\sin(kd/2\cos\theta). \quad (11.7)$$

Many non-scanning antenna arrays utilize the same array factor and no phase shift between the individual radiators. However, more generic (phased) arrays usually use an arbitrary (not necessarily 0 or π) progressive phase shift between the individual radiators, which leads to a varying array factor and a varying array radiation.

Note: A dipole array shown in Figure 11.7 is called the *broadside array* when operating at $\theta = \pi/2$ (and $\phi = \pi/2$). It is called the *endfire array* when operating at $\theta = 0$.

11.3 ARRAY FACTOR FOR IDENTICAL RADIATORS

11.3.1 Array Factor of the Array of N Dipoles

One could easily prove using trigonometric manipulations that the array factor of two dipoles from Eq. (11.5b) can be represented in the form,

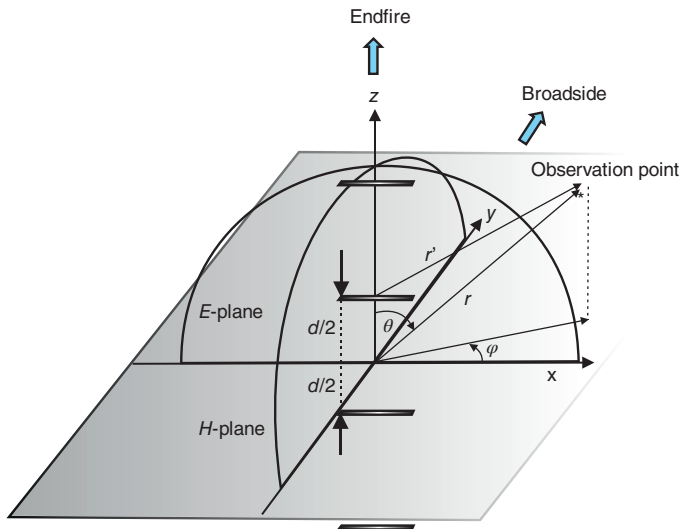


Figure 11.7 Broadside and endfire linear arrays.

$$AF = \frac{\sin(Nkd/2\cos\theta)}{\sin(kd/2\cos\theta)}, \quad (11.8a)$$

where $N = 2$. This equation is trivially expanded to an array of N dipoles separated by the distance d . The proof of Eq. (11.8a) for arbitrary N is straightforward but somewhat lengthy [1].

For small values of the argument ($\theta \rightarrow \pi/2$), the array factor given by Eq. (11.8a) simplifies to

$$AF = \frac{\sin(\frac{N}{2}x)}{\frac{1}{2}x}, \quad x = kd\cos\theta, \quad |x| \ll 1 \quad (11.8b)$$

so that the array factor is similar to the *sinc function* in the vicinity of the main beam. This suggests that an array will always have a pattern with the main beam surrounded by a large number of smaller *sidelobes*.

11.3.2 Gain of the Array Factor

It might appear at first sight that the gain factor N is lost in Eq. (11.8a). However, when the argument of both sine functions tends to zero in Eq. (11.8a), one asymptotically has

$$AF = \frac{\sin(Nkd/2\cos\theta)}{\sin(kd/2\cos\theta)} \rightarrow N \quad (11.9a)$$

so that the array factor does provide the expected electric-field array gain (N times the electric field of the individual radiator) in the selected direction.

11.3.3 Sidelobes

Array nulls and *array sidelobes* in the vicinity of the main beam are predicted by Eq. (11.8a) as well as by Eq. (11.8b). A conventional term is *sidelobe ratio*, which is the ratio of the main beam directivity to that of the first sidelobe. For large arrays, it is approaching a constant factor of 13.3 dB [2].

11.3.4 Grating Lobes

The array factor in Eq. (11.8a) indicates that a maximum field multiplication by N occurs whenever $x = kd \cos \theta = \pm 2n\pi$, not only at $\theta = \pi/2$. All such unwanted maxima with $n = 1, 2, 3, \dots$ are called the *grating lobes*. For smaller element spacings, such maxima do not occur in the “visible” space. This is because the equation

$$|\cos \theta| = \frac{2n\pi}{kd} \geq \frac{2\pi}{kd} > 1 \quad (11.9b)$$

cannot be solved for real-valued elevation angles, $0 \leq \theta \leq \pi$. The necessary condition for the absence of grating lobes is therefore a sufficiently small radiator spacing, that is

$$\frac{2\pi}{kd} > 1 \Rightarrow \frac{\lambda}{d} > 1 \Rightarrow d < \lambda. \quad (11.9c)$$

However, this condition is generally not sufficient for all possible arrays. The more restrictive common rule stating that the *half-wave or smaller spacing precludes grating lobes* should be used instead [2].

Example 11.1

Assume an array with spacing $d = \lambda$. Where does the grating lobe occur?

Solution: According to Eq. (11.9b),

$$|\cos \theta| = \frac{2\pi}{kd} = 1 \Rightarrow \theta = 0^\circ, 180^\circ. \quad (11.9d)$$

Thus, two grating lobes will occur in addition to the main beam, which occurs at $\theta = 90^\circ$, i.e. at broadside.

11.4 ARRAY RADIATED POWER AND ARRAY DIRECTIVITY

A naïve guess is to assume that the total power radiated by an array of identical radiators is equal to the power of an individual radiator (or *isolated radiator*) times the number of elements, N . This equality may not be satisfied, even for radiators without *mutual coupling*. The reason is that the electric fields of array elements are added with *different phase shifts* for different points in space, which leads to different total powers. The corresponding proof is given in Example 11.2 and in Figure 11.8.

Therefore, a straightforward assumption involving the definition of directivity from Chapter 3 that would result in the maximum array directivity in the form,

$$D_{max} = 10 \log_{10} N + D_{max}^0, \quad (11.10)$$

where D_{max}^0 is the directivity of an isolated radiator, is not valid either.

The array directivity could only be estimated for isotropic radiators where a result similar to Eq. (11.10) can be obtained. However, inclusion of element pattern

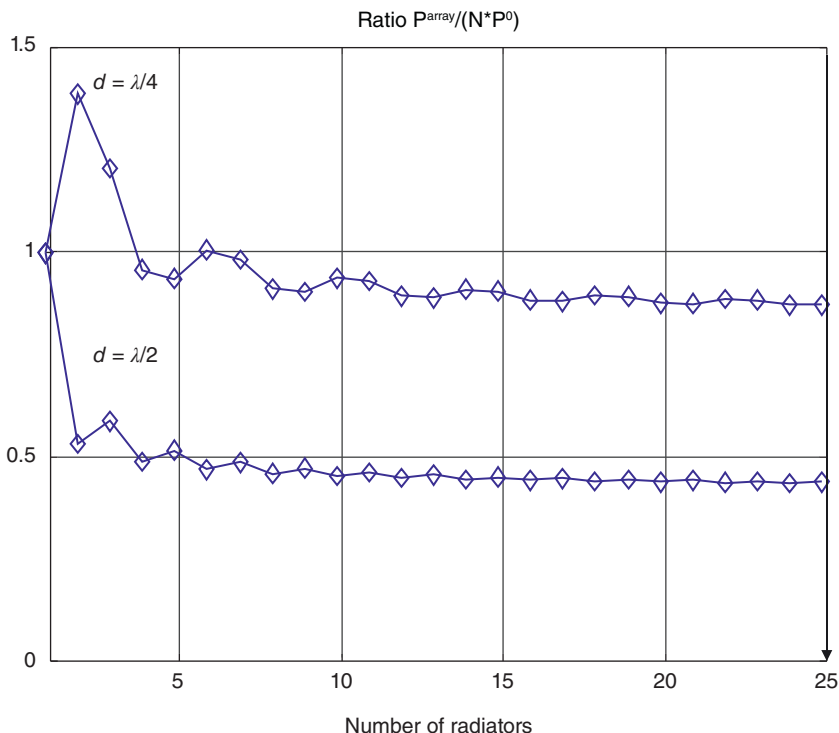


Figure 11.8 Power ratio $P_{rad}^N / (NP_{rad}^0)$ at two different element spacings for the linear broadside array of small dipoles.

effects greatly increases the difficulty of array directivity computations. Only a few analytical results are available for realistic linear arrays, in the form of infinite trigonometric series [3].

Example 11.2

Compare radiated far-field power of an individual small dipole with the power of N identical small dipoles assembled in a linear array configuration shown in Figure 11.7. Assume the same feed current I_0 and check if the array radiates N times more power than the single dipole.

Solution: In the first case, the total radiated power is given by an integral of the squared magnitude of the electric field, $E_\theta^0(r, \theta, \phi)$, from Eq. (11.1). Omitting all constant factors (they will cancel out later anyway), one has

$$P_{rad}^0 \cong \int_0^{2\pi} \int_0^\pi [1 - \sin^2 \theta \cos^2 \phi] \sin \theta d\theta d\phi. \quad (11.11)$$

In the second case, we use Eq. (11.5c) and (11.9a) and obtain

$$P_{rad}^N \cong \int_0^{2\pi} \int_0^\pi \left[\frac{\sin(Nkd/2\cos\theta)}{\sin(kd/2\cos\theta)} \right]^2 [1 - \sin^2 \theta \cos^2 \phi] \sin \theta d\theta d\phi. \quad (11.12)$$

Figure 11.8 shows the numerically computed ratio, $P_{rad}^N / (NP_{rad}^0)$, as a function of the number of radiators and at two different values of the element spacing.

One can see that this ratio is generally *less than one*. The corresponding MATLAB script follows:

```
M      = 180;
thetas = [0:pi/M:pi-pi/M];
phis   = [0:2*pi/M:2*pi-2*pi/M];
stept  = thetas(2) - thetas(1);
stepp  = phis(2) - phis(1);
E0 = zeros(M, M);
for m = 1:M
    for n = 1:M
        E0(m, n) = sqrt((1 - sin(thetas(m)).^2.*cos(phis(n)).^2));
    end
end
% Array
N = 25; % Max number of elements
PN = zeros(N, 1);
PA = zeros(N, 1);
for e = 1:N
    % Array factor
    lambda = 1; % Wavelength
    k      = 2*pi/lambda; % Wavenumber
```

```

d      = lambda/2;      % Array element spacing
AF     = sin(e*k*d/2*cos(thetas))./...
% Array factor
          sin( k*d/2*cos(thetas));
for m = 1:M
    for n = 1:M
        PN(e) = PN(e) + stepp*stept*E0(m, n)^2;
    end
end
PN(e) = e*PN(e);
for m = 1:M
    for n = 1:M
        PA(e) = PA(e) + stepp*stept*E0(m, n)^2*AF(m)^2;
    end
end
end

```

11.5 DIRECTIVITY OF THE ARRAY AND DIRECTIVITY OF THE ARRAY FACTOR

Eq. (11.10), rewritten in the form $D = D_{AF} + D^0$ (in decibel), is satisfied in one special case: for an *isotropic radiator* where the second factor in square brackets in the integrand on the right-hand side of Eq. (11.12) is equal to one. Furthermore, D^0 is equal to zero in decibel. Thus, for an array of isotropic radiators, the array directivity is simply the *directivity of the array factor*, D_{AF} . In the general case, one could write (in decibel)

$$D(\theta, \phi) = D_{AF}(\theta, \phi) + C(\theta, \phi), \quad (11.13)$$

where $C(\theta, \phi)$ is a more likely positive contribution due to the radiation of an individual non-isotropic radiator. To obtain quantitative estimates for $C(\theta, \phi)$, we must evaluate all field integrals numerically as described in Example 11.2 and in Chapter 3.

It is therefore a common practice to study the directivity of the array factor, $D_{AF}(\theta, \phi)$. Even this study constitutes significant difficulties. A much smaller contribution $C(\theta, \phi)$ can then be found separately when necessary.

11.6 CONCEPT OF A SCANNING ARRAY

11.6.1 Progressive Phase Shift(s)

We again consider the case of an array of two dipoles shown in Figure 11.6, when the upper dipole now has a phase shift of $+\beta/2$ and the lower dipole has a phase shift

of $-\beta/2$. Mathematically (and in practice), the phase shift is coming from a certain delay factor τ (lead or lag) in time, that is

$$\exp(j\omega(t \pm \tau)) = \exp(j\omega t \pm j\beta). \quad (11.14)$$

The *progressive (incremental) phase shift* β is usually implemented through the delay lines. Eq. (11.4) is then transformed to

$$E_{\theta}^{1,2} = j\eta \frac{kI_{1,2}l_A \exp(-jkr) \exp(\pm j(kd/2\cos\theta + \beta/2))}{8\pi r} \sqrt{1 - \sin^2\theta \cos^2\phi}. \quad (11.15)$$

One can see that the phase factor is additive with the argument of the array factor, i.e. the substitution can be made $kd \cos \theta \rightarrow kd \cos \theta + \beta$. Hence, the array factor given by Eq. (11.8a) for two dipoles and by Eq. (11.9a) in the general case is transformed to

$$AF = \frac{\sin(N \frac{1}{2}(kd \cos \theta + \beta))}{\sin(\frac{1}{2}(kd \cos \theta + \beta))} \quad (11.16)$$

given that the progressive phase shift between the individual radiators is β . For example, for an array of five radiators, the phase shifts could become

$$-2\beta, -\beta, 0, \beta, 2\beta. \quad (11.17)$$

The total phases are indeed defined to within a constant: any extra constant phase could be added to every radiator without changing the result.

11.6.2 Scanning the Main Beam

It was shown that the array factor in Eq. (11.16) is maximized when its argument *approaches zero*. Following this logic, the main beam of the array could be moved electronically by changing β . Assume that we want to maximize the array factor of a broadside array for a certain scanning direction, say $\theta = \theta_0$. Then, we should choose the phase shift or phase delay β from the equality

$$kd \cos \theta_0 + \beta = 0 \Rightarrow \beta = -kd \cos \theta_0. \quad (11.18)$$

This is the basic idea behind scanning. As an example, Figure 11.8 shows electric field distributions for a scanning array of eight dipoles above a ground plane in a two-dimensional space obtained via full-wave 2D FDTD simulations. To better observe and highlight weak signal propagation around the array, the only electric

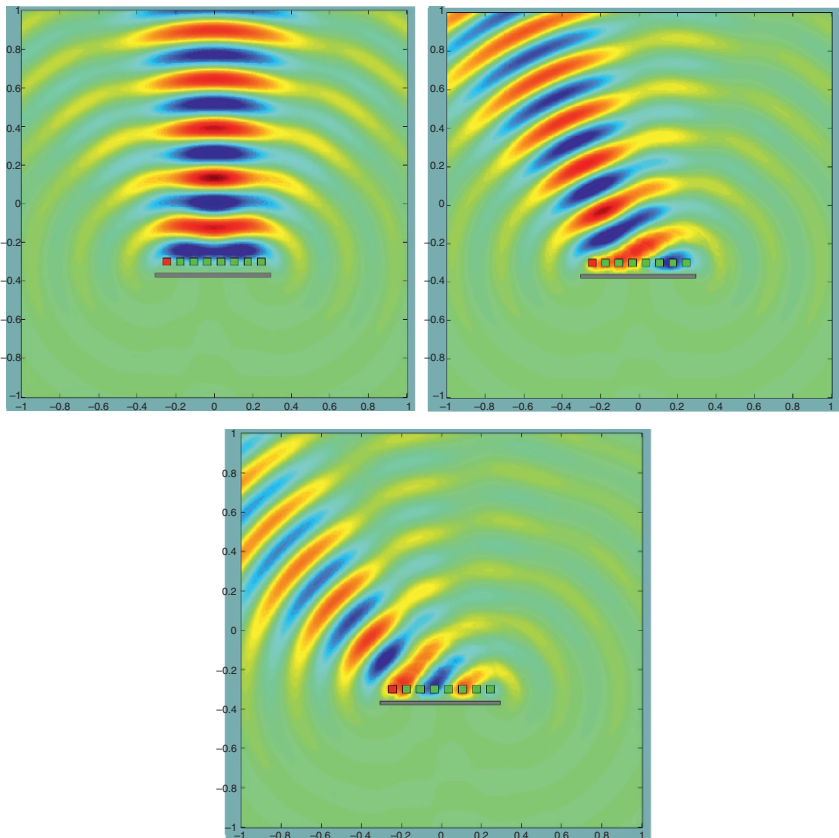


Figure 11.9 A dipole array behavior (cross section) in a two-dimensional space for different progressive phase shifts (FDTD simulations). Top left – the phase shift is zero; top right – the phase shift corresponding to a 30° scan from zenith; bottom – the phase shift corresponds to a 60° scan. The array in Figure 11.9 has been so constructed that one could visually recognize the main beam and sidelobes.

field component is plotted in Figure 11.9 using a linear scale, in the array's H-plane.

REFERENCES

1. C. A. Balanis, *Antenna Theory: Analysis and Design*, Wiley, New York, 2016, fourth edition.
2. R. C. Hansen, *Phased Array Antennas*, Wiley, New York, 2009, second edition.

3. W. L. Stutzman and G. A. Thiele. *Antenna Theory and Design*, Wiley, New York, 2012, third edition.

PROBLEMS

- 1***. 1. Describe in your own words meaning of the array factor. Why is it critical in the antenna array analysis?
2. A linear broadside array (the incremental phase shift between individual radiators is zero) of 10 resonant $\lambda/2$ dipoles at 1 GHz has all radiators separated by $\lambda/2$. Using Antenna Toolbox
- (A) Estimate the maximum array directivity in dB.
 - (B) Compare this result with Eq. (11.10) and estimate the deviation.
 - (C) Plot the array directivity pattern in the H-plane.
- 2***. 1. What is a sidelobe?
2. Using Antenna Toolbox, demonstrate the presence of sidelobes and find the sidelobe ratio (main beam to the first lobe) at a fixed frequency and by varying the separation distance of array elements with the help of a linear array of 10 $\lambda/2$ dipoles. Assume $\lambda/2$ dipole separation. The individual dipole radiator is designed for operation at 1 GHz.
3. Does the sidelobe ratio approach the theoretical value of 13.3 dB [2]?
- 3***. 1. What is a grating lobe?
2. Demonstrate the presence of grating lobes at a fixed frequency and by varying the separation distance of array elements with the help of the linear array of 10 $\lambda/2$ dipoles. The individual dipole radiator is designed for operation at 1 GHz. At which radiator separation distance does the first set of grating lobes occur?
- 4***. Based on Antenna Toolbox, write a MATLAB script that calculates peak directivity from a broadside array of $\lambda/2$ spaced dipoles as a function of N , number of elements. Do the following:
- (a) Create a dipole by using the `design` function, with a resonance at 1 GHz. Tilt this dipole so that it lies flat on the XY plane.
 - (b) Create a linear array of dipoles, by using the dipole designed in (a). Vary N from 2 to 30 and calculate the directivity at $az = 0, el = 90$. Plot the directivity at zenith as a function of N .
 - (c) Repeat the task (b), but this time, use a rectangular array. Vary the `Size` from (2×2) to (8×8) , increasing the number of elements by 1 along each dimension at each step.

- (d) Repeat the exercise in (c), but this time, set the array to have a triangular lattice.
- (e) Overlay the results for directivity from (c) and (d) on a single plot as a function of size.

Clearly label the axis in all plots. Provide titles and legends where appropriate.

SECTION 2 LINEAR ARRAYS

11.7. Broadside Linear Array	287
11.8. Array Amplitude Taper	290
11.9. Binomial Broadside Array	291
11.10. Dolph-Chebyshev Broadside Array	294
11.11. Endfire Linear Array	295
11.12. Hansen-Woodyard Endfire Array	297
11.13. Linear Array for Arbitrary Scan Angles	297
11.14. Superdirectivity	298
References	301
Problems	301

11.7 BROADSIDE LINEAR ARRAY

For the *broadside array*, we scan at $\theta_0 = 90^\circ$ in Figure 11.7, which corresponds to $\beta = 0$ in Eq. (11.18) and to the array factor from Eq. (11.9a), i.e.

$$AF = \frac{\sin(Nkd/2\cos\theta)}{\sin(kd/2\cos\theta)}. \quad (11.19)$$

The maximum directivity of the array factor will now be computed analytically. According to the definition of directivity in Chapter 3 and after choosing $U(\theta) = AF(\theta)^2$, $U_{max} = N^2$, one has

$$D_{AFmax} = \frac{U_{max}}{U_0} = \frac{N^2}{\frac{1}{4\pi} \int_0^{2\pi} \int_0^\pi AF(\theta)^2 \sin\theta d\theta d\phi} = \frac{N^2}{\frac{1}{2} \int_0^\pi AF(\theta)^2 \sin\theta d\theta}. \quad (11.20)$$

The corresponding integral in the denominator is computed analytically, which yields the exact result [1]

$$D_{AFmax} = \frac{N^2}{N + 2 \sum_{n=1}^{N-1} (N-n) \text{sinc}(nkd)}, \quad \text{sinc}(x) = \frac{\sin(x)}{x}. \quad (11.21)$$

Note that a slightly different definition of the *sinc* function is used here. The directivity precisely equals N for array spacings that are multiples of half wavelength. For other spacing values, the result nonlinearly depends on the array spacing and on the number of array elements. The corresponding expression in dB is

$10\log_{10}D_{AFmax}$. A more general expression for the directivity as a function of the elevation angle is obtained using the known value of U_0 , i.e. $D_{AF}(\theta) = U(\theta)/U_0$. This function is easily computed numerically.

Example 11.3

For a broadside array of 10 radiators, compute the radiation pattern of the array factor at three different values of the array spacing: quarter wave, half wave, and one wave.

Solution: The corresponding solution is shown in Figure 11.10a. This is not the analytical but rather a numerical solution obtained via numerical evaluation of the integral $\frac{1}{4\pi} \int_0^{2\pi} \int_0^\pi AF(\theta)^2 \sin\theta d\theta d\phi$. The corresponding MATLAB script follows (note the offset of 20 dB in MATLAB polar plot).

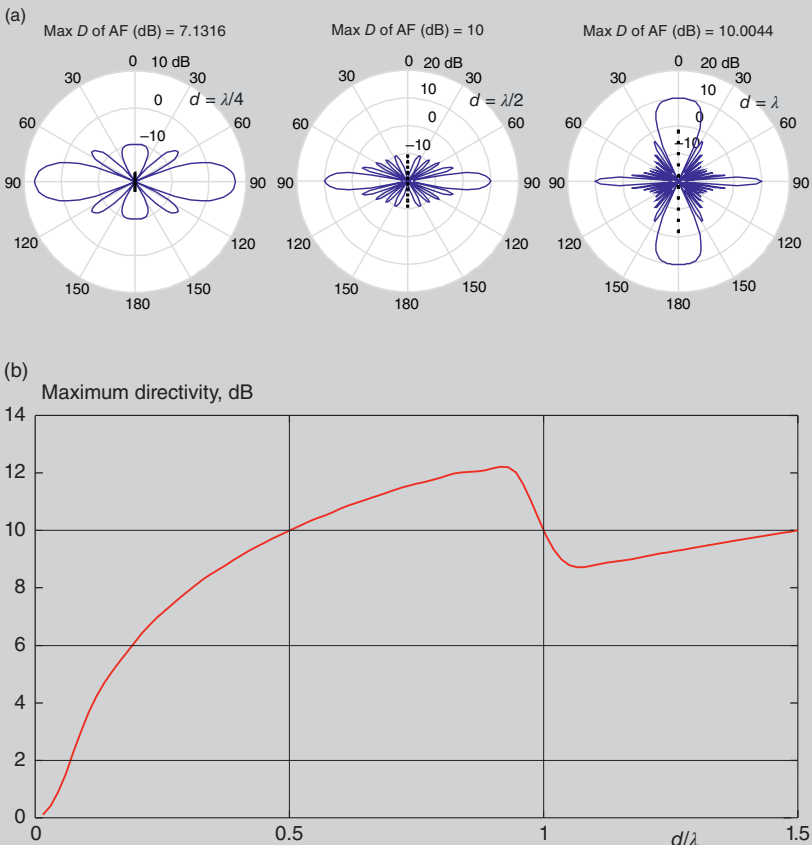


Figure 11.10 (a) Directivity patterns of the array factor for the broadside array of 10 radiators at different element spacings d . Very strong grating lobes appear in the last case. This result is independent of the radiator type. (b) Maximum directivity of the broadside array as a function of array spacing. This result is independent of the radiator type.

```

P      = 360;
thetas = [[0:pi/P:pi-pi/P] [pi:-pi/P:0]]; % Full thetas
N      = 10;          % Number of elements
f      = 1e9;          % Frequency
lambda = 3e8/f;       % Wavelength
k      = 2*pi/lambda; % Wavenumber
d      = lambda/4;     % Array element spacing
beta   = 0;           % Phase shift
psi    = k*d*cos(thetas) + beta;
AF     = sin(N/2*psi)./sin(1/2*psi); % Array factor
U = AF.^2;
step = thetas(2) - thetas(1);
U0 = 1/(4*pi)*(2*pi)*step*sum(AF(1:P).^2.*sin(thetas(1:P)));
% Directivity of the array factor
D = U/U0;
thetam = [pi/2-thetas(1:P) pi/2+thetas(P+1:end)];% MATLAB arg
Offset = 20;
DdB = 10*log10(D) + Offset;
DdB(find(DdB < 0)) = 0;           % Eliminate negative values
polar(thetam, DdB, 'b'); hold on; % Polar plot (full pattern)

```

Example 11.3 indicates that the array directivity reaches its maximum value at approximately half-wave spacing. This result could be also proved using the analytical expression from Eq. (11.21).

Example 11.4

For a broadside array of 10 radiators, compute the maximum directivity as a function of the element spacing.

Solution: To solve this problem, we will use the analytical result: Eq. (11.21). The corresponding result is shown in Figure 11.10b. The corresponding MATLAB code follows:

```

clear all;
N      = 10;          % Number of elements
f      = 1e9;          % Frequency
lambda = 3e8/f;       % Wavelength
k      = 2*pi/lambda; % Wavenumber
M = 100;
for m = 1:M
    d(m) = m*lambda/(M/1.5); % Array element spacing
    % Maximum directivity (Hansen)
    SUM = 0;
    for n = 1:N-1

```

```

SUM = SUM + (N-n)*sin(k*d(m)*n)/(k*d(m)*n);
end
DMAX = N^2/(N + 2*SUM);
DMAXdB(m) = 10*log10(DMAX)
end
plot(d/lambda, DMAXdB, 'r'); grid on; hold on
plot(d/lambda, 10*log10(N)*ones(size(d)), 'b');

```

Example 11.4 shows that the best broadside array spacing for the maximum directivity without the grating lobes is approximately half wave or slightly greater.

11.8 ARRAY AMPLITUDE TAPER

Figure 11.10a indicates one major problem with the broadside arrays with uniform amplitudes: the presence of significant sidelobes around the main beam. To entirely avoid or suppress sidelobes to an acceptable level, an *amplitude taper* may be introduced. It means that we will weigh the excitation amplitudes for every array element. The center elements typically have larger amplitudes whereas the border elements – smaller amplitudes. The taper is symmetric versus the array center.

Eq. (11.19) will not work for the amplitude taper. We need to go back to the original expression Eq. (11.4). For an even number of array elements, $N = 2M$, we denote the excitation amplitudes for one symmetric half of array elements by a_1, \dots, a_M , with the element a_1 being closest to the center. Then the array factor is given by

$$\begin{aligned}
AF = & a_1(\exp(+jkd/2\cos\theta) + \exp(-jkd/2\cos\theta)) \\
& + a_2(\exp(+j3kd/2\cos\theta) + \exp(-j3kd/2\cos\theta)) \\
& + \dots a_M(\exp(+j(2M-1)kd/2\cos\theta) + \exp(-j(2M-1)kd/2\cos\theta))
\end{aligned} \tag{11.22a}$$

or, which is the same,

$$AF = 2 \sum_{n=1}^M a_n \cos((2n-1)kd/2\cos\theta). \tag{11.22b}$$

For an odd number of array elements, $N = 2M + 1$, we denote the excitation amplitudes for one symmetric half of array elements by a_2, \dots, a_{M+1} . The center element at the origin has the amplitude excitation of $2a_1$. Then the array factor is given by

$$AF = a_1(1 + 1) + a_2(\exp(+jkd \cos \theta) + \exp(-jkd \cos \theta)) + \dots + a_M(\exp(+jMkd \cos \theta) + \exp(-j2Mkd \cos \theta)) \quad (11.23a)$$

or, which is the same,

$$AF = 2 \sum_{n=1}^{M+1} a_n \cos((n-1)kd \cos \theta). \quad (11.23b)$$

Do not forget to divide a_1 by two when using this expression in practice.

11.9 BINOMIAL BROADSIDE ARRAY

The *binomial taper* eliminates the sidelobes of the broadside array entirely. It is given by a *Pascal triangle* shown in Table 11.1. The taper is rather sharp at the array center.

However, the directivity of the main beam decreases. Example 11.5 and Figure 11.11 illustrate the use of the binomial taper. Compared to Figure 11.10a for the uniform array excitation, the directivity of the main beam decreases by approximately 3 dB.

TABLE 11.1 Array weighting coefficients for the binomial taper.

N										
1	1									
2	1 1									
3	1 2 1									
4	1 3 3 1									
5	1 4 6 4 1									
6	1 5 10 10 5 1									
7	1 6 15 20 15 6 1									
8	1 7 21 35 35 21 7 1									
9	1 8 28 56 70 56 28 8 1									
10	1 9 36 84 126 126 84 36 9 1									

Example 11.5

For a broadside array of 10 radiators with the binomial taper, compute the radiation pattern of the array factor at different values of the array spacing: quarter wave, half wave, and one wave.

Solution: The corresponding solution is shown in Figure 11.11. This is a simple numerical solution. The corresponding MATLAB script follows (again note the offset of 20 dB):

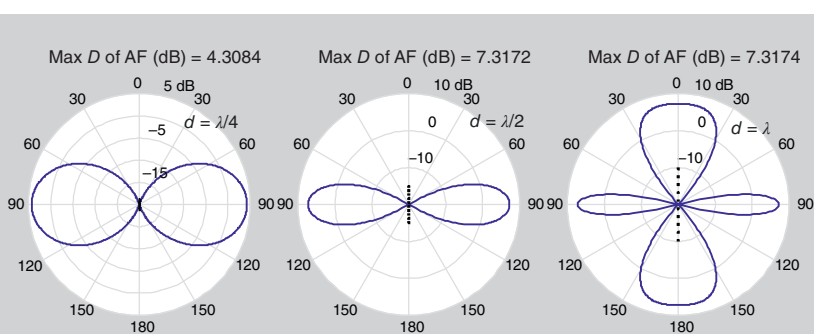


Figure 11.11 Directivity patterns of the array factor for the broadside array of 10 radiators with the binomial taper at different element spacings d . Very strong grating lobes appear in the last case.

```

P      = 360;
thetas = [[0:pi/P:pi-pi/P]; [pi:-pi/P:0]]; % Full thetas
N      = 10;          % Number of elements
f      = 1e9;         % Frequency
lambda = 3e8/f;      % Wavelength
k      = 2*pi/lambda; % Wavenumber
d      = lambda/4;    % Array element spacing
taper = [126 84 36 9 1]/126; % Binomial coefficients
AF = zeros(size(thetas));
if ~mod(N, 2)
    M = N/2;
    for m = 1:M+0
        AF = AF + taper(m)*2*cos((2*m-1)/2*k*d*cos(thetas));
    end
else
    M = (N-1)/2;
    for m = 1:M+1
        AF = AF + taper(m)*2*cos((m-1)*k*d*cos(thetas));
    end
end

% Directivity of the array factor (with offset in dB)
U = AF.^2;
step = thetas(2) - thetas(1);
U0 = 1/(4*pi)*(2*pi)*step*sum(AF(1:P).^2.*sin(thetas(1:P)));
D = U/U0;
thetam = [pi/2-thetas(1:P) pi/2+thetas(P+1:end)];
Offset = 20;
DdB = 10*log10(D) + Offset;
DdB(find(DdB < 0)) = 0;
polar(thetam, DdB, 'b');

```

TABLE 11.2 Array weighting coefficients for Chebyshev taper. The sidelobe level is 20 dB below the main beam.

<i>N</i>		0.6111	1.0000	0.6111	
3		0.5761	1.0000	1.0000	0.5761
4		0.5176	0.8326	1.0000	0.8326
5		0.5406	0.7768	1.0000	0.7768
6		0.5439	0.6942	0.9157	1.0000
7		0.5799	0.6603	0.8751	1.0000
8		0.6014	0.6153	0.8121	0.9503
9		0.6416	0.5944	0.7780	0.9214
10					

11.10 Dolph-Chebyshev BROADSIDE ARRAY

Figure 11.11 indicates that the binomial taper significantly decreases the broadside array gain. An alternative is the *Dolph-Chebyshev array taper*. This weighting distribution allows us control the sidelobe level at a certain prescribed value while maintaining nearly the same or a slightly lower gain of the main beam as compared to the uniform distribution [2, 3]. The idea is to write down the array factor in a polynomial form, determine all secondary maxima, and impose an upper bound on those maxima by equating their values to a certain prescribed value. In contrast, for the binomial taper, no secondary maxima should occur.

A simple implementation of the Dolph-Chebyshev distribution is given by MATLAB function $w = \text{chebwin}(L, r)$ (Signal Processing ToolboxTM), which returns the column vector w containing the length L Chebyshev window whose Fourier transform sidelobe magnitude is r dB below the mainlobe magnitude. Table 11.2 shows the Dolph-Chebyshev array taper for $r = 20$ dB obtained using this function. Example 11.6 implements the corresponding Dolph-Chebyshev broadside array. The uniform sidelobe level of -20 dB is clearly seen.

Example 11.6

For a broadside array of 10 radiators with the Dolph-Chebyshev taper, compute the radiation pattern of the array factor at different values of the array spacing: quarter wave, half wave, and one wave.

Solution: The corresponding solution is shown in Figure 11.12. This is a simple numerical solution. The corresponding MATLAB script follows (note the offset of 20 dB):

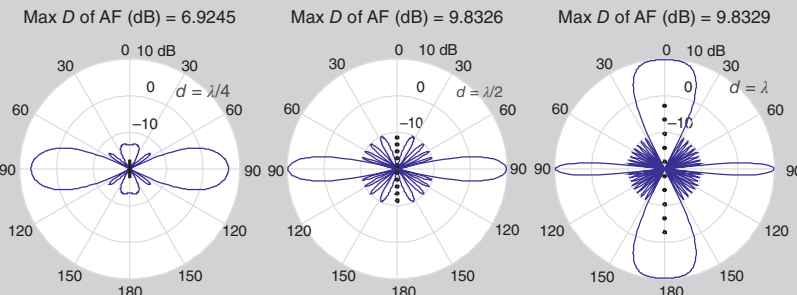


Figure 11.12 Directivity patterns of the array factor for the broadside array with 10 radiators with the Dolph-Chebyshev taper at different element spacings d . Very strong grating lobes appear in the last case.

```

P      = 360;
thetas = [[0:pi/P:pi-P] [pi:-pi/P:0]]; % Full thetas
temp   = (length(thetas)-1)/2;
% Array factor
N      = 10;           % Number of elements
f      = 1e9;          % Frequency
lambda = 3e8/f;        % Wavelength
k      = 2*pi/lambda;  % Wavenumber
d      = lambda/4;     % Array element spacing
AF = zeros(size(thetas));
bw = chebwin(N, +20); % Chebyshev window
if ~mod(N, 2)
    M = N/2;
    taper = bw(M:-1:1); % Chebyshev taper
    for m = 1:M+0
        AF = AF + taper(m)*2*cos((2*m-1)/2*k*d*cos(thetas));
    end
else
    M = (N-1)/2;
    taper = bw(M+1:-1:1); % Chebyshev taper
    taper(1) = taper(1)/2;
    for m = 1:M+1
        AF = AF + taper(m)*2*cos((m-1)*k*d*cos(thetas));
    end
end
% Directivity of the array factor (with offset in dB)
U = AF.^2;
step = thetas(2) - thetas(1);
U0 = 1/(4*pi)*(2*pi)*step*sum(AF(1:P).^2.*sin(thetas(1:P)));
D = U/U0;
thetam = [pi/2-thetas(1:P) pi/2+thetas(P+1:end)];
Offset = 20;
DdB = 10*log10(D) + Offset;
DdB(find(DdB < 0)) = 0;
polar(thetam, DdB, 'b');

```

11.11 ENDFIRE LINEAR ARRAY

For the *endfire array*, we scan at $\theta_0 = 0^\circ$ in Figure 11.7, which, according to Eq. (11.18) corresponds to the following incremental phase shift:

$$kd \cos \theta_0 + \beta = 0 \Rightarrow \beta = -kd. \quad (11.24)$$

The array factor given by Eq. (11.16) becomes

$$AF = \frac{\sin(N\frac{1}{2}(kd \cos \theta + \beta))}{\sin(\frac{1}{2}kd \cos \theta + \beta)} = \frac{\sin(N\frac{1}{2}kd(\cos \theta - 1))}{\sin(\frac{1}{2}kd(\cos \theta - 1))}. \quad (11.25)$$

The maximum directivity of the array factor will be again computed analytically. According to the definition of directivity in Chapter 3 and after choosing $U(\theta) = AF(\theta)^2$, $U_{max} = N^2$, one has

$$D_{AFmax} = \frac{U_{max}}{U_0} = \frac{N^2}{\frac{1}{4\pi} \int_0^{2\pi} \int_0^\pi AF(\theta)^2 \sin \theta d\theta d\phi} = \frac{N^2}{\frac{1}{2} \int_0^\pi AF(\theta)^2 \sin \theta d\theta}. \quad (11.26)$$

The corresponding integral in the denominator is computed analytically, which yields the *exact result* [1]

$$D_{AFmax} = \frac{N^2}{N + 2 \sum_{n=1}^{N-1} (N-n) \text{sinc}(2nkd)}, \quad \text{sinc}(x) = \frac{\sin(x)}{x}. \quad (11.27)$$

This expression replicates the result for the broadside array Eq. (11.21), but with the element spacing halved. Also, the directivity of the array factor precisely equals N for spacings that are multiples of a quarter wavelength.

Example 11.7

For an endfire array of 10 radiators, compute the maximum directivity as a function of the element spacing.

Solution: We could reuse the results of Example 11.4 and Figure 11.10b but with the x -scale in Figure 11.10 divided by two.

While the behavior of the maximum directivity looks similar to the maximum directivity of the broadside array, the entire radiation pattern of the endfire array is quite different as it will be seen in Example 11.8 and in Figure 11.13.

Example 11.8

For an endfire array of 10 radiators, compute the radiation pattern of the array factor at different values of array spacing: quarter wave, half wave, and one wave.

Solution: The corresponding solution is shown in Figure 11.13. This is not the analytical but rather a numerical solution obtained via numerical evaluation of the integral $\frac{1}{4\pi} \int_0^{2\pi} \int_0^\pi AF(\theta)^2 \sin \theta d\theta d\phi$. It essentially replicates Example 11.3. The only changes to be made in the corresponding MATLAB script are:

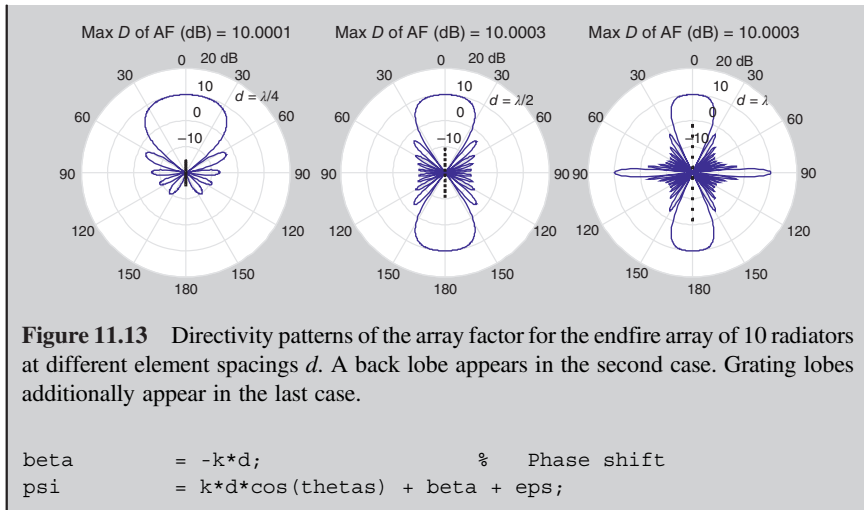


Figure 11.13 Directivity patterns of the array factor for the endfire array of 10 radiators at different element spacings d . A back lobe appears in the second case. Grating lobes additionally appear in the last case.

```

beta      = -k*d; % Phase shift
psi       = k*d*cos(thetas) + beta + eps;

```

11.12 Hansen-Woodyard ENDFIRE ARRAY

This is an endfire array with an improved directivity of the main beam (increase of approximately 2.5 dB). At the same time, the sidelobe level increases from approximately -13.3 dB to -9 dB [2]. Instead of Eq. (11.24), we should use a slightly different phase shift:

$$kd \cos \theta_0 + \beta = 0 \Rightarrow \beta = -\left(kd + \frac{\pi}{N}\right). \quad (11.28)$$

The computations for the Hansen-Woodyard array are performed similar to the computations for the ordinary endfire array from Example 11.8. Figure 11.14 shows the comparison results for the two endfire arrays with quarter-wave spacing and with 10 radiators each.

11.13 LINEAR ARRAY FOR ARBITRARY SCAN ANGLES

Broadside and endfire arrays are the two limiting cases of a linear array scanning in arbitrary direction in the yz -plane in Figure 11.7. The corresponding result for the maximum directivity of the array factor for uniform amplitude distribution is again an exact analytical expression, which is given in the form [1]:

$$D_{AF \max} = \frac{N^2}{N + 2 \sum_{n=1}^{N-1} (N-n) \operatorname{sinc}(nkd) \cos(nkd \cos \theta_0)}, \quad \operatorname{sinc}(x) = \frac{\sin(x)}{x} \quad (11.29)$$

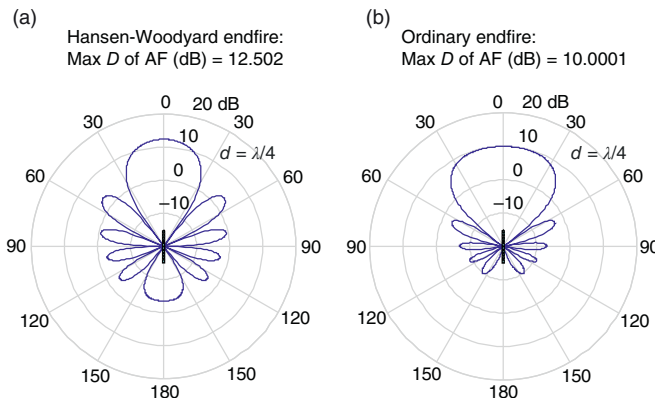


Figure 11.14 Directivity patterns of the array factor for Hansen-Woodyard array (a) and the ordinary endfire array (b), respectively, with quarter-wave spacing and with 10 radiators each.

where θ_0 is the corresponding scan angle. When $\theta_0 = \pi/2$, we will have the result for the broadside array given by Eq. (11.21).

11.14 SUPERDIRECTIVITY

The Hansen-Woodyard array is a first example of an array with a modest *superdirectivity*. The term “superdirective” (or *supergain*) broadly means a directivity that is *higher* than obtained with the same array length and elements uniformly excited (constant amplitude and constant phase) [1].

Another example is given by a broadside array of seven radiators with quarter-wave spacing [1]. Instead of the uniform amplitude distribution,

$$a_1 = 0.5, \quad a_2 = 1, \quad a_3 = 1, \quad a_4 = 1 \quad (11.30a)$$

in Eq. (11.23b), we will use [1]

$$a_1 = -8.264/2, \quad a_2 = 7.122, \quad a_3 = -3.933, \quad a_4 = 1.443. \quad (11.30b)$$

Note the negative amplitude values mean that the array elements in Eq. (11.30b) must be driven with different phases. Pattern comparison is discussed in Example 11.9 and is shown in Figure 11.15. One can see that the superdirective property indeed increases the sidelobes.

Another truly amazing extreme example is given by a broadside array of nine isotropic radiators with *overall length* $\lambda/4$ (*element spacing is* $\lambda/32$) and weighting coefficients in the form [4]:

$$\begin{aligned} &[17787318.7374/2 - 14253059.7032 \\ &7161483.1266 - 2062922.9994 \quad 260840.2268]; \end{aligned} \quad (11.30c)$$

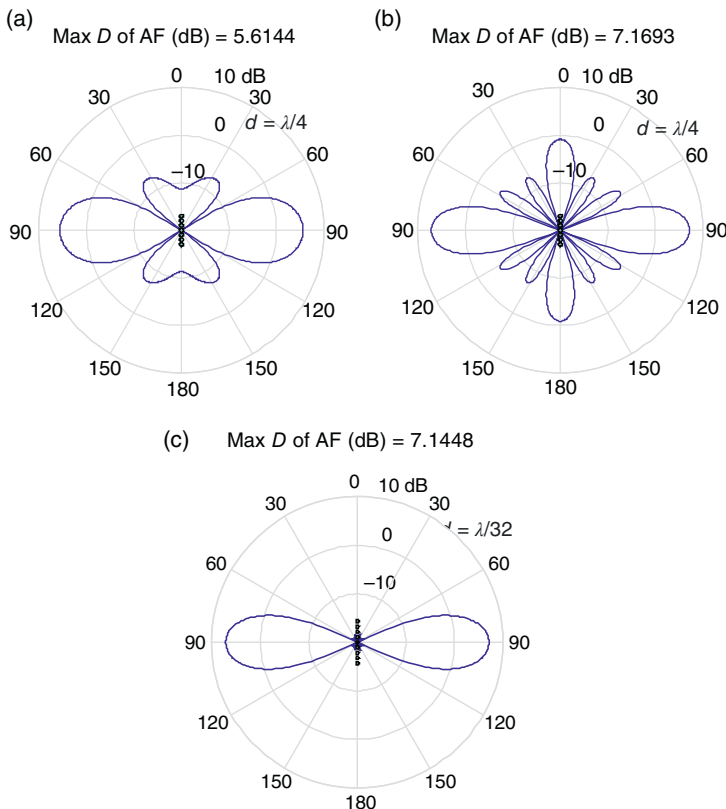


Figure 11.15 (a,b) Directivity patterns of the array factor for the broadside array with seven radiators and with the amplitude/phase taper following Eq. (11.30a) (uniform taper) and Eq. (11.30b) (“superdirective” taper), respectively. (c) Directivity pattern of the array factor for the broadside array with nine radiators and with the amplitude/phase taper following Eq. (11.30c) (“superdirective” taper).

The corresponding pattern looks nearly perfect – cf. Example 11.9 and Figure 11.15c. A problem with this design is a very high tolerance sensitivity. To check the sensitivity, you might want to slightly change the spacing values in Eq. (11.30c) and observe the results.

Example 11.9

Implement the broadside array tapers from Eq. (11.30b).

Solution: For Eq. (11.30a) and, (11.30b), the corresponding solution is given in part by the MATLAB code:

```
N      = 7;          % Number of elements
f      = 1e9;        % Frequency
```

```

lambda      = 3e8/f;          % Wavelength
k           = 2*pi/lambda;    % Wavenumber
d           = lambda/4;        % Array element spacing
taper = [0.5 1 1 1];
taper = [-8.264/2 7.122 -3.933 1.443];
AF = zeros(size(theta));
if ~mod(N, 2)
    M = N/2;
    for m = 1:M+0
        AF = AF + taper(m)*2*cos((2*m-1)/2*k*d*cos(theta));
    end
else
    M = (N-1)/2;
    for m = 1:M+1
        AF=AF+taper(m)*2*cos((m-1)*k*d*cos(theta));
    end
end

```

The rest of the code follows Examples 11.5 and 11.6. The result is shown in Figure 11.15.

For Eq. (11.30c), one has

```

%   Array factor
N           = 9;            % Number of elements
f           = 1e9;           % Frequency
lambda      = 3e8/f;         % Wavelength
k           = 2*pi/lambda;    % Wavenumber
d           = lambda/32;       % Array element spacing
beta        = 0;             % Phase shift
taper = [0.5 1 1 1];
taper = [17787318.7374/2 -14253059.7032 7161483.1266 -2062922.9994
260840.2268];
AF = zeros(size(theta));
if ~mod(N, 2)
    M = N/2;
    for m = 1:M+0
        AF = AF + taper(m)*2*cos((2*m-1)/2*k*d*cos(theta));
    end
else
    M = (N-1)/2;
    for m = 1:M+1
        AF=AF+taper(m)*2*cos((m-1)*k*d*cos(theta));
    end
end

```

The rest of the code follows Examples 11.5 and 11.6. The result is shown in Figure 11.15.

REFERENCES

1. R. C. Hansen, *Phased Array Antennas*, Wiley, New York, 2009, second edition.
2. C. A. Balanis, *Antenna Theory: Analysis and Design*, Wiley, New York, 2016, fourth edition.
3. C. L. Dolph, “A current distribution for broadside arrays which optimizes the relationship between beam width and side-lobe level,” *Proc. IRE*, vol. 34, pp. 335–348, 1946.
4. R. C. Hansen, *Electrically Small, Superdirective, and Superconducting Antennas*, Wiley, New York, 2006.

PROBLEMS

- 1***. A linear broadside array (the incremental phase shift between individual radiators is zero) of 10 resonant $\lambda/2$ dipoles at 1 GHz is considered with the uniform amplitude distribution. Using Antenna Toolbox, estimate the value of the correction factor $C(\theta, \phi)$ from Eq. (11.13) in the direction of the main beam for different radiator spacings (quarter lambda, half lambda, and lambda spacing).
- 2.** Solve the task of Example 11.3 using Hansen’s summation formula given by Eq. (11.21). How different is the result?
- 3***. A linear broadside array (the incremental phase shift between individual radiators is zero) of 10 resonant $\lambda/2$ dipoles at 1 GHz is considered subject to the binomial taper. Using Antenna Toolbox, generate the analog of Figure 11.11 and estimate the value of the correction factor $C(\theta, \phi)$ from Eq. (11.13) in the direction of the main beam in every case (quarter lambda, half lambda, and lambda spacing). *Hint:* use the `AmplitudeTaper` property to simulate your design.
- 4***. A linear broadside array (the incremental phase shift between individual radiators is zero) of 10 resonant $\lambda/2$ dipoles at 1 GHz is considered subject to the Dolph-Chebyshev taper. Using Antenna Toolbox, generate the analog of Figure 11.12 and estimate the value of the correction factor $C(\theta, \phi)$ from Eq. (11.13) in the direction of the main beam in every case (quarter lambda, half lambda, and lambda spacing). *Hint:* use the `AmplitudeTaper` property and `chebwin` function to simulate your design.
- 5***. A linear broadside array (the incremental phase shift between individual radiators is zero) of 15 radiators at 1 GHz is considered subject to the Dolph-Chebyshev taper.
 1. Generate the analog of Figure 11.12 for quarter lambda, half lambda, and lambda spacing using Example 11.6 as a base.

2. Using Antenna Toolbox, generate a similar figure and estimate the value of correction $C(\theta, \phi)$ from Eq. (11.13) for an array of 15 resonant dipoles at 1 GHz in the direction of the main beam in every case (quarter lambda, half lambda, and lambda spacing). *Hint:* use the `AmplitudeTaper` property and `chebwin` function to simulate your design.
6. 1. Could the directivity of the main beam for the array factor of a broadside array with N radiators and with the uniform amplitude distribution be greater than $10\log_{10}N$? Justify your answer.
2. Repeat for the ordinary endfire array.
7. Generate the analog of Figure 11.14a for Hansen-Woodyard array when scanning at 45° from zenith in Figure 11.7.

SECTION 3 PLANAR ARRAYS

- 11.15. Theoretical Gain Pattern of a Finite 2D Array 303**
- 11.16. Design of Small 2D Arrays: Impedance Bandwidth Improvement and Directivity 308**
- 11.17. Corporate Series Feed – Wilkinson Power Dividers 312**
- 11.18. Corporate (Parallel) Feed 314**
- References 315**
- Problems 316**

11.15 THEORETICAL GAIN PATTERN OF A FINITE 2D ARRAY

11.15.1 Gain of the Main Beam

All planar arrays are broadside, not endfire. The directive gain of a large finite and generally mutually coupled 2D phased array with M by N regularly spaced elements is determined by the expression first suggested by Hannan [1] and repeatedly cited by Hansen [2, 3] and others. Namely, with reference to Figure 11.16,

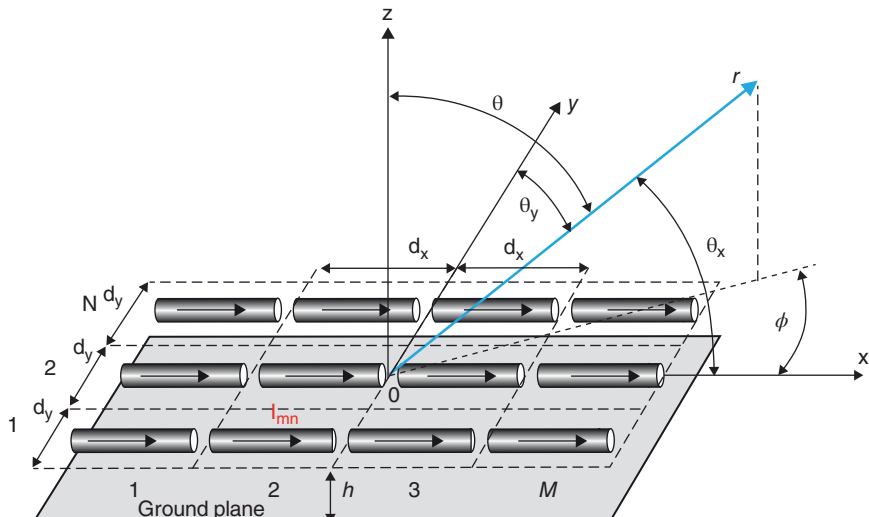


Figure 11.16 Planar array geometry and unit cell dimensions.

$$D(\theta, \phi) = MN \frac{4\pi A}{\lambda^2} \cos \theta, A = d_x d_y. \quad (11.31)$$

Here, λ is the wavelength, θ is the *scan* elevation angle, and d_x, d_y are the dimensions of the *array unit cell*. This equation was first suggested based on the “natural guess” that the directivity of the large array is exactly equal to the directivity of the large (compared to the wavelength) aperture. The directivity of an aperture with a uniform impinging electric field in free space exactly coincides with Eq. (11.31) [4].

Furthermore, since the effective area of an element should be proportional to its projected area in the direction of interest, the element gain should have a cosine variation with the angle as stated in Eq. (11.31). Based on this semi-intuitive reasoning, Eq. (11.31) has been formulated.

Despite the lack of initial theoretical justification, it was shown by Oliner and Malech [5] (and also mentioned by Hansen, Ref. [2]) that Eq. (11.31) can be exactly proven for radiating slots and dipoles. Let us consider a *non-scanning* array first. In the case of the non-scanning array pointing toward zenith, $\theta = 0$, so that Eq. (11.31) can be used to predict the gain in dB at zenith (at broadside) in the form:

$$D = 10 \log_{10} \left[MN \frac{4\pi d_x d_y}{\lambda^2} \right] \text{dB} \quad (11.32)$$

11.15.2 Array Factor

The directivity pattern of the array factor of the *scanning planar array* in Figure 11.16 is conveniently expressed in terms of *direction cosines* in Figure 11.16 [6]. It is given by a two-dimensional sum,

$$\begin{aligned} AF(\theta, \phi) &= \left| \sum_{m=1}^M \sum_{n=1}^N I_{mn} \exp(j(m d_{rx} \tau_x + n d_{ry} \tau_y)) \right|, \\ d_{rx} &= \frac{2\pi d_x}{\lambda}, \quad d_{ry} = \frac{2\pi d_y}{\lambda}, \quad \tau_x = \cos \theta_x - \cos \theta_{xs}, \quad \tau_y = \cos \theta_y - \cos \theta_{ys} \\ \cos \theta_{xs} &= \frac{\psi_x}{d_{rx}}, \quad \cos \theta_{ys} = \frac{\psi_y}{d_{ry}}. \end{aligned} \quad (11.33)$$

Here,

I_{mn} are (real) excitation weights (currents/voltages in the feed); $I_{mn} = 1$ with no taper.

θ_x and θ_y are two angles from the Cartesian axes x and y to the scanning direction \mathbf{r} in Figure 11.16. Their cosines are the direction cosines.

ψ_x and ψ_y are the progressive phase shifts between array elements.

When scanning at zenith, the direction cosines of the radius vector specifying the desired scan direction (the beam maximum), $\cos\theta_{xs}$ and $\cos\theta_{ys}$, are both equal to zero.

After some manipulations, the array factor from Eq. (11.33) in the vicinity of the main beam can be simplified as [4, 6]

$$AF(\theta, \phi) = \frac{\sin x \sin y}{x - y}, \quad x = \frac{1}{2}Md_{rx}\tau_x, \quad y = \frac{1}{2}Nd_{ry}\tau_y, \quad (11.34)$$

which is the *Fraunhofer scalar diffraction pattern* of the corresponding rectangular aperture.

11.15.3 Pattern of an Individual Element

Eq. (11.33) and (11.34) are not sufficient for establishing the complete array radiation pattern. They need to be further augmented with the pattern of an individual element. We will omit this step since the dipole (the radiator under study) pattern close to zenith is very uniform and since the corresponding contribution is expected to be rather small in the main beam of large planar arrays.

11.15.4 Array Directivity

We will consider an array scanning at zenith, i.e. for $\cos\theta_{xs} = \cos\theta_{ys} = 0$, first. We will attempt to find the directivity of the array factor by combining results of Sections 1.1–1.3. We know that the array factor itself is given by Eq. (11.34) whereas its maximum directivity is already known: it is given by Eq. (11.32). Using those two facts, we could write the directivity pattern of the array factor in the vicinity of main beam in the form:

$$D_{AF} = 10 \log_{10} \left[NM \frac{4\pi d_x d_y}{\lambda^2} \left(\frac{\sin x \sin y}{x - y} \right)^2 \right] \text{dB}, \quad (11.35)$$

$$x = \frac{1}{2}Md_{rx}\cos\theta_x, \quad y = \frac{1}{2}Nd_{ry}\cos\theta_y.$$

We will next assume that Eq. (11.35) holds in the vicinity of the main beam for any scan angle. For the *E-plane scan* (xz-plane in Figure 11.16), one has $\theta_x + \theta = 90^\circ$, $\theta_y = 90^\circ$. Therefore, Eq. (11.35) simplifies to

$$D_{AF} = 10 \log_{10} \left[NM \frac{4\pi d_x d_y}{\lambda^2} \left(\frac{\sin x}{x} \right)^2 \right] \text{dB}, \quad x = \frac{1}{2}Md_{rx}\sin\theta. \quad (11.36)$$

For the *H-plane scan* (yz-plane in Figure 11.16), one has $\theta_y + \theta = 90^\circ$, $\theta_x = 90^\circ$. Therefore, Eq. (11.35) simplifies to

$$D_{AF} = 10 \log_{10} \left[NM \frac{4\pi d_x d_y}{\lambda^2} \left(\frac{\sin y}{y} \right)^2 \right] \text{dB}, \quad y = \frac{1}{2} N d_{ry} \sin \theta. \quad (11.37)$$

11.15.5 Application Example

The geometry of the unit cell in the array under study is shown in Figure 11.17 (see also Figure 11.18 for the overall array assembly). The radiator is a “ribcage” dipole with a conical matching network close to the antenna feed to be connected to a balun. The overall size of the radiator is slightly less than the size of the unit cell.

In the particular case of an 8×8 array and with reference to the notations of Figure 11.16, we use the following parameters in Eq. (11.36) and (11.37):

$$N = 64, \quad d_x = d_y = 240 \text{ mm}, \quad k = \frac{2\pi}{\lambda}, \quad \lambda = c_0/f. \quad (11.38)$$

11.15.6 Comparison Between Theory and Numerical Simulations

The numerical simulations have been carried out for the array of center-fed ribcage with Ansys HFSS commercial CEM software. The spacing from the ground plane was 150 mm. Figure 11.18 shows the overall array structure. The numerical solution was obtained with a perfectly matched layer (PML) box and used about 100 000 tetrahedra. Figure 11.19 shows the numerical directive gain (dashed curve) versus theoretical directivity [Eq. (11.37) – solid curve] in the H-plane at two frequencies of interests.

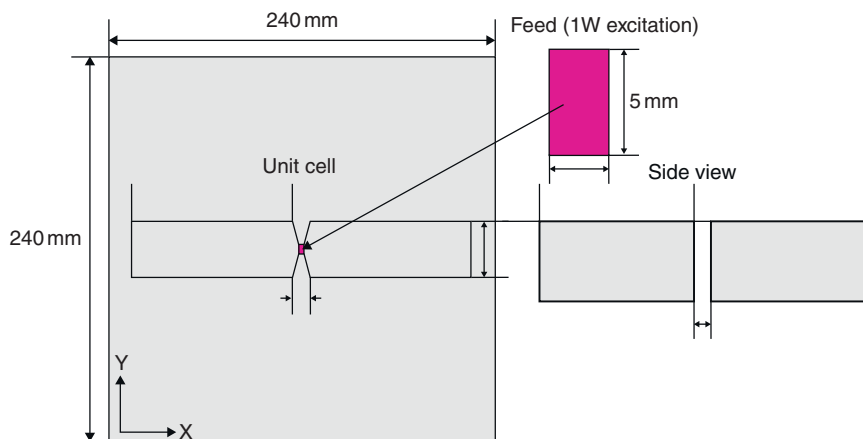


Figure 11.17 The array unit cell on the size of 240×240 mm.

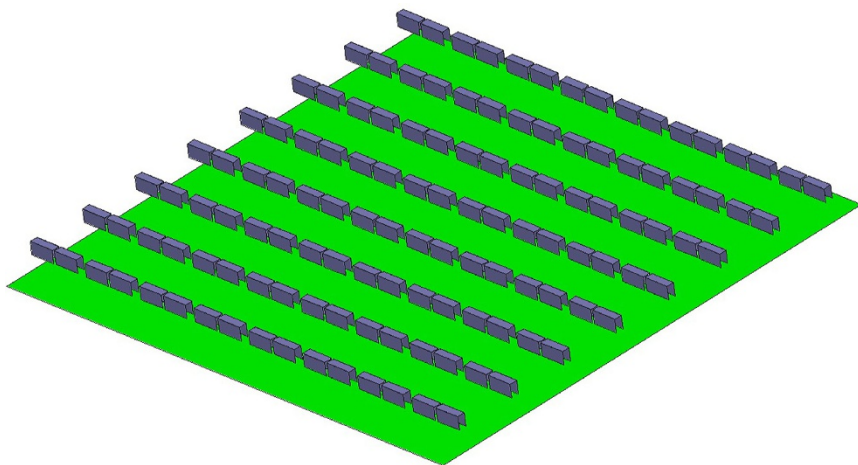


Figure 11.18 Theory versus numerical simulations of an 8×8 array of dipoles on the total size of 1.96×1.96 m.

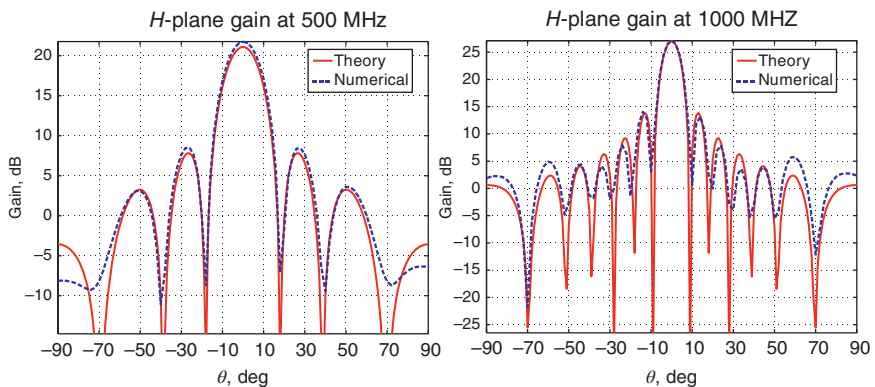


Figure 11.19 Theory (directivity of the array factor only) versus numerical simulations (accurate array directivity with taking into account the directivity of individual radiators) for an 8×8 array of dipoles on the total size of 1.96×1.96 m. Scanning at zenith is considered.

The theoretical and numerical data agree quite well despite the sophisticated nature of the dipole radiators, presence of the ground plane, etc. This confirms the theoretical estimates given by Eq. (11.35) through (11.37). Note that experimental data obtained for the same array (cf. Figure 11.2 of this chapter) at 500 MHz confirm the gain and the slope of the main beam to within 1.5 dB.

Example 11.10

Check the results of Figure 11.19 against Eq. (11.32) for the array directivity at zenith.

Solution: A simple MATLAB script

```

f          = 0.5e9;                      % Frequency
lambda    = 3e8/f;                      % Wavelength
k          = 2*pi/lambda;                % Wavenumber
M          = 8;
N          = 8;
dx         = 0.24;
dy         = 0.24;
DAF        = 10*log10(N*M*4*pi*dx*dy/lambda^2)

```

predicts directivity of 21.1 dB at 500 MHz and of 27.1 dB at 1 GHz, which is again in a good agreement with Figure 11.19.

11.16 DESIGN OF SMALL 2D ARRAYS: IMPEDANCE BANDWIDTH IMPROVEMENT AND DIRECTIVITY

In this section, we will present some design results for *small arrays*. We will in particular establish theoretical/numerical results for impedance bandwidth improvement and for the array directivity with full-wave numerical simulations. As an example, we will consider arrays of blade dipoles above the ground plane.

Antenna impedance becomes active antenna impedance [2, 3] in an array of all radiators excited simultaneously. Accurate analytical expressions for active or scan impedances of infinite arrays exist [2, 3, 7]. However, this is not the case for small arrays.

11.16.1 Unit Cell Structure and Geometry Parameters

For small arrays, the unit cell structure is crucial since it is not only the benchmark against which we will compare the performance of various finite arrays, but also, it serves as the basic building block for those arrays.

The unit cell shown in Figure 11.20 comprises of a resonant blade dipole of half length L and width W placed over a finite ground plane of dimensions $S_x \times S_y$ at a height h (120 mm). A conical impedance matching structure is included to control the impedance match between the feed point and the dipole. A wide-blade dipole is chosen to enable a wider impedance bandwidth and a simpler impedance matching network.

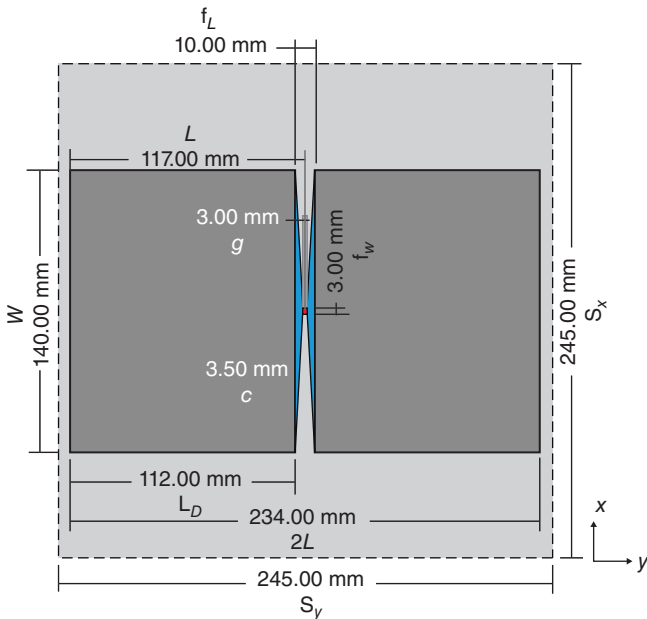


Figure 11.20 Top view of a unit cell consisting of a resonant dipole above a ground plane (dotted line is the border of the unit cell).

11.16.2 Simulation Setup and Impedance Results for a Unit Cell Radiator

The unit cell was again modeled in Ansys HFSS. All the metal portions were assigned a boundary condition of perfect electric conductor (PEC). The feed was modeled as a lumped port with the impedance of $50\ \Omega$. The unit cell was surrounded by a radiation box with the boundary condition of the PML assigned to it. A discrete frequency sweep from 0.2 to 1.2 GHz was applied. The impedance bandwidth definition we use is $S_{11} < -10\ \text{dB}$, which translates to a VSWR of 2 on the feed line. Figure 11.21 shows the S_{11} obtained over the frequency range 0.2–1.2 GHz. The results indicate that the unit cell configuration is resonant around 850 MHz and possesses a fractional bandwidth of 35%.

11.16.3 A 2×1 Array

We now investigate whether impedance bandwidth improvement can be obtained by using one more identical unit cell placed either along the x -axis or along the y -axis. We chose to replicate along the y -axis. Our goal is to achieve a bandwidth of at least 2.3 : 1, where the bandwidth is defined by

$$B = \frac{f_U}{f_L}. \quad (11.39)$$

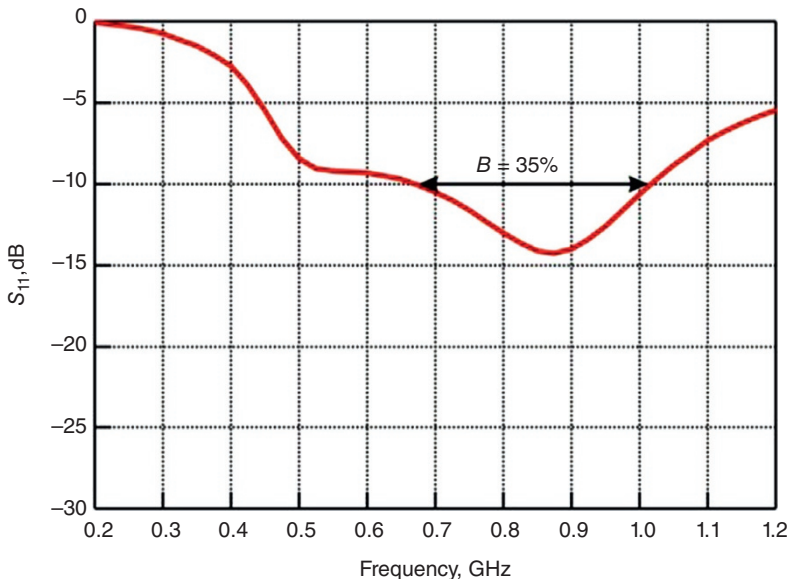


Figure 11.21 Reflection coefficient S_{11} for the isolated unit cell comprising of the resonant blade dipole over a finite ground plane.

Here, f_U and f_L represent the upper and lower frequencies of the band which satisfies the $S_{11} < -10$ dB criterion. The 2×1 array is shown in Figure 11.22a, along with the port numbering scheme. In this case, we have two ports, but due to symmetry, we only need the reflection coefficient data from either port. The antennas are excited simultaneously and are not intended to have the scanning capability. The simulation setup remains the same as before. It is clear from Figure 11.22b that we can indeed achieve a larger bandwidth with the 2×1 array as compared to the single radiator. The bandwidth achieved over the frequency range 0.4–1.0 GHz is approximately 2.5 : 1.

11.16.4 The 3×1 , 2×2 , 4×1 , 3×2 , 3×3 , 4×2 , 4×4 Arrays

Eight different array configurations chosen for investigation are shown in Figures 11.22 and 11.23, respectively. The corresponding S_{11} performance of these arrays is shown in the second column of the figures.

Clearly all these arrays exhibit superior bandwidth performance as compared to the isolated unit cell radiator, and the maximum impedance bandwidth achievable by these arrays is greater than 2.5 : 1. The edge elements of these finite arrays exhibit a somewhat wider impedance bandwidth as compared to the non-edge elements.

This is an illustration of the fact that the array bandwidth is typically larger than the bandwidth of a single radiator. The reason is a *mutual coupling* between individual radiators [2]. The resonant frequency is close to the resonant frequency of the individual patch antenna.

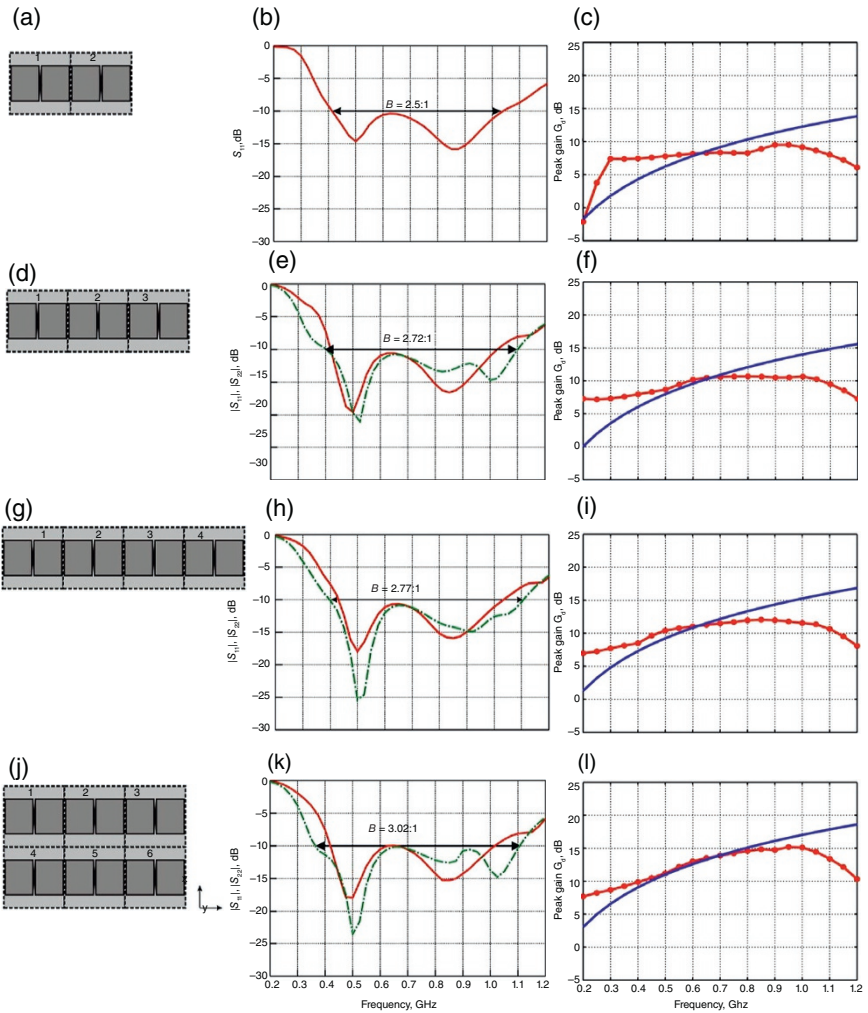


Figure 11.22 The geometry for the 2×1 , 3×1 , 4×1 , and 3×2 arrays is shown in the first column (a, d, g, j). The second column (b, e, h, k) provides the S_{11} (solid red curve) and the S_{22} (dashed-dotted green curve). The third column (c, f, i, l) provides a comparison between the theoretical (solid blue curve) and the simulated (dotted red curve) peak broadside directivity of these arrays.

11.16.5 Peak Broadside Directivity – Theoretical and Simulation Results

For a large array that is uniformly excited, the peak directive gain is restated here using the variables defined in Figure 11.20 as:

$$D = \frac{4\pi N_x N_y S_x S_y}{\lambda^2}. \quad (11.40)$$

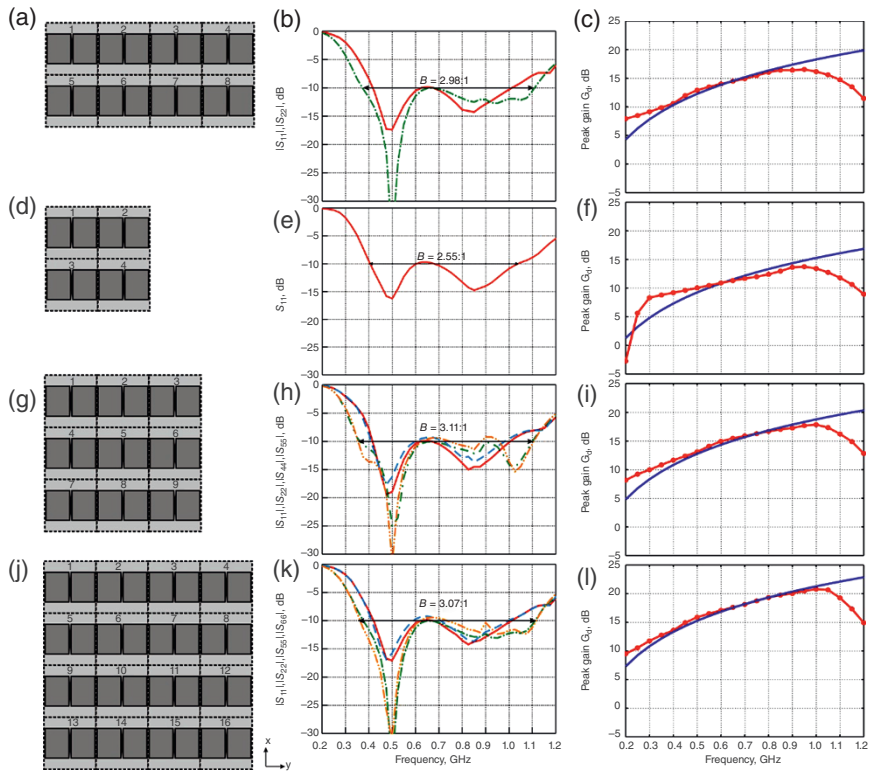


Figure 11.23 The geometry for the 4×2 , 2×2 , 3×3 and 4×4 arrays is shown in the first column (a, d, g, j). The second column (b, e, h, k) provides the S_{11} (solid red curve) and the S_{22} (dashed-dotted green curve). The third column (c, f, i, l) provides a comparison between the theoretical (solid blue curve) and the simulated (dotted red curve) peak broadside directivity of these arrays.

In general, close to the center frequency of 700–800 MHz, all arrays considered above achieve the theoretical gain. Barring a couple of cases (2×1 , 2×2 at 0.2 GHz), all the arrays exceed the theoretical estimate for the directivity predicted by the array area rule at lower frequencies. At the center of the band, the rectangular and square arrays perform much better than their linear counterparts. At higher frequencies, the peak broadside directivity exhibits a significant drop-off.

11.17 CORPORATE SERIES FEED – WILKINSON POWER DIVIDERS

Corporate-fed networks are typically used to provide power splits of 2^n , such as $n = 2, 4, 8, \dots$ and so on. For an antenna array, this type of feed is more general and versatile because it provides the designer with more control over the amplitude

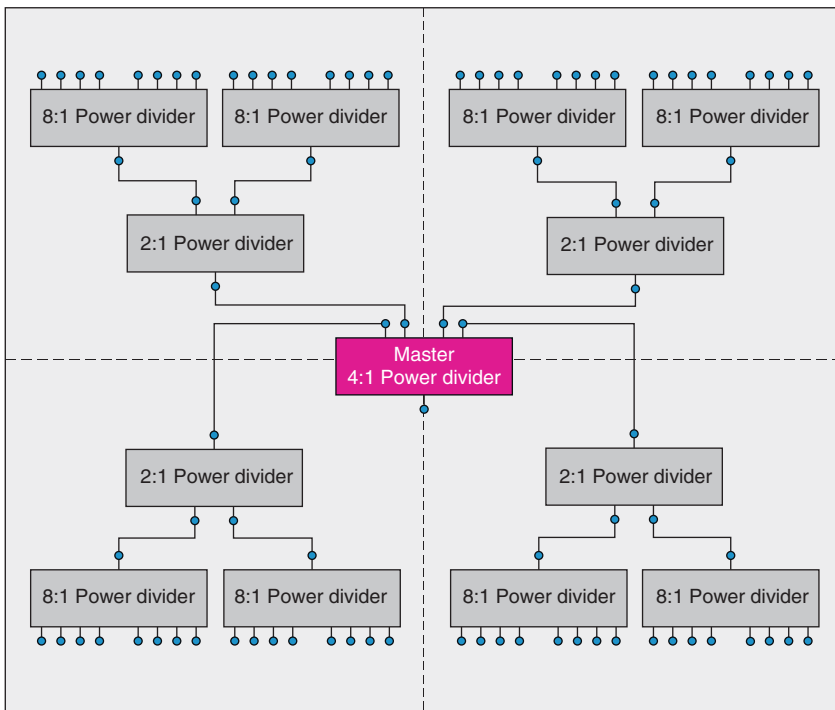


Figure 11.24 Corporate-feeding network used for the 64-element antenna array.

and phase of each element. The case in point is an 8×8 array shown in Figure 11.18. For this 64-element antenna array, a corporate feed network is constructed using $2:1$, $4:1$, and $8:1$ Wilkinson dividers as shown in Figure 11.24.

The array is divided into four sub-arrays having 16 elements in each 4×4 module. Within each module, each individual element is fed by two $8:1$ power dividers, which in turn are fed by one $2:1$ divider. Then, each module is fed by a master $4:1$ divider. In total, the feed network is composed of one $4:1$ master divider, four $2:1$ dividers, and eight $8:1$ dividers.

The performance of Wilkinson power dividers may be simulated in Ansys HFSS; the typical data are shown in Figure 11.25 for a 500 MHz–1 GHz array in Figure 11.18 with 130 mil FR4 used for the power divider design. Using a low-loss dielectric instead of FR4 will significantly improve the performance, especially at higher frequencies.

The estimated total divider loss at 1 GHz is $0.7(2:1) + 1(4:1) + 2(8:1) = 3.7$ dB. Another 1.5 dB is coming from the cable adapters. Using a low-loss substrate instead of the 130 mil FR4 would allow us to reduce the realized gain loss by about 3 dB.

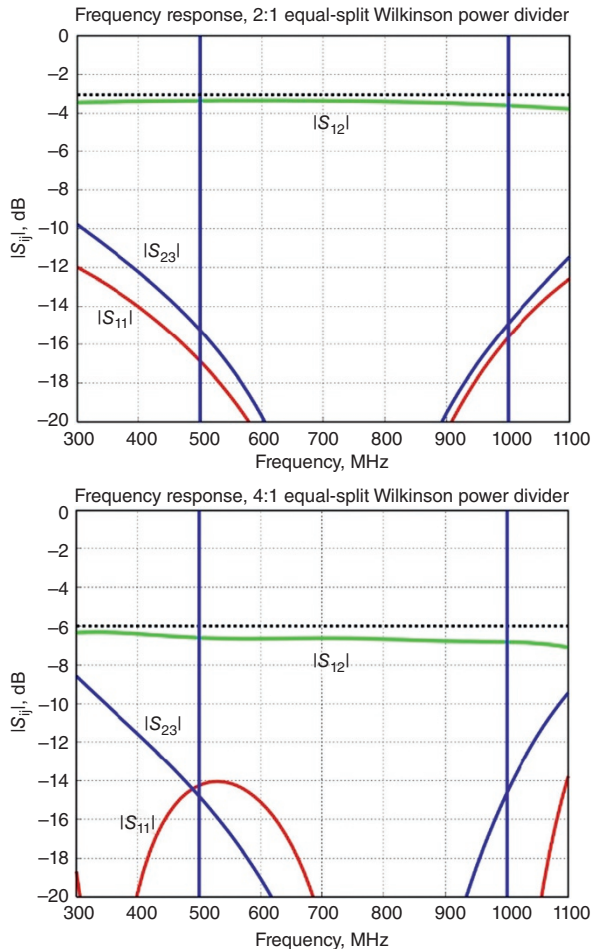


Figure 11.25 Simulated behavior of two (2 : 1, 4 : 1) series Wilkinson dividers used in hardware prototypes. The loss is given by the deviation of S_{12} from the theoretical dashed line.

11.18 CORPORATE (PARALLEL) FEED

Another example of the corporate feed is shown for a small patch antenna array in Figure 11.26. A patch antenna has a typical impedance of 300–500 Ω at the radiating edge and 0 Ω at the centerline. Therefore, an inset should be introduced in Figure 11.26 in order to match it to a different impedance, say 100 Ω . In Figure 11.26, two 100 Ω transmission lines (TLs) are combined in parallel, which would give us an impedance of 50 Ω . To match this impedance to another 100 Ω transmission line, a quarter-wave transformer is introduced. Finally, a vertical coaxial connector of 50 Ω characteristic impedance is connected in Figure 11.26

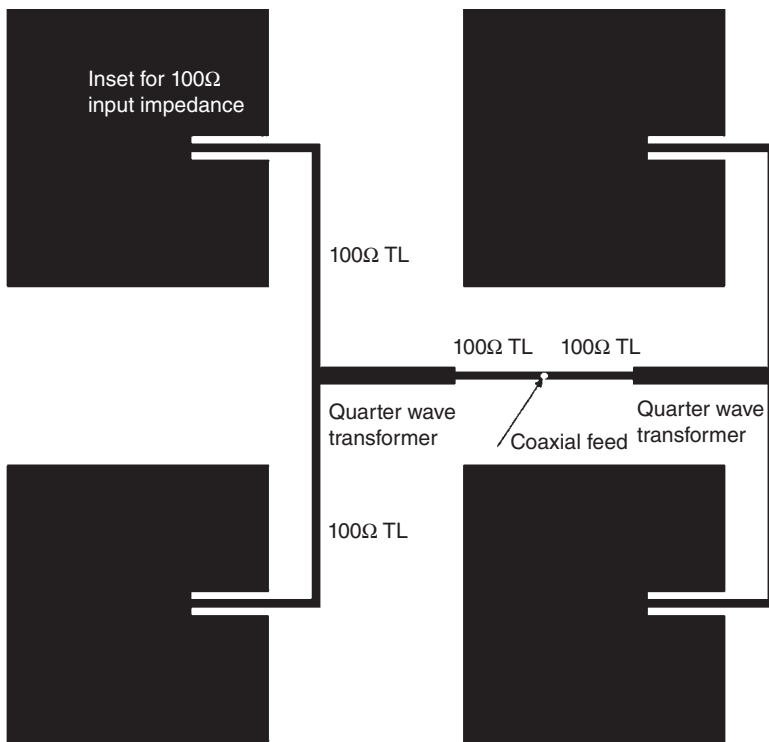


Figure 11.26 Example of the corporate feed for a 2×2 patch antenna array using the probe master feed.

to the two 100Ω transmission lines. The coaxial probe feed sees both TLs in parallel, i.e. it sees 50Ω . Other numerous examples of the corporate feed are possible – see Ref. [8] at the end of this section.

REFERENCES

1. P. W. Hannan, “The element-gain paradox for a phased-array antenna,” *IEEE Trans. Antennas Prop.*, vol. 12, no. 4, pp. 423–433, 1964.
2. R. C. Hansen, *Phased Array Antennas*, Wiley, New York, 2009, second edition.
3. R. C. Hansen, “Phased arrays,” In *Antenna Engineering Handbook*, J. L. Volakis, Ed., McGraw-Hill, New York, 2007, fourth edition.
4. C. A. Balanis, *Antenna Theory: Analysis and Design*, Wiley, New York, 2016, fourth edition.
5. A. A. Oliner and R. G. Malech, “Mutual coupling in infinite scanning arrays,” In *Microwave Scanning Antennas*, Vol. II, R. C. Hansen, ed., Academic Press, New York, 1966.
6. W. H. Von Aulock, “Properties of phased arrays,” *Proc. IRE*, vol. 48, no. 10, pp. 1715–1727, 1960.

7. S. Makarov and A. Puzella, "Scan impedance for an infinite dipole array: Hansen's formulas vs. Ansoft HFSS simulations," *IEEE Antennas Prop. Magazine*, vol. 49, no. 4, 2007, pp. 143–156.
8. D. P. Gray, C. B. Ravipati, and L. Shafai, "Corporate fed microstrip arrays with non-radiating edge fed microstrip patches," in *1998 Antennas and Propagation Society International Symposium*, 1998, pp. 1130–1133, June 1998.

PROBLEMS

1. A planar broadside 4×4 array of patch antennas has the size of $1 \times 1'$ at 2.45 MHz. It is built using a 4.67 mm or $3/16''$ thick acrylic substrate at $\epsilon_r = 3.0$. Analytically estimate the maximum array directivity in dB.
2. A broadside directed-power array has 16 radiators in total. They could be assigned either as a linear array or as a planar square array. In every case, the spacing between the radiators is $\lambda/2$, in any direction. Which array has a higher gain?
- 3*. Verify Figure 11.19 for the planar array directivity using Antenna Toolbox simulations for an 8×8 array of straight resonant dipoles.

Suggested example: Wideband Blade Dipole Antenna and Array.

Hint: A sample MATLAB code could be used:

```
%> 8 X 8 Array of Dipoles Backed by Reflector
clc;
clearvars;
close all;
%> Create Dipole Backed by Reflector
f = 500e6;
d = design(dipole,f);
d.Length = 230e-3;
d.Tilt = 90;
d.TiltAxis = [0 1 0];
r = design(reflector,f);
r.Exciter = d;
r.GroundPlaneLength = inf;
r.GroundPlaneWidth = inf;
%%
a = rectangularArray;
a.Size = [8 8];
a.Element = r;
a.RowSpacing = 240e-3;
a.ColumnSpacing = 240e-3;
figure
show(a)
```



Index

- Antenna
antenna designer, MATLAB, 251–252
backlobe, 116
balun, 103, 108, 110
center frequency, 26
circularly polarized, 119, 259
complex reflection coefficient, 19
directivity, 84, 87, 211
Friis equation, 95
impedance bandwidth, 10, 26
impedance matching, 137
input impedance, 8
isotropic, 84
loss resistance, 2
omnidirectional, 40
passive RFID tag, 33
polarization, 34, 156, 211, 212, 264
polarization mismatch, 35
power transfer between two antennas, 4
radiation density, 86
radiation efficiency, 7
radiation intensity, 86
radiation pattern, 80
radiation resistance, 2
reactance, 9
reflection coefficient, 19, 23
resistance, 9
resonant, 2, 108, 141
tuning and matching, 6, 185, 189–192
- Antenna array
array, 18, 119, 124, 271, 279, 292, 304
array factor, 119
bandwidth, 10, 26, 174, 177, 264, 308–310
grating lobes, 279
impedance, 8, 10, 20, 26, 38, 45, 46, 75, 137
progressive phase shift, 124
linear, 24, 31, 87
Modeling in Antenna Toolbox:
 Laboratory Session #12 Part 1 of online materials
Modeling in Antenna Toolbox:
 Laboratory Session #12 Part 2 of online materials
non-scanning, 271–273, 277, 304
scanning, 271
sidelobes, 278, 279
- Balun
broadband, 141
Dyson, 108
ferrite split snap-on core, 113
high frequency transformer, 110
Marchand, 110
power divider or splitter, 108
resonant balun, 108
split-coaxial, modeling, 103

- Dipole antenna
 antenna backlobe gain, 150
 balun, 137, 138, 150
 blade dipole, 137–141, 147–149,
 151, 153
 bowtie dipole, 137–139
 broadband antenna type, 141
 broadside direction, 135
 endfire direction, 135
 frequency independent antennas, 144
 impedance, analytical formula, 140
 impedance matching, 137
 impedance matching lumped circuit, 137
 log-periodic antennas, 145
 matching and tuning, 6, 137
 Modeling in Antenna Toolbox:
 Laboratory Session #6 Part 1 of online
 materials, (AU: Not found)
- Modeling in Antenna Toolbox:
 Laboratory Session #6 Part 2 of online
 materials, (AU: Not found)
 monopole, 135, 136, 150
 non-resonant travelling wave, 141
 notch antenna, 148
 radiation pattern, 136–139, 147
 resonance, first, 136, 140
 small dipole antenna, 71, 75, 156, 173
 spherical wave, 143
 standing resonant wave, 141
 tapered slot, 144
 travelling wave antenna, 141
- Input impedance
 antenna reactance, 9, 172
 antenna resistance, 9
 complex reflection coefficient, 19
 have wave resonance, 11
 impedance bandwidth, 10, 26
 incident wave, 19
 power angle, 9
 power reflection coefficient, 23
 reflected wave, 19
 scattering parameters, 18, 24
 voltage reflection coefficient, 19
 voltage standing wave ratio, 26
- Loop antenna
 axial mode of radiation, 167
 balun, 155, 156
 electric dipole, 156
- electromagnetic duality, 156
 horizontal polarization, 156
 impedance, 157, 160, 165, 166, 168
 magnetic dipole, 156
 matching, 156, 160, 165, 168
 Modeling in Antenna Toolbox:
 Laboratory Session #7 of online
 materials, (AU: Not found)
 parallel resonance, 160
 parallel RLC lumped circuit, 160
 quarter-wave-circumference-loop, 162
 radiation pattern, 156, 159, 163, 165
 resonance, 156, 158, 159, 161, 165, 169
 series resonance, 159
 series RLC lumped circuit, 159
 small loop, 156–159, 161,
 163–165, 168
 vertical polarization, 156
- Patch/PIFA antenna
 bandwidth, 199–202, 206, 207, 215
 conductor loss, 204
 co-polar directivity, 210
 co-polarization, 210
 cross-polarization, 211
 cross-polarization isolation, 211
 dielectric loss, 203
 dominant component of electric field, 211
 feeding, patch antenna, 199, 200, 206,
 207, 209
 feeding, PIFA antenna, 220–222,
 224, 231
 fields, 197, 198, 206, 209, 211–213
 impedance, 200–202, 206–208, 216,
 219–227, 230, 231
 low-loss conventional patch antenna, 201
 mesh subdivision, 207
 Modeling in Antenna Toolbox:
 Laboratory Session #9 of online
 materials, (AU: Not found)
 partial quality factor, 204
 PIFA antenna, 214, 219, 230
 polarization, 197, 199, 206, 209–211,
 218, 219
 radiating edges of the patch, 199
 radiation pattern, 198, 199, 209
 resonance, 207, 209, 210, 220, 222–225
 resonant mode of operation, 200
 space-wave, 203
 surface-wave, 203

- Polarization
 circular, 87
 circular polarization ratio, 264
 dual polarized, 264
 elliptical, 87
 horizontal polarization, 156
 left-handed circularly polarized, 119
 linear, 87
 polarization bandwidth, 264
 polarization mismatch, 34
 vertical polarization, 156
- Radiation pattern
 backlobes, 116
 co-polar directivity, 211
 co-polarization, 211
 cross-polarization, 212
 cross-polarization isolation, 212
 directivity, 84
 far-field, 75
 front-to-back ratio, 129
 near field, 75
 power radiated per unit solid angle, 86
 radiating field, 75
 radiating near field region, 75
 radiation intensity, 86
 reactive near field, 75
 realized gain, 91
 sidelobes, 278
 sidelobes ratio, 279
 transition region, 75
- Small antennas
 bandpass filter, 189
 bandwidth, 171–178, 180, 182,
 185, 189
 electrically small antenna, 172, 185
 electromagnetic resonator, 175
 half power small antenna
 bandwidth, 174
 maximum bandwidth ever
 possible, 177
 open resonators, 175
 quality factor of an antenna, 175–178
 radiation efficiency, 180
 small dipole antenna, 173, 182
 small loop antenna, 173, 183,
 185, 191
 small monopole antenna, 191
 tuning, 185, 186, 189, 191, 192
 wheeler Chu limit, 176–177, 179
- Traveling-wave antennas
 active antenna region, 245
 axial-mode, 242
 cavity-backed, 246
 equiangular spiral antenna, 246
 feeding-region, 247
 helical antenna, 241–243, 246
 normal mode, 241
 transmisison region, 246
 Yagi-Uda antenna, 233, 238–240

WILEY END USER LICENSE AGREEMENT

Go to www.wiley.com/go/eula to access Wiley's ebook EULA.